THERMODYNAMIC PROPERTIES OF VAPOURS

A thesis presented for the degree of
Doctor of Philosophy
in
Chemical and Process Engineering

at the
University of Canterbury
Christchurch
New Zealand

by
Rakesh Malhotra
(1983)

Dedicated to my parents

ACKNOWLEDGEMENTS

I wish to express my gratitude to Professor A. G. Williamson. His indispensable interest, advice, forebearance and drive to finish any task by 'YESTERDAY', has inspired me to accomplish this project 'TODAY'. Thanks are due to Dr. P. J. McElroy for his guidance and assistance, especially to reduce my scrawl into a meaningful thesis, while Professor Williamson was on leave. Also, I express my gratitude to Professor R. Battino (Dayton Univ., Ohio, USA) for his indispensable patient guidance in part of this work, during his visit to Canterbury University in 1980.

Many thanks are due to technical staff (especially Mr. D. Brown) of the Chemical and Process Engineering Department for their timely skillful assistance in the construction of the apparatus, and Mr. F. Downing of the Chemistry Department for his glass-blowing.

I wish to acknowledge the receipt of Postgraduate Research Scholarship from the University Grants Committee NZ. Also, thanks are due to Prof. R. B. Keey who made sure that I never experienced any financial problems, in the later stages of this work.

I wish to acknowledge the help of the Civil Engineering Department in permitting me to use their computer facilities and word processor system for typing this thesis. Thanks are due especially to Dr. D. Scott and Mr. J. Ritchie (Civil Engineering Dept.) for their valuable assistance in familiarising me with the system.

I wish to thank Ambika Prasad for her patient proof reading of the manuscript and Prasad for assistance with the diagrams. Thanks are due to Miss L. K. Anderson for her assistance with the typing in Greek symbols in the text. Also, I would like to thank especially to Mrs. P. Thomas for her care and attention rendered in xeroxing the thesis.

Last but not least, my special thanks are due to my parents for their continual encouragement from a distance.

CONTENTS

CHAPTER 5 **OPERATING PROCEDURE**

CHAPTER 6 **EXPERIMENTAL RESULTS**

SUMMARY

A new method (Couldwell et al., 1978) has been developed for the measurement of the second virial coefficients of condensable gases. This method evaluates the second virial coefficients in terms of three pressure measurements (temperature maintained constant) and avoids the difficult volume calibration associated with former p-V-T-n and other volumetric methods.

Measurements are reported for n-hexane at temperatures of 323.15, 328.15, 338.15, 348.15, 358.15 amd 373.15 K, and for benzene and cyclohexane at temperatures of 323.15, 348.15 and 373.15 K. The influence of surface adsorption of the vapours on the measurement of second virial coefficients is observed. It is suggested that future measuremets be made for loading pressure less than 0.34 to 0.4 times the saturation vapour pressure of the gases, corresponding to a region of monolayer adsorption.

The influence of the third virial coefficient is determined, thus enabling the estimations of the "true" second virial coefficients which are at variance with the literature values (Dymond and Smith, 1980). Reasons are advanced to explain this anomaly. The results interpreted in the same manner, as the literature values, are in agreement with the latter.

In a parallel study, an existing apparatus (McElroy et al., 1980) has been modified to measure unlike interaction second virial coefficients (Battino et al., 1983). The excess second virial coefficients $(B_{12} - (B_{11}+B_{22})/2)$ for benzene, cyclohexane and n-hexane vapour binary mixtures have been measured at the temperatures 298.15,

323.15, 348.15, 373.15 and 398.15 K. The method permits the interaction second virial coefficients, B_{12}, to be determined with an accuracy three times better than that can be obtained from measurement of second virial coefficients of the mixtures.

The lower temperature measurements are affected by surface adsorption. A postulated mathematical model (Shannon, 1976) has been checked to calculate a correction for surface adsorption. The interaction virial coefficient values, for benzene + cyclohexane, are compared with B_{12} values in the literature and the values obtained from empirical correlations.

CHAPTER 1

INTRODUCTION

1-1 Scope

The ability to understand and accurately predict p-V-T-n properties of gases, vapours and their mixtures is vital for design purposes in chemical process industries and for the determination of other important thermodynamic behaviour such as chemical and phase equilibria. Knowledge of the latter is essential for rational design of separation operations such as distillation, absorption and extraction.

Knowledge of p-V-T-n properties of gases and vapours, as well as enabling calculations of the thermodynamic properties of a real system also contributes to our understanding of intermolecular forces. The latter, with the application of statistical thermodynamic principles (eg. Hill, 1962), provide the means of predicting the pure and mixture properties of both condensed and gaseous phases.

Provided the equation of state measurements meet the criteria of high precision, freedom from systematic errors and sufficient range, they can give definitive information about the intermolecular potential (Knobler, 1983). But a very few measurements of volumetric methods come up to this standard. This work aims to determine the "true" second virial coefficients of pure components, of high precision.

1-2 Historical Development

Intensive study of the subject since the classical work of Boyle in 1662, and major advances by Charles, Dalton, Avogadro and Amagat over the intervening period in the nineteenth century, has been condensed into a simple mathematical relation, generally known as perfect gas law :

$$pV = RT\Sigma_i\, n_i \qquad (1.1)$$

where p represents the pressure, V the total volume, n_i the quantity of component i, R the gas constant and T the absolute temperature.

The perfect gas relation may also be derived from molecular considerations, using statistical mechanics (eg. Hill, 1962), or from the kinetic theory of gases (eg. Hirschfelder, Curtiss and Bird, 1954). But these relationships describe the behaviour of only a perfect gas, or the limiting behaviour of a real gas as pressure tends to zero.

Subsequent work has involved modification of the perfect gas equation of state, to secure a better representation of the p-V-T-n properties of real gases. Van der Waals in 1883, proposed the first practical two-parameter equation to improve over the ideal gas law. Other two-parameter equations of state are those of Dieterici, Berthelot and Redlich-Kwong (Scott, 1976). Unfortunately these are successful in representing experimental data over only limited density and temperature ranges. The more cumbersome equations of state available have more than two constants and are more accurate in the regions of

higher density. An extreme example of such relations, is the Benedict, Webb and Rubin equation proposed in 1940. It has eight constants, which are determined empirically for each substance. Even so they are only valid in the region of fitted experimental data and extrapolation outside this region is risky.

The virial equation of state has the advantage over the empirical relations, in its theoretical connection with the inter-molecular forces and thus the possibility of its extrapolation (Mason and Spurling, 1969), outside the experimental data region.

Mason and Spurling (1969) and Knobler (1978) have provided a detailed discussion of the volumetric properties of pure gases and mixtures. Cox and Lawrenson (1973) have discussed p-V-T-n behaviour of single gases.

1-3 The Virial Equation of State

In 1901, Kamerlingh Onnes first suggested the polynomial

$$pv = A + \frac{B''}{v} + \frac{C''}{v^2} + \frac{D''}{v^4} + \frac{E''}{v^6} + \frac{F''}{v^8} \qquad (1.2)$$

to fit p-v-T data. However, the volumetric properties of a gas at low or moderate densities are suitably described by the virial equation of state expressed :

as either the volume explicit (or Leiden) form

$$pv = RT(1 + B(T)/v + C(T)/v^2 + \ldots) \qquad (1.3)$$

or the pressure explicit (or Berlin) form

$$pv = RT + \beta(T)p + \gamma(T)p^2 + \ldots \tag{1.4}$$

where v is the molar volume. B(T) and C(T) are the second and third virial coefficients for the volume series. $\beta(T)$ and $\gamma(T)$ are the second and third virial coefficients for the pressure series.

Several authors (Epstein, 1952; Putnam and Kilpatrick, 1953; and Mavridis, 1976) have proposed procedures to derive the relations between the coefficients of the pressure series and those of the volume series. However, for the infinite series, inverting one series into the other and then equating the coefficients, leads to unique relations between the two sets of coefficients, as follows:

$$B(T) = \beta(T) \tag{1.5}$$

$$C(T) = \gamma(T)RT + B^2(T) \tag{1.6}$$

Kell (1982) has also derived the relations between the virial coefficients of both the pressure and density series for the compressibility factor z and for z^{-1} and log z up to the fifth virial coefficient, and has displaced in a pattern that assists the convenient transformation between them.

Statistical thermodynamics (Hill, 1962) also provides a theoretical basis for the virial equation of state in which the virial coefficients correspond successively to the interactions between pairs, triplets, etc. of molecules. Elabd (1976) has also used a new method for calculation of statistical mechanical expressions for the virial coefficients.

Second virial coefficients can be used in numerous ways to derive further properties of gases or vapours. Hirschfelder et al. (1954) have summarized the deviations of some thermodynamic functions from the ideal values, in terms of the virial coefficients.

For a gas or vapour mixture, the virial coefficients B_m and C_m depend on the composition, usually given by mole fraction x_i and represented as averages of all possible interactions between groups of molecules.

$$B_m = \sum_i \sum_j x_i x_j B_{ij} \tag{1.7}$$

$$C_m = \sum_i \sum_j \sum_k x_i x_j x_k C_{ijk} \tag{1.8}$$

For a binary mixture

$$B_m = x_1^2 B_{11} + 2x_1 x_2 B_{12} + x_2^2 B_{22} \tag{1.9}$$

and

$$C_m = x_1^3 C_{111} + 3x_1^2 x_2 C_{112} + 3x_1 x_2^2 C_{122} + x_2^3 C_{222} \tag{1.10}$$

where x_1 and x_2 are the mole fractions of components 1 and 2.

Consequently three second virial coefficients B_{11}, B_{22} (the pure component virial coefficients) and B_{12} (interaction virial coefficient) are needed to describe the binary interactions in a binary mixture. Similarily the third virial coefficient of a mixture needs four terms : C_{111}, C_{222}, C_{112}, C_{122}. The terms C_{112} and C_{122} are third virial coefficients of the unlike molecular interaction.

For mixtures, it is convenient to define an excess second virial coefficient

ε, and two excess third virial coefficients ζ_1 and ζ_2.

$$\varepsilon = B_{12} - (B_{11} + B_{22})/2 \tag{1.11}$$

$$\zeta_1 = C_{112} - (2C_{111} + C_{222})/3 \tag{1.12}$$

$$\zeta_2 = C_{122} - (C_{111} + 2C_{222})/3 \tag{1.13}$$

Using these definitions, equations (1.9) and (1.10) become

$$B_m = x_1 B_{11} + x_2 B_{22} + 2x_1 x_2 \varepsilon \tag{1.14}$$

$$C_m = x_1^3 C_{111} + x_2^3 C_{222} + 3x_1 x_2 (x_1 \zeta_1 + x_2 \zeta_2) \tag{1.15}$$

1-4 The Principle of Corresponding States

The Principle of Corresponding States (Guggenheim, 1967) asserts that the behaviour and properties of the molecules with the same functional form for their intermolecular potential, can be correlated using the critical properties of the components as scaling factors. Thus for the interaction second virial coefficients of a pure substance or a mixture :

$$B_{ii}/V_i^c = f(T/T_i^c) \tag{1.16a}$$

$$B_{ij}/V_{ij}^c = f(T/T_{ij}^c) \tag{1.16b}$$

where V_i^c and T_i^c are the critical properties of a pure substance and V_{ij}^c and T_{ij}^c are pseudo critical properties of the mixture. The most widely used extensions to the simple principle are

a) McGlashan and Potter's (1962) equation for n-alkanes

$$B/V^c = 0.430 - 0.886(T^c/T) - 0.694(T^c/T)^2 - 0.0375(n-1)(T^c/T)^{4.5} \quad (1.17)$$

where n is the number of carbon atoms in the hydrocarbon chain. Several authors (Guggenheim and Wormald, 1965; Dantzler and Knobler, 1969; Pandya and Williamson, 1971) have suggested the applicability of equation (1.17) to molecules other than the alkanes.

b) The Pitzer-Curl (1957) correlation, modified by Tsonopoulos (1974) to fit at low reduced temperature (T_R <0.75)

$$Bp^c/RT^c = f^{(0)} + \omega f^{(1)} \quad (1.18)$$

where $$f^{(0)} = 0.1445 - 0.33(T^c/T) - 0.1385(T^c/T)^2 - 0.0121(T^c/T)^3 - 0.000607(T^c/T)^8 \quad (1.19)$$

$$f^{(1)} = 0.0637 + 0.331(T^c/T)^2 - 0.423(T^c/T)^3 - 0.008(T^c/T)^8 \quad (1.20)$$

and ω is Pitzer's acentric factor (Pitzer et al., 1955).

Combining rules have been used to predict pseudocritical properties, to fit the interaction coefficients for mixtures into the same frame-work. The most common of these are (Prausnitz, 1969)

for temperature $$T^c_{12} = (T^c_1 T^c_2)^{0.5} \quad (1.21)$$

for volume $$V^c_{12} = 1/8(V^{c\,1/3}_1 + V^{c\,1/3}_2)^3 \quad (1.22)$$

for chain length $$n_{12} = (n_1 + n_2)/2 \quad (1.23)$$

and for the acentric factor

$$\omega_{12} = (\omega_1 + \omega_2)/2 \qquad (1.24)$$

Pandya and Williamson (1971) used McGlashan and Potter's corresponding states treatment for n-alkanes, together with Barker and Linton's average chain length concept and expressions for the pure component critical temperature and volume. They fitted an analytical relation for T^c and V^c against chain length for pure n-alkanes, to yield a general expression for B as a function of n, the chain length and T, the absolute temperature only.

1-5 The Principle of Congruence

The principle of Congruence allows the prediction of mixture properties within a family or homologous series from the knowledge of the pure component or other mixture behaviour of that series. Barker and Linton (1963) and Dantzler et al. (1968) have illustrated the application of the principle of congruence to the second virial coefficients of gas mixtures.

Koh and Williamson (1980) have reviewed the principle of Congruence for the estimation of the properties of mixtures of homologues from the properties of the pure components.

1-6 Second Virial Coefficient and Intermolecular Potential

There is an established connection between the macroscopic domain of virial coefficients and microscopic domain of intermolecular forces. Statistical mechanics provides a method for determination of the equation of state and other thermodynamic properties of a gas in terms of its intermolecular potential. Keller and Zumino (1959) considered the inverse problem and observed that in the classical statistical mechanics, the second virial coefficients, in the virial expansion of the equation of state of a gas, uniquely determine the intermolecular potential provided that the potential is monotonic. Frisch and Helfand (1960) also observed that, in general, second virial coefficient data are only able to define the width of the potential well as a function of its depth and repulsive branch.

However, the traditional practice of force fitting the data to crude potential energy functions do not allow the full value of the information contained in the property to be realized. Cox et al. (1980) described a new iterative procedure using second virial coefficient data, to enable information about intermolecular potential to be obtained. Smith et al. (1980) gave a demonstration of the new method, on the inversion of second virial coefficient data derived from an undisclosed potential energy function and found the derived potential parameters to be most satisfactory in the agreement with the original parameters. Smith et al. (1981) examined the applicability of the method to real and imperfect pseudoexperimental data incorporating random errors, calculated from a known potential energy function. The

procedure was also shown to be satisfactory when applied to the experimental data for argon.

Arora et al. (1980) used binary diffusion coefficient data with accurate virial coefficients data to yield (m 6,8) potential parameters. They claimed that these potentials derived with the aid of the Chapman-Eskong theory, could predict accurate viscosities.

Thus the virial equation of state may be employed to extract information on intermolecular forces. This has been hindered to some extent by an inadequate approach in experimental measurement of the second virial coefficient. Truncation of the equation of state at the second virial coefficient B, may prevent determination of the "true" B value and prevent observation of the effect of triplet molecular interaction.

1-7 Measurement of Second Virial Coefficients

An intensive effort has been made in this laboratory for more than a decade to develop an experimental technique to avoid this shortcoming. This investigation involves the development of a new method (Couldwell et al., 1978) for obtaining accurate B values for pure substances.

In addition accurate determination of the interaction second virial coefficients, B_{12}, in mixtures, have been made via measurements of the pressure change on mixing at constant volume. To enable testing of the mixing rules described in Section 1-4, B_{12} must be measured with sufficient accuracy.

The determination of B_{12} from measurements of the mixture

second virial coefficient, B_m, (equation 1.19) can result in uncertainties up to three times the uncertainty in each pure component second virial coefficient measurement.

The excess second virial coefficient can be related to the pressure change on mixing at constant volume and temperature (Knobler et al., 1959).

$$\varepsilon \approx \frac{RT\Delta p}{2x_1x_2p^2(1 + \Delta p/p)} \qquad (1.25)$$

where Δp is the change in system pressure on mixing and p is the initial system pressure. Then using equation (1.11), B_{12} may be determined directly with greater accuracy than by other methods.

The relation between the isothermal Joule-Thomson coefficient, ϕ and the second virial coefficient for pure components is

$$\phi = \lim_{p \to 0} (\partial H/\partial p)_T = B_{ii} + T(dB_{ii}/dT) \qquad (1.26)$$

For gas mixtures, the Joule Thomson coefficient measurements give information on dB_m/dT and not on dB_{12}/dT. However, the enthalpy of mixing of vapours at low pressure, is related to ε by the equation

$$\lim_{p \to 0} H_m^E/p = 2x_1x_2(\varepsilon - T d\varepsilon/dT) \qquad (1.27)$$

and an accurate measurement of H_m^E can provide an accurate description of the behaviour of ε and therefore B_{12} over a wide range of temperature.

In addition to giving B_{12} values more accurate than those obtained from B_m, the excess second virial coefficient, ε is often required in thermodynamic calculations. For example in the study of

liquid vapour equilibria (i.e. multicomponent distillation) ε is required for conversion of accurate vapour pressure measurements into excess chemical potentials.

As stated earlier, a prime purpose of this investigaion is to measure second virial coefficient of pure components, and excess second virial coefficient of mixtures, with sufficient accuracy, to enable the testing of mixing rules.

CHAPTER 2

REVIEW OF EXPERIMENTAL METHODS

A. PURE COMPONENTS

2-1 Classification of Methods

Many methods of pure component second virial coefficient measurements have been extensively reviewed and their accuracy and limitations discussed (Couldwell, 1975; Cox and Lawrenson, 1973; Mason and Spurling, 1969). This review concentrates on the experimental techniques and their accuracy reported in the literature since 1972.

Most of the experimental techniques involving p-V-T-n measurements, can be categorised into two fairly well-defined groups: low pressure, and high pressure measurements. In both cases measurements may be made directly on the gas or it may be compared with another gas, whose properties are well established.

In addition to p-v-T methods, other gas properties, which depend on its non-ideality, may be measured and problems associated with volume calibration or surface adsorption avoided.

Since the measurements of pressure, temperature, density and number of moles are common to many of the methods, a brief summary of these is given.

2-2 Measurement of Experimental Quantities

Hala et al. (1967) have discussed laboratory techniques of measuring pressure and temperature in great detail.

2-2.1 Pressure Measurement

The SI unit of pressure is the Newton per square metre, Nm^{-2}, which is also called the Pascal (Pa). For convenience, the bar, which is equal to 10^5 Pa, is used in reporting p-v-T data. The standard atmosphere has now been defined as 1.01325 bar exactly.

In relative determination of virial coefficients, it is usually sufficient to know the absolute pressure to only a few parts in 10^4. The need for the highest possible accuracy in these measurements is conveniently concentrated in the determination of pressure ratios (Casado et al., 1951), small pressure difference (McGlashan and Potter, 1962) and pressure equality (Bottomley et al., 1958a). Under favourable conditions, sensitivities of a few parts in 10^6 can be achieved in each of these kinds of determinations. A similar sensitivity is reported for the pressure determination for this work.

Pressure measurements can be divided into two basic sections low pressure or high pressure measurements. Low pressures are generally measured by mercury manometer. Such measurements require accurate values of local acceleration due to gravity, g and of the density of mercury, ρ. This in turn requires the manometer to be thermostated. The height of each leg of mercury manometer is usually measured with a

precision cathetometer and an overall accuracy of ±5 Pa can usually be achieved.

High pressures can be measured with multiple manometers, consisting of a number of mercury manometers in series. These are inconvenient to use, having the problem of temperature control, reading many mercury heights to account for one pressure reading and applying corrections for the weight of the air column in each tube (Hala et al., 1967). The adsorption of sample gas on the mercury and correction for it (Kemball and Rideal, 1946) can be overcome by placing a differential pressure transducer in the apparatus as shown in Figure 2-1.

Another standard measuring device for higher pressures is the free piston gauge, based on balancing an unknown pressure of fluid (oil for instance) on a freely moving piston, by placing weights on it, as shown in Figure 2-2. This device has the advantage that the weight on the piston directly fixes the pressure of the system. However, the device suffers from three principal sources of error: friction, leaking of the pressure transmitting fluid through annulus between the piston and cylinder, and distortion of the gauge. Warowny et al. (1978b) have reported corrections for the effect of thermal expansions and elastic deformation of the piston and cylinder. They have also discussed the calibration of weights and corrections for the effects of local gravity and air buoyancy.

Besides the mercury manometer and free piston gauges, there are other types of gauges in use. Gehrig and Lentz (1977) used Bourdon gauges to measure pressures up to 300 MPa. The Bourdon gauge is essentially an arc of flattened metal tube, with its open end connected to the equipment in which pressure is measured and its other (sealed) end free. The difference between the pressure applied to the tube and that surrounding the tube, causes motion of the free end and this

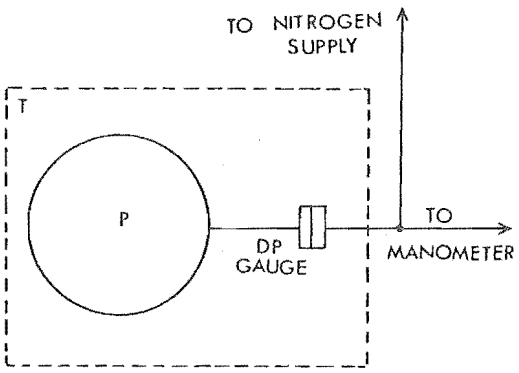

FIGURE 2-1

NULL PRESSURE INDICATOR

DP = DIFFERENTIAL PRESSURE

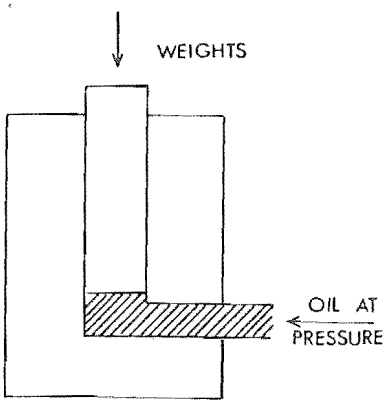

FIGURE 2-2

SIMPLE FREE-PISTON GAUGE

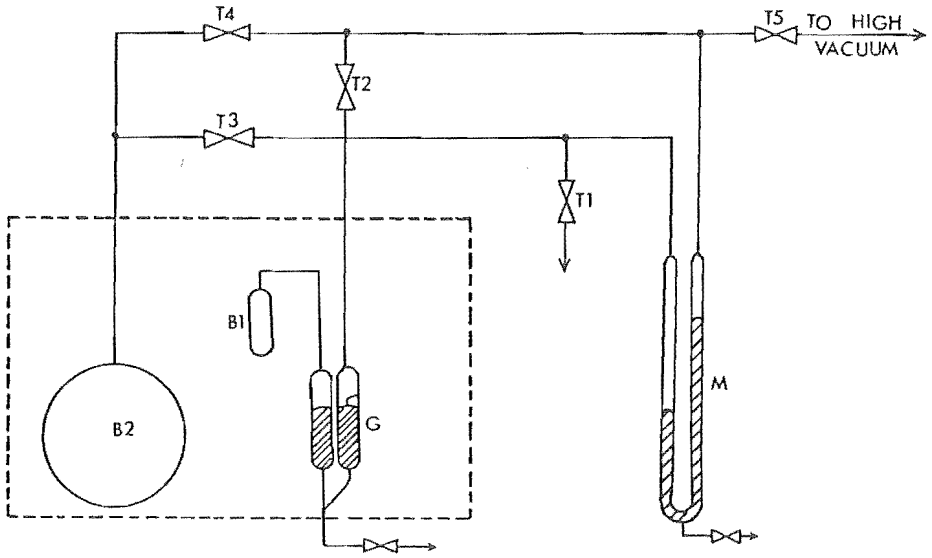

FIGURE 2-3

p-V-T-n METHOD (Baxendale et al., 1951)

motion is transmitted by a gear train or linkage to a pointer indicator on a pressure scale. The best of these devices generally have a precision of 0.1%.

David and Hamann (1953) also measured high pressures up to 1250 atmospheres, using "Budenberg" standard test gauges of the Bourdon tube type.

Anderson et al. (1968) used a Quartz Bourdon gauge for pressure below 170 kPa, reporting uncertainities up to 38 Pa. These differ from the Bourdon tube type in using a fused quartz spiral tube in the place of the bourdon tube. Another type of Quartz bourdon type gauge measures pressure by the amount of electric currrent that is necessary to apply to electromagnetic coils to oppose and exactly balance the rotation of the tube.

Benedict (1937) used a Manganin resistance gauge, which operates on the principle of changing resistance of the wire subjected to pressure. (Manganin is an alloy of copper (80 to 84%), manganese, nickel and iron). The pressure coefficient of resistivity is about 1.1×10^{-6} ohms per bar and is linear over a wide pressure range. The estimated maximum error in the absolute pressure was 0.2% up to 2000 atmospheres and 0.3% from 2000 to 7400 atmospheres. The precision of these devices also depends on that of the dead weight gauge tester against which they are generally calibrated.

A number of pressure transducers relying on the change in electronic and magnetic properties with pressure, have been developed. These transducers can be either variable capacitance or variable reluctance type. The former has a metal diaphragm which moves with respect to a fixed plate, changing the thickness of dielectric between the plates. Using a suitable bridge circuit, the variation in the capacitance can be measured and calibrated against pressure. The

variable reluctance type transducer has a movable magnetic diaphragm. The magnetic diaphragm is positioned between two magnetic output coils, such that any displacement of the diaphragm caused by applied pressure changes the inductance between the two coils. The resulting voltage output can be calibrated against the pressure.

The quartz crystal pressure measuring device works on the principle that the crystal oscillates at a given frequency at a constant pressure. The sensor probe of this device has a reference oscillator, whose resonant frequency is independent of the pressure. The difference between the quartz crystal oscillator frequency and that of the reference oscillator is a measure of the pressure applied to the crystal. These devices can have a precision of $\approx 10^{-3}$ Pa over a pressure range up to 800 bars.

2-2.2 Temperature Measurement

In the International Practical Temperature Scale (IPTS) 68 (Rossini, 1970), the unit of thermodynamic temperature (T) is the Kelvin (K), defined as the fraction 1/273.16 of the thermodynamic temperature of the triple point of the water. T is also expressed in celsius temperature (t) by

$$t = T(K) - 273.15 \qquad (2.1)$$

The unit of celsius temperature is the degree celsius (^{o}C), which is, by definition, equal in magnitude to the Kelvin.

Nicholas and White (1981) have reviewed temperature measurement devices and their calibrations. The platinum resistance thermometer is

an accurate temperature measuring device, which determines the ratio of a resistance at given temperature to that of a thermostatted standard resistance, within the International Practical Temperature Scale ranging from -182.97 to 630.5°C.

The quartz thermometer is also an accurate and convenient device, when it is used on differential mode. The absolute temperature is measured as the difference of the temperatures of one probe in the system and other at a reference point, preferably the ice point.

2-2.3 Density Measurement

The most direct method to measure density or molar volume, is to determine both the mass of gas and the volume it occupies separately. At high pressure, the mass of gas may be determined by direct weighing (Cherney et al., 1949). The volume of the apparatus is determined by observing the mass of fluid of known density (mercury or distilled water) which fills the apparatus. However, accurate determination of volume is difficult.

Some experiments determine density by refractive index or nuclear magnetic resonance technique. Others use techniques such as Burnett method (Section 2-3.2.3) and other expansion methods (Section 2-3.1.7), to avoid direct density measurement.

2-2.4 Amount of Gas

Lambert et al. (1949) obtained the number of moles by extrapolating a plot of pV versus p to zero pressure using the

truncated linear pressure series virial equation

$$pV = n(RT + \beta p) \qquad (2.2)$$

The value of n obtained from the intercept is then used with the limiting slope, $n\beta$, to obtain the second virial coefficients. Such methods assume that the number of moles of gas in the apparatus remain constant and the third virial coefficient is zero.

Casado et al. (1951) reported inability to reproduce isotherms of pv versus p for benzene in successive runs. Hamann and Pearse (1952) noticed apparent non-linearity of pv with p, for methyl chloride and methyl bromide and attributed this to the effects of adsorption or of higher terms in the virial equation of state. Whytlaw-Gray and Bottomley (1957) considered the effect of the third virial coefficient to be unlikely to be as great as that apparently observed, and attributed curvature in pv versus p isotherms, to the effect of adsorption. They observed this effect to be minimum and constant, for scrupulous clean apparatus and entirely grease clean mercury.

Eubank and Kerns (1973) observed the effects of adsorption in the Burnett apparatus calculation as indicated by an apparent shift of the apparatus constant.

2-2.5 Reference Gases

Some experiments involve comparison of the behaviour of the sample gas with that of a reference gas under the same conditions to determine second virial coefficients. Generally the reference gas is more nearly ideal than the gas under investigation, or is one with well

known p-v-T properties in the region of the experiment. The most commonly used reference gases are nitrogen, helium and argon, for which second and third virial coefficients are well known over a wide range of temperature. Other reference gases used are dried air (Barton and Hsu, 1969), oxygen (Casado et al., 1951), carbon tetrafluoride (Hajjar and MacWood, 1970) and neon (Wallace et al., 1964).

2-3 Experimental p-v-T Methods

Ellington and Eakin (1963) reviewed the techniques for p-v-T measurements, and stressed the need for increased accuracy in the data, to obtain derived thermodynamic properties of reasonable accuracy. The obvious but cumbersome experimental approach to determine B, C, D... at a particular temperature is to measure sufficient values of p, V, and n, that the virial coefficients can be uniquely determined using the virial equation of state.

$$pV/nRT = 1 + nB/V + n^2C/V^2 + n^3D/V^3 + \ldots \qquad (2.3)$$

where B, C, D... are the functions of temperature. Knobler (1978) has reclassified p-V-T-n measurements by keeping two of the quantities n, p, V, T constant, and determining the dependence of the remaining two on each other. However, it is experimentally inconvenient to keep p, V constant and show dependence of n and T on each other. Also keeping p, T constant, there is no useful information gained having V and n as variant. Besides V and n may not be measured with required accuracy.

2-3.1 Low Pressure p-V-T-n Experimental Methods

2-3.1.1 p-V-T-n Method

Roper (1940) extended the gas density method for atomic weight determination, to measure the second virial coefficients of olefins. The method involves measuring the pressure of a weighed amount of the gas in a globe of known volume, at a given temperature. Roper determined the mass of gas in the globe by weighing it evacuated and filled, making use of an almost identical counterpoise to provide buoyancy and adsorption correction. In transforming p-V-T-n data into p-v-T, Roper calculated B using the truncated form of equation (2.3).

$$B = \frac{pv^2}{RT} - RTv \qquad (2.4)$$

Barton and Hsu (1969) used a similar method to that of Roper (1940) with the modification of the addition of a metal diaphragm sensing device between the sample and reference gas (dried air) on the mercury manometer side. This prevented mercury pressure problems at the high temperatures and contamination of the sample with mercury vapours. Baxendale et al. (1951) used a small mercury null manometer G (in the constant temperature bath) between the sample in the bulb B1 and external manometer M as shown in Figure 2-3. The nitrogen let into the apparatus through T1, to balance the vapour pressure, was contained mainly in the ouffer bulb B2 of a capacity of 3 litres. This was immersed in the thermostat to prevent fluctuations in the pressure of

the gas due to change in room temperature.

Kolysko et al. (1972) used a modified differential mercury manometer (Figure 2-4) having platinum pins incorporated in an electric circuit and sealed into each limb of the manometer, to indicate the null position, as recorded by a sensitive galvanometer. They determined the second virial coefficients at very low pressure, using the equation

$$\beta = \lim_{p \to 0} (pv - RT)/p \qquad (2.5)$$

Eon et al. (1971) used a similar design of apparatus to measure the vapour pressure of pure substances. They calculated pressure series second virial coefficients using the relation

$$\beta = \mathcal{V} - RT/p \qquad (2.6)$$

Pathak (1979) used the same relation (equation 2.6) to calculate pressure series second virial coefficients. The apparatus (Figure 2-5) consisted of a flask connected to null manometer M1, which in turn was connected to another manometer M2. The vapour pressure of the sample was given by

$$p = \Delta hM1 + \Delta hM2 \qquad (2.7)$$

where $\Delta hM1$ and $\Delta hM2$ are the differences of the heights of mercury levels in M1 and M2.

2-3.1.2 Boyle's Method

Boyle apparatus as shown in Figure 2-6, is based on the

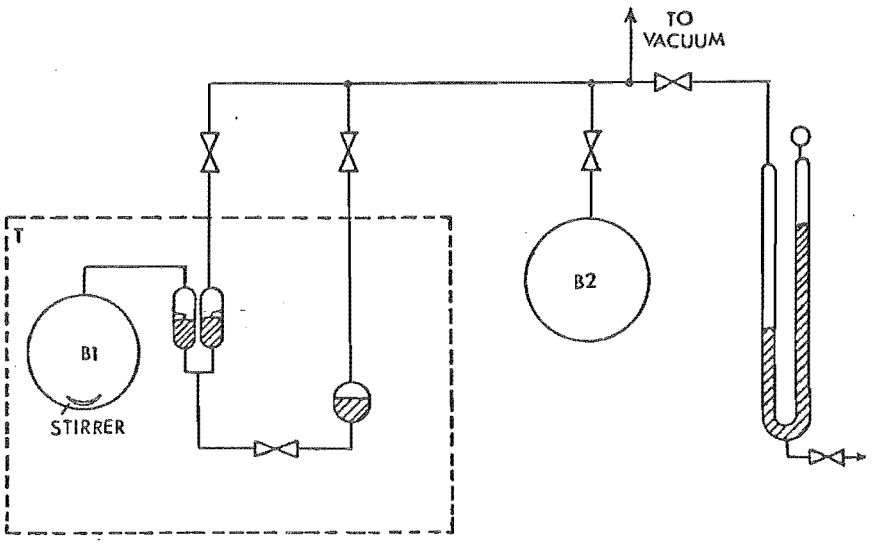

FIGURE 2-4

p-V-T-n METHOD (Kolysko et al., 1972)

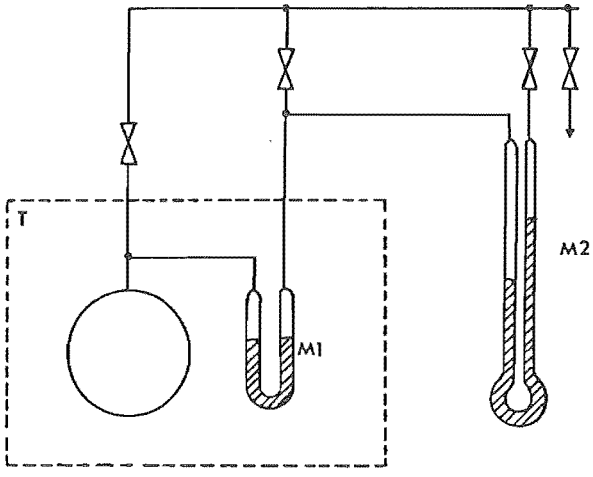

FIGURE 2-5

p-V-T-n METHOD (Pathak, 1979)

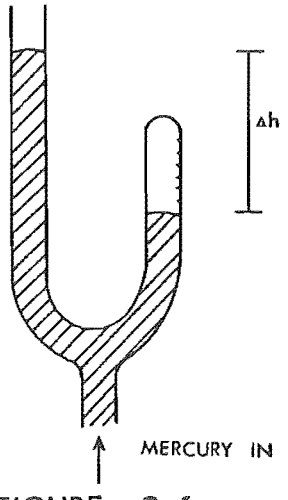

FIGURE 2-6

BOYLE'S LAW APPARATUS

principle, that for a given mass of a perfect gas at constant temperature, the volume is inversely proportional to the pressure. The deviations of a real gas from perfect behaviour may be used to determine the second virial coefficient.

Alexander and Lambert (1941) described a simple Boyle apparatus (Figure 2-7), in which gas is compressed into a graduated tube using a mercury column. Lambert et al. (1949) used it in an extensive investigation of organic vapours and their mixtures. Cawood and Patterson (1932) modified the Boyle apparatus, using a graduated tube projection on a much larger bulb (Figure 2-8), to measure non ideality at high pressures. Baxendale et al. (1951) constructed a simple apparatus (Figure 2-9) to calculate the gas imperfection coefficient α, given by the equation

$$v = RT/p + \alpha \qquad (2.8a)$$

where α is function of pressure given by

$$\alpha = \beta + \gamma p \qquad (2.8b)$$

and β and γ are second and third virial coefficients. The sample gas was compressed through a series of predetermined and accurately known volumes. This process required only the volume ratios rather than the exact volume.

Andon et al. (1957) adopted this method to calculate the second virial coefficients assuming that

$$\alpha = \beta \qquad (2.9)$$

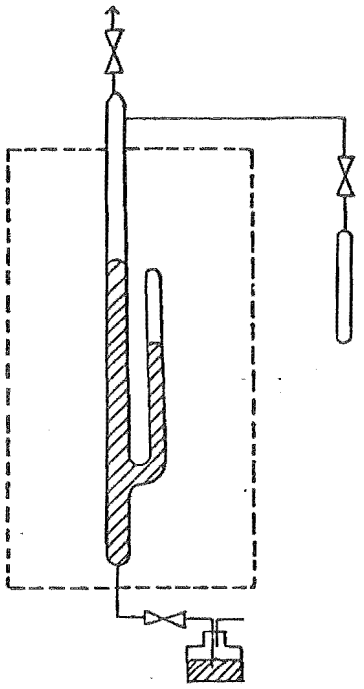

FIGURE 2-7
BOYLES APPARATUS (Alexander & Lambert, 1941)

FIGURE 2-8

HIGH PRESSURE BOYLE'S LAW APPARATUS

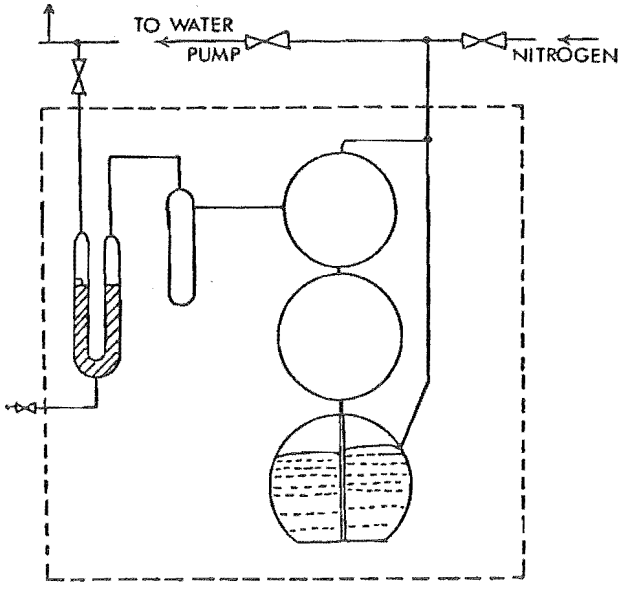

FIGURE 2-9

FIXED VOLUME BOYLE'S APPARATUS
(Baxendale et al., 1951)

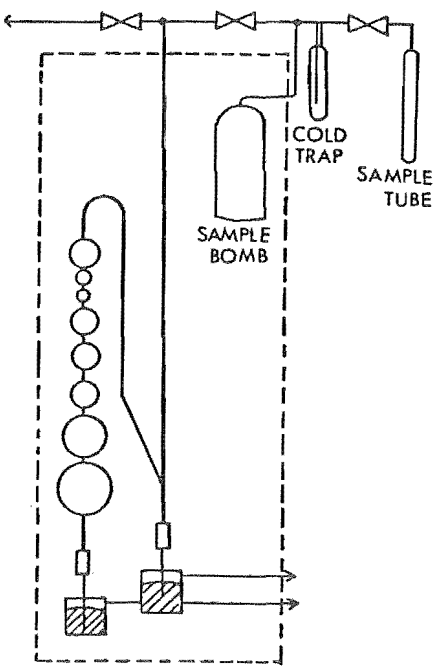

FIGURE 2-10
VARIABLE VOLUME PIEZOMETER

Cox and Andon (1958) devised their measurement technique to avoid adsorption errors (see Section 3-5).

Knoebel and Edmister (1968) devised a variable volume piezometer (Figure 2-10) constructed of various sized spherical glass bulbs, such that on each compression, the pressure increased by approximately one half the initial pressure. They used it to measure β of pure substances as well as their mixtures.

Hajjar et al. (1969) used an apparatus with four glass bulbs interconnected by smaller tubes (Figure 2-11), the volume of each bulb and that of capillary tip being previously calibrated with respect to reference lines. They measured the amount of the sample by confining the pure liquid over mercury in the calibrated tip. They varied the sample and measured the pressure, as it was vaporised and expanded through the various bulbs.

Cottrell and Hamilton (1956) developed an apparatus (Figure 2-12), where a null point detector is used to separate the gas under investigation from the reference gas (nitrogen) in contact with the mercury. The sample is expanded into a series of accurately known volumes and the pressure is determined by using a differential pressure transducer and an external manometer.

The calculation of the second virial coefficients from the Boyle apparatus and its modifications is the same in most cases. From the pressure series virial equation

$$pV = nRT + n\beta p \qquad (2.10)$$

a plot of pV versus p results in a straight line having slope $n\beta$ and the y axis intercept at nRT. From the density series equation

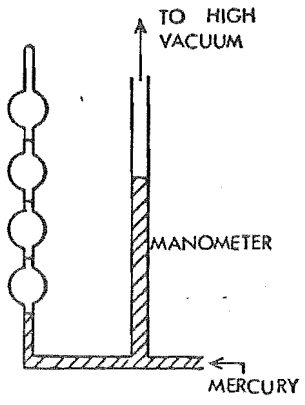

FIGURE 2-11

FIXED-VOLUME BOYLE APPARATUS

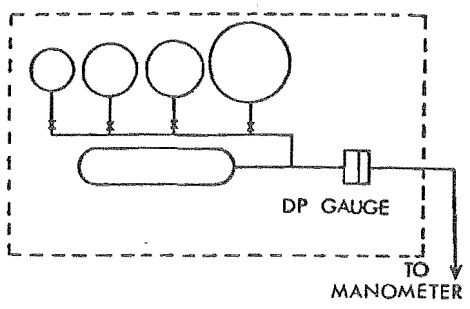

FIGURE 2-12

MERCURY-FREE EXPANSION APPARATUS

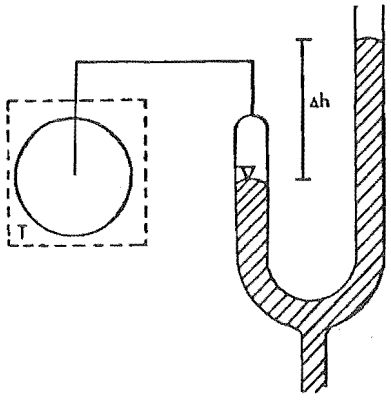

FIGURE 2-13

CONSTANT VOLUME GAS THERMOMETER

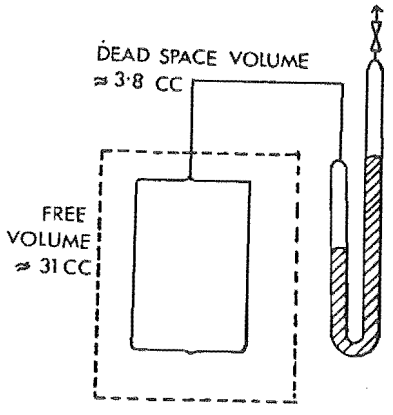

FIGURE 2-14

CONSTANT VOLUME GAS THERMOMETER (Johnston & Weimer, 1934)

$$pV = nRT\ (1 + nB/V) \qquad (2.11)$$

a plot of pV versus 1/V gives a straight line of slope n^2BRT and y-axis intercept at nRT.

2-3.1.3 Gas Thermometer

The constant pressure or constant volume gas thermometer is an experimental arrangement in which the amount of gas and either the volume or pressure are kept constant, while the temperature changes. Mason and Spurling (1969) have reviewed both methods. These methods have not been so commonly used in recent times. However, constant - volume gas thermometers are more common than constant pressure gas thermometers.

The constant volume gas thermometer (Figure 2-13) has certain limitations, as varying the temperature, varies the density, because of "dead space" in the manometer and connecting capillary which are not held at the same temperature as the "constant" volume. Giauque et al. (1927) used a graphical method to apply corrections for the amount of gas in that section of the capillary within the temperature gradient. Johnston and Weimer (1934) made the thermometer bulb (Figure 2-14) especially large in order to diminish the importance of the "dead space" correction. Still they made the usual correction for the portion of the gas present in the "dead space", with the several regions at their appropriate temperatures treated separately.

The manometer may be maintained at the same temperature, limiting the range of the temperature for performing the experiment.

This problem can be overcome by using a null indicator kept at the same temperature as the sample gas and an external manometer with nitrogen to balance the nulling pressure.

Most of the gas thermometer arrangements involve three main experimental difficulties, especially at low temperatures. These are uncertainty of pressure determination, inability to keep temperature constant for the time necessary to reach equilibrium and uncertainty in the determination of the quantity of gas contained in the "dead space". Kistemaker and Keesom (1946) suggested a double constant volume apparatus (Figure 2-15) loaded to different gas densities (ρ_1 and ρ_2) and surrounded by a single copper mantle, ensuring both volumes at the same temperature. They overcame the experimental difficulties when measuring isotherms at the low temperatures by using a X-ray shadowgraph method which read the manometers quickly and accurately. The "dead space" problem was reduced by making such volumes as small as possible. Two points on the pv isotherm measured simultaneously at low pressure, enabled a second virial coefficient to be determined, using the equation

$$(pv)_1 - (pv)_2 = RTB(\rho_1 - \rho_2) \qquad (2.12)$$

Keller (1955) avoided the "dead space" difficulties by measuring the gas in these volumes after the completion of the experiment. He fitted his results with the density series equation

$$pV/nRT = 1 + (n/V)B + (n/V)^2C \qquad (2.13)$$

Khodeeva et al. (1966) constructed an apparatus (Figure 2-16) similar to a constant volume gas thermometer. They used mercury as pressure transmitting and isolating fluid to separate the sample from

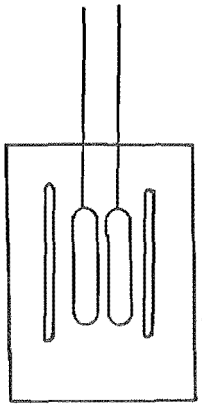

FIGURE 2-15

LOW TEMPERATURE CONSTANT-VOLUME APPARATUS

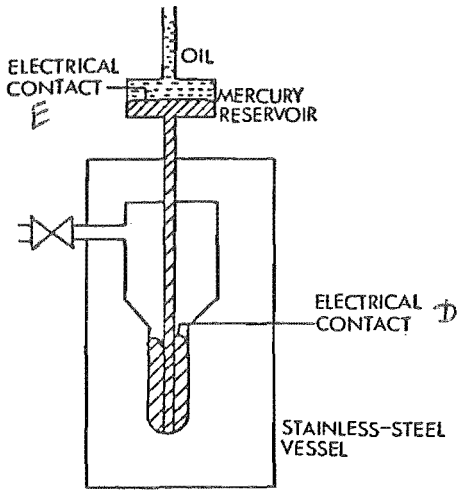

FIGURE 2-16

CONSTANT VOLUME GAS THERMOMETER (Khodeeva et al, 1966)

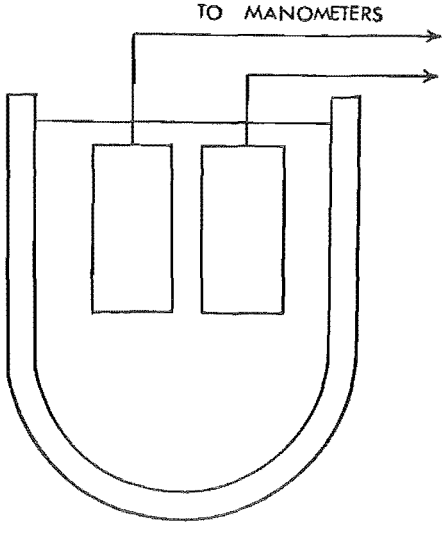

FIGURE 2-17

DIFFERENTIAL PRESSURE APPARATUS

piston gauge. An electric contact D monitors mercury level in the vessel and another contact E measures the position of mercury - oil interface. Bottomley and Nairn (1977) used a constant volume gas thermometer technique at sub atmospheric pressures to provide second virial coefficients at 300-500 K.

2-3.1.4 Differential Methods

Low pressure experiments may be performed using a method in which the sample gas behaviour is compared with that of a reference gas whose equation of state is well known in the pressure and temperature range of the experiment. These methods are of five kinds :

1). differential pressure methods involving the experimental arrangement, in which at constant volume, the difference in the pressure is measured after the same change in the temperature for each gas;

2). differential volume method (Section 2-3.1.5) involving the measurement of small change in volumes necessary to restore exact pressure equality after the two gases (initially at the same pressure and volume) have been subjected to the same change in temperature;

3). differential compression method (Section 2-3.1.6) involving the measurement of pressure difference, when the two gases are confined to nearly identical volumes at constant temperature;

4). differential expansion method (Section 2-3.1.7) involving the difference between the volume expansion at constant pressure, when the two gases initially at the same pressure are expanded;

5). comparative gas density balance method (Section 2-3.1.8)

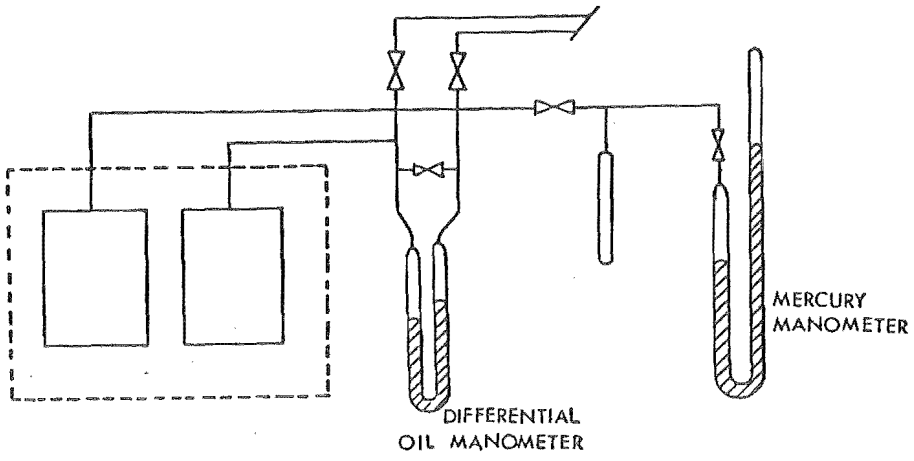

FIGURE 2-18

DOUBLE CONSTANT VOLUME GAS THERMOMETER
(Varekamp & Beenakker, 1959)

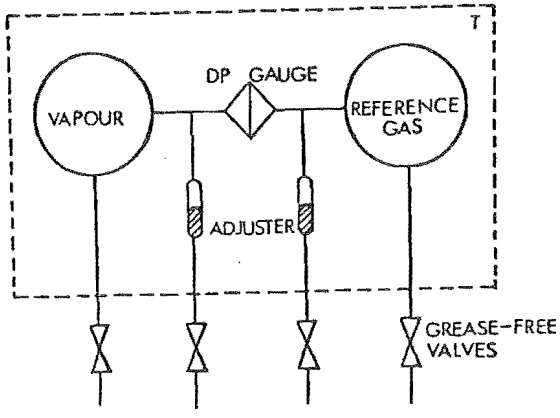

FIGURE 2-19

DIFFERENTIAL VOLUME APPARATUS

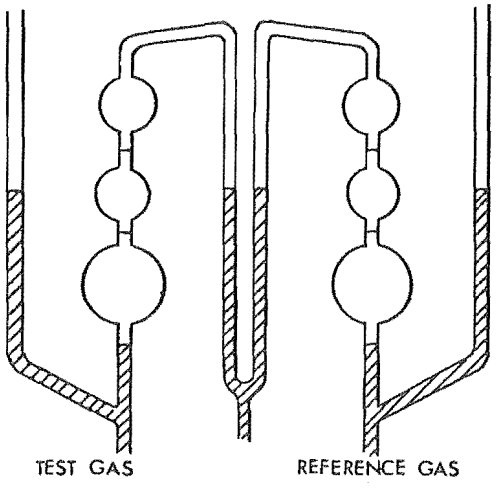

FIGURE 2-20

DIFFERENTIAL COMPRESSION
APPARATUS

involving the measurement of pressure of each gas at the point where they have equal densities at constant temperature.

Differential Pressure Method

Long and Gulbransen (1936) modified the single constant volume gas thermometer (Figure 2-14) of Johnston and Weimer (1934) into a "double" constant volume gas thermometer (Figure 2-17) with independent absolute manometers. The method consisted of a direct comparison of the properties of the gas in question with the known p-v-T behaviour of helium. Varekamp and Beenakker (1959) further developed this method (Figure 2-18), using only one absolute manometer instead of two. They used a differential manometer instead of the second absolute manometer. Both bulbs are filled with reference gas and an unknown gas at the same pressure and temperature. The apparatus is then heated by 1 K and the resulting pressure difference read from the differential manometer. The pressure difference may directly be related to the change in the second virial coefficient as a function of temperature. The data are treated by using the following equation of state.

$$p = Ad(1 + Bd) \qquad (2.14)$$

where p is the pressure in the normal atmospheres

A is the ratio of the absolute temperature and 273.15 K

B is the second virial coefficient and

d is the density expressed in Amagat units.

The values of the different quantities for the gas in the reservoir 1 and 2 may be denoted with the indices 1 and 2 and the values at the initial and final temperatures may be indicated by i and

f respectively . An expression of $p_1^i p_2^f / p_2^i p_1^f$ can be simplified (neglecting any higher order terms in B) to the expression

$$\Delta p/p_1^f = (B_2^f - B_2^i)d_2 - (B_1^f - B_1^i)d_1 \qquad (2.15)$$

where the gas 1 is the reference gas and Δp is equal to $p_2 - p_1$.

2-3.1.5 Differential Volume Method

Bottomley (1960) proposed a method (Figure 2-19) in which the specimen vapour and the reference gas are confined at equal pressure and temperature on two sides of a null manometer. A substantial change in the temperature unequally changes the pressure of the two gases. The small change in volume required to restore exact pressure equality is simply related to the change in second virial coefficient of the vapour.

When the expansion is in the pressure series, the relation is

$$\beta_1 - \beta_2 = \Delta V/n \qquad (2.16)$$

When the expansion is in the volume series (Bottomley and Spurling, 1964), then

$$B_1 - B_2 = \frac{V_1}{n}\left(\frac{p_1V_1}{nRT_1} - 1\right) - \frac{V_2}{n}\left(\frac{p_2V_2}{nRT_2} - 1\right) \qquad (2.17)$$

p_1/RT_1 and p_2/RT_2 in equation (2.17) can be replaced by

$$n/V_1 + (n/V_1)^2B_1 \quad \text{and} \quad n/V_2 + (n/V_2)^2B_2 \qquad (2.18)$$

Bottomley and Spurling (1964) used this method to determine the second

virial coefficient of n-butane.

2-3.1.6 Differential Compression

Hamann and Pearse (1952) devised a differential method (Figure 2.20) to measure small differences of pressure when a gas under investigaion and a reference gas are confined to nearly identical volumes in accurately calibrated burettes connected to opposite sides of a differential manometer. The differential pressure is noted for compression of both gases to equal volumes at the same temperature.

McGlashan and Potter (1962) used a similar type of apparatus (Figure 2-20), stressing the fact that only volume ratios rather than the volumes need to be known accurately. These apparatus suffer from the limits of the temperature range placed on it by the use of mercury for the compression. From two successive compressions (A and B) of gas initially occupying all three bulbs to where they occupy only one bulb, two second virial coefficients (B'_{12} and B'_{13}) can be calculated. The final value of the second virial coefficient is obtained by averaging

$$B = (B'_{12} + 2B'_{13})/3 \qquad (2.19)$$

The uncertainty in the determination of B'_{12} is twice that in B'_{13}. Vilcu and Birhala (1975) used the same method to find second virial coefficients of benzene, hexane and methyl chloride. To minimise the error due to vapour adsorption on glass, they washed the piezometer feed lines with vapours two to three times, prior to feeding the vapour into the burette. Feng and Melzer (1972) described an undergraduate apparatus similar to that of McGlashan and Potter (1962) for

determining the second virial coefficients of vapours.

2-3.1.7 Differential Expansion

The experimental arrangement for this method (Figure 2-21) consists of two volumes in intimate thermal contact, two gas pipettes and a differential manometer connected across the lines going to two volumes. Two volumes are filled with the reference gas and the unknown gas at exactly the same pressures. The two gases are expanded to constant pressure by the removal of weighed amounts of mercury. The difference in the weight between removed quantities of mercury gives the difference between the volume expansions of the two gases (Bottomley et al., 1950). Bottomley et al. (1958a) expressed this difference in volumes expension at the same pressure, as the volume ratio to calculate the second virial coefficient of benzene using the relation

$$\frac{R_p}{R_o} = \frac{1 + B_{benzene}\,p/RT}{1 + B_{nitrogen}\,p/RT} \qquad (2.20)$$

where R_p = (benzene volume)/(nitrogen volume) at pressure p and

R_o is an intercept when the results R_p and p are fitted by the method of least squares to a line $R_p = R_o + ap$.

Thomaes and Van Steenwinkel (1960) used this technique at low temperature. However, since the mercury volume adjuster was not at these low temperatures for practical reasons, some of each of the reference and sample gases was also at the volume adjuster temperature.

Bottomley et al. (1958a) avoided this problem at the cost of the temperature range being limited by the mercury. Kappalo et al. (1963)

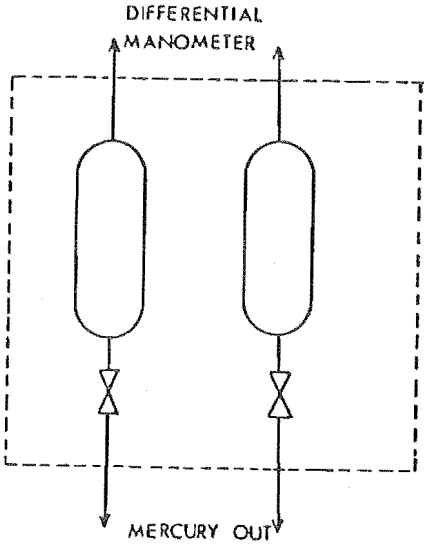

FIGURE 2-21

DIFFERENTIAL EXPANSION METHOD

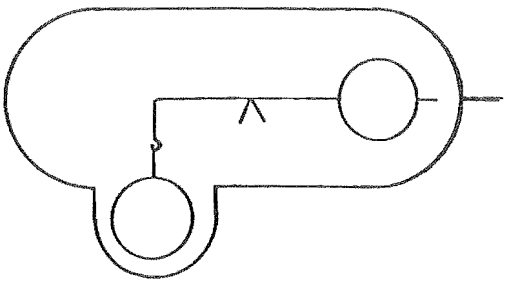

FIGURE 2-22

GAS DENSITY BALANCE

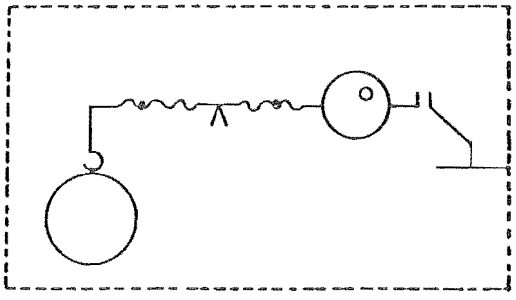

FIGURE 2-23

GAS DENSITY BALANCE
(Casado et al., 1951)

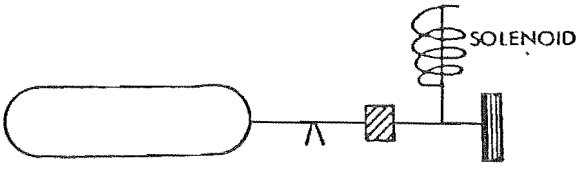

FIGURE 2-24

GAS DENSITY BALANCE
(Hajjar & MacWood, 1970)

avoided the weighing of large amount of mercury by expanding the two gases by approximately equal and pre-determined amounts and attaining pressure equality by small volume adjustments.

2-3.1.8 Comparative Gas Density Balance

Edwards (1917) developed the gas density balance (Figure 2-22) for determination of gas densities and hence molecular weights. Whytlaw-Gray et al. (1931), Casado et al. (1951), Hajjar and MacWood (1968) and Wallace et al. (1964) used modifications of this method to determine the second virial coefficients. The gas density microbalance arrangement consists of a buoyancy bulb suspended at one end of a balance beam, the whole being enclosed in gas tight chamber. The pressure of two gases, reference and gas under investigation, are measured at which they have equal densities as shown by balance of the buoyancy bulb. The truncated pressure series virial equation written in terms of molecular weight of the gas, M and the density, ρ, is then used in the form

$$Mp/\rho = RT + \beta p \qquad (2.21)$$

Explicit equations in the density of each gas may be equated which give a value of the unknown virial coefficient as follows

$$\beta_2 = \frac{RT}{p_2}\left[\frac{M_2 p_2}{M_1 p_1}\left(1 + \frac{\beta_1 p_1}{RT}\right) - 1\right] \qquad (2.22)$$

The subscripts 1 and 2 refer to reference and the sample gases respectively.

Edwards (1917) used pairs of adjustable counter weights to balance the buoyancy globe. Casado et al. (1951) had a series of hemispherical depressions on the either side of central fibre suspensions (Figure 2-23) having two steel balls placed in the each arm of the beam, to balance the float at the zero point for a series of different densities. The beam carried at one end, a suspended buoyancy bulb, which was balanced by a smaller bulb with a hole in it, of very nearly the same weight and having the sum of its internal and external surfaces nearly equal to the external surface of the buoyancy bulb.

Hajjar and MacWood (1970) mounted vertically on the beam, a permanent magnet (Figure 2-24), which could swing freely in the annular space of the solenoid mounted inside the balance. A constant current, 60 ma maximum, when passed through the solenoid, afforded a method of changing the range of the balance without opening it.

Di Zio et al. (1966) used a precision analytical balance (Figure 2-22) to determine second virial coefficients, without reference to the properties of any other materials. They expressed the buoyant mass m by equation

$$m = \rho' M V_E \qquad (2.23)$$

where ρ' is the molar density of the vapour; M is the molecular weight of the vapours and V_E is the effective float volume.

They made a series of buoyant mass determinations at constant temperature and successively lower pressures. For low pressure using equation (2.23), the virial equation of state truncated after the second term can be expressed as

$$\frac{p}{m} = \frac{RT}{MV_E} + B\frac{RT}{(MV_E)^2}m \qquad (2.24)$$

Thus a plot of p/m versus m should yield a straight line. B can then be calculated from the slope, intercept and absolute temperature. Thus, the procedure has the advantage of a single filling of the apparatus and injecting the vapours into the apparatus either as a gas or as a liquid, without even knowing its amount.

2-3.1.9 Other Volumetric Methods

Multiple precise pressure measurement methods are favoured compared to those involving individual measurements of volume and quantity of material. Couldwell et al. (1978) described a technique (Section 3-2), which relied only on a sequence of pressure measurements and which is critically dependent on the exact additivity of the volumes. The method accounted for the effect of third virial coefficients. Ewing and Marsh (1979) described a differential Burnett expansion technique, where only pressure differences are measured. The apparatus consisted of three bulbs. Marsh and Williamson (1981) combined the advantages of two techniques and proposed a five bulb technique, which does not require the absolute pressure to be known accurately. The apparatus (Figure 2-25) consists of two bulbs on the vapour side and three bulbs on the reference side.

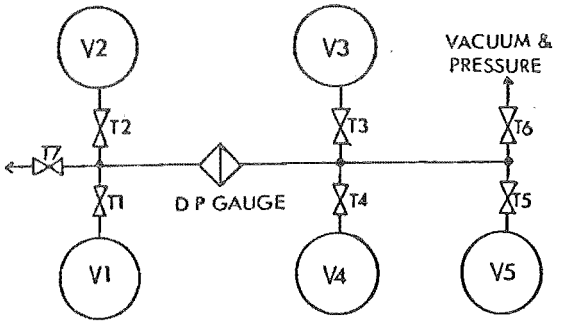

FIGURE 2-25

MULTIPLE PRESSURE MEASUREMENTS METHOD

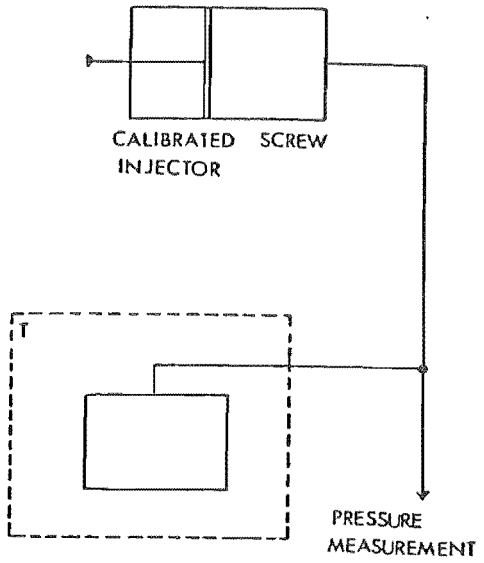

FIGURE 2-26

HIGH PRESSURE P-V-T-n METHOD

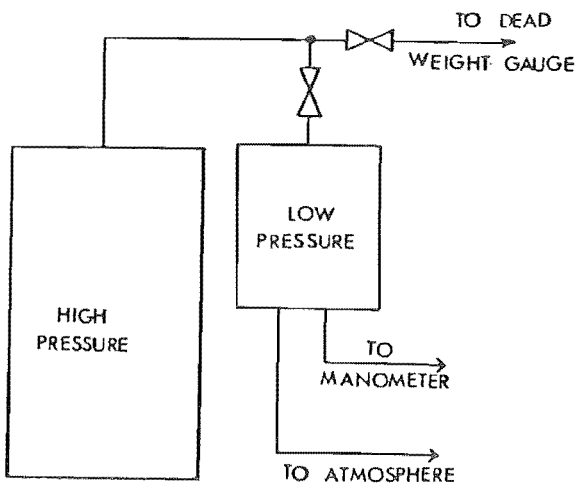

FIGURE 2-27

BEAN APPARATUS

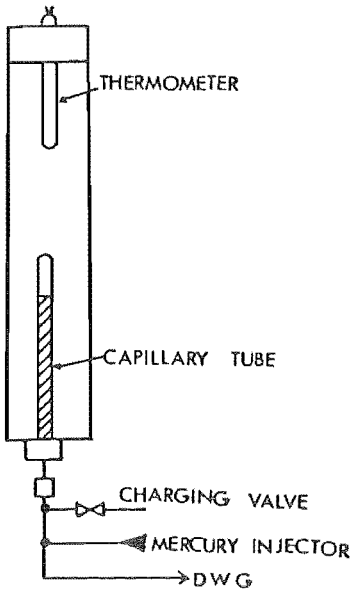

FIGURE 2-28

HIGH PRESSURE BOYLE APPARATUS

2-3.2 High Pressure p-v-T Experimental Methods

Almost all high pressure, p-v-T measurements are of a direct nature rather than of relative type to determine the second virial coefficients.

2-3.2.1 p-V-T-n Method

The direct and simple method to obtain p-V-T-n data is to weigh the gas confined in a piezometer of known volume at measured temperature and pressure (Benedict, 1937). However, this method is not used very frequently at high pressures.

Kell and Whalley (1965) and Kell et al. (1968) described a method of determining the equation of state of a condensable vapour without measuring its volume independently, and without knowing the thermodynamic temperature accurately. Kell and Whalley (1965) constructed a high-temperature high-pressure vessel (Figure 2-26) into which known amounts of liquid can be injected by a calibrated screw injector. Observations for pressures and corresponding masses can be noted for subsequent additions to measure compressibilities of vapours. Kell et al. (1968) reported several advantages of the methods. It did not necessarily require the volume of the high temperature vessel being stable for long periods except during the measurement of one isotherm. Only a small volume of the experimental fluid is contained in a narrow bore tube used in the region of temperature gradient between the thermostat and room temperature. The method did not require the sample to be very

pure as the non-ideality is composition dependent and has only a second order effect. It needed only the temperature being known accurately on the thermodynamic scale.

Hou and Martin (1959) studied the p-v-T properties of trifluoromethane using a steel isometric bomb, of calibrated volume. They obtained a series of pressure and temperature measurements for one charging of a known amount of trifluoromethane. On the completion of the run, they recovered the sample and weighed it as a check on the initial determination.

Lentz (1969) used a high pressure cylinder built of austenitic steel provided with a sapphire window and an O-ring sealed moving piston which allows the volume to vary. The position of the piston and hence the volume, can be accurately determined, by reading the ruler through the sapphire window. On working at high temperature, they found it convenient to increase the temperature and let the pressure increase at constant volume. Gehrig and Lentz (1977) used the same apparatus to study p-v-T behaviour for benzene in the range of 5 to 300 MPa, and 323 to 683 K. At constant filling, they reduced the volume in order to get isochores.

David and Hamann (1953), Abraham and Bennet (1960) and Straty and Prydz (1970) performed fixed volume experiments in conjunction with normal volume determination to obtain the quantity of the gas used. They first confined the unknown quantity of gas at a measured pressure in a high pressure cell of a fixed, known volume, immersed in a temperature regulated bath. Then they determined the quantity of gas in the cell by expanding the high-pressure gas to a measured pressure near one atmosphere in a large known volume of evacuated glassware immersed in a constant temperature bath. The procedure needs correction to be made for sample gas contained in the dead spaces of both the high-

pressure cell and normal volume apparatus. White et al. (1960) introduced a valve which allowed isolation of the dead space volume from the test volume. Thus at the end of the pressure and temperature measurement, they isolated the test volume by closing the valve and pumped away the gas. Then they expanded the sample in the pressure vessel to low pressure to determine the amount of gas.

Michels et al. (1952) used the same method to measure the second virial coefficients of helium, at low temperature for pressures up to 1000 atmospheres. They found the use of mercury to be unacceptable to ensure constant volume during the measurement and separate the gas from the oil of a free piston gauge at low temperature. They used a null-pressure indicating diaphragm differential pressure indicator to seperate the gas from the oil.

Solbrig and Ellington (1963) used the method (Figure 2-27) developed by Bean (1930). High-pressure vessel of known volume is charged with a known mass of gas to a high density. Then isometric data is obtained for this density at increasing temperatures to the highest temperature desired or the limiting pressure of the equipment. Then some of the gas is bled out of the vessel into low-pressure vessel, the amount bled determined and the data procedure is repeated for next isometric. The sequence is repeated to the lowest density convenient. The amount of the gas in the high-pressure vessel for last isometric is determined.

The sum of successive masses bled out of vessel is checked against the mass originally charged to determine whether all steps of procedure were executed carefully.

2-3.2.2 Boyle Type Compressions

The simplest free compression type of apparatus (Figure 2-28) consists of a high pressure capillary tube in which the sample is confined under high pressure over mercury. The volume of the sample can be measured visually with a cathetometer (Gornowski et al., 1947; Connolly and Kandalic, 1960; Singh and Kudchadker, 1979) or by a resistance wire placed along the axis of the tube (Walters and Smith, 1952). Similar techniques have been used by others (Cherney et al., 1949; Couch et al. 1961; Day and Felsing, 1952). They used a calibrated mercury injector and determined the volume of the gas by measuring the amount of mercury that is used to compress the gas. The method can be used at up to 500 atmospheres (Mason and Spurling, 1969). Douslin et al. (1969) pushed this method to its limit of precision.

Michels et al. (1935) and Schamp et al. (1958) used the fixed volumes compression apparatus (Figure 2-29), which consists essentially of an inverted glass burette consisting of a number of calibrated bulbs connected by capillary tubes, into which the sample is compressed. The burette is placed in a pressure vessel in which the bottom part is filled with mercury and top part ouside the burette with the oil of high-pressure system. Fused platinum contacts in the capillary determine the accurate volumes between two consecutive contacts.

2-3.2.3 Burnett Method

Burnett (1936) devised a multiple expansion method (Figure

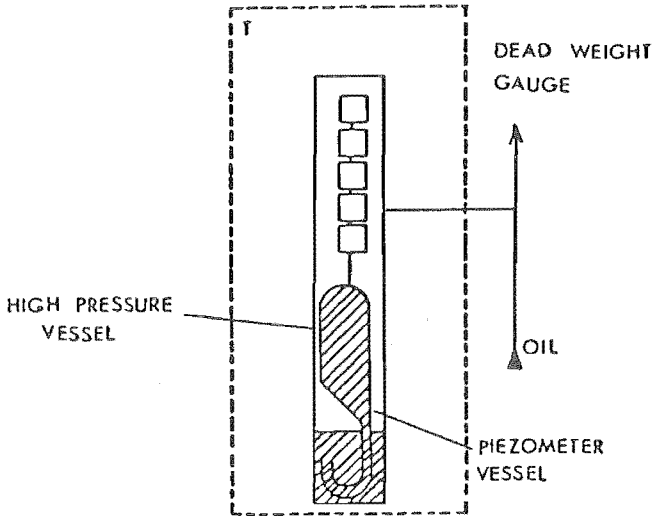

FIGURE 2-29

FIXED VOLUME HIGH PRESSURE BOYLE APPARATUS

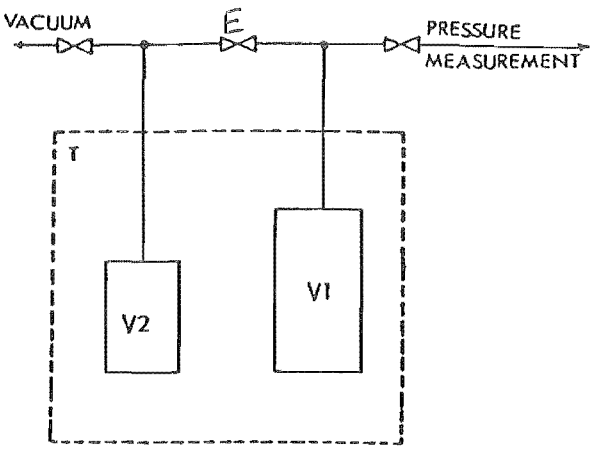

FIGURE 2-30

BURNETT APPARATUS

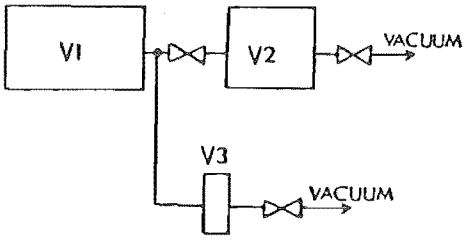

FIGURE 2-31

THREE CHAMBERS BURNETT APPARATUS

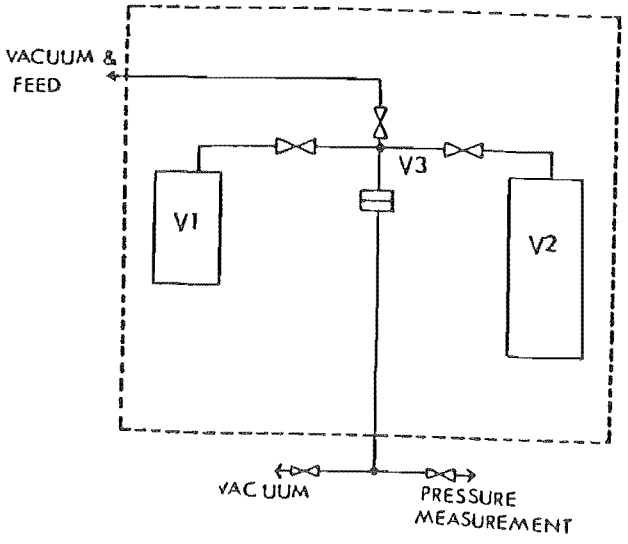

FIGURE 2-32

MODIFIED BURNETT APPARATUS

2-30) that eliminates all volume and mass measurements and involves experimental observations of pressure and temperature only. Initially the pressure of an unknown quantity of gas, confined at fairly high pressure in V_1, is measured. The gas is expanded into V_2 through expansion valve E and the pressure is again measured after thermal equilibrium is achieved. Valve E is then closed again and V_2 is evacuated. This process is continued until the pressure is sufficiently low. The apparatus, being mercury free, can be used to relatively high temperatures.

Burnett (1936) and Silberberg et al. (1959) discussed the calculation procedure. The compressibility factor

$$z = pV/nRT = 1 + \beta p + \gamma p^2 + \ldots \qquad (2.25)$$

is used as a measure of deviation from ideality. The number of moles before and after the xth expansion may be expressed using the equation (2.25)

$$n_{x-1} = \frac{p_{x-1} V_1}{z_{x-1} RT} \qquad (2.26a)$$

$$n_x = \frac{p_x (V_1 + V_2)}{z_x RT} \qquad (2.26b)$$

and since n_{x-1} equals n_x then

$$\frac{p_{x-1}}{p_x} = \frac{V_1 + V_2}{V_1} \cdot \frac{z_{x-1}}{z_x} \qquad (2.27a)$$

where the ratio $(V_1 + V_2)/V_1$ is expressed as the Burnett apparatus

constant, N. Hence equation (2.27a) becomes

$$\frac{p_{x-1}}{p_x} = N\frac{z_{x-1}}{z_x} \qquad (2.27b)$$

There is strong experimental and theoretical evidence to support the assertion that $\lim_{p->0} z=1$ (Silberberg et al., 1959). This limit applied to equation (2.27b) leads to the relations

$$\underset{p_x->0}{\text{Limit}} \frac{p_{x-1}}{p_x} = \underset{p_{x-1}->0}{\text{Limit}} \frac{p_{x-1}}{p_x} = N \qquad (2.28a)$$

$$\underset{p_x->0}{\text{Limit}} \frac{p_x}{p_{x-1}} = \underset{p_{x-1}->0}{\text{Limit}} \frac{p_x}{p_{x-1}} = \frac{1}{N} \qquad (2.28b)$$

If the compressibility factor isotherm is linear with pressure, both p_{x-1}/p_x versus p_{x-1} and p_x/p_{x-1} versus p_x will give linear graphs, considerably facilitating an accurate extrapolation and the value of the apparatus constant.

Silberberg et al. (1959) considered a special case, when the isothermal variation of the compressibility factor with the pressure may be considered to be linear.

$$z = 1 + \beta p \qquad (2.29a)$$

In such cases equation (2.27b) becomes

$$(p_{x-1})/p_x = N + (N-1)\beta p_{x-1} \qquad (2.29b)$$

The graphical determinations of the apparatus constant, N, is made easily and accurately by using a gas with a linear compressibility factor isotherm (Anderson et al., 1968). Helium is well suited as the

calibrating gas for the Burnett apparatus, because of extensive literature values of z, linearity of z versus p, and low values of the second virial coefficients which test the apparatus sensitivity. Thus the intercept on the ratio axis, of the best straight line through a plot of the pressure ratios observed with these gases versus their corresponding pressures determines N. Having determined the value of N, the second virial coefficient, β, may then be calculated from the slope.

Hall and Canfield (1970) proposed a method for reducing Burnett compressibility data by a nonlinear least-squares analysis. This procedure produced apparatus constants and virial coefficients which are consistent with the data within least mean squares. Wielopolski and Warwony (1978) proposed a fast least-squares method for simultaneous determination of virial coefficients and Burnett constants. The method does not require any estimates of virial coefficients. It needs only a rough estimate of the apparatus constant.

Heichelheim et al. (1962) introduced a third chamber of smaller volume to the apparatus (Figure 2-31) to permit a choice in the percentage by which the density is reduced for any particular expansion.

Silberberg et al.(1967) reported that for an overall accuracy of 0.05% in the compressibility factor, the uncertainity in N must be reduced to only a few parts in 100,000. Anderson et al. (1968) observed an unusual shift in the apparatus constant determined from the zero pressure limit of pressure ratio, during the investigation of acetone at 25°C. The value of N increased with the temperature and was at 150°C only slightly less than the helium value. The isothermal adsorption model of Langmuir correctly predicted the shift in the apparatus constant.

Eubank and Kerns (1973) presented three methods of treatment of physical adsorption errors: alter the apparatus, isochoric coupling with Burnett data and correction of the Burnett data by an adsorption correction. Katayama and co-workers (1980) constructed a Burnett expansion apparatus, which can be also used for the pressure change method (Knobler, 1967) to obtain interaction second virial coefficient of mixtures. Ohgaki et al. (1982) further improved the apparatus for measurements at high temperature of up to 125°C. They coated the cells and connecting valves with gold to reduce the effect of gas adsorption on the walls. Mansoorian et al. (1977) made vapour pressure and p-v-T measurements for ethane using the Burnett isochoric method.

The Burnett method in its basic form has been used by a number of workers (Lee and Edmister, 1970; Prasad and Viswanath, 1980; Prasad and Kudchadker, 1978; Warowny et al., 1978b; Waxman and Hastings, 1971; and Weir et al., 1967).

Kell et al. (1978) measured the second virial coefficient of helium from 0 to 500°C by the two temperature gas expansion method. The gas expansions were made both from the low temperature vessel to high and from the high to the low.

Hall and Eubank (1974) have suggested a variation (Figure 2-32), which they claim offers some significant advantages over the conventional Burnett apparatus, the main one being that of simplicity. The valves and fittings are minimal to reduce the possibility of leaks. The ability to open both sides of the differential pressure cell to vacuum enables a null check after each Burnett expansion.

2-3.3 Other Experimental Methods

One of the major difficulties in the previous direct p-v-T measurements is that of calibrating and measuring the volumes. This can be surmounted by the measurement of some other intrinsic property which depends on gas non-ideality.

2-3.3.1 Joule Thomson Coefficient

Rybolt (1981) discussed a virial treatment of the Joule and Joule-Thomson coefficients. These methods have at least two advantages over piezometric measurements of p-v-T properties. First, the extent of the imperfection can be measured directly, rather than as a small difference between two large quantities. Second, the results are free from errors due to adsorption, especially for vapours containing hydroxyl or other strongly polar groups and for p-v-T measurements at temperatures appreciably below the critical. The isenthalpic coefficient $(\partial T/\partial p)_H = \mu$, is related to isothermal coefficient, $(\partial H/\partial p)_T = \phi$, by the relationship

$$\phi = - \mu C_p \qquad (2.29)$$

Francis et al. (1969) constructed a flow calorimeter, fitted with an adjustable throttle, for the measurement of the pressure and temperature dependence of the enthalpy of vapours. Charnley et al. (1953) and Francis et al. (1969) measured isothermal Joule-Thomson

coefficients by passing the test gas through a throttle valve or porous plug. At a measured initial temperature, the pressure drop is measured for the gas flowing through the throttle at a known flow rate. The gas is heated (or cooled) to attain its original temperature, with the amount of energy required to do this being measured. The isothermal Joule-Thomson coefficient, ϕ, is given by

$$\phi = \frac{H_{(p_2)} - H_{(p_1)}}{p_2 - p_1} \tag{2.30}$$

where the subscripts 1 and 2 refer to the upstream and downstream sides of the throttle. Using the pressure series virial equation of states (equation 1.4) and equation (2.30) and carrying out the integration, Francis et al. (1969) obtained the expression

$$\phi = (\beta - T d\beta/dT) + (\gamma - T d\gamma/dT)(p_1 + p_2)/2 + \ldots \tag{2.31}$$

where β, γ are pressure series virial coefficients. A plot of ϕ versus $(p_1 + p_2)/2$ thus gives the quantity $(\beta - T d\beta/dT)$ and $(\gamma - T d\gamma/dT)$. The zero pressure values of both ϕ and μ are finite, for example, the zero pressure values of ϕ depends only on B. Thus

$$\phi_0 = B - T(dB/dT) \tag{2.32}$$

The major disadvantage of the Joule Thomson coefficient method is that B is not obtained directly but can only be obtained by adopting a particular functional form expressing B in terms of T. For example, the functional form adopted by Wormald (1975) is such that

$$B = \sum_{i=0}^{n} b_i T^{-i} \tag{2.33}$$

where n is the number of terms. Exponent i may be specified. Then

$$B - T(\partial B/\partial T) = b_0 + \sum_{i=1}^{n} b_i (T^{-i} + iT^{-i}) \qquad (2.34)$$

Thus measurement of ϕ at atleast n different temperatures enables estimation of the parameters b_i and B may be obtained.

Pocock and Wormald (1975) constructed a calorimeter with an adjustable throttle to measure the isothermal Joule-Thomson coefficient of nitrogen. They considered in detail the heat leaks in flow calorimeters and developed a method for their analysis. Wormald (1975) encountered the same problem of inconsistency of isothermal Joule-Thomson coefficients of benzene. Al-Bizreh and Wormald (1977, 1978) modified the fixed throttle flow calorimeter to measure isothermal Joule-Thomson coefficients of benzene, cyclohexane, hexane and alkanes and tests indicated the heat leaks to be negligible. Clarke et al. (1979) reported developments in the construction and performance of flow calorimeters for the measurements of isothermal Joule-Thomson coefficients of the condensable vapours at low pressures.

The adiabatic Joule-Thomson coefficient, $(\partial T/\partial p)_H$, is determined by measuring the temperature difference across a throttling device at a constant pressure drop. Three types of throttling devices have been used : valves or orifices, axial-flow porous plugs, and radial flow porous plugs.

The valves or orifices have been abandoned in use in favour of porous plugs (axial or radial flow, Figure 2-33). The major drawback is of heat leaks. Axial flow plugs have less heat leak problem than valves. King and Potter (1962) advocated axial flow porous plugs for ease of fabrication. Burnett (1923) and Sage et al. (1936) used radial flow porous plugs though they have undesirable features of cost and

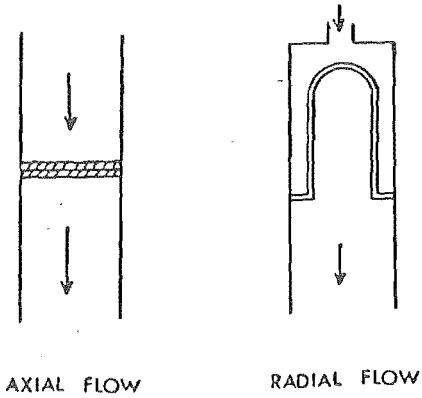

FIGURE 2-33

POROUS PLUGS

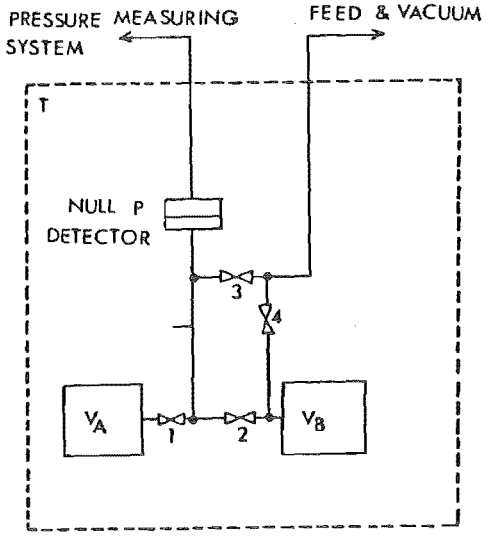

FIGURE 2-34

BURNETT APPARATUS FOR B_{12}

difficulty of fabricating the hollow structure.

Johnston (1946) used a radial porcelain plug having the distinct advantage of the low thermal conductivity of the material and possibility of reducing errors resulting from the heat leaks across the throttle. Stockett and Wenzel (1964) used extensive modification of the valve (Johnston, 1946) in their apparatus.

The adiabatic Joule-Thomson coefficient can also be expressed in terms of the second virial coefficient. Combining equations (2.29) and (2.33) μ is expressed as

$$\mu = - 1/Cp(\beta - Td\beta/dT) \qquad (2.35)$$

2-3.3.2 Sound Velocity

The velocity of sound in a real gas is dependent on both temperature and pressure and these dependencies can be expressed as a virial expansion (Knobler, 1983).

$$C^2(T, p) = y_o RT/M + A_1(T)p + A_2(T)p^2 + \ldots \qquad (2.36)$$

where $y_o(T)$ is the specific heat ratio in the zero pressure limit.

M is the molecular weight and

A_1 and A_2 are acoustic virial coefficients. A_1 is related to the ordinary second virial coefficient by the expression (Grimsrud and Werntz, 1967) for monotonic gas

$$A_1(T) = 2y_o/M \left(B(T) + 2T/3(dB/dT) + 2T^2/15(d^2B/dT^2) \right) \qquad (2.37)$$

The temperature dependence of the second virial coefficient can be represented by the relation

$$B(T) = \alpha + \xi/T \tag{2.38}$$

where α and ξ are constants. Substituting for B(T) in equation (2.37), we obtain

$$A_1(T) = 2y_0/M\ (\alpha + 3\xi/5T) \tag{2.39}$$

Thus by plotting A_1 from the velocity of sound measurements, as a function of T^{-1}, the constants α and ξ, and hence the second virial coefficients are determined. Grimsrud and Werntz (1967) and Kessler and Osborne (1980a, b) used this method for the determination of the second virial coefficient of helium for temperatures ranging from 1.28 to 3.816 K.

Knobler (1983) reported a different analysis to represent the second virial coefficient by a general polynomial

$$B(T) = \sum_{j=1}^{k} a_j T^{(5-j)/2} \tag{2.40}$$

which gives

$$A_1(T) = \sum_{j=1}^{k} a_j y_j T^{(5-j)/2} \tag{2.41a}$$

with

$$y_j(T) = (\rho_0/m)[2 + (\rho_0-1)(5-j) + (\rho_0-1)^2(5-j)(3-j)/4\rho_0] \tag{2.41b}$$

The coefficient a_j can be determined by fitting A_1 by least squares. This method of analysis is very sensitive to the polynomial

chosen for B which must represent satisfactorily both the first and second derivatives.

2-3.3.3 Optical and NMR Methods

Ashton and Guggenheim (1956) have discussed a refractive index method involving the measurement of refractive index as a function of gas pressure at constant temperature, to calculate B, using the relation

$$(n^2 - 1/n^2 + 2)RT/p = p^o[1 + (\lambda - B)/V] \qquad (2.42a)$$

where n is the refractive index,

p is the molar polarisation,

λ is the refractivity second virial coefficient as a function of temperature,

B is the density series second virial coefficient, and

p^o is the limiting value of p at zero density

Since λ is the less than the experimental error in B (Mason and Spurling, 1969), the equation (2.42a) may be written as

$$(n^2 - 1/n^2 + 2)RT/p \simeq p^o(1 - B/V) \qquad (2.42b)$$

and hence B may be calculated from measurements of the refractive index and pressure. Kerl (1982) proposed scannning wavelength interferometry method for precise investigation of the refractive index of gases and their dependence on wavelength, temperature and pressure.

Lipsicas et al. (1961) used NMR measurement methods to obtain the compressibility of gases, whose nuclei have non-zero spin, over a wide range of pressures and temperatures. This technique uses a

reference gas with known compressibility, at the conditions of the experiment and in the same apparatus to obtain the apparatus constant. The method is useful for obtaining p-v-T data where the speed rather than accuracy is important.

2-3.3.4 Clapeyron Equation and Specific Heat Measurements

The Clapeyron equation can be stated as

$$dp_s/dT = \Delta H_v/T\Delta v \qquad (2.43a)$$

where ΔH_v is the enthalpy of vaporisation, p_s is the saturated vapour pressure and Δv is the molar change in volume on vaporisation, represented by

$$\Delta v = v_g - v_l \qquad (2.43b)$$

where v_g and v_l are the molar volumes of the gas and liquid phases respectively. Substituting for v_g from the truncated pressure series virial equation, the Clapeyron equation becomes

$$\beta = \frac{\Delta H_v}{T(dp/dT)_s} + v_l - RT/p \qquad (2.44)$$

Rearranging equation (2.43a), using the volume series virial equation gives

$$RT(1 + B/v_g + C/v_g^2 + \ldots)/p_s = v_l + \frac{\Delta H_v}{T(dp/dT)} \qquad (2.45)$$

Aston et al. (1946) used this equation to determine the second

virial coefficeints of but-1-ene.

Measurements of the vapour heat capacity as a function of the pressure may be made at the same time as heat of vaporisation. Waddington et al. (1947) described an improved constant flow calorimeter to measure heat capacity and heat of vaporisation of the components. Scott et al. (1947) checked their calculations of β from ΔH_v, by measurements of the heat capacity of the vapours, whose variation with the pressure is related to the temperature dependence of the virial coefficient by the equation.

$$\lim_{p \to 0} (\partial Cp/\partial p)_T = - T(d^2B/dT^2) \qquad (2.46)$$

Todd et al. (1978) have improved McCullough and Waddington's (1968) vapour flow calorimeter, to achieve more precise control of conditions and convenience in the operation. Meyer et al. (1980) have used a similar method to measure the second virial coefficients of n-alkyl acetates.

2-3.3.5 Other Indirect Methods

Spertell (1972) investigated on a theoretical level, the possibility of determining the second virial coefficient of a pure component (B_{22}) from gas liquid chromatography. The method developed rests upon the elution of an isotopic form of the carrier gas in extremely small quantity so that infinite dilution is very nearly approached.

Kamenetskii (1973) has obtained an analytical expression, whereby the second virial coefficient of any gas can be determined from

the viscosity. They claim the accuracy of the calculated B(T) to be adequate enough for the determination of compressibilities with an accuracy of 0.3% to 0.5%.

Slawsky et al. (1959) developed a device to observe the behaviour of gases undergoing rapid dynamic processes, either compression or expansions. The data obtained initially from these devices are pressure - density curves.

B. MIXTURES

2-4 Experimental Methods For Measurement of Interaction Second Virial Coefficients

Recently Knobler (1978) has reviewed experimental methods for the determination of the second virial coefficients of the mixtures of gases. The wide variety of experimental methods, described above, to determine the second virial coefficients of pure substances, can also be applied to mixtures. However, the information obtainable on the interaction virial coefficient will be poor due to the accumulation of experimental errors. For a binary mixture expressed by equation (1.9), at equimolar concentration, the interaction virial coefficient is given by

$$B_{12} = 2B_m - (B_{11} + B_{22})/2 \qquad (2.47)$$

If the mixture and pure virial coefficients B are determined to $\pm\delta B$, then the maximum error in B_{12},

$$\delta B_{12} \approx 3\delta B \qquad (2.48)$$

is three times that of the pure component data. The adsorption problem experienced in the determination of B for pure substances can be enhanced in mixtures (Pavlyuchenko, 1970).

There are a few methods that are applicable only to gas mixtures and these will be discussed below.

2-4.1 Measurement of the Excess Volume or Pressure on Mixing

No PVT technique has been devised to determine the interaction virial coefficient directly, because of the dependence of mixture behaviour on the like as well as the unlike interactions (Knobler, 1978). However at low pressure, the change in either volume or pressure on mixing gases at constant pressure or constant volume respectively are directly proportional to ε, defined by equation (1.11).

Edwards and Roseveare (1942) and Gorski and Miller (1953) used the technique to measure the volume change of mixing of gases at constant pressure. Two gases are loaded into separate volumes at equal pressures. After measuring the pressure, the gases are mixed and the volume of the mixing chamber is adjusted to bring the pressure of the mixture back to the initial (pre-mixing) pressure as determined by a differential pressure transducer. The volume change is measured by mercury added or withdrawn from a burette. If we ignore the higher virial coefficient, ε may be expressed as

$$\varepsilon = \Delta v/(2x_1x_2) \qquad (2.49)$$

McElroy (1968) and Ratzsch and Freydank (1971) used the same method to determine the interaction second virial coefficient of binary gas mixtures.

Knobler (1967) modified the apparatus (Knobler et al., 1959) for the determination of interaction second virial coefficient, making use of a pressure transducer. Two pure components are loaded into separate volumes V_1 and V_2 at equal pressures. The loading pressure is then measured and the gas is mixed in V_1 and V_2 using cold finger

(trap) technique. Initially a third isolated volume is filled to the same pressure as the loading pressure, and after mixing, is compared with the mixture pressure directly using a differential pressure transducer. Pasco et al. (1980) observed that measurements involving polar substances are particularly susceptible to error. They observed the effects of adsorption, as one of the sources of the errors. McElroy et al. (1980) and Marsh and Rogers (1983) used the same method and applied an adsorption correction to the measurements of ε.

Bell and Dunlop (1981) and Martin et al. (1982) used a Texas Instrument Co. Quartz spiral gauge (Bell and Dunlop, 1982) to measure Δp, eliminating the need for manometric fluids. Katayama et al. (1980) described an improved apparatus based on the pressure change method (Knobler, 1967) to be also used for the Burnett expansion method. Ohgaki et al. (1982) constructed an apparatus for measurements in the high temperature and high pressure region.

Hall and Eubank (1973) proposed an experimental technique to make direct measurements of interaction second virial coefficent (B_{12}) using a normal Burnett p-v-T apparatus (Figure 2-34) , and mixing of two gases at constant volume, not necessarily being initially at the same pressure. The method requires initial pressure measurements of two components i and j, in volumes V_A and V_B respectively and the final pressure measurement of mixtures of both components mixed in volumes V_A, V_B and V_C. The value B_{12} is then determined from the observed temperature and initial and final pressures, and the pure component compressibility factors (or densities). The pure component second virial coefficients and the mixture composition are not required. They claim that the proposed analysis leads to a smaller uncertainty in B_{12} measurement compared to other previous techniques. Also these measurements are only slightly less accurate than pure component second

virial coefficients measured in the same Burnett apparatus.

Hall and Eubank (1974) also proposed a scheme to measure excess volume and hence the interaction virial ceofficient of mixtures at low density, using a Burnett apparatus. Holste et al. (1980) described the apparatus based on Burnett mixing method (Hall and Eubank, 1973, 1974), to measure the interaction second virial coefficients of mixture of helium and carbon dioxide.

2-4.2 Gas Solubility Method

Addition of an inert gas (1) to a system in which a substance (2) is in equilibrium with its condensed phase, liquid or solid can alter the vapour pressure of the second component (Knobler, 1978). It means, if the total pressure in the system is p and the mole fraction of (2) in the vapour phase is x_2, the partial pressure px_2 is not equal to p_2^0, the vapour pressure of the pure substance. Assuming the condensed phase to be incompressible and that the inert gas is only sparingly soluble in the condensed phase, the alteration in the vapour pressure is attributable to the change in the chemical potential of the vapour, because of interaction between the vapour and the inert gas. Under the conditions $p>>p_2^0$ and $x_2<<x_1$ the interaction second virial equation can be found using the expression

$$RT\ln(px_2/p_2^0) = (V_2^0 - 2B_{12} - B_{11})/p + \ldots \qquad (2.50a)$$

Hence it is possible, from the measurement of x_2 as a function of p, to obtain the value of B_{12}, if the molar volume v_2^0 of the pure condensed phase and the equation of the inert gas are known.

Miller et al. (1972) reported another form, frequently used to

calculate the values of B_{12}. It is expressed as

$$RT\ln(px_2/p_2^0) = v_2^0(p - p_2^0) + B_{22}p_2^0 - 2RT(x_1B_{12} - x_2B_{22})/v_m(x) + RT\ln[pv_m(x)/RT] \quad (2.50b)$$

where $v_m(x)$ is the molar volume of the mixture, obtained by approximations.

Kretschmer and Wiebe (1951) used this method to measure the solubility of propane and butane in ethanol. Najour and King (1966) determined the solubility of Naphthalene in the various gases by spectrophotometrically measuring the vapour concentration of the solid naphthalene at various temperatures and pressures. They used the expression

$$\ln[C_2/C_2^0] = [v_2^S - 2B_{12}(T)]d/\mathcal{V} \quad (2.51)$$

where C_2/C_2^0 is the ratio of the vapour concentrations in the presence and absence respectively, of the compressed gas

d is the relative gas density

$\mathcal{V}$ is the molar volume of the gas (component 1) at the standard temperature and pressure.

$\mathcal{V}_2^S$ is the molar volume of the solid component (2).

D'Avila et al. (1976) have used gas solubility method to measure B_{12} of mixtures of heavy hydrocarbons with nitrogen and methane. Malesinska (1980) has proposed a method for an improved determination of the second cross virial coefficient B_{12} using gas solubility data, and concluded that B_{12} values are not reliable, if data on vapour - liquid equilibria are not thermodynamically consistent.

Ohgaki et al. (1982) have developed a new method for gas solubility measurement for the purpose of obtaining reference value of

vapour-liquid equilibria at high pressures. This method involved only one initial volume calibration of gas-adsorption vessel.

2-4.3 The Chromatographic Method

Laub and Pecsok (1974) have reviewed in great detail, the determination of virial coefficients by gas-liquid chromatography. The method is related to the gas-solubility technique and requires that the carrier gas (inert gas) is insoluble in the stationary phase. Cruickshank et al. (1966) have discussed the analysis of this technique.

Pecsok and Windsor (1968) calculated the interaction second virial coefficients of some hydrocarbon-hydrocarbon gas mixtures from gas liquid chromatography. The discrepency between GLC and static results, especially when using ethane, is attributed to the solubility of carrier gas in the stationary liquid. They made an appropriate correction for this solubility effect and observed that the corrected GLC values were in good agreement with static data.

Knobler (1978) quotes that under the optimal conditions, the values of B_{12} can be determined to ± 2 cm^3 mol^{-1}, but typical uncertainties are about 10 to 20 cm^3 mol^{-1}. Appreciable solubility of the carrier gas in the stationary phase decreases the precision of the measurement.

2-4.4 Flow Calorimetric Measurements

At low density, the enthalpy of mixing, H^E, for a binary

vapour mixture provides information about $d\varepsilon/dT$ via the relation

$$\lim_{p\to 0} (H^E/p) = 2x_1x_2(\varepsilon - Td\varepsilon/dT) \qquad (2.52)$$

However, the analysis requires some functional form to be assumed for the relation between ε and T, so that the values of $H^E/2x_1x_2p$ can be predicted from known values of ε, and can be compared with experimental values. Judd et al. (1980) fitted the known values of ε for the mixture of benzene and cyclohexane, to a function of the form

$$\varepsilon = a + b \exp(c/T) \qquad (2.53)$$

which in turns leads to

$$H^E/2x_1x_2p = a + b(1 + c/T)\exp(c/T) \qquad (2.54)$$

The heat of mixing measurements should enable estimation of the parameters and hence, estimation of ε. This process also, suffers from the disadvantage of not being able to measure ε directly. ε is obtained by adopting a particular functional form expressing ε in terms of T (eg. equation 2.53). But it does provide a more accurate description of the behaviour of ε over a wide range of temperature.

Wormald (1969b) built a flow calorimeter to measure H^E of vapours. Doyle et al. (1981) improved the flow calorimeter and used it to measure H^E for acetone + trichloromethane vapours. Judd et al. (1980) designed and built a non-adiabatic flow calorimeter for low pressure measurement of the enthalpy of mixing of benzene and cyclohexane vapours. They concluded H^E/p measurements to be of most promising use in the low temperature region where adsorption is a problem in the experiments used for dtermining ε. Shannon (1976)

suggested that for a given set of $\Delta H^E/p$ measurements at various temperatures (T_1 and T_n), a two level iterative process can be used to evaluate $d\varepsilon/dT$ at each temperature, provided ε and H^E/p are known at one temperature T_1.

CHAPTER 3

THE METHODS USED IN THIS WORK AND ERROR ANALYSIS

A. PURE COMPONENT

3-1 Introduction

O'Neill and Pandya (Couldwell et al., 1978) built an apparatus to measure the second virial coefficients of pure substances. The latters' results for n-hexane varied from the generally accepted literature values (Dymond and Smith, 1980), sufficiently to warrant further investigation. Couldwell (1975) rebuilt the apparatus, with some improvement such as keeping the central valve arrangement out of contact with oil bath. Unfortunately, the results scattered at 328.15 and 343.15 K, because of the presence of oil traces in the apparatus, due to insufficiently scrupulous cleaning following an accidental breakage.

However, the previous investigation provided the impetus to redesign and rebuild the improved version of the apparatus, enclosed in an air thermostat to avoid oil contact completely.

3-2 The Method

Consider a simple apparatus of two bulbs having equal volumes, up to valves H1 and H2, and with a small bulb connected to the section between H1 and H2 having total volume ΔV and coupled to a pressure transducer and another valve H3 (Figure 3-1).

The condensable gas under investigation is introduced into the volume V_1 and ΔV through H3 and H1, while the second cell is kept evacuated. The pressure of n moles of gas occupying volume V_1, is measured. H1 is closed and the gas occupying volume ΔV is evacuated and the n moles of the gas remaining are transferred completely into the second cell, of volume V_2. Pressure is measured again of the n moles of the gas occupying volumes V_2 and ΔV. Now the gas is allowed to expand to occupy the volume V_1, V_2 and ΔV. After these three pressure measurements, the gas is transferred again to cell 1, for a second loading at reduced pressure. This procedure is repeated for the third and subsequent runs until further reduction of the pressure results in unacceptable errors (Table 3-2).

Three truncated pressure series virial equations can be written for each loading of n moles at constant temperature corresponding to the three volumes

$$p_1V_1 = nRT + n\beta p_1 + n\gamma p_1^2 \qquad (3.1)$$

$$p_2(V_2 + \Delta V) = nRT + n\beta p_2 + n\gamma p_2^2 \qquad (3.2)$$

$$p_3(V_1 + V_2 + \Delta V) = nRT + n\beta p_3 + n\gamma p_3^2 \qquad (3.3)$$

By eliminating V_1 and $(V_2 + \Delta V)$ from equations (3.1 - 3.3), it

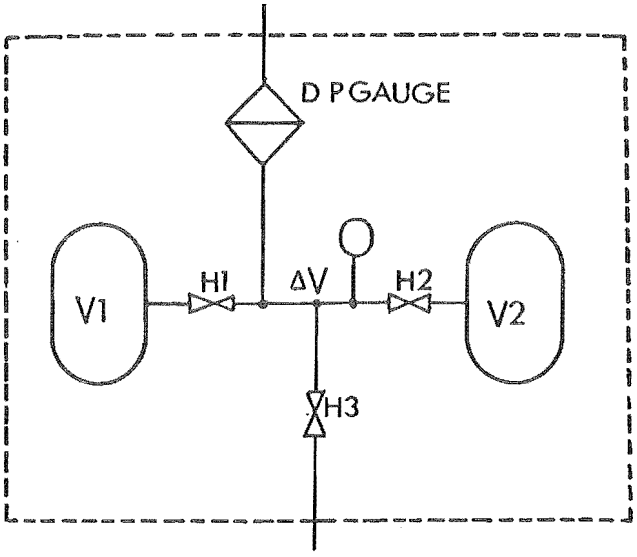

FIGURE 3-1

Basis of Apparatus (This Work)

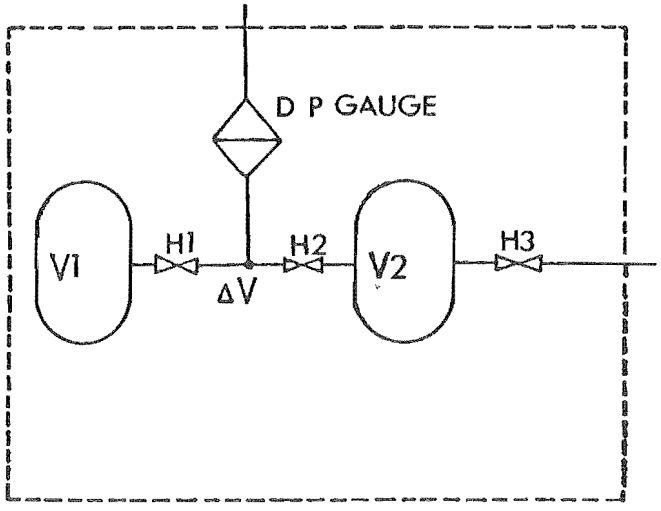

FIGURE 3-2

Simplified Couldwell's (1975) Apparatus

follows that

$$\beta + \gamma(p_1 + p_2 - p_3) = RT(1/p_3 - 1/p_1 - 1/p_2) \qquad (3.4)$$

This can be rewritten as :

$$\beta_{apparent} = \beta + \gamma(p_1 + p_2 - p_3) \qquad (3.5)$$

where $\beta_{apparent} = RT(1/p_3 - 1/p_1 - 1/p_2)$ (3.5b)

and $\beta = \underset{(p_1 + p_2 - p_3) \to 0}{\text{Lt.}} \beta_{apparent}$ (3.6)

Consequently, a plot of $\beta_{apparent}$ versus $(p_1 + p_2 - p_3)$ yields the "true" second virial coefficient β, as the intercept and the third virial coefficient γ as the limiting slope of the plot. If there is non-constancy of temperature, then equation (3.5b) can be rewritten as

$$\beta_{apparent} = R(T_3/p_3 - T_1/p_1 - T_2/p_2) \qquad (3.7)$$

Equation (3.7) can also be expressed in terms of the variation of the temperatures T_2 and T_3 from T_1.

$$\beta_{apparent} = RT_1\left[\frac{(1 + \frac{\Delta T_3}{T_1})}{p_3} - \frac{1}{p_1} - \frac{(1 + \frac{\Delta T_2}{T_1})}{p_2}\right]$$

$$= RT_1\left(\frac{1}{p_3} - \frac{1}{p_1} - \frac{1}{p_2}\right) + RT_1\left(\frac{\Delta T_3}{T_1 p_3} - \frac{\Delta T_2}{T_1 p_2}\right) \qquad (3.8)$$

where $\Delta T_3 = T_3 - T_1$

and $\Delta T_2 = T_2 - T_1$

If the density series virial equation is truncated after the second virial coefficient term, then the three equations applicable to each loading of n moles of the gas in the apparatus are as follows

$$p_1 = \frac{n}{V_1}RT + \left(\frac{n}{V_1}\right)^2 BRT \qquad (3.9)$$

$$p_2 = \left(\frac{n}{V_2 + \Delta V}\right)RT + \left(\frac{n}{V_2 + \Delta V}\right)^2 BRT \qquad (3.10)$$

$$p_3 = \left(\frac{n}{V_1 + V_2 + \Delta V}\right)RT + \left(\frac{n}{V_1 + V_2 + \Delta V}\right)^2 BRT \qquad (3.11)$$

After eliminating V_1 and V_2 from these equations, an iterative process is used, that chooses β as as initial value of B, to satisfy the equations (3.9 - 3.11). The better value of B is chosen until it satisfies all the equations, (appendix A3). As with the pressure series, a value of "true" second virial coefficient can be obtained by plotting these density series virial coefficients against ($p_1 + p_2 - p_3$) and extrapolating to zero pressure.

The test of the accuracy of this method would be its coincident intercepts (Scott and Dunlop, 1962), as the convergence of the pressure or density series virial equation suggests (equation 1.5).

Comparison with Couldwell's analysis

Couldwell's (1975) technique involved the calibration of ΔV (Figure 3-2). He assumed n moles of the condensable vapours occupying volume V_1 and ΔV, instead of volume V_1 as in this work. Three truncated pressure series virial equations, when rearranged gave an equation similar to expression (3.4) which leads to

$$\beta_{apparent} = RT\left(\frac{1}{p_3} - \frac{1}{p_1} - \frac{1}{p_2}\right) + \frac{\Delta V}{n} \qquad (3.12)$$

The current interpretation has the advantage of eliminating the need to determine ΔV.

3-3 Error Analysis

The basic assumptions for evaluation of $\beta_{apparent}$ using equations (3.1 - 3.3) have been that

1. The temperature of the bath is constant for the whole run.
2. The amount of material in the vapour phase is constant for the whole run.
3. volume V_3 is the sum of the volumes V_1 and V_2.

An error analysis involves a check on two types of errors, non-constancy and uncertainties. Non-constancy in the temperature is checked by equation (3.7). The change in the number of moles of the gas during the run may be attributed to the possible adsorption on the glass cell wall or incomplete transfer of the sample from cell 1 to cell 2. Volume V_3 may not be identical to the sum of the volumes V_1 and V_2, because of inconsistency in closing of the valves. There may be error in the physical measurement, for example, of temperature and pressure, because of uncertainties inherent in the thermometer and pressure gauges.

The three pressure series equations truncated at β, relevant to this method are

$$p_1V_1 = n_1RT_1 + n_1\beta p_1 \qquad (3.13)$$

$$p_2V_2 = n_2RT_2 + n_2\beta p_2 \qquad (3.14)$$

$$p_3V_3 = n_3RT_3 + n_3\beta p_3 \qquad (3.15)$$

Dividing equations (3.13 - 3.15) by p_1, p_2 and p_3 respectively and

rearranging them in the form :

$$(n_1+n_2-n_3)\beta = V_1+V_2-V_3 + n_3R\frac{T_3}{p_3} - n_1R\frac{T_1}{p_1} - n_2R\frac{T_2}{p_2} \quad (3.16)$$

If we now write

$$V_3 = V_1 + V_2 \pm \delta V \quad (3.17.i)$$

$$n_2 = n_1 \pm \delta n_2 \quad (3.17.ii)$$

$$n_3 = n_1 \pm \delta n_3 \quad (3.17.iii)$$

$$T_1 = T_1 \pm \delta T_1 \quad (3.17.iv)$$

$$T_2 = T_1 \pm \Delta T_2 \pm \delta T_2 \quad (3.17.v)$$

$$T_3 = T_3 \pm \Delta T_3 \pm \delta T_3 \quad (3.17.vi)$$

$$p_1 = p_1 \pm \delta p_1 \quad (3.17.vii)$$

$$p_2 = p_2 \pm \delta p_2 \quad (3.17.viii)$$

$$p_3 = p_3 \pm \delta p_3 \quad (3.17.ix)$$

so that equations (3.17.i to iii) account for inconsistent error in volume (V_3) and number of moles during p_2 and p_3 measurements, while equations (3.17.iv to ix) account for uncertainties in the physical measurements of temperature and pressure. The non-constancy in the temperature, ΔT_2 and ΔT_3, during p_2 and p_3 measurements can be accounted for in equations (3.7 and 3.8). Here, the analysis assumes the temperature (T), being constant for the whole run, to account for only uncertainty (δT_i) in the temperature measurement. Hence,

$$T_1 = T_2 = T_3 = T \quad (3.17.x)$$

Substituting for V_3, n_2, T_1, T_2, T_3, p_1, p_2, and p_3 in equation (3.16)

gives

$$(n_1 \pm \delta n_2 \pm \delta n_3)\beta \pm \delta V = R\left[\frac{(n_1 \pm \delta n_3)(T \pm \delta T_3)}{p_3 \pm \delta p_3} - \frac{n_1(T \pm \delta T_1)}{p_1 \pm \delta p_1}\right.$$
$$\left. - \frac{(n_1 \pm \delta n_2)(T \pm \delta T_2)}{p_2 \pm \delta p_2}\right] \qquad (3.18)$$

On rearranging equation (3.18) gives

$$\beta\left(1 \pm \frac{\delta n_2 + \delta n_3}{n_1}\right) \pm \frac{\delta V}{n_1} = RT\left[\frac{(1 \pm \frac{\delta n_3}{n_1})(1 \pm \frac{\delta T_3}{T})}{p_3(1 \pm \delta p_3/p_3)}\right.$$
$$\left. - \frac{(1 \pm \frac{\delta T_1}{T})}{p_1(1 \pm \frac{\delta p_1}{p_1})} - \frac{(1 \pm \frac{\delta n_2}{n_1})(1 \pm \frac{\delta T_2}{T})}{p_2(1 \pm \frac{\delta p_2}{p_2})}\right] \qquad (3.19)$$

which can be further rearranged to

$$\beta_{apparent} = RT\left(\frac{1}{p_3} - \frac{1}{p_1} - \frac{1}{p_2}\right) + RT\left[\frac{1}{p_3}\left(\pm\frac{\delta n_3}{n_1} \pm \frac{\delta T_3}{T} \pm \frac{\delta p_3}{p_3}\right)\right.$$
$$\left. - \frac{1}{p_1}\left(\pm\frac{\delta T_1}{T} \pm \frac{\delta p_1}{p_1}\right) - \frac{1}{p_2}\left(\pm\frac{\delta n_2}{n_1} \pm \frac{\delta T_2}{T} \pm \frac{\delta p_2}{p_2}\right)\right] \pm \frac{\delta V}{n_1}$$
$$\pm\left(\frac{\delta n_2 \pm \delta n_3}{n_1}\right)\beta \qquad (3.20)$$

If we now assume that the errors are cumulative, we can write equation (3.20) as

$$\beta_{apparent} = RT\left(\frac{1}{p_3} - \frac{1}{p_1} - \frac{1}{p_2}\right) \pm RT\left(\frac{\delta p_3}{p_3^2} + \frac{\delta p_1}{p_1^2} + \frac{\delta p_2}{p_2^2}\right)$$
$$\pm R\left(\frac{\delta T_3}{p_3} + \frac{\delta T_1}{p_1} + \frac{\delta T_2}{p_2}\right) \pm RT\left(\frac{\delta n_3}{p_3 n_1} + \frac{\delta n_2}{p_2 n_1}\right) \pm \left(\frac{\delta n_2 + \delta n_3}{n_1}\right)\beta$$
$$\pm \delta V/n \qquad (3.21)$$

With the further assumption that

$$[\delta p_3] \approx [\delta p_2] \approx [\delta p_1] \approx [\delta p]$$

$$[\delta T_3] \approx [\delta T_2] \approx [\delta T_1] \approx [\delta T]$$

$$[\delta n_3] \approx [\delta n_2] \approx [\delta n_1] \approx [\delta n]$$

and that

$$p_1 \approx p_2 \approx p \text{ and } p_3 \approx p/2$$

where p is the loading pressure p_1.

We may express the error in terms of the higher pressure (p_1) and the corresponding temperature of bath (T), to obtain

$$\beta_{obs} = \beta_{real} \pm \frac{6RT\delta p}{p^2} \pm \frac{4R\delta T}{p} \pm \frac{3RT\delta n}{pn_1} \pm \frac{2\delta n}{n_1}\beta \pm \frac{\delta V}{n_1} \qquad (3.22)$$

where $\beta_{obs} = \beta_{real} \pm \delta\beta_{max}$

β_{obs} is the value of $\beta_{apparent}$ calculated from the experimentally measured quantities and β_{real} is the error free apparent second virial coefficient. The maximum uncertainty is this

$$\delta\beta_{max} = \pm\left[\frac{6RT\delta p}{p^2} + \frac{4R\delta T}{p} + \frac{3RT\delta n}{pn_1} + \frac{2\delta n}{n_1}\beta_{app.} + \frac{\delta V}{n_1}\right] \qquad (3.23)$$

Quantitative error analysis shows that only the first two terms on the R.H.S. contribute significantly to $\delta\beta_{max}$. Hence the maximum uncertainty is

$$\delta\beta_{max} \approx \pm\left[\frac{6RT\delta p}{p^2} + \frac{4R\delta T}{p}\right] \qquad (3.24)$$

The uncertainty (δp) in the pressure measurement is the sum of the uncertainties in the pressure gauges (Section 3-4).

If for each pressure measurement, n complete sets of Bar_1, Bar_2 and DWG readings were taken, the error in the pressures from

which second virial coefficient is calculated, could be divided by $\sqrt{n}$ (Topping, 1955). Hence probable uncertainty (δq) in the pressure measurement is

$$\delta q = \delta p/\sqrt{n}$$

Since it is most unlikely that each probable error is maximum all the time, the probable error ($\delta\beta_{probable}$) in $\beta_{apparent}$ determination will be assigned by taking the square root of the sum of the squares of main contributing sources.

$$\delta\beta_{probable} = \pm\left[\left(\frac{6RT\delta q}{p^2}\right)^2 + \left(\frac{4R\delta T}{p}\right)^2\right]^{0.5} \qquad (3.25)$$

where δq is the probable uncertainty in the pressure measurement.

3-4 Error Limitation

The error in the analysis of the results arises from two principle sources: instrumental uncertainties and experimental limitations.

Instrumental uncertainties occur mainly in pressure and temperature measurement. Haywood (1977) has discussed in detail, a proposed standard procedure for measuring the repeatability and estimating the accuracy of the measuring instrument. The instrumental uncertainties are differentiated into random and systematic uncertainties to assess the accuracy of an instrument at the time of measurement.

Experimental limitations are in the control of the air

thermostat temperature, transfer of component from one cell to another and closing of "Hoke" valves. The valves need to be closed slowly and uniformly each time, so that the vapour trapped inside the valve volume is a minimum and nearly the same in the quantity, each time. Equation (3.7) takes care of any drift in the thermostat temperature.

3-4.1 Uncertainty in the Pressure Measurement

The two differential pressure transducers used, were commercial model; MKS "Baratron", available from MKS Instruments, Inc. of Burlington, Massachusetts, USA. Baratron 1, Type 170M-25B, had a sensor head model 315BH-10, serial No. 17490, which was installed in the air thermostat. Baratron 2, Type 170M-25C had a sensor head model 315BH-10, serial No. 56832, which was insulated in a cotton wool jacket and installed outside the air bath.

Both Baratrons' digital readout units had a scale from -10 to +10 volts, indicating 0 to 10 mm Hg of differential pressure at the pressure head, i.e. 1 Baratron volt corresponding to 1mm Hg of the differential pressure. The reading -x volts indicated the reference gas pressure at the reference port (Pr_1) of the head, being higher by x mm Hg than the sample pressure at the system port (Ps_1).

3-4.1.1 Baratron 1

The Baratron 1's null and full scale positions were stable within ±0.0001 and ±0.002 volts respectively in a full day. Null and full scale of Baratron 1 were always adjusted just before

measurement.

The stability of Baratron 1 zero was within ±0.002 volts. When both sides of the Baratron were exposed to line pressure between 10.00 mm and 1 atmosphere, the maximum shift noted in the Baraton zero was 30 mV or ±0.0ϕ15 volts. When one atmosphere pressure was exerted on the positive side of Baratron, with vacuum on the reference side, the Baratron zero was displaced in the positive direction by 0.005 volts. This correction is not necessary, as both sides of the Baratron were exposed to pressure or evacuated simultanously within 10.00 mm Hg.

3-4.1.2 Baratron 2

The Baratron 2's null and full scale positions were stable within ±0.0002 and ±0.002 volts respectively. The stability of the Baratron zero was within ±0.001 volts. There was no effect on Baratron zero, of increased line pressure on both sides of the Baratron. One absolute atmospheric pressure exerted on the positive side of the Baratron, displaced the Baratron zero in the positive direction by 0.004 volts. However, Baratron 2 had never more than 10.00 mm Hg absolute pressure on the system side.

Since the final pressure measurement was required in units of one particular instrument, Baratron 1 was calibrated against Baratron 2 within the error of ±0.01 volts. Baratron 2 was then calibrated against the air dead weight gauge within ±0.01 mm Hg.

3-4.1.3 Systematic Baratron Uncertainty

The systematic uncertainty in the Baratron (MKS Baratron, 1975) because of non-linearity , hysteresis and ambient temperature change,according to the manufacturer, is 0.08% of the reading. Since the uncertainty is value dependent, both Baratrons are used up to a maximum differential pressure of 2 mm Hg, corresponding to 2 volts only. Table 3-1 gives the accumulation of the maximum uncertainties in measuring pressure of 10^5 Pa, in the experimental conditions, using Baratron 1 and 2 only upto maximum 2 volts. Assuming that the systematic and Baratron zero uncertainties are included in the calibration of one gauge against the another, the maximum error is considered to be only ±5 Pa.

3-4.1.4 Ruska Dead Weight Gauge

According to Ruska Instrument Corporation, Houston (Ruska Dead Weight Gauge, 1976), accumulation of uncertainties in the pressure measurement is 99 ppm. The systematic uncertainty in the reported value of the area of the piston (model; 2465-778-60, serial No. 23165, Piston; TL-416) is estimated to be 79 ppm. Hence the total uncertainty in the gauge excluding systematic uncertainty is 20 ppm.

Table 3-1 **Maximum uncertainty in measuring 10^5 Pa pressure**

Types of Uncertainties	Reported Uncertainties	Uncertainties ± mmHg	Uncertainties ± Pa
Baratron 1 (in thermostat)			
Baratron zero		0.002	0.3
Systematic uncertainty	0.08 % (a)	0.002	0.3
Uncertainty converting Bar 1 into Bar 2 units		0.010	1.3
Baratron 2 (in Laboratory)			
Baratron zero		0.001	0.1
Systematic uncertainty	0.08 % (a)	0.002	0.3
Uncertainty converting Bar 2 into DWG units		0.010	1.3
Dead Weight Gauge			
linearity uncertainty in DWG measurement	20 ppm (b)	0.015	2.0
Total		0.042	5.6

(a) MKS Baratron (1975) Design Note.

(b) Ruska Dead Weight Gauge (1976) Operating Manual.

3-4.2 Temperature Uncertainty

A "Hewlett Packard" quartz thermometer calibrated against a "Rosemount" Platinum resistance thermometer, was used to measure the temperature of the air thermostat. The uncertainity in the temperature measurement was within ±0.005 K.

3-4.3 Error Due to Change in Content of the System

When transferring a sample from cell 1 to cell 2, during an experimental run, the degree of completion of the transfer could be observed on Baratron 1. The maximum incomplete transfer at the end of the process for benzene and n-hexane corresponded to a pressure of 0.04 Pa which in turn corresponded to δn of about 2×10^{-8} moles at 323.15 K. However for cyclohexane, the maximum incomplete transfer at the end of the process, corresponded to about 10^{-7} moles. This change is quite significant, and it makes the third term in the equation (3.23), quite significant at the low working pressure range corresponding to 3 to 4×10^{4} Pa.

The number of moles could also change because of surface adsorption, but as discussed in Section 3-5, this effect is believed to be small, because of the measurements taken below the pressure range corresponding for p/p° equal to or less than 0.6. However, the analysis, because of surface adsorption as discussed in Section 3-5 gives valuable suggestions for the starting loading pressure. Also the "Hoke" valves may not be closed with the same consistency and may

Table 3-2 **Maximum Error in $\beta_{apparent}$ Measurement**

$px10^{-4}$ (Pa)	(A)= $\frac{6RT\delta p}{p^2}$ ($cm^3\ mol^{-1}$)	(B)= $\frac{4R\delta T}{p}$ ($cm^3\ mol^{-1}$)	$\sqrt{(A^2 + B^2)}$ ($cm^3\ mol^{-1}$)
1	748.0	16.6	748.2
2	187.0	8.3	187.2
3	83.0	5.5	83.2
4	47.0	4.2	47.2
5	30.0	3.3	30.2
6	21.0	2.8	21.2
7	15.0	2.4	15.2
8	12.0	2.1	12.2
9	9.0	1.8	9.2
10	7.0	1.7	7.2

(A) = First term in the equation (3.23)

(B) = Second term in the equation (3.23)

$\sqrt{(A^2 + B^2)}$ = The probable error

cause error in the number of moles and hence pressure measurement. Care is taken to close the "Hoke" valve as slowly as possible to minimise the pressure difference across the valve.

Couldwell (1975) has shown that only the first two terms of the equation (3.23) have a significant contribution to $\delta\beta_{max}$. Hence only two terms have been used to calculate the limits of the error bands. However, Table 3-2 gives the maximum errors assuming that

$R = 8.3144\ Pa\ m^3\ mol^{-1}\ K^{-1}$, $T = 300$ K, $\delta T = 0.005$ K, for a range of pressure varying from 1×10^5 Pa to 1×10^4 Pa. The error δp is considered to be 5 Pa, including uncertainty in the pressure measurement and errors caused by inconsistent closing of the "Hoke" valves. Since most of the pressure measurements readings are observed in at least three complete sets, the probable error is considered to be 3 Pa, and it reduces the error to 0.6 times the maximum error in $\beta_{apparent}$ measurement.

3-5 Effect of Surface Adsorption on the Second Virial Coefficient

Alexander and Lambert (1941) and Lambert et al. (1949) considered the discrepancy between the calculated values using Berthelot equation and the observed values of B, due to adsorption of vapours on the apparatus surface. However, they observed practically no difference in the value of B , when the surface/volume ratio in their apparatus was increased by the addition of glass wool.

Bottomley and Reeves (1957) first discussed the significance of vapour adsorption in relation to determinations of second virial coefficients of vapours. They emphasized the allowance for the adsorption of the vapours on the walls in the unfavourable cases, where B was less than 1000 $cm^3\ mol^{-1}$. They considered the uncertainties in the second virial coefficient could be up to 100 $cm^3\ mol^{-1}$. Bottomley et al. (1958a), and Bottomley and Reeves (1958c) applied the necessary corrections to their results for the second virial coefficients of benzene and n-hexane. Cox and Andon (1958) also considered errors due to adsorption and they minimised this source of error by allowing the vapours to come in contact with all the surfaces of the compression

bulbs before making measurements. Bottomley and Reeves (1957) and Bottomley et al. (1965) have presented some data on the extent of adsorption of organic vapours on "Pyrex" and "Borosilicate" glass surfaces, which may be used in high precision gas-volumetric measurements.

Eubank and Kerns (1973) observed the effects of adsorption in Burnett apparatus calculations as indicated by an apparent shift of the apparatus constant. They suggested careful preparation of an apparatus having reduced scrupulous clean surface area for the sample gas, to reduce the adsorption effects.

When calculating high precision gas volumetric measurements, it is necessary to optimise the working pressure range, keeping in mind, the expected errors of the low pressure measurements (Table 3-2) and the expectation of adsorption of vapours on the glass surface, at higher pressures. Most volumetric measurements have been made in the pressure range of 60 to 70% of the saturation pressure. Bottomley and Reeves (1957) have speculated on a tendency towards greater adsorption in the cases where the measurements have been carried to 70% saturation or more.

In this work, the effect of expanding n moles of gas from volume V_1 or V_2 into volumes $V_1 + V_2$, is to halve the total pressure and double the surface area. Unless the adsorption isotherm is such that halving the pressure, halves the adsorption of number of moles per unit area, a change in the number of adsorped moles will occur and hence affect the measurement of $\beta_{apparent}$. Assuming the change in the number of moles, is only due to surface adsorption, three pressure series virial equations can be written as

$$p_i V_i = n_i RT + n_i \beta \tag{3.26}$$

where $i = 1, 2, 3$ corresponding to three measurements.

n_i = number of the moles in the ith measurement.

For the number of moles to be same at the end of the measurement, n_i should be approximately equal to n_2 and n_3. Assuming,

n_{a_i} = number of the moles adsorbed on to the surface in the ith measurement.

$$n_i = n - n_{a_i}$$

Hence for n_1, n_2 and n_3 to be equal,

$$n_{a^1} = n_{a^2} = n_{a^3} \tag{3.27}$$

To evaluate the effect of surface adsorption, a standard BET isotherm (Brunauer et al., 1938) was used. The BET isotherm can be written as

$$n_a = \frac{N^0 ACp}{(p^\circ - p)[1 + (C-1)(p/p^\circ)]} \tag{3.28}$$

where n_a = number of moles adsorbed onto the surface,

N^0 = number of moles per unit area required to form a monolayer,

A = adsorptive surface area

C = an isotherm parameter, and is estimated for benzene, cyclohexane and n-hexane for adsorption of the vapours on glass surface,

p° = saturation vapour pressure of the gas,

p = working pressure of the gas.

Equation (3.28) can be rearranged to

$$\theta = \frac{Cp/p^{\circ}}{(1 - p/p^{\circ})[1 - p/p^{\circ} + Cp/p^{\circ}]} \qquad (3.29)$$

where θ is the fraction of the surface covered with a monolayer.

Most of the data for surface adsorption of benzene, cyclohexane and n-hexane on pyrex glass, are reported only up to relative pressure p/p° corresponding to 0.34 to 0.4.

In this work, the adsorption isotherm (Cusumano and Low, 1970) is analysed for surface adsorption of benzene on porous glass at 31.5°C. They noted that the amount of benzene adsorbed was almost linear up to p/p° equal to 0.34.

Cusumano and Low (1970) also plotted a graph for apparent surface coverage (θ) for adsorption at 32°C as a function of the relative pressure. Noting the value of θ is 0.2 for p/p° corresponding to 0.34 for monolayer formation, and substituting in equation (3.29), the value of C for benzene is calculated to be 4.2. One square metre surface needs 4×10^{-6} moles of benzene, having cross sectional area of 42 A^2 and lying flat on the surface. Using the above parameters and p° equal to 1360 mm Hg at 373.15 K and assuming that the adsorptive area of each cell (1) or (2) is its geometric area (0.6 m^2), the variation in the number of moles with varying p/p° was investigated using equation (3.28). The results are illustarated in Figure (3-3).

The hypothetical isotherm (Figure 3-3) is justified on comparison with the adsorption isotherm (Figure 3-4) for experimentally observed data (Cusumano and Low, 1970). The benzene adsorbed at the relative pressure equal to approximately 0.34, is six times the benzene adsorbed at relative pressure 0.05 (Figure 3-3)

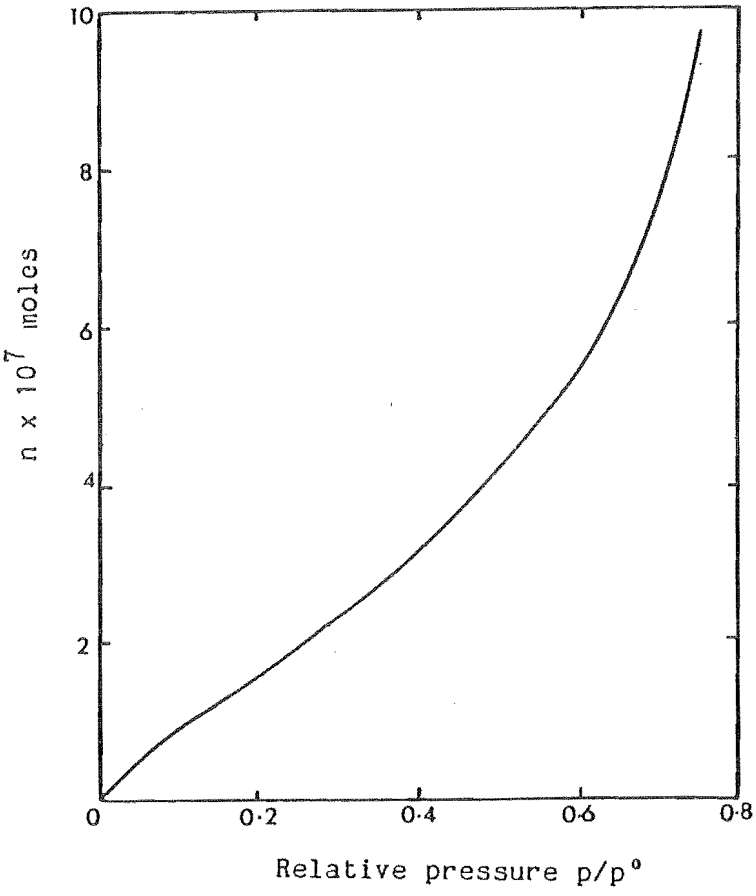

FIGURE 3-3

The Hypotical Adsorption Isotherm for benzene at 373.15 K.

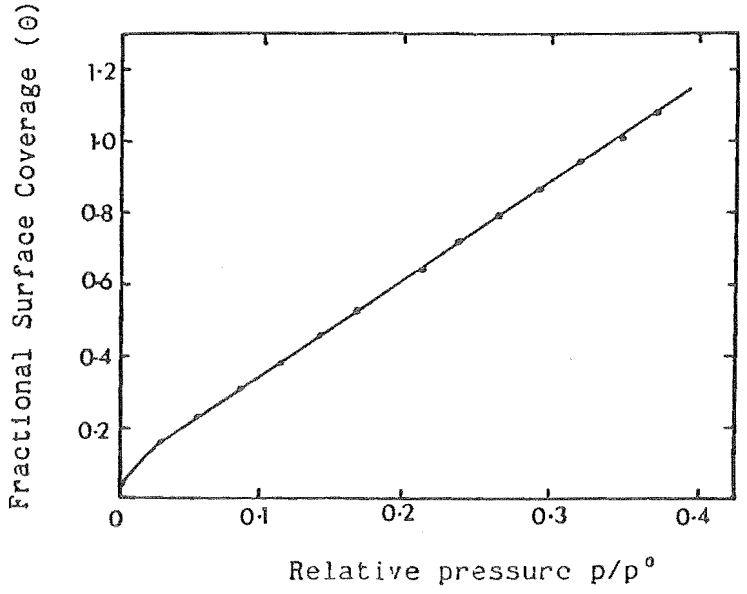

FIGURE 3-4

The Experimental adsorption Isotherm of Benzene, as function of the Relative Pressure

while the experimentally observed benzene adsorbed is five times for the same range (Figure 3-4). It is assumed that

$$p_1 \approx p_2 \approx 2p_3$$

For p_3 measurement, the surface area is approximately doubled, as the vapours are expanded in cell (1) and cell (2). Therefore, the total number of moles adsorbed on to the glass surface is also twice the number of moles for any relative pressure. Table 3-3 shows the number of moles of benzene vapours adsorbed on the glass surface for given initial loading pressure represented as the relative pressure (p/p°). Obviously, there is a possibility of significant change in number of moles caused by the multimolecular layer adsorption at the higher pressures. This may cause a significant error in β measurement equation (3.23) for maximum loading pressure corresponding to relative pressure (p/p°) being greater than 0.7.

Table 3-3 **Relative Pressure and Number of Moles Adsorbed**

p_1/p°	$\frac{\delta n_1 x 10^7}{\text{moles}}$	p_3/p°	$\frac{\delta n_3 x 10^7}{\text{moles}}$
0.8	12.2	0.40	6.2
0.7	7.7	0.35	5.4
0.6	5.5	0.30	4.6
0.5	4.2	0.25	3.9
0.4	3.2	0.20	3.2
0.3	2.3	0.15	2.3
0.2	1.6	0.10	1.6

Considering the case of benzene at 300 K, the saturated vapour pressure p^0 is 11732 Pa. The loading pressure p_1 corresponding to p/p^0 equal to 0.8 is approximately equal to 9385 Pa. Assuming the volume of each cell equal to approximately 1000 cm^3 and R equal to 8.3144 $Pa\,m^3\,mol^{-1}\,K^{-1}$, the number of moles of benzene in the system correspond to $4x10^{-3}$ moles. The third term in equation (3.23) contributes its uncertainty in β measurement equal to 243 $cm^3\ mol^{-1}$. Assuming β is of the order of -1500 $cm^3\ mol^{-1}$, the fourth term corresponds to 1 $cm^3\ mol^{-1}$. Thus there is a significant effect, of adsorption of the vapours on the surface, on the measurent of β.

This suppports the experimental observation (Bottomley et al., 1965) that adsorption effects are significant for acetone at 50°C and 350 mm Hg pressure (62.5% saturation). For an adsorption isotherm like that of benzene on glass, with up to a monolayer for p/p^0 corresponding to 0.34 is linear isotherm, there is negligible effect of adsorption.

In this work, the results for the measurement of the second virial coefficient are unaffected by the surface adsorption, provided the number of moles adsorbed, in the three pressure measurements remain constant (Section 3-2). Table 3-3 shows that the number of moles adsorbed in any of the three measurements is nearly constant, when the maximum loading pressure is less than 60% of saturation vapour pressure and is unaffected by surface adsorption for any of the three pressure measurements close to maximum loading pressure corresponding to p/p^0 equal to 0.4. Several authors (Brunauer et al., 1938; Cusumano et al., 1970) have claimed monolayer adsorption isotherm up to a relative pressure (p/p^0) of 0.34, and that the adsorption isotherm is nearly linear, between p/p^0 of 0.05 and 0.35.

Gawdzik et al. (1976) compared the adsorption isotherms of benzene, n-hexane and cyclohexane on porous glass beads using a gas adsorption chromatography method. They showed that adsorption isotherms for cyclohexane and benzene are comparable, while that for n-hexane is steeper than the former. Boulton et al. (1966) have also compared benzene and cyclohexane adsorption isotherms on silica gel, expecting the benzene isotherm to lie slightly above than that of cyclohexane, in the monolayer region. Thus, similar inferences for the adsorption isotherms of cyclohexane and n-hexane at various temperatures, and the maximum loading pressure being less than 70% of saturation vapour pressure, may be drawn.

B. MIXTURES

3-6 The Experimental Method

This method is based on measurements of the pressure change Δp, on mixing of two pure gases initially at the same pressure and temperature, at constant temperature and volume. Referring to Figure 3-5, two equal sized volumes are filled to equal pressure with two pure gases. Using the pressure series virial equation of state:

$$pV = n_i(RT + \beta_{ii}p + \gamma_{iii}p^2 + \ldots) \tag{3.30}$$

where $i = 1, 2$ refer to component (1) and (2) respectively,

p = the pressure,

V = the volume of each cell,

T = temperature of the bath,

n_i = number of moles of the gas of component i,

β_{ii} = second virial coefficient of the pressure series,

γ_{iii} = third virial coefficient of the pressure series.

Equation (3.30) can be rearranged in terms of V, for i components, added and then divided by $\Sigma_i n_i$ to give

$$2V/\Sigma n_i = RT/p + \Sigma x_i \beta_{ii} + (\Sigma x_i \gamma_{iii})p + \ldots \tag{3.31}$$

Upon mixing the two components and maintaining the bath temperature constant, the pressure series virial equation of state for the mixture can be written as :

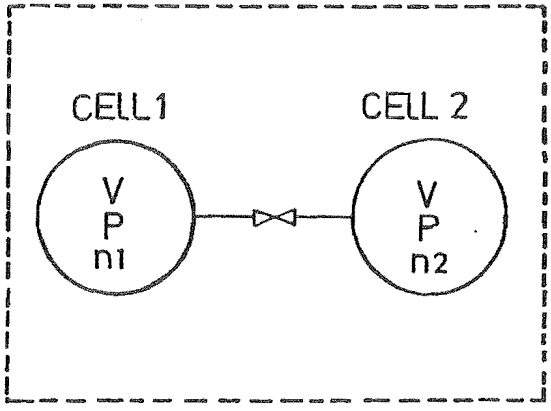

FIGURE 3-5

Simplified Interaction Second Virial Coefficient Method

$$p_m(2V) = \Sigma n_i(RT + \beta_m p_m + \gamma_m p_m^2 + \ldots) \qquad (3.32)$$

where the subscript m stands for the mixture. Rearranging the equation (3.32) gives

$$2V/\Sigma n_i = RT/p_m + \beta_m + \gamma_m p_m + \ldots \qquad (3.33)$$

Comparing equation (3.31) with (3.33), and rearranging it gives

$$\beta_m - \Sigma x_i \beta_{ii} = RT(1/p - 1/p_m) - \gamma_m p_m + (\Sigma x_i \gamma_{iii})p + \ldots \qquad (3.34)$$

The definition of β_m for a binary mixture can be written as in equation (1.14)

$$2x_1x_2\varepsilon = \beta_m - x_1\beta_{11} - x_2\beta_{22} \qquad (3.35)$$

Now if γ_m is defined by equation (1.15) as

$$\gamma_m = x_1\gamma_{111} + x_2\gamma_{222} + 3x_1x_2(x_1\xi_1 + x_2\xi_2) \qquad (1.15)$$

where ξ_1 and ξ_2 are the pressure series excess third virial coefficients and p_m is defined as

$$p_m = p + \Delta p \qquad (3.36)$$

then substituting equations (3.35, 1.15, and 3.36) in equation (3.34) and rearranging gives

$$2x_1x_2\varepsilon = \frac{RT\Delta p}{p^2(1 + \Delta p/p)} - 3x_1x_2(x_1\xi_1 + x_2\xi_2)p$$
$$-3[x_1x_2(x_1\xi_1 + x_2\xi_2) + x_1\gamma_{111} + x_2\gamma_{222}]\Delta p \qquad (3.37)$$

Shannon (1976) has discussed the advantages of this analysis over that developed by Knobler (1967), though the latter has the advantage that the final expression involves the use of the volume series virial coefficient directly.

3-7 Error Analysis

The influence of the third virial coefficient is negligible (Section 3-7.2), for the experiments likely to be carried out at about 2 to 4 x 10^4 Pa. Hence equation (3.37) can be rewritten, with the first term on the right hand side dominant,

$$\varepsilon_{\text{apparent}} \simeq \frac{RT\Delta p}{2x_1x_2p^2(1 + \Delta p/p)} \tag{3.38}$$

for the error analysis. $\varepsilon_{\text{apparent}}$ can be related to "true" or "real" ε by a correction $\delta\varepsilon$.

$$\delta\varepsilon = \varepsilon - \varepsilon_{\text{apparent}} \tag{3.39}$$

Basic assumptions for the evaluation of ε are

1. The temperature of the bath is constant for the whole run.
2. Both components are at the same initial pressure.
3. The total amounts of the each substance in the vapour phase remain constant.
4. The volumes of both cells are the same.

The errors likely to occur, using this technique, can be classified into two categories:

1. errors inherent in the physical measurements, for example: the

temperature, the pressure and the change in the pressure, $\delta\varepsilon'$,

2. errors caused by changes in the unmeasurable extensive properties of the system, for example:

a) Effect of third virial coefficient ($\Delta\varepsilon$)

b) Effect of unequal loading pressure ($\delta\varepsilon_p$)

c) Effect of surface adsorption ($\delta\varepsilon_a$)

Therefore, $\delta\varepsilon$ in equation (3.39) can be mathematically expressed as the summation of errors

$$\delta\varepsilon = \delta\varepsilon' + \Delta\varepsilon + \delta\varepsilon_p + \delta\varepsilon_a \tag{3.40}$$

3-7.1 Estimation of Errors

The measured variables are Δp, p and T. The calculations of x_1 and x_2 depend on p, T and the assumption of the equal mixing volumes.

Using the usual notation for errors, and substituting in equation (3.38) gives

$$(\varepsilon_{apparent} + \delta\varepsilon') =$$

$$\frac{RT\left(1 + \frac{\delta T}{T}\right)\Delta p\left(1 + \frac{\delta\Delta p}{\Delta p}\right)}{2x_1\left(1 + \frac{\delta x_1}{x_1}\right)x_2\left(1 + \frac{\delta x_2}{x_2}\right)\left(p^2\left(1 + \frac{\delta p}{p}\right)^2\left(1 + \frac{\Delta p}{p}\right)\left[1 + \frac{\delta\left(1 + \frac{\Delta p}{p}\right)}{\left(1 + \frac{\Delta p}{p}\right)}\right]\right)} \tag{3.41}$$

where $\delta\varepsilon'$ is the uncertainty in $\varepsilon_{apparent}$, as the result of the uncertainties inherent in the temperature, the pressure and the pressure change on mixing measurements. Retaining only 1st. order

terms in the uncertainties, equation (3.41) becomes

$$\varepsilon_{apparent}\left(1 + \frac{\delta\varepsilon'}{\varepsilon_{apparent}}\right) \approx$$

$$\frac{RT\Delta p}{2x_1x_2(p^2 + p\Delta p)}\left(1 + \frac{\delta T}{T} + \frac{\delta\Delta p}{\Delta p} + \frac{\delta x_1}{x_1} + \frac{\delta x_2}{x_2} + \frac{2\delta p}{p} + \frac{\delta\Delta p}{p}\right) \quad (3.42)$$

Since both Δp and $\delta\Delta p \ll p$, equation (3.42) simplifies to

$$\delta\varepsilon'/\varepsilon_{apparent} \approx \frac{\delta T}{T} + \frac{\delta\Delta p}{\Delta p} + \frac{\delta x_1}{x_1} + \frac{\delta x_2}{x_2} + \frac{2\delta p}{p} \quad (3.43)$$

The term $\delta x/x$ is further dependent on p, T, and the equality of mixing volumes. Shannon (1976) observed that the inequality of the mixing volume is a second order effect and may be ignored. The correction for mole fraction can be expressed as the correction in the number of moles of the components 1 and 2.

$$(x_1 + \delta x_1) = (n_1 + \delta n_1)/(n_1 + n_2 + \delta n_1 + \delta n_2) \quad (3.44)$$

On rearranging, it gives

$$x_1\left(1 + \frac{\delta x_1}{x_1}\right) = \frac{n_1}{n_1 + n_2}\left(1 + \frac{\delta n_1}{n_1} - \frac{\delta n_1}{n_1 + n_2} - \frac{\delta n_2}{n_1 + n_2}\right) \quad (3.45)$$

Though the errors are cumulative, but for the first two terms having δn_1 in equation (3.45), the sign and magnitude has to be the same and there will therefore be some cancellation. Hence

$$\pm\frac{\delta x_1}{x_1} = \pm\frac{\delta n_1}{n_1} \mp \frac{\delta n_1}{n_1 + n_2} \pm \frac{\delta n_2}{n_1 + n_2} \quad (3.46)$$

Since in the experiment

$$n_1 \approx n_2 \approx n/2$$

and $$\delta n_1 \approx \delta n_2 \approx \delta n/2$$

equation (3.46) simplifies as

$$\frac{\delta x_1}{x_1} = \pm \frac{\delta n}{2n} \pm \frac{\delta n}{2n} = \frac{\delta n}{n} \qquad (3.47)$$

Substituting these results in the equation (3.43)

$$\frac{\delta \varepsilon'}{\varepsilon} = \pm \frac{\delta T}{T} \pm \frac{\delta \Delta p}{\Delta p} \pm \frac{2\delta n}{n} \pm \frac{2\delta p}{p} \qquad (3.48)$$

The relative sizes of each term can be illustrated by taking a hypothetical situation. The pressure difference can be read (including zero error) to ±0.01 Pa. The thermostat temperature can be held constant to ±0.02 K and the absolute pressure can be determined to ± 10 Pa. Taking a case where T = 323 K, p = 24080 Pa, Δp = 5.6 Pa, gives a value of ε = 51.9 $cm^3\ mole^{-1}$, using equation (3.38) with $x_1 = x_2 = 0.5$ and substituting these values into the equation (3.48), disregarding the third term, gives

$$\delta\varepsilon' = \pm 51.9\left(\frac{0.02}{323} + \frac{0.1}{5.6} + \frac{2x10}{24080}\right) \quad cm^3\ mol^{-1}$$

$$\delta\varepsilon' = \pm 1.0 \quad cm^3\ mol^{-1}$$

$$\varepsilon = 51.9 \pm 1.0 \quad cm^3\ mol^{-1}$$

The analysis shows that the measurement of the pressure difference contributes the major part of the error in ε. The effect is more pronounced at lower loading pressure. Halving the loading pressure, increases the relative errors in the measurement of pressure (δp) and pressure difference ($\delta\Delta p$), twofold and fourfold respectively.

3-7.2 The Effect of the Third Virial Coefficients

Equation (3.38) needs justification for the omission of the effect of the third virial coefficient. Rearranging equations (3.37) gives

$$\varepsilon = \varepsilon_{apparent} + \Delta\varepsilon$$

$$= \frac{RT\Delta p}{2x_1x_2p^2(1 + \frac{\Delta p}{p})} - \frac{3}{2}p(1 + \frac{\Delta p}{p})(x_1\xi_1 + x_2\xi_2)$$

$$- \frac{3\Delta p}{2x_1x_2}(x_1\gamma_{111} + x_2\gamma_{222}) \qquad (3.49)$$

ξ_1 and ξ_2 are the pressure series excess third virial coefficients. From the definition of $\varepsilon_{apparent}$ in the equation (3.38), $\Delta\varepsilon$ is given by

$$\Delta\varepsilon = -\frac{3}{2}p(1 + \frac{\Delta p}{p})(x_1\xi_1 + x_2\xi_2) - \frac{3p}{2x_1x_2}(x_1\gamma_{111} + x_2\gamma_{222}) \qquad (3.50)$$

Experimental data on the third virial coefficients are rare. However for the purposes of calculating the effect of neglecting third virial coefficient, the latter may be estimated using Chueh and Prausnitz's (1967) corresponding states type correlation.

$$\frac{C}{V_c^2} = (0.232\ T_R^{-0.25} + 0.468\ T_R^{-5})[1 - e^{(1 - 1.89T_R^2)}]$$

$$+ de^{-(2.49 - 2.35T_R + 2.70T_R^2)} \qquad (3.51)$$

where T_R is the reduced temperature (T/T^c)

Knowing the critical properties of the components T^c and V^c,

one can estimate C and hence γ using equation (1.6). Orentilecher and Prausnitz's (1967) approximation,

$$\gamma_{ijk} = (\gamma_{iii}\gamma_{jjj}\gamma_{kkk})^{(1/3)} \qquad (3.52)$$

may be used to calculate γ_{112} and γ_{122}. Using equations (1.12 and 1.13), ξ_1 and ξ_2 can then be evaluated and hence $\Delta\varepsilon$ can be estimated.

Shannon (1976) evaluated the values of ξ_1 and ξ_2, knowing only critical constants T^c and V^c of the pure components, benzene and cyclohexane. Evaluating equation (3.50), using estimated values of ξ_1, ξ_2, γ_{111} and γ_{222} gives

$$\Delta\varepsilon = 1.5 \times 10^{-5} p + 7.1 \times 10^{-3} \quad \text{cm}^3\ \text{mol}^{-1} \qquad (3.53)$$

This shows that neglecting the second term in the equation (3.53), the estimation of $\varepsilon_{\text{apparent}}$ may have a systematic error of about ± 2 cm^3 mol^{-1}, for a pressure range of 10^5 Pa. Since this work is likely to be carried out at about 3 to 4×10^4 Pa, the error due to neglecting the third virial coefficients is likely to be negligible, about ± 0.5 cm^3 mol^{-1}.

3-7.3 The Effect of Unequal Loading Pressure

Referring to Figure 3-5, assuming that loading pressure in the second volume is $(p + \delta p_2)$; the pressure series virial equation of state, truncated at β_{11} can be written for the two equal volumes as

$$pV = n_1(RT + \beta_{11}p + \ldots) \qquad (3.54)$$

$$(p+\delta p_2)V = n_2[RT + \beta_{22}(p+\delta p_2) + \ldots] \qquad (3.55)$$

These equations may be rearranged to give

$$\frac{2V}{(n_1+n_2)} = \frac{x_1 RT}{p} + x_1\beta_{11} + \frac{x_2 RT}{p+\delta p_2} + x_2\beta_{22} \qquad (3.56)$$

Using $p_m = p + \Delta p$, in equation (3.33) truncated to second term gives

$$\frac{2V}{(n+n)} = \frac{RT}{p+\Delta p} + \beta_m \qquad (3.57)$$

Equating equations (3.56 and 3.57), and using equation (3.35) gives

$$2x_1x_2\varepsilon = \frac{x_1RT}{p} + \frac{x_2RT}{p(1+\frac{\delta p_2}{p})} - \frac{RT}{p(1+\frac{\Delta p}{p})} \qquad (3.58)$$

where $\varepsilon \simeq \varepsilon_{apparent} + \delta\varepsilon_p$

Using the binomial expansion to the linear term $(1+\delta p_2/p)^{-1}$ where $\delta p_2 << p$, on rearranging gives

$$2x_1x_2\varepsilon = \frac{RT\Delta p}{p^2(1+\Delta p/p)} - \frac{x_2RT\delta p_2}{p^2} \qquad (3.59)$$

Substituting for $\varepsilon_{apparent}$ from equation (3.38), and on rearranging, $\delta\varepsilon_p$ represents the error, due to unequal loading pressures, given by

$$\delta\varepsilon_p \simeq \pm\frac{RT\Delta p}{2x_1p^2} \qquad (3.60)$$

Using the particular example in Section 3-7.1, and assuming that the loading pressure in volume V_2 can be balanced within 0.1 Pa, then

the corresponding error is

$$\delta\varepsilon_p = \pm 0.4 \text{ cm}^3 \text{ mol}^{-1}$$

3-7.4 The Effect of Surface Adsorption

The basic assumption in this analysis, is constancy in the total number of moles in the vapour phase, during the whole run. However, the total number of moles in the vapour phase may be altered because of surface adsorption. The effect of mixing is to halve the partial pressure and double the surface area. A change in total pressure is inevitable, if the adsorption isotherm is not linear with respect to partial pressure for that region.

Referring to Figure 3-5, the pressure series virial equation of state for the volume V_1 and V_2 on loading are

$$pV_1 = (n_1 - n_{a1})RT + (n_1 - n_{a1})\beta_{11}p \qquad (3.61)$$

$$pV_2 = (n_2 - n_{a2})RT + (n_2 - n_{a2})\beta_{22}p \qquad (3.62)$$

where n_{a1} and n_{a2} refer to the number of the moles adsorbed on to the surface of each cylinder before mixing.

After mixing

$$(p + \Delta p)(V_1 + V_2) = (n_1 + n_2 - n'_{a1} - n'_{a2})RT + (n_1 + n_2 - n'_{a1} - n'_{a2})\beta_m(p + \Delta p) \qquad (3.63)$$

where n'_{a1} and n'_{a2} refer to moles adsorbed after mixing. Multiplying equation (3.61) by $x_1/p(n_1-n_{a1})$ and equation (3.62) by $x_2/p(n_2-n_{a2})$ and then on rearranging we get

$$x_1\beta_{11} = \frac{n_1 V_1}{(n_1 + n_2)(n_1 - n_{a1})} - \frac{x_1 RT}{p} \tag{3.64}$$

$$x_2\beta_{22} = \frac{n_2 V_2}{(n_1 + n_2)(n_2 - n_{a2})} - \frac{x_2 RT}{p} \tag{3.65}$$

Both volumes V_1 and V_2 are equal. Dividing equation (3.63) by $(p+\Delta p)/(n_1+n_2-n'_{a1}-n'_{a2})$ and rearranging gives

$$\beta_m = \frac{2V}{(n_1 + n_2 - n'_{a1} - n'_{a2})} - \frac{RT}{p+\Delta p} \tag{3.66}$$

Substracting the sum of the equations (3.64 and 3.65) from equation (3.66) gives

$$2x_1 x_2 \varepsilon = 2x_1 x_2 \varepsilon_{apparent} + \frac{V}{n_1 + n_2 - n'_{a1} - n'_{a2}}\left[2 - \frac{n_1 - n'_{a1}}{n_1 - n_{a1}} - \frac{n_2 - n'_{a2}}{n_2 - n_{a2}}\right] \tag{3.67}$$

where $\varepsilon = \varepsilon_{apparent} + \delta\varepsilon_a$

Hence

$$\delta\varepsilon_a = \frac{(n_1 + n_2)V}{2n_1 n_2}\left[\frac{n'_{a1} - n_{a1}}{n_1} + \frac{n'_{a2} - n_{a2}}{n_2}\right] \tag{3.68}$$

In this work, since $n_1 \simeq n_2 \simeq n/2$

$$\delta\varepsilon_a = V[n'_{a1} - n_{a1} + n'_{a2} - n_{a2}]/n_1^2 \tag{3.69}$$

To evaluate the effect of surface adsorption, n_{a1} and n_{a2} can

be calculated using equation (3.28)

$$n_{a_i} = \frac{N_i^0 ACp}{(p_i^0 - p_i)[1 + (C-1)(p_i/p_i^0)]} \qquad (3.70)$$

where N_i^0 is the number of moles of component i, per unit area required to form monolayer,

A = the adsorptive area of each cell,

C = an isotherm parameter,

p_i^0 = the saturation vapour pressure of the component i.

To evaluate the number of moles adsorbed after mixing n'_{a1} and n'_{a2}, it is assumed that the mixture isotherm is a linear combination of the individual isotherms. The event of mixing two components is to double the surface area and to halve the partial pressure for each component. Consequently

$$n'_{a_i} = \frac{N_i^0 A'Cp'_i}{(p_i^0 - p'_i)[1 + (C - 1)p'_i/p_i^0]} \qquad (3.71)$$

where A' = 2A, Double the adsorptive surface area of each cell,

and $p'_i = p_i/2$, the partial pressure of each component, after mixing.

Substituting for A' and p'_i in equation (3.71) and rearranging gives

$$n'_{a_i} = \frac{N_i^0 ACp_i}{(p_i^0 - p_i/2)[1 + (C - 1)p_i/2p_i^0]} \qquad (3.72)$$

Hence knowing n_{a_i} and n'_{a_i} for the both components, $\delta\varepsilon_a$ can be evaluated. However, two sources of errors still exist.

1. The isotherm parameter (C) for benzene and cyclohexane is

assumed to be 100 (Barbernics et al., 1974), for the adsorption of a nonpolar substance on to a polar substrate. However, C may not be necessarily 100 and it may affect the correction.

2. There is speculation of multilayer formation for the relative pressure p_i/p_i^0 above 0.4.

3-7.5 Other Sources of Uncertainties

Shannon (1976) speculated on the effect of impurities and inert gases in the mixture, on the interaction second virial coefficients. Residual mixture in the mixing volumes from previous measurements or inert gases left from the degassing procedure could be causes of adulteration in the mixture. Treating the system as a multicomponent mixture, and making allowance for the maximum likely impurity, Shannon calculated the error to be negligible.

CHAPTER 4

EXPERIMENTAL EQUIPMENT

A. PURE SUBSTANCE

4-1 Description of the Experimental Equipment

A detailed line diagram of the apparatus is shown in Figure 4-1. The individual items of the apparatus are discussed in the following sections in detail, covering where applicable, the design, materials and methods of construction, and the tests used to prove the item's integrity during its operation.

4-1.1 Vacuum Lines, Taps and Ampoules

The vacuum lines were made either of "Pyrex" glass or copper tube. Most of the glass manifold was clamped to a frame affixed to the floor. It had either ground-glass vacuum stopcocks (G1 to G14) or high vacuum glass and teflon taps (T1 to T9) ["Young"]. The latter were used to provide the grease free region for the organic vapours. Most of the remaining valves (W1 to W8) were metallic valves with Swagelok fittings ["Whitey"; type B43S4].

Most of the metallic manifold outside the thermostat, was affixed to the wall and was insulated by a 1 inch thick cotton wool layer to reduce the effect of varying ambient temperature. Organic

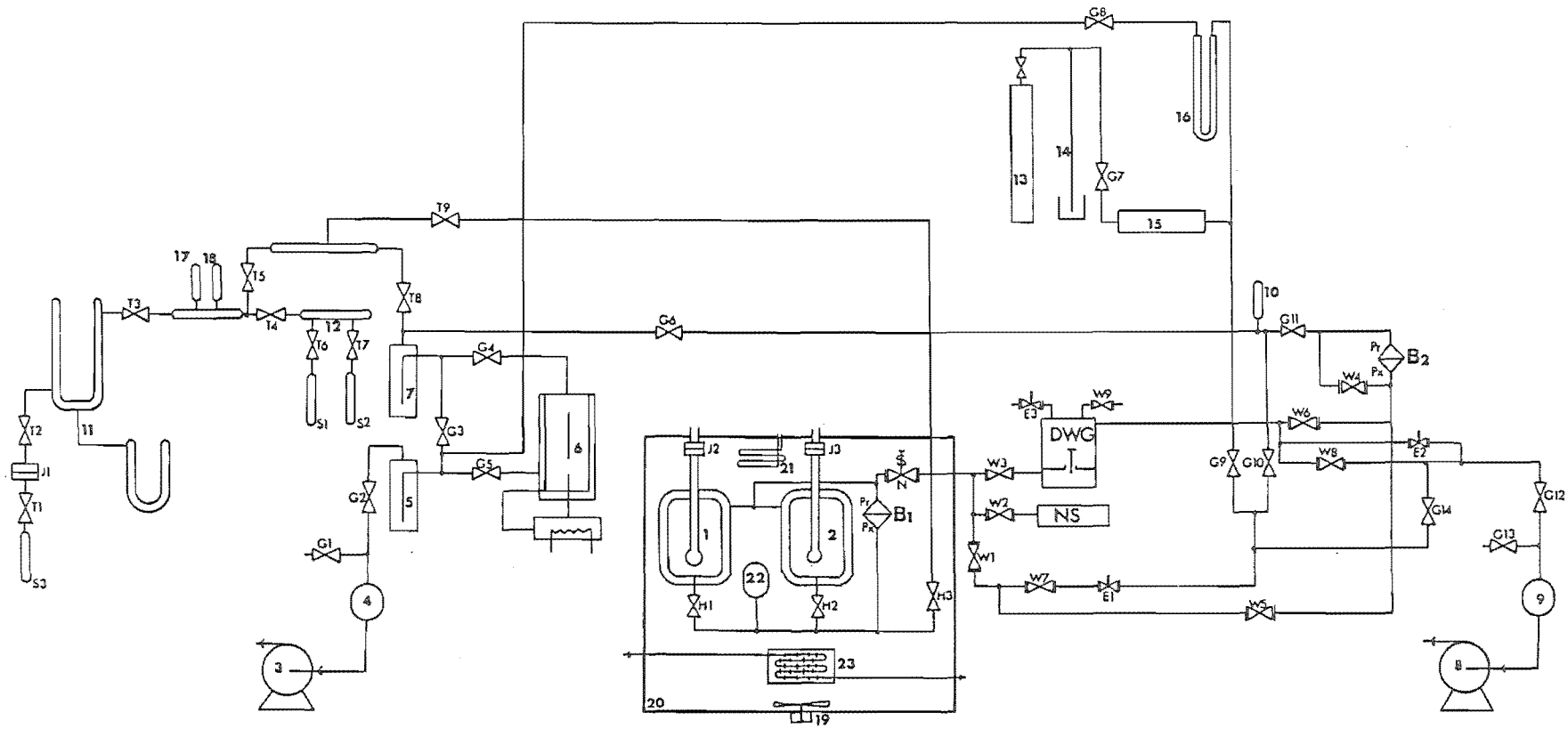

FIGURE 4-1 APPARATUS LINE DIAGRAM

Key to Figure 4-1

(1) A double walled glass cell of approximately 1000 cm^3 capacity, having cold finger, extended to about two thirds of the depth of the inner portion of the cell.

(2) A glass cell similar to cell (1) and connected to it by glass to metal seals and "Hoke" valves [model 4618N4]

(3) Two-stage rotary vacuum pump, ["Jigtool"; model SEUSO H6605]

(4) 1000 cm^3 glass globe.

(5) Liquid air cooled cold trap.

(6) The mercury diffusion pump.

(7) Liquid air cooled cold trap.

(8) Two-stage rotary vacuum pump, ["Edwards"; model 2SC20A]

(9) 1000 cm^3 glass globe.

(10) Penning Gauge Head [Edwards"; model 5MF]

(11) Degassing manifold with a "Soveril" teflon joint J1 to connect bulk storage ampoule.

(12) Loading manifold, mounted with two sample ampoules.

(13) Dry oxygen-free nitrogen supply (NZ Industrial Gases Ltd.).

(14) Mercury safety valve to allow the nitrogen to escape, should the pressure exceed one atmosphere.

(15) Tube containing dry silica gel, to dry nitrogen gas.

(16) Mercury manometer to calibrate National Semiconductor NS approximately.

(17) Pirani Gauge Head [Edwards; model G6B].

(18) Penning Gauge Head [Edwards; model 6].

(19) Electric motor drive to the fan inside the bath.

(20) Air thermostat

(21) Spiral coil for compressed air

(22) 100 cm^3 glass bulb

(23) Heat exchanger

S1 to S3	Sample ampoules
E1 to E3	"Edwards" neddle valves
G1 to G14	Ground glass vacuum stopcocks
H1 to H3	"Hoke" valves
J1 to J3	Soveril teflon joints
N	"Nupro" bellow sealed valve
T1 to T9	"Young" teflon taps
W1 to W9	"Whitey" valves
V1	Cylinder regulating valve
DWG	"Ruska" dead weight gauge
NS	National Semiconductor pressure transducer
Pr	Reference port of Baratron pressure gauge
Px	System port of Baratron pressure gauge
B_1	"Baratron 1" installed inside the bath
B_2	"Baratron 2" (installed outside the bath) connected to DWG

vapours were introduced into the cells (1 and 2) on opening the valves H1, H2 and H3 ["Hoke"; model 4618N4]. A fine control needle valve E1 ["Edwards" type OSIC] was used to check the flow of nitrogen through the bellows sealed valve N ["Nupro"; type B-4H] inside the thermostat to introduce nitrogen into the outer volumes of cells (1 and 2). All the valves except E1, were capable of maintaining 10^{-2} Pa vacuum or better for periods of at least one week. E1 always, showed a gradual leak. However, the valve E1 was advantageous, as it provided control to prevent the reference side of Baratron 1, being overloaded relative to the sample gas pressure.

The cold traps (5 and 7) were demountable, the ground glass joints being grease sealed. These traps were immersed in liquid air to remove moisture, organic vapours and mercury from the system.

4-1.2 Vacuum Pumps and Gauges

Two vacuum pumps (3 and 8) were used in the whole experimental set-up. The backing pump (3) for the whole apparatus was a two-stage rotary vacuum pump ["Jigtool"; model SEUSO H6605]. This pump, by itself achieved a system pressure of less than 5 Pa. It was used in conjunction with the mercury diffusion pump (6) designed and built, in glass, by Mr. F. Downing of the Chemistry Department. When cold trapped, the rotary and diffusion pumps were capable of reducing the whole experimental system to better than 10^{-4} Pa.

The second vacuum pump (8) was also a two-stage rotary pump [Edwards"; model 2SC20A] which was used to evacuate the bell jar on the air piston Dead Weight Gauge to 150 to 200 Pa. Two glass globes (4 and 9) of capacity 1000 cm^3 were used as traps, to avoid the accidental flow of oil into the apparatus, as a consequence of the pump stopping under vacuum.

The vacuum in the glass manifold was checked by a Pirani-Penning Gauge ["Edwards"; model 4] with a Pirani Gauge Head (17) ["Edwards"; model G6B] and a Penning Gauge Head (18) ["Edwards"; model 6] mounted on the manifold. The vacuum on the reference side of Baratron 2, was checked by a Pirani/Penning type Vacuum Gauge ["Edwards"; model 2A] with a Penning Gauge Head (10) ["Edwards; model 5MF] mounted on the glass manifold close to the Baratron 2 Head Sensor.

4-1.3 Sample Degassers and Loading Manifold

Bell et al. (1968) and Battino et al. (1971) have described an apparatus for rapid degassing of the liquid. The former is based on vacuum sublimation of small volumes of frozen material, while the latters' method facilitates the rapid degassing of the liquid sample of the order of 500 cm^3.

The degassing manifold (11) was built for degassing liquid samples of the order of 100-150 cm^3, on the lines suggested by Bell et al. (1968). The degassers were made of "Pyrex" glass. The sample ampoule could be connected to the degassing unit by a demountable teflon joint J1 ["Soveril"; type SVC15], capable of maintaining a vacuum of 0.5 Pa for 2 to 3 hours.

Two storage sample ampoules, were made from "Pyrex" glass tubes and "Young" Taps. The taps were oriented in such a way that the PTFE seals seated on the surface of the sample side of the tap. The barrel seal (on the atmosphere side) was backed by a second O-ring ["Viton"; type V160-4C-P4]. The degassing (11) and loading (12) manifolds, could be isolated from the rest of the apparatus, by tap T5 to facilitate the loading of degassed sample from the degassing unit to the sample storage ampoule.

4-1.4 High Pressure Nitrogen Supply

The oxygen-free dry nitrogen, used to balance the sample gas pressure in the cell, was drawn from a "New Zealand Industrial Gases

Ltd." cylinder (13). The nitrogen was throttled, using an ordinary NZIG reducing regulator V1, into a tube (15) packed with dry silica gel. A mercury safety valve (14) was connected between the supply and the apparatus, to safe-guard against over-pressure above one atmosphere. The dried nitrogen was bled through G9, E1, W7, W1 and N, into the outer volume of cells 1 and 2, so that Baratron 1 showed a slightly greater pressure on the nitrogen side than on the system side.

A mercury in glass manometer (16), mounted on a rigid frame, was positioned between the vacuum pump (3) and the National Semiconductor pressure gauge NS, to calibrate the latter approximately from zero to atmospheric pressure (Section 5-3.1).

4-1.5 Air Bath Thermostat

The apparatus was enclosed in a demountable air bath (20), especially designed (Singh, 1979), for this work to operate at temperatures of up to at least 150°C. It was constructed 50 cm$\frac{1}{2}$ above the floor surface, on a rigid frame affixed to the floor. This reduced the effect of vibrations being carried to the sensitive instruments on the bench attached to the wall.

The dimensions of the bath were 90 cm x 90 cm x 110 cm. It was constructed of stock aluminium sheet. The space between the double walls, 10 cm$\frac{1}{2}$ apart, was packed with glass wool and the edges were covered by "Hardy Therm" asbestos board. The detachable parts of the air bath had silicone rubber seals on the surfaces to ensure tight contact with the rest.

A second double walled open bath of capacity nearly 0.175 m^3,

was installed on a frame inside the main air bath. The double walls were 8 cm thick, packed with glass wool and covered with "Hardy Therm". Finned aluminium extrusions were fixed to the outer walls of the small bath to provide additional heat capacity. A rectangular finned tube heat exchanger (23) was installed at the bottom of the inside bath and was connected to a cooling water supply to enable cooling of the bath when necessary.

The air in the bath was vigorously circulated using a fan (19) installed inside the bath and driven by a 1/4 hp and 1425 rpm AC motor ["Crompton Parkinson"; type E65], fixed to the main frame outside the bath with its shaft aligned to the centre of the bath. A stainless steel cylinder, having bearings fixed at its both ends, had the shaft passing through it and locked into the assembly. The cylindrical assembly was inserted into the bath from the bottom and was held there by bolting it to the main frame. The shaft inside the bath had a centrifugal fan fixed to it. The protruding end of the shaft from the bath was connected to the motor shaft by slipping an ordinary PVC tube on both. This reduced the vibrations conveyed to the bath.

The energy required to maintain the air bath at constant temperature was provided by two heaters. The temperature control equipment is discussed in detail in Section 4-2. The base heat consisted of 36 light bulbs ["Philips"; 15 watt], in parallel and uniformly distributed in four rows, on the outside wall of the inner bath. Observations showed that bulbs screwed firmly to the brackets had a shorter life time, due to vibrations, than those just slipped into the brackets. The voltage supply to the base heat, was controlled by a "Variac" transformer. The base heat provided 85% of the required energy, while the rest was supplied by twenty two bulbs, as required by the temperature controller. These bulbs were also connected in

parallel and arranged in two rows, around the bath, in between the four rows of the base heat. The temperature controller (Shannon, 1976) was an S.C.R. proportional temperature controller, with an appropriate thermistor inserted into the bath.

Several times, during transfer of condensable vapours from one cell to another, liquid air was poured into the cold fingers. A spiral heat exchanger (21) was installed inside the bath, with its two ends protruding out of the bath. One end was connected to the compressed air supply and the other had a long rubber tube connection to reach the bottom of the cold finger. Compressed air, at the bath temperature obtained from the system, speeded the process of emptying the cold finger and reheating the cell back to the bath temperature.

A metallic frame was installed, just above the heat exchanger, to support the cells (1 and 2) and connecting tube. The "Hoke" valves were connected to the apparatus either with metal to glass seals or "Cajon VCR" connectors, soldered in place using "Easy Flow" high temperature solder. Connections out of the air bath were made with "Swagelok" [type 316] connectors.

The outer jackets of both cells (1 and 2) were coupled together and coupled via a "Nupro" valve to the nitrogen side of Baratron gauge 1 which isolated the system.

The pressure transducer, Baratron 1 Head Sensor (detailed discussion in Section 4-4b), was installed on the frame. Both ports of Baratron 1, system side Px_1 and reference side Pr_1, are provided with fittings ["Cajon"; type 4VCR] and mating halves. The coupling glands are machined to accept 1/4 inch O.D. tube. The Px_1 port had access to sample gas, while Pr_1 port had access to nitrogen.

4-1.6 The Sample Gas Cells

The sample gas cells (1 and 2), each having an approximate volume of 1000 cm^3, were constructed of "pyrex" glass and placed inside the thermostat. The analysis of the results did not require the volumes of the cells to be known exactly (Section 3-2). The cells were double walled, with nitrogen gas occupying the outer volume at a pressure equal to the internal pressure of the sample occupying the inner volume of the cell. This prevented distortion of the cell caused by changes in pressure. The double walled design of the cell also reduced the effect of slight fluctuations in the bath temperature on to the temperature inside the cell. A cold finger extended two thirds of the length into the inner portion of each of the cells. The cold finger was connected by a joint ["Soveril"; type SVL30], to another tube of similiar diameter, just protruding out of the upper surface of the bath. The cold finger facilitated the transfer of the condensable materials into the cells, using liquid air in the cold fingers. During the experiment, this access was closed by a wooden rod which almost filled the cold finger, to minimise convective heat exchanges with the surroundings.

A dummy bulb identical to the sample gas cell in dimensions was constructed (not shown in the Figure 4-1), and was mounted inside the air thermostat at the same level as other gas cells. A tube of the same diameter as the cold finger but open at both ends extended two thirds of the length into the inner portion of the dummy bulb and the quartz thermometer (or Pt. Resistance thermometer) probe was inserted into the tube. The stability of the temperature inside the inner volume of the

dummy bulb was expected to be the same as inside the inner volume of both sample gas cells.

A glass bulb of volume 100 cm^3 (22) was installed on the line between cell 1 and cell 2, to permit the removal of a significant quantity of material by evacuation, to change the starting pressure for successive measurements.

4-2 Thermostat Control Devices

The whole apparatus was set up in an air conditioned laboratory controlled to 25±2°C. Bath temperature control was achieved using an SCR proportional temperature controller (Shannon, 1976) with a glass encapsulated NTC thermistor of appropriate resistance (between 5 to 10 K ohms at the operating temperature), immersed in the air bath. The circuit diagram is shown in Figure 4-2. The controller basically consisted of an amplifier, to amplify the output voltage from a bridge formed of a thermistor, fine and coarse temperature control resistors and a 470 ohms resistance. The amplified voltage fired a uni-junction transistor, which in turn pulsed the silicon controlled rectifier to pass current proportionally, through the heater. The controller was kept in a simple wooden enclosure, maintained at 30±0.1°C, by an adjustable Bimetal thermostats ["Sunvic"; type TS]. It was observed that long term drift was decreased significantly by keeping the controller electronics at constant temperature.

The air bath temperature was controlled to better than ±0.01°C over two hours. The maximum very long term drift was observed to be a tenth of a degree, and followed the room temperature variation of 3 to 4°C. However, the variation of temperature inside

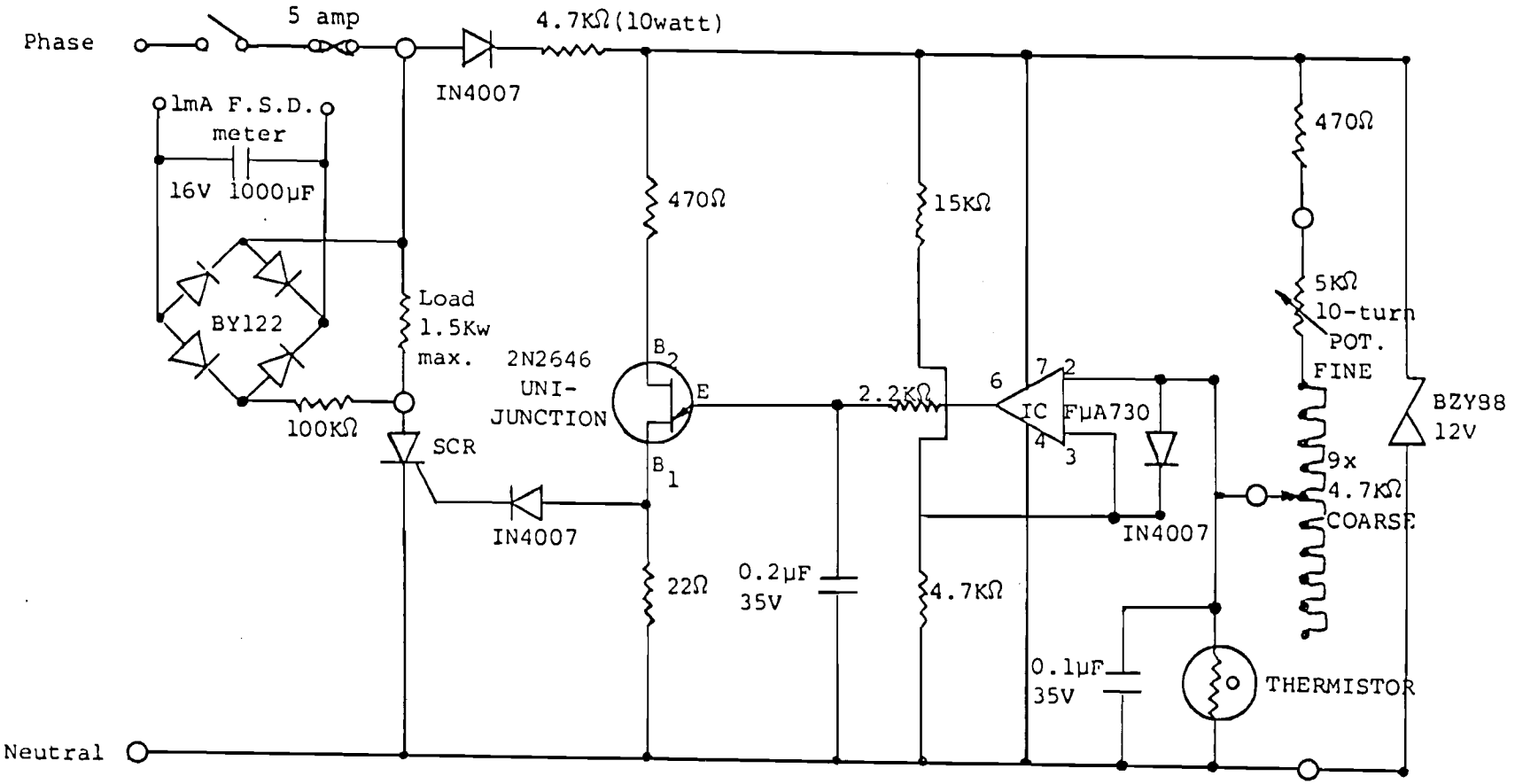

FIGURE 4-2

Thermostat Bath Proportional Temperature Controller

the dummy bulb, in the bath was normaly less than $\pm 0.005^{o}C$ over a period of a measurement.

A thermistor of nearly the same resistance as that of the controller sensor, was kept either inside the bath, at the same level as the controller sensor or inserted into the dummy bulb and was connected to a chart recorder through a Wheatstone bridge (Figure 4-3). One thermistor (10 k ohms) clamped close to the experimental area, was connected to the chart recorder through another Wheatstone bridge. The whole set-up enabled the observation of the temperature stability in the room, inside the bath or inside the dummy bulb.

4-3 Temperature Measurement

In the earlier part of this work, the temperature inside the dummy bulb was measured using a Platinum Resistance Transfer Standard ["Rosemount"; model WS104HL, serial No. 409] and a Precision Comparison Bridge ["Rosemount"; model VLF51A-150]. The ice point (Nicholas and White, 1981) was carefully established in a dewar flask, having equilibrium between crushed ice and air saturated distilled water. The probe was calibrated at the ice point and its resistance at $0^{o}C$ was 25.505 ohms. DSIR, Wellington, NZ calibrated the same probe in 1977 and reported the resistance equal to 25.4924 ohms, at the ice point.

For the later stages of the work, a quartz thermometer ["Hewlett Packard"; type 2801A] was used to measure the temperature inside the dummy bulb. The thermometer was used in the differential mode. One probe was dropped into the dummy bulb and the other probe dipped into transformer oil in a tube, was immersed into the ice bath.

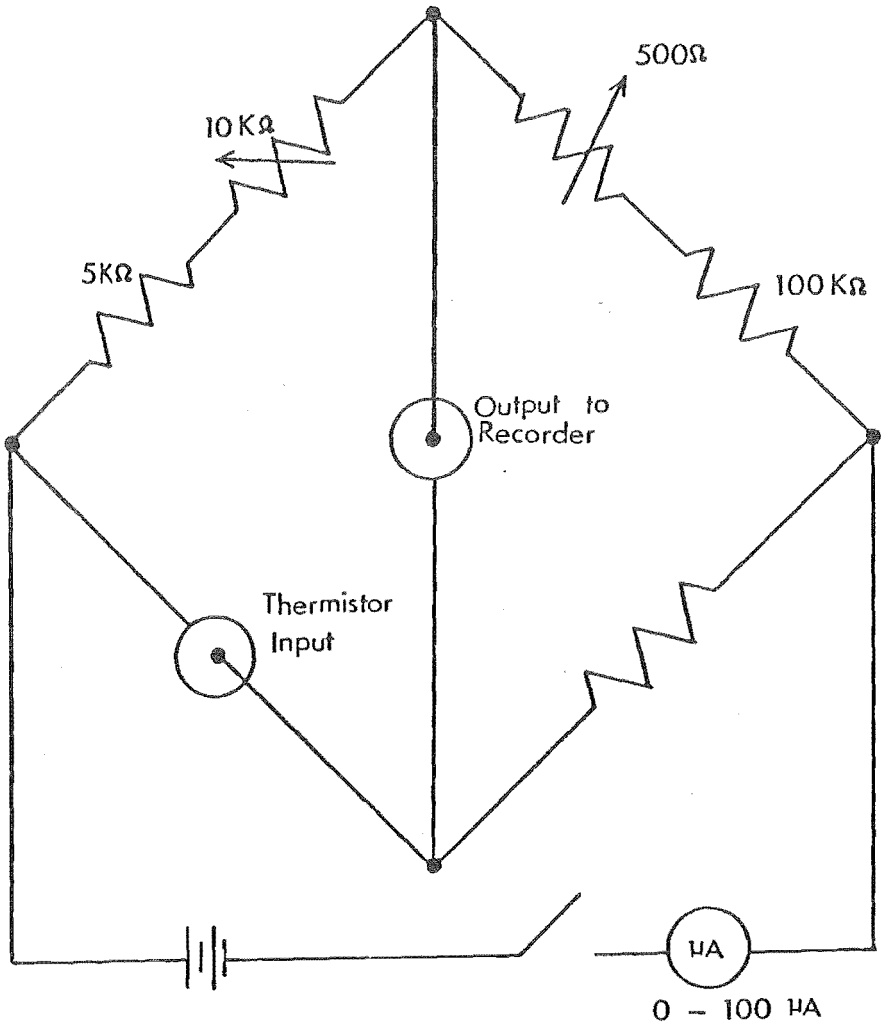

FIGURE 4-3 D.C. THERMISTOR BRIDGE

The difference between the bath temperature and ice temperature was then read directly on the meter. The zero reading of the quartz thermometer was checked by immersing both probes in the ice bath. Any deviation of the zero reading was used to correct the estimated bath temperature.

However, it should be emphasised that in this work, it was more essential to know the shift in the temperature of the system, from one measurement to another in one complete run, rather than the precise temperature of the bath. The quartz thermometer, with its digital display, facilitated observation of small temperature changes.

4-4 Pressure Measuring Devices

Pirani and Penning gauges were used in the line to check the vacuum. A mercury in glass manometer was installed between the vacuum pump (3) and the National Semiconductor gauge (NS), to calibrate the latter. Two MKS Baratrons and one air piston Dead Weight Gauge (DWG), were installed in the line, as shown in Figure 4-1, to measure the pressure of the sample gas.

a.) National Semiconductor Gauge

A temperature compensated absolute pressure transducer, ["National Semiconductor"; type LX1600A] was installed, as shown in Figure 4-1, on the line leading to the reference port Pr_1 of Baratron 1, through valve W2. It was calibrated from 0 to 7.6 volts, for a pressure range from 0 to 760 mm Hg (Section 5-3.1). The output was read on an automatic digital multimeter ["Philips"; type PM 2517X]. It had a maximum static error band of 3%, and was suitable for the approximate

estimation of reference pressure and loading of the appropriate weights on the piston of dead weight gauge (Section 5-2.2).

b.) Baratrons

Two differential pressure gauges ["MKS Baratron"; type 170M series] were installed in the apparatus. Both sensors (bakeable single sided design)[Type 315-BH-10] had a standard full scale range of 10.00 mm. The sensor is recommended (MKS Baratron Pressure Meter; Type 170, 1977) for 10 mm Hg unidirectional differential pressure measurements, and is usable with any corrosive gas compatible with the materials of construction of the gauge (Inconel and stainless Steel). The sensor of Baratron 1 has its corrosion resistant baffle plate, diaphragm and sensor body exposed to the sample gas (Px port). The other side of the sensor is exposed to non-corrosive and clean nitrogen gas (Pr port). These gauges are generally recommended for the use of higher pressure on the Px port of the sensor.

Baratron 1 sensor was used as a unidirectional differential pressure measurement device. It was installed in the bath as discussed in the Section 4-1.5. Baratron 2 was used for the absolute pressure measurement, with reference port Pr_2 of the sensor exposed to continuous vacuum. It was installed outside the bath, in the same manner as Baratron 1 Sensor. Port Px_2 of sensor, was connected to the DWG through W6 and to reference side Pr_1 of Baratron 1, through the "Nupro" valve N and the "Whitey" valves (W1 and W5) as shown in Figure 4-4. The reference side port (Pr_2) was subjected to continuous vacuum through G11 enabling measurement of the absolute pressure inside the bell jar of the dead weight gauge.

According to the Instruction manual for the MKS Baratron Pressure Meter, Type 170 (1977), calibration for negative pressure is

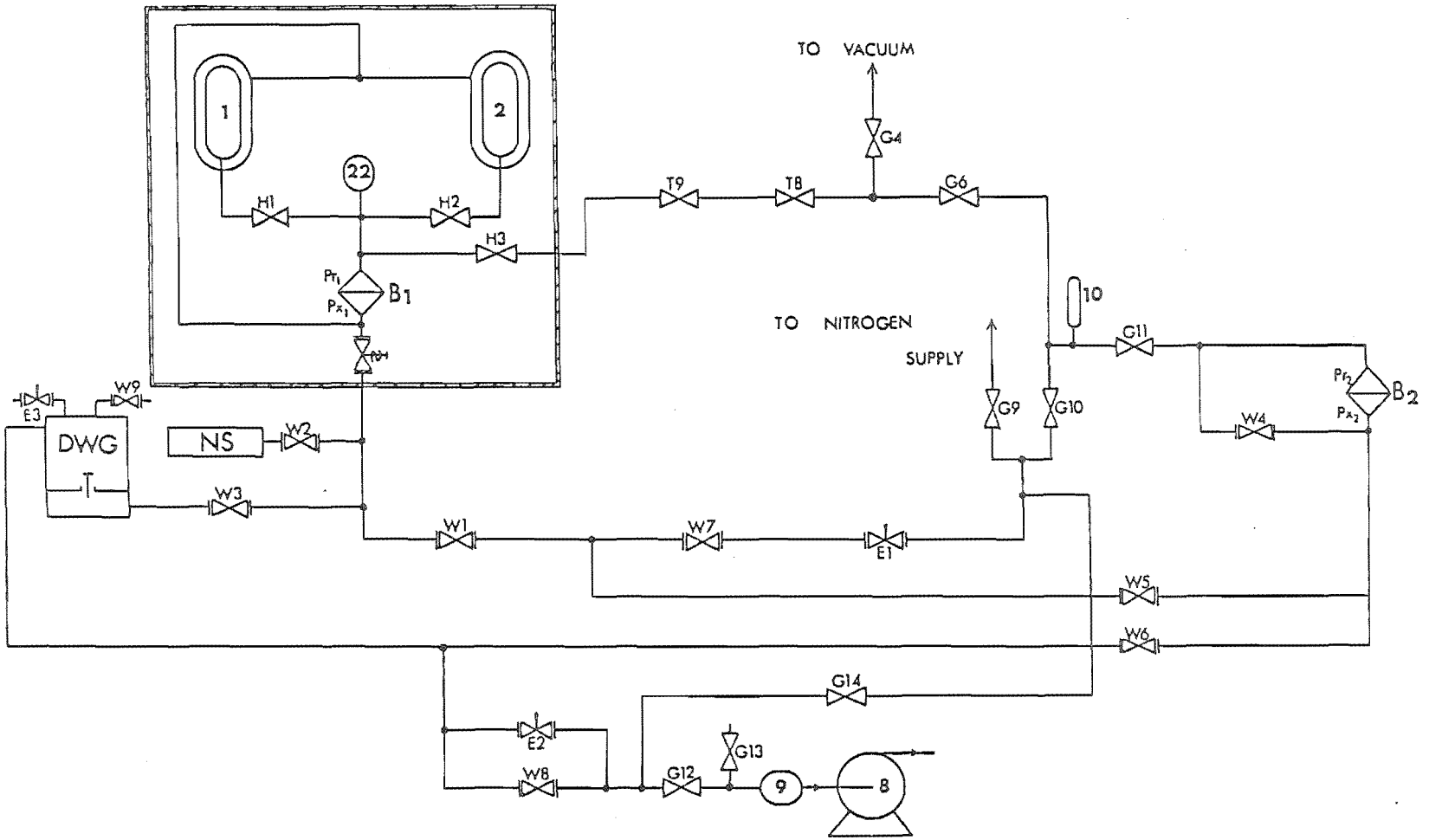

FIGURE 4-4 CIRCUIT DIAGRAM OF VALVES & CELLS ARRANGEMENT

relatively good over 20.0% of the Head range. However, because of the need for cross calibration of Baratron 1 with Baratron 2, the reference port Pr_1 of Baratron 1 was exposed to pressures above those on the sample side, but it was unidirectional in all the measurements. It was used only below 2.00 mm of negative differential pressure, to avoid the 2 to 3% of error at negative full head range. The calibration was observed to be reproducible and is reported in Appendix A5.

Electronics unit accessories for the type 170M series, consisted of bakeable Head Adaptor [type 170M-35], Pressure Indicator, [type 170M-6] and (5.5 Digits) Digital Readouts [type 170M-25]. The bakeable Head Adaptor had two temperature compensation controls to permit the Baratron to read pressure directly and without requiring any further correction to the readings. The Pressure Indicator provided excitation to the Head and converted the head output to a proportional DC output of +10.0 volts full scale. The Digital Readout Units converted the analog output (+10.0 volts) to a visual display. The performance of Baratrons is already discussed in Section 3-5.

During the course of the work, the Baratron Digital Readout Units developed faults, particularly during the use of Tesler Coil leak detectors on the line. Thus the Baratrons should always be disconnected. The power to the Baratrons and the DWG was supplied through an "APEX" Isolating Transformer, to reduce the effect of minor variations in line voltage arising from other equipment in the laboratory.

c.) Air Piston Dead Weight Gauge

An air piston dead weight gauge DWG ["Ruska"; model 2465] was installed for the measurement of the pressure of nitrogen. It was located in a draft and vibration free location on a fixed and levelled

table. The pressure connection to it had access to nitrogen gas through W3. The manifold connecting the top of the DWG table, was connected to the sample port Px_2 of Baratron 2, through W6 and to the vacuum pump (8) through E2 and W8 (Figure 4-4).

A bell jar was placed on the gauge, using an O-ring with a light grease sealing. The "Whitey" valve, W9, open to the atmosphere, was connected to a wide opened tube with cotton plug, to prevent the contamination of gauge by dust particles in the laboratory atmosphere. A thermometer was provided in the side of the gauge to indicate the gauge temperature.

B. MIXTURES

4-5 Description of the Experimental Equipment

A detailed line diagram of the apparatus is shown in Figure 4-5. Shannon (1976) has given a detailed description of the existing apparatus to measure the interaction second virial coefficients of the mixtures. A brief description of the individual items of the apparatus with certain alterations (Battino, 1980) are given in this section.

The vacuum lines were all made of "Pyrex" glass. The backing pump (4) for the whole apparatus was a two-stage rotary vacuum pump ["Jigtool"; model SEVSO G4372]. The mercury diffusion pump (3), used in conjunction with the rotary pump, was capable of achieving a system pressure of 10^{-2} Pa, in the whole apparatus, when cold trapped. The vacuum gauges on the lines were Vacuum Pirani, with a gauge head ["Edwards"; model M6A] and Vacuum Penning with a gauge head ["Edwards"; model 6].

The loading manifold consisted of four sample storage ampoules, made of "Pyrex" glass tube and teflon taps ["Young"]. The sample degasser and loading manifold were identical to that described in the Section 4-1.3.

The high pressure nitrogen supply set-up was identical to that described in section 4-1.4. Nitrogen was throttled using a NZIG reducing regulator (V1) and passed through a bed of dry silica gel. The dry nitrogen was then passed through a shut-off valve (V2) into an adjustable volume valve (V3). The adjustable bellows of the valve, controlled the adjustment of desired nitrogen pressure. Further

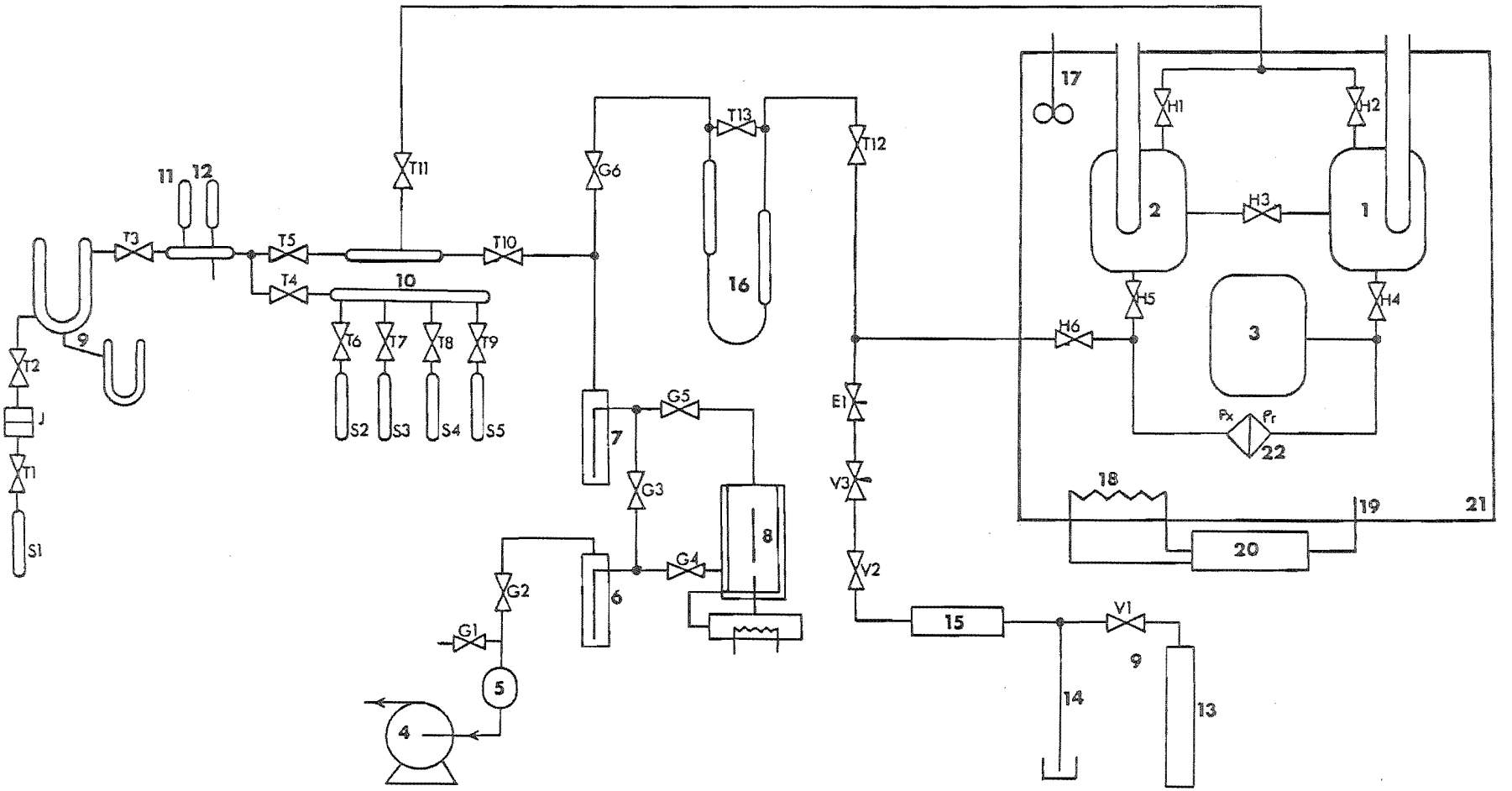

FIGURE 4-5 APPARATUS LINE DIAGRAM

Key to Figure 4-5

(1) Stainless steel vessel of approximately 6000 cm^3 capacity, having a cold fingure and a 10 mm diameter entrance tube made from copper and connected to the sample ampoule through V1.

(2) Similar to vessel (1), and connected to the sample ampoule through V2 and to vessel (1) through V3.

(3) Similar to vessel (1) and (2), and connected to vessel (1) and the sample side of the Baratron through V4.

(4) Two-stage high vacuum pump ["Jigtool"; model 5EVSO G4372].

(5) 1000 cm^3 glass globe.

(6) Liquid air cooled cold trap.

(7) same as (6)

(8) Mercury diffusion pump.

(9) Degassing manifold with a "Soveril" teflon joint J1, to connect the bulk sample ampoule.

(10) Loading manifold, mounted with four sample ampoules.

(11) Pirani Gauge Head ["Edwards"; Model M6A]

(12) Penning Gauge Head ["Edwards"; Model 6]

(13) Dry oxygen-free nitrogen supply [NZ Industrial Gases Ltd.]

(14) Mercury safety valve.

(15) Tube containg dry silica gel

(16) Mercury manometer.

(17) The stirrer

(18) Controller heater

(19) Thermistor

(20) Proportional temperature controller

(21) Stainless steel thermostat

(22) Baratron

E1	"Edwards" needle valve
G1 to G6	Ground glass vacuum stopcock
H1 to H6	"Hoke" valves
T1 to T11	Teflon taps ["Youngs"]
V1	NZIG nitrogen supply regulator
V2	Shut-off valve
V3	Adjustable volume bellow valve

nitrogen was passed through a needle valve E1 ["Edwards"; type OSIC] which monitored the flow of nitrogen to the transducer and manometer.

4-5.1 Thermostat

A stainless steel tank (21) of 150 litres capacity and dimensions 50 cm x 50 cm x 60 cm was mounted on a platform designed to slide up and down on a frame. Heat transfer oil ["BP"; TH65HB] having a vapour flash point of 220°C was used as bath fluid to stand a maximum temperature of 150°C. A single six-bladed propeller (17), powered by a 300 Watt motor, was used to stir the bath. The fluid movement was vigorous enough to reflect any variation in the temperature of the bath in 2 to 5 seconds.

A 5 kW (maximum) immersion heater was used as a base heater, but was limited to 1 kW to prevent oil charring due to high heat flux at element surface. A "Pyrotenax" heater of 800 watts, used as a controller heater (18), consisted of 35 metres of "Pyrotenax" wire [type copper sheathed] of resistance 0.315 ohms per metre at 20°C on a frame surrounding the cylinder. An S.C.R. proportional thermostat temperature controller (20), (as described in Section 4-2) with the appropriate thermistor (19) immersed in the oil as the sensor, was used for the temperature control. The bath top was covered with removable wooden strips and glass wool. The bath temperature control was better than ±0.01°C over long periods. The long term drift over 24 hours was also better than ±0.01°C. Bath cooling was achieved by passing mains water through a coil of 15 metres of copper tubing of 5 mm diameter, mounted on the same frame as the "Pyrotenax" heater.

A portable spiral heat exchange was used to heat air to bath

temperature, when needed to reheat the cold finger. The heat exchanger consisted of 1 metre, 10 mm diameter copper tube coiled into a 50 mm diameter coil. The outlet was then put deep into the cold finger, with the spiral heat exchanger in the thermostat bath. The compressed air out of the exchanger was upto 90% of the bath temperature within 10 to 15 minutes.

4-5.2 Mixing Cylinders and Assembly

The three mixing cylinders, each of 6 litres capacity, were constructed from stainless steel [Type 316]. Each cylinder had a 10mm diameter copper entrance tube. Cylinders (1 and 2) had two cold fingers. "Hoke" valves [model 4618N4] were used for the valve assembly (see Figure 4-5) which connected the cylinder assembly. The pressure transducer was attached to the valve assembly with "Cajon" [type 4VCR] fittings. The complete assembly was mounted onto the thermostat support frame and joined to the vacuum system through glass-metal seals.

Before constructing the complete assembly, the cylinders, which had been electropolished internally, and the valve assembly were thoroughly washed, degreased and cleaned. After testing for leaks in the cylinder and valve assembly,each cylinder, the valve assembly and pressure transducers were baked in an oven under a vacuum of 0.1 Pa or better (Shannon, 1976). The cylinders and pressure transducers were held at 400^{o}C for 3 to 4 hours. The valves, because of their temperature limitation of 310^{o}C, were baked at 300^{o}C for 3 to 4 hours.

4-6 Temperature Measurement

The temperature was measured using a Platinum Resistance thermometer ["Rosemount"; model WS104HL; serial no. 240] and a precision comparison bridge ["Rosemount"; model VLF51-150]. The resistance of the probe at $0^{o}C$ was measured to be 25.5221 ohms. DSIR Wellington (1977), NZ reported the resistance of the same probe equal to 25.5151 ohms.

4-7 Pressure Measuring Devices

A mercury manometer was used to measure the initial loading pressure in each experimental run. A differential pressure transducer [MKS "Baratron"] was used to ensure equality of the pressure of component 1 and component 2, and later to observe the change in the pressure on mixing of the two components.

a.) Mercury Manometer

The manometer was constructed of 25 mm i.d. "Veridia" precision bore tubing. The mercury was washed and then air was bubbled through it, in a solution of 10% nitric acid. After thorough washing with distilled water a number of times, the mercury was partially dried by passing through a filter paper having a pin-hole in it. The mercury was then distilled under vacuum. Finally purified distilled mercury was loaded into the manometer under vacuum.

The mercury manometer was enclosed in a cabinet lined with 10

mm polystyrene sheet to minimize the air draughts around it. Two 20 watt fluorescent tube lights fixed at the back, lit the mercury surfaces. Two sliding brass collars were used to hood and collimate the light from the mercury surfaces. A 50 mm slit in the front of the cabinet allowed the mercury level to be measured with a "Precision Tool & Instrument Company Ltd." Cathetometer [No. H546]. The Cathetometer was sited so that the vertical measuring bar was equidistant from both manometer legs, to avoid refocussing of the telescope. The measuring bar was checked for vertical alignment using the spirit level on the telescope, to eliminate relevelling adjustment of the telescope between the individual readings.

b.) MKS Baratron

The "Baratron" obtained from MKS Instruments Inc. of Burlington, Massachusetts, USA, consisted of a pressure Head [type 90H-1E, serial no. K5197] of range 130 Pa (1 mm) and Indicator [type 90M-XR, serial no. K5106]. The MKS company provided the calibration with a claimed resolution of 1.3×10^{-4} Pa. The "Px" and "Pr" ports of the Baratron were joined to the cylinder and valve assembly respectively using "Cajon" fittings. The Px port was connected to the sample side (cell 1 and 3), and the Pr port was connected to the nitrogen supply and cell (2), cut off by valves H6 and H5 respectively (see Figure 4-5).

The sensor had a close fitting jacket of mild steel around it, with the flanges sealed and the interior filled with fibre-glass insulation. A "snorkel" was used to lift the triaxial cables from the sensor out of the bath to the preamplifier. The "snorkel" was also packed with fibre glass to prevent cooling by the ambient air in the laboratory.

CHAPTER 5

OPERATING PROCEDURE

A. PURE SUBSTANCES

5-1 Introduction

Prior to loading the system cell 1 (item no. (1) in Figure 4-1) with the sample, the reference side of Baratron 1 (inside the bath) was calibrated against the system side of Baratron 2 (Section 5-3.2), and the latter's system side was calibrated against the dead weight gauge (Section 5-3.3), so that the final pressure of the sample could be expressed in dead weight gauge (DWG) units. The materials were purified and prepared for loading as discussed in Section 5-4.

5-2 Operating Procedure

The initial step for each experimental run was to evacuate the whole system to better than 0.01 Pa vacuum, as indicated by the Penning gauge. The "Hoke" valves H1, H2, H3 and the "Nupro" valve N were wide open. All the valves in the system were also opened (Figure 4-1) except

1. W6 cutting off DWG from the system side of the Baratron 2,
2. W3 cutting off DWG from the reference side of the Baratron 1,

3. G9, G10, W7 cutting off the supply of nitrogen to the reference side of the Baratron 1,
4. T3 cutting off the sample degassing unit from the main line,
5. T6, T7 cutting off the sample ampoules from the main line,
6. G8 cutting off the mercury in manometer from the main line,

An indication of the total vacuum, apart from the Penning gauge, were given by Baratron 1 and 2's outputs, indicating zero differential pressure on both the sides of the Baratron 1 and 2.

5-2.1 Loading of the Sample in the Cell 1

The sample was initially degassed in the large degassing unit (Section 5-4.1). Before loading the sample in the Cell 1, it was again degassed two to three times in the sample ampoule. Baratron 1 zero was checked and adjusted to read zero.

H2 was shut. T8 was shut to isolate the degassing and loading manifold from the vacuum. Liquid air was poured into the cold finger of the cell 1, prior to the opening of tap T6 of the sample ampoule. The desired amount of the sample was evaporated from the sample ampoule taking precautions that

a. there was an adequate amount of liquid air in the cold finger of cell 1, and
b. T6 was open just enough, to ensure no overloading on the system side of the Baratron 1, which could affect the Baratron 1 zero.

After loading the sample, H1 and H3 were shut. Air at the thermostat temperature was run through the cold finger to evaporate the liquid air and heat the cell to the bath temperature.

H1 was slightly opened and the sample was expanded to the sample port (Px_1) of Baratron 1. Nitrogen pressure was exerted on the reference port (Pr_1) of Baratron 1 simultaneously through E1, W7 and W1, so that neither side of the Baratron was overloaded at any time. The nitrogen pressure was adjusted to be more than the sample pressure because the -ve side of the Baratron 1 had been calibrated against the +ve side of the Baratron 2 (Section 5-3.2).

Generally three hours were allowed to elapse after loading of the sample to ensure that it had attained equilibrium with the temperature of the bath. The equilibrium was also ensured by observing the constant differential pressure on Baratron 1.

5-2.2 Measurement of Pressure p_1 of the Sample in Cell 1

Full Scale and Null positions of both Baratrons were checked and adjusted to read 10.0000 and 0.0000 volts. W4 was opened to check and adjust Baratron 2 zero to read 0.0000 volts. The temperature of the bath was read using the Quartz thermometer and/or Platinum Resistance Thermometer.

Referring to Figure 4-1, H1 was slowly shut, till it was only half a turn open. N was then shut. The initial reading on the Baratron 1 was noted down when enough time had elapsed for the Baratron reading to be nearly constant. The procedure of closing the valve H1 slowly in steps and waiting till the Baratron reading was constant, was repeated, till it was completely shut. Before starting the pressure measurement, it was confirmed that

a. the opening of the cold finger to the atmosphere was blocked by the piece of wood and a screw cap.

b. H1 and H2 were shut properly.

c. N was shut and Baraton 1 was reading constant, ensuring that the sample had reached equilibrium with the temperature of the bath.

N was opened. National Semiconductor NS pressure transducer indicated the approximate pressure of nitrogen on the reference side of the Baratron 1. W3 was opened to connect the reference side of the Baratron 1 to the dead weight gauge. Both, the needle valve E3 and the "Whitey" valve W9 on the top of the Jar of DWG were shut. It was ensured that W7 was shut, so that there was no gradual leak of nitrogen through E1.

The test report of calibration - pressure gauge weights (RUSKA dead weight gauge, 1976) reports designation of each weight, its corresponding true mass (kg) and denomination in pressure (MPa). The pressure, corresponding to tare component (piston assembly), was substracted from the approximated pressure of nitrogen. Then the difference of the pressure was balanced by placing the appropriate combination of weights on the piston. The bell jar was placed on the DWG table (ensuring proper fit on O-ring, with a light grease sealing). W8 was opened to pump the inside of the jar. W6 was opened after one minute which ensured that the reference port of Baratron 2 was never overloaded and it read less than 10.00 volts indicating absolute pressure less than 10.00 mm inside the jar.

At the balanced position of the pressure by weights on the piston, the latter started rising up, from the cylinder assembly of the dead weight gauge. By adjusting W8 and E3, the position of the floating piston was monitored such that the bottom surface of the weight was in line with the mark on the jar within 1 mm. Only then the motor was started and kept in operation till the weights had acquired

some momentum.

At this position various pairs of Baratron 2 and Baratron 1 readings were noted (Appendix A6), indicating absolute pressure inside the bell jar and differential pressure on both the sides of Baratron 1. Piston temperature and the weights on the piston were noted.

A few observations of Baratron pair readings were repeated for slightly different pressure on the reference side of the Baratron 1, without changing any weight on the piston. Baratron 2 zero was checked by opening W4.

5-2.3 Measurement of Pressure p_2 of the Sample in Cell 2

After measuring p_1, the excess of the sample occupying the volume ΔV in the apparatus (Figure 4-1) had to be removed, so that only n moles of the sample in cell 1 could be used to measure p_2 and p_3. Both ports of the Baratron had to be evacuated simultaneously to avoid the accidental over-pressuring of any port.

Excess of the sample in volume ΔV could be returned to sample ampoule S2 (Figure 4-1). The latter was covered with liquid air and the sample in it was degassed once or twice. T8 was shut to prevent the excess of sample from cell 1, going into the diffusion pump. H3 was slightly opened. Nitrogen could be pumped through N, W1, W7, E1 and G14, using rotary pump (8). The two valves H3 and N were so adjusted that the differential pressure onto both the ports of Baratron 1 was within the range of its reading, while the sample was being transferred from cell 1 to the sample ampoule S2, and nitrogen was pumped out of the outer volume of cell 1.

After most of the sample had been transferred to sample

ampoule S2, T8 was opened to pump away the rest of the sample, using rotary pump (3) and the diffusion pump. H2 was also opened to ensure removal of any sample initially left in cell 2. This was a good check on the complete transfer of the sample from cell 2 to cell 1 in the previous run. H3 was then closed.

Another liquid air distillation was carried out to transfer the sample across from cell 1 to cell 2. To ensure complete transfer, the cold finger was topped with the liquid air for nearly one hour. Baratron 1 differential pressure close to ±0.005 volts for half an hour indicated complete transfer.

As discussed in the Section 5-2.1, the sample was expanded to the system port of the Baratron. Generally three hours elapsed before the measurement of pressure p_2 of the same number of moles as in cell 1. The "Hoke" valve H2 was ensured to be shut and p_2 was measured as discussed in Section 5-2.2.

5-2.4 Measurement of Pressure p_3 of the sample

After measuring pressure p_2 of the sample in cell 2, the sample had to be expanded into cell 1 and cell 2, to measure pressure p_3 of n moles of sample, occupying volume $V_1 + V_2$. H2 was opened. The excess of nitrogen had to be pumped through N, W1, W7, E1 and G14, as discussed in Section 5-2.3. H1 and N were so adjusted that there was never overloading of the pressure on either side of the Baratron 1, and the sample was expanded in both cells. Generally up to one hour elapsed after this step for the system to achieve equilibrium and to take measurement of pressure p_3.

H1 and H2 were shut, as discussed in Section 5-2.2. The pressure p_3 was measured.

5-3 Calibration of Gauges

As already mentioned it was considered appropriate to read the system pressure in dead weight gauge (DWG) units only. Baratron 1 was calibrated against Baratron 2 (Section 5-3.2), which in turn was, calibrated against the dead weight gauge (Section 5-3.3).

5-3.1 Calibration of National Semiconductor Gauge

The National Semiconductor (NS) gauge used to measure the approximate pressure of nitrogen on the reference side of Baratron 1, was calibrated against mercury pressure in a glass manometer. Its full scale was adjusted to read 7.6 volts at 1 atmosphere pressure.

G18 was opened to pump one side of the mercury manometer. The nitrogen was expanded to the NS gauge through G9, E1, W7, W1 and W2. The pressure was read as the difference of mercury heights in the manometer and as NS gauge output corresponding to the absolute pressure, on the "Philips" multimeter. The nitrogen pressure was increased in steps of 50-70 mm Hg to one atmosphere and corresponding NS gauge outputs were read on the multimeter. Then pressure was decreased in steps and the calibration was repeated. The NS gauge was adjusted to read 0 to 7.6 volts, corresponding to 0 to 760 mm Hg pressure.

5-3.2 Calibration of Baratron 1 against Baratron 2

Baratron 1 units were converted into Baratron 2 units, as the latter's DVM was found to have a good linearity in the whole scale. The reference side of the Baratron 1 was calibrated against the positive side of Baratron 2, to enable the shortest connection between the two (Figure 4-4), through N, W1, W5. The calibration was repeated at each temperature at which the experiment was carried out.

Full Scale and Null positions of both the Baratrons' digital volt meters were checked and adjusted to read 10.000 and 0.000. All the valves were open except W2, W3, W6, W8, G9, G10, G14 (Figure 4-4). after achieving vacuum as good as 10^{-5} torr in the whole system, the zero's of both Baratrons were adjusted by closing G4 to the vacuum. H3 and W4 were shut.

Nitrogen was expanded through G9, into the outer volume of cells (1 and 2) and the system connecting to Pr_1 port of Baratron 1 and Px_2 port of Baratron 2 (Figure 5-1). At equilibrium, the outputs on both Baratron DVMs were noted. The procedure was repeated for slightly varied pressures. The sum (ΔS) of Baratron 2 and Baratron 1 was plotted against Baratron 1 values (Appendix A5). This was expected to give a straight line through the origin. For example, if Bar_1 reads -2.0 volts corresponding to 2 mm Hg of absolute pressure on reference port (Pr_1) of Bar_1, then Bar_2 should read +2.0 volts corresponding to same 2 mm Hg of absolute pressure on the system port (Px_2) of Bar_2 (Figure 5-1). Hence,

$$\Delta s = Bar_1 + Bar_2 \qquad (5.1)$$

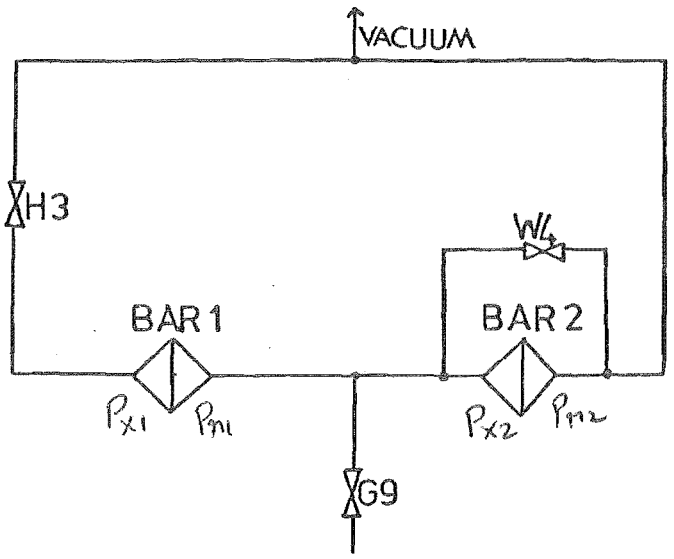

FIGURE 5-1

Circuit Diagram of the Apparaturs for the Calibration

Baratron 1 against Baratron 2

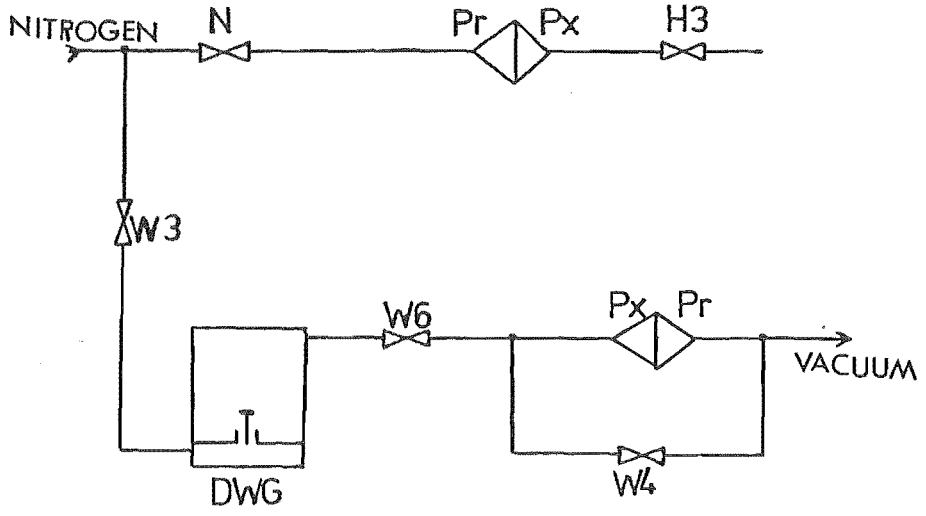

FIGURE 5-2

Circuit Diagram of the Apparatus for Calibration of Baratron 2

against Dead Weight Gauge

To read Bar_1 into Bar_2 units, Δs for corresponding Bar_1 reading was subtracted from it. Hence

$$\text{corrected } Bar_1 = Bar_1 - \Delta s \qquad (5.2)$$

For example,

Assuming $Bar_1 = -2.0000$ volts; $Bar_2 = 1.9995$ volts

$\Delta s = -0.0005$ volts

From equation (5.2)

$$\text{corrected } Bar_1 = -1.9995 \text{ volts}$$

The calibration was checked often, in between the subsequent runs. It was found to be consistent within ±0.005 volts. The calibration of Baratron 1 against Baratron 2, varied at the different temperature of the bath and all the calibrations are plotted in Appendix A5.

5-3.3 Calibration of Baratron 2 against DWG

Both sides of the Baratron 1 were pumped to 0.01 Pa. A nitrogen pressure of 10.000 mm Hg was applied to the system port of Baratron 1 through H3 (Figure 5-2). Roughly the same nitrogen pressure was applied on to the reference port of Baratron 1 through the "Nupro" valve.

The nitorgen pressure on Pr_1 port of Baratron 1 was measured using no weight on the piston of the DWG. For the balanced position indicated by the floating piston (Section 5-2.2), a few Bar_2 and Bar_1 observations were noted. The pressure exerted by the piston was corrected for the piston temperature. For these observations, the sum

of Bar_1, Bar_2 and DWG (indicating the system pressure P_s on Baratron 1, Section 6-1.3) was averaged and was always found to be within ±0.004 mm Hg. The Bar_2 value corresponding to the DWG pressure was noted.

For the same Bar_1 reading, the process was repeated by varying weights on the piston. The least square straight line was fitted to the data pairs of Bar_2 reading and DWG pressures, holding nearly the same differential pressure on Baratron 1 within ±0.005 mm. The relationship between Bar_2 and DWG was found to be

$$Bar_2(Volts) = 0.999602 \times DWG\ P(mm\ Hg) \qquad (5.3)$$

5-4 Materials

Benzene

"Koch Light Laboratory Ltd." benzene (thiophene free); grade "puriss" A.R., 95% distilling between 79.5 and 80.5°C was used as base stock.

Cyclohexane

"Koch Light Laboratory Ltd." cyclohexane "puriss" of guaranteed purity >99% was used as base stock.

n-Hexane

"Phillips" Research grade n-hexane, lot 1377 of guaranteed purity of 99.99 moles % was used without further purification.

5-4.1 The Purification of the Components

Benzene and cyclohexane needed further purification. They were distilled using a "Nester/Faust Mfg. Corp." Auto Annular Teflon Spinning Band Distillation Column. The middle 50% of the distilled component was collected at the reflux ratio of 1:30. The purity of the component was checked to be greater than 99.98 moles %, using a Gas Chromatograph ["Shimadzu"; type GC-R1A], with a flame ionization detector and "porapak Q" column.

Before loading samples in the sample manifold, the components were thoroughly degassed by multiple distillation in the degassing manifold (item 11 in Figure 4-1), using liquid air as the coolant. The manifold was evacuated between successive distillations, while the fluid was held frozen with liquid air. After approximately five distillations, the fluid was transferred to the sample ampoule S1 (item 12 in Figure 4-1).

B. MIXTURES

5-5 Operating Procedure

Prior to loading the system with the components, all the taps and valves were open (Figure 4-5). The whole apparatus was evacuated to below 0.05 Pa for at least twelve hours. The pressure transducer was adjusted and zeroed. The thermostat temperature was noted and the temperature controller was set.

Valves H2, H3 and H5 were closed. With tap T10 closed, an estimated amount of the first component was allowed to evaporate from the sample ampoule to solidify onto the liquid air cooled cold finger of cell 1. After half an hour, valve H1 was closed. Using hot compressed air at almost the thermostat temperature, the remaining coolant in the cold finger was removed and the latter was warmed. Tap T10 was opened to evacuate the sample supply line. After waiting another hour, H2 was opened and tap T10 closed. An excess of component 2 required to balance the pressure in the cell 1, was transferred into cell 2. The cold finger was warmed to the thermostat temperature.

Both cold fingers were blocked using wooden blocks and the top of the bath was covered with a 1" thick sheet of glass wool. After another 3 to 4 hours, tap T12 was closed and shut-off valve V2 opened. Dry nitrogen was admitted to the pressure transducer and the mercury manometer through V3 and needle valve E1, until the pressure transducer was zeroed or brought to within 130 Pa of the pressure in cell 1 and reference cell. The valve V3 was used to control the fine adjustment of zero of the pressure transducer by adjusting the bellows. The pressure on the mercury manometer was then measured. This gave the

initial loading pressure (p). The temperature of the bath was measured. Tap T12 was opened to evacuate the nitrogen from the system.

After evacuating the nitrogen, valve H6 was closed and H5 opened. Tap T4 was opened and T10 closed. Valve H2 was opened slightly to bleed the excess of the component 2 from cell (2) to the sample ampoule containing that component, until zero pressure differential was indicated on the transducer.

After giving time for the cells to equilibrate, H3 was opened. Then valve H4 was carefully and slowly closed and the reading on the pressure transducer noted. This was the zero pressure difference reading. H5 was closed to avoid an overload of deflection from the reference side, when the mixture was frozen.

Liquid air was poured into one of the cold fingers of cell 1 or cell 2. About half an hour was given, for the mixing of the contents of both cylinders. The frozen cold finger was heated back to thermostat temperature and allowed to come to thermal equilibrium. Valve H5 was opened.

This technique is called the "Open Tap" technique, as the pressure being nearly same in all three cells, H3 and H5 were wide open to allow the pressure fluctuations to settle down, before closing H4. Though H5 is closed before inducing mixing in either cell, it is opened again to measure the pressure change. By these means, the effect of volume changes caused by opening and shutting the valves is avoided and the likelihood of a transducer zero shift is greatly reduced.

Once the reading on the pressure transducer remained constant for several hours, it was noted. The reading of the pressure transducer gave the change in system pressure on mixing (Δp). The zero shift might also be checked again by opening valve H4, once the measurement had been completed. In practice the zero pressure

difference reading before and after mixing had been reported within 0.01 Pa (Shannon, 1976). Later the sample was distilled out of the cells into the ampoule containing used components. All the taps and valves were opened and the system evacuated in the preparation of the subsequent run.

Thus the whole operating procedure, gave the three required variables (equation 3.28), namely

1. the initial pressure of the system (p),
2. the temperature of the experiment (T), and
3. the change in pressure (Δp), after the mixing of two components and the equipment had returned to the initial temperature.

5-5.1 Materials

Materials for these experiments were prepared as discussed in Section 5-4.

CHAPTER 6

EXPERIMENTAL RESULTS

A. PURE COMPONENTS

6-1 Organisation of Raw Data and Calculation Procedure for the Results

The raw data for each loading of the apparatus comprises of

1. bath and piston temperature,
2. weights on the piston of dead weight gauge and
3. outputs of the differential pressure gauges, Baratron 1 and Baratron 2, at the balanced position of DWG gauge, for any pressure measurement.

6-1.1 Temperature

The bath temperature, when measured by the platinum resistance thermometer, is corrected for the resistance of the standard resistance at that temperature, using the calculation procedure shown in Appendix A1.

The bath temperature, when measured by the Quartz thermometer is read as the difference of temperatures ($T_1 - T_2$), where T_2 is the temperature for the probe immersed inside the ice bath and T_1 is the

temperature for the probe immersed inside the dummy bulb in the air bath. The reported temperatures in the tables are the tempertures corrected for the zero difference ($T_1 - T_2$) at the ice point. This was observed to be $-0.045^{o}C$, with both probes immersed at the same level, inside the ice bath.

6-1.2 DWG Pressure

The pressures exerted by the individual weights on the piston are corrected for the change in the area of the piston and for the piston temperature at the time of pressure measurement as described in Appendix A2. The sum of the pressures exerted by each weight on the piston (for balanced position) and that exerted by the piston alone gives the total DWG pressure.

6-1.3 Total Pressure

The simple diagram of the pressure measuring circuit is shown in Figure 6-1.

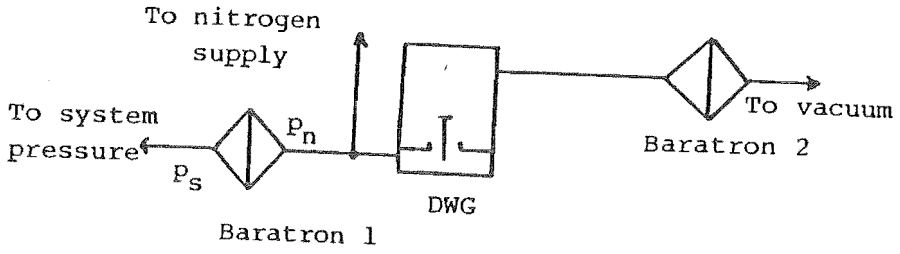

FIGURE 6-1

Pressure Measuring Circuit

System pressure (p_s) is indicated as the differential pressure, (in Bar_1 units, V') compared to that of nitrogen (p_n) on Baratron 1. Hence,

$$p_s - p_n = Bar_1\ (V')$$
$$p_s = Bar_1\ (V') + p_n \qquad (6.1)$$

Nitrogen pressure is the sum of DWG pressure (in mm Hg units) and pressure inside the bell jar, on top of DWG table, as indicated by the absolute pressure (in Bar_2 units, V) on Baratron 2. Hence,

$$p_n = Bar_2\ (V) + DWG\ (mm\ Hg) \qquad (6.2)$$

substituting in equation (6.1)

$$p_s = Bar_1\ (V') + Bar_2\ (V) + DWG\ (mm\ Hg) \qquad (6.3)$$

As per calibration of Bar_1 against Bar_2 (section 5-3.2) and calibration charts for correction to Baratron 1 readings at all temperatures as plotted in Appendix A5, the corrected Bar_1 is expressed as

$$Corr.\ Bar_1\ (V) = Bar_1\ (V') - \Delta s \qquad (5.2)$$

where corrected Bar_1 is display of the differential pressure (volts) on Baratron 1, corrected to read in Bar_2 (V) units. Δs is the sum of (Bar_1 + Bar_2) for any particular Bar_1 reading. Hence

$$p_s = [(Bar_1 - \Delta s) + Bar_2]\ (V) + DWG\ (mm) \qquad (6.4)$$

Since $1\ Bar_2\ (V) = 0.999602 \times DWG\ (mm)$ (5.3)

$$p_s(mm) = (Bar_1 - \Delta s + Bar_2)/0.999602 + DWG \quad (6.5a)$$

and $$p_s(pascal) = p_s(mm) \times 133.3224 \quad (6.5b)$$

6-1.4 Organisation of Data

Appendix A6 (Part I) gives one complete set of the original instrument readings, and sample calculations for the determination of the total pressure. Three pressure measurements at the respective temperatures for each run are tabulated in Appendix A7, for n-hexane, benzene and cyclohexane.

Using the iterative technique described in Section 3-2, the volume series second virial coefficient $B_{apparent}$ can be calculated as explained in Appendix A3. The calculated results of $\beta_{apparent}$ and $B_{apparent}$ are tabulated at their corresponding values of $(p_1 + p_2 - p_3)$ in the order of decreasing pressure in Tables 6-1 to 6-12.

6-2 Analysis Procedure For the Results

From equation (3.5a)

$$\beta_{apparent} = \beta + \gamma(p_1 + p_2 - p_3) \quad (6.6a)$$

$$= RT(1/p_3 - 1/p_1 - 1/p_2) \quad (6.6b)$$

Straight line regression coefficients (a and b) are deduced by the method of weighted least squares analysis (Appendix A4) for the set of $\beta_{apparent}$ and $(p_1 + p_2 - p_3)$ pairs using the form

$$y = a + bx \tag{6.7}$$

where y is apparent second virial coefficient ($\beta_{apparent}$) and x is the pressure term $(p_1 + p_2 - p_3)$. Comparing equations (6.6a) and (6.7), "a" corresponds to the pressure series "true" second virial coefficient β and "b" corresponds to the third virial coefficient γ. The regression coefficients "a" and "b" are reported, in Tables 6-1 to 6-12, for the results for second virial coefficients of n-hexane, benzene and cyclohexane at various temperatures.

By plotting $\beta_{apparent}$ against $(p_1 + p_2 - p_3)$, we obtain β as the intercept, where

$$\beta = \lim_{(p_1 + p_2 - p_3) \to 0} \beta_{apparent} \tag{6.8}$$

This determines a pressure series "true" second virial coefficient at the temperature T for the component under investigation.

$B_{apparent}$ when plotted against $(p_1 + p_2 - p_3)$, should produce a line that intersects the y-axis at the same point as obtained from graph of $\beta_{apparent}$ versus $(p_1 + p_2 - p_3)$ as requirement in equation (3.~~11~~ 5),

$$\beta = B \qquad (3.~~11~~\ 1.5)$$

The regression coefficients (a' and b') for the set of $B_{apparent}$ and $(p_1 + p_2 - p_3)$ are obtained by the same weighted least squares analysis

method (Appendix A4), using the form $y' = a' + b'x$, where y' corresponds to $B_{apparent}$ for the pressure term $(p_1 + p_2 - p_3)$ represented as x. However, a' may not necessarily correspond to volume series "true" second virial coefficient B, and "b'" is not the third virial coefficient C, as a linear relationship similar to equation (6.6a), still need to be established between the $B_{apparent}$ and the pressure term $(p_1 + p_2 - p_3)$.

The plots are shown in the Figures 6-1 to 6-12. Each plot has a line perpendicular to the x-axis at the point TP, to indicate the value of $(p_1 + p_2 - p_3)$ corresponding to a loading pressure equal to 0.6 times the saturation vapour pressure of the vapours at that temperature. The bold line error bands on both sides of the pressure series straight line fit indicate the maximum error band width, $\Delta\beta_1$ corresponding to a maximum error equal to 5 Pa in each of the pressure measurements. The broken line error bands indicate the probable error band width, $\Delta\beta_2$ corresponding to a probable error of 3 Pa in each of the pressure measurements. As is obvious, the error width widens with the decrease in the loading pressure for each set.

Besides showing the analysis procedure for the second virial coefficients $\beta_{apparent}$ and $B_{apparent}$, Appendix A6 (Part II) also shows sample calculations for their correlation and comparison with other workers' results (see Chapter 7 for the tables and figures for comparison). The literature values for the components have been taken from Dymond and Smith (1980) and the smooth curve has been plotted through the best existing data. It is also demonstrated that the existing measurements reported in the literature may be in error due to the neglect of the effect of the third virial coefficient.

Hayden and O'Connell (1975) and Tsonopoulos (1974) estimations, described in Appendices A8 and A9, have been used to compare the

results.

Having determined the experimental values of the second virial coefficients, the information is used to obtain the two adjustable parameters of the Lennard-Jones (6-12) potential, using the procedure described by Hirschfelder et al. (1954). The values of parameters σ and ε/k are compared with the literature values.

A quantity k_b is defined by

$$k_b = B(T_2)/B(T_1) \tag{6.9}$$

The ε/k is determined by the trial and error solution of the equation .

$$k_b = \left[\frac{B^*(kT_2/\varepsilon)}{B^*(kT_1/\varepsilon)}\right] \tag{6.10}$$

ε/k may be first approximated using the values calculated from boiling temperature (T_b), melting temperature (T_m) or critical temperature (T^c) using equations

$$\varepsilon/k = 1.15\ T_b \tag{6.11.1}$$

$$\varepsilon/k = 1.92\ T_m \tag{6.11.2}$$

$$\varepsilon/k = 0.77\ T^c \tag{6.11.3}$$

The collision diameter is obtained from

$$b_0 = 1.2615\ \sigma^3 = \left[\frac{B(T_1)}{B^*(T_i^*)}\right] \tag{6.11.4}$$

(3.11)

where T_i is either T_1 or T_2.

6-3 Calculated Results

Calculated results for n-hexane, benzene and cyclohexane are organised in this section. Each Table (Tables 6-1 to 6-12) reports the pressure term, $(p_1 + p_2 - p_3)$ and corresponding $\beta_{apparent}$ and $B_{apparent}$ for a particular run, in the order of decreasing loading pressure. Each run is weighted according to the likely error in the measurement of maximum loading pressure, p_1, in that particular run and is given by equation

$$W_i = 1/E1_i \qquad (6.12)$$

where $E1_i$ is the probable error, $\delta\beta_{probable}$, in β measurement, as expressed by equation (3.25). W_i is the "weight".

The regression coefficients, using weighted least-squares straight line analysis as detailed in Section 6-2 and Appendix A4, for the pressure series (a and b) and for the volume series (a' and b') are also reported along with each table.

6-3.1 Results for n-hexane

Apparent second virial coefficients $\beta_{apparent}$ and $B_{apparent}$ of n-hexane have been calculated from the raw data recorded in Tables A7-1 (Appendix A7) at temperatures 323.15, 328.15, 338.15, 348.15, 358.15, 373.15 K The results are tabulated in Tables 6-1 to 6-6 and are plotted in Figures 6-2 to 6-7. The standard error in the extrapolated

values of B and β are also tabulated and range from ± 30 to ± 50 $cm^3\ mol^{-1}$. However, as is obvious from the plots, that the precision of $\beta_{apparent}$ or $B_{apparent}$ determined in same pressure ranges, as used by other workers, is within ± 10 to ± 25 $cm^3\ mol^{-1}$.

Some of the sets of measurements have been repeated for n-hexane and some runs for n-hexane at various temperatures have been discarded because loading pressure is much greater than 0.6 times the saturation vapour pressure of vapours at those temperatures. These runs are tabulated in the following tables.

Table 6-1. **Results for Hexane at 323.15 K**

Run No.	$(p_1 + p_2 - p_3)$ / Pa	$\beta_{apparent}$ / $cm^3\ mol^{-1}$	$B_{apparent}$ / $cm^3\ mol^{-1}$
6	62332	-1528	-1475
11	60515	-1556	-1502
1	57492	-1510	-1462
7	52322	-1565	-1516
12	50789	-1555	-1508
2	48034	-1604	-1559
8	43878	-1550	-1512
13	42592	-1565	-1527
3	40934	-1521	-1487
9	36782	-1503	-1474
14	35695	-1551	-1521
4	34165	-1517	-1489
10	30793	-1621	-1593
15	29892	-1561	-1536
5	29076	-1658	-1631

Pressure Series

$a = -1605\ cm^3\ mol^{-1}$ Standard error = $42\ cm^3\ mol^{-1}$

$b = 1.120 \times 10^{-3}\ cm^6\ mol^{-2}$ Standard error = $8.402 \times 10^{-4}\ cm^6\ mol^{-2}$

Volume Series

$a' = -1606\ cm^3\ mol^{-1}$ Standard error = $40\ cm^3\ mol^{-1}$

$b' = 2.002 \times 10^{-3}\ cm^6\ mol^{-2}$ Standard error = $7.986 \times 10^{-4}\ cm^6\ mol^{-2}$

FIGURE 6-2

Extrapolation of observations for n-hexane to zero pressure at 323.15 K

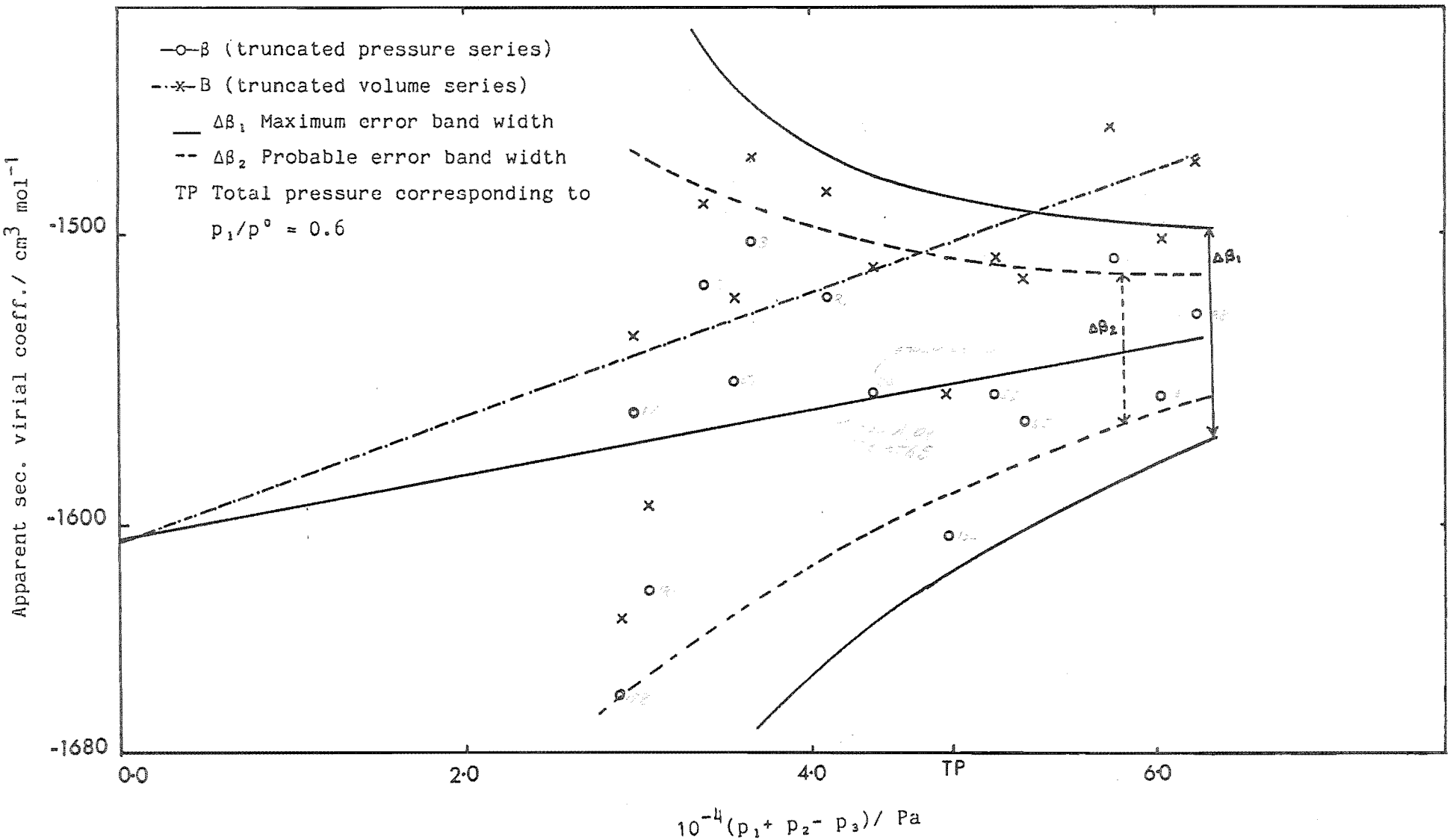

Table 6-2. **Results for Hexane at 328.15 K**

Run No.	$(p_1 + p_2 - p_3)$ / Pa	$\beta_{apparent}$ / $cm^3\ mol^{-1}$	$B_{apparent}$ / $cm^3\ mol^{-1}$
1	73440	-1535	-1473
7	65320	-1568	-1510
2	61624	-1568	-1513
8	54976	-1579	-1533
3	51837	-1579	-1530
9	46077	-1529	-1491
4	43424	-1571	-1533
5	36502	-1580	-1548

Note : Run 6 (Table A7-1.2b) has loading pressure (p_1) higher than the desired loading pressure and hence is not included in the Table (6-2) for weighted least square analysis.

Pressure Series

$a = -1607\ cm^3\ mol^{-1}$ Standard error = $37\ cm^3\ mol^{-1}$

$b = 7.848 \times 10^{-3}\ cm^6\ mol^{-2}$ Standard error = $6.184 \times 10^{-4}\ cm^6\ mol^{-2}$

Volume Series

$a' = -1604\ cm^3\ mol^{-1}$ Standard error = $34\ cm^3\ mol^{-1}$

$b' = 1.615 \times 10^{-3}\ cm^6\ mol^{-2}$ Standard error = $5.749 \times 10^{-4}\ cm^6\ mol^{-2}$

FIGURE 6-3

Extrapolation of observations for n-hexane to zero pressure at 328.15 K

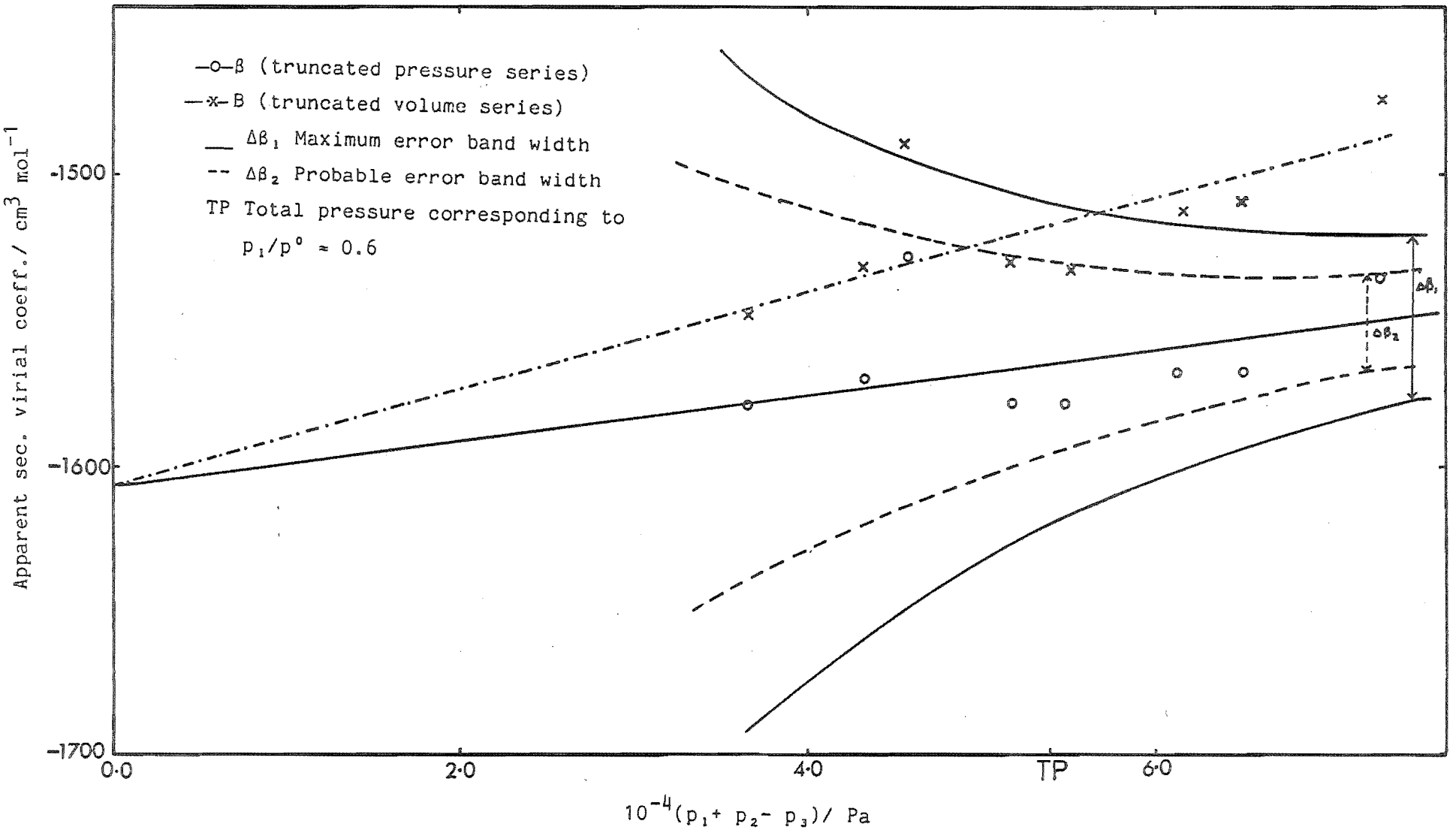

Table 6-3. **Results for Hexane at 338.15 K**

Run No.	$(p_1 + p_2 - p_3)$ / Pa	$\beta_{apparent}$ / $cm^3\ mol^{-1}$	$B_{apparent}$ / $cm^3\ mol^{-1}$
1	82769	-1375	-1320
2	69532	-1360	-1315
3	58321	-1383	-1344
4	48928	-1362	-1331
5	40991	-1455	-1425
6	34359	-1354	-1333

Pressure Series

$a = -1408\ cm^3\ mol^{-1}$ Standard error = $51\ cm^3\ mol^{-1}$

$b = 4.879 \times 10^{-3}\ cm^6\ mol^{-2}$ Standard error = $7.590 \times 10^{-4}\ cm^6\ mol^{-2}$

Volume Series

$a' = -1409\ cm^3\ mol^{-1}$ Standard error = $49\ cm^3\ mol^{-1}$

$b' = 1.149 \times 10^{-4}\ cm^6\ mol^{-2}$ Standard error = $7.227 \times 10^{-4}\ cm^6\ mol^{-2}$

FIGURE 6-4

Extrapolation of observations for n-hexane to zero pressure at 338.15 K

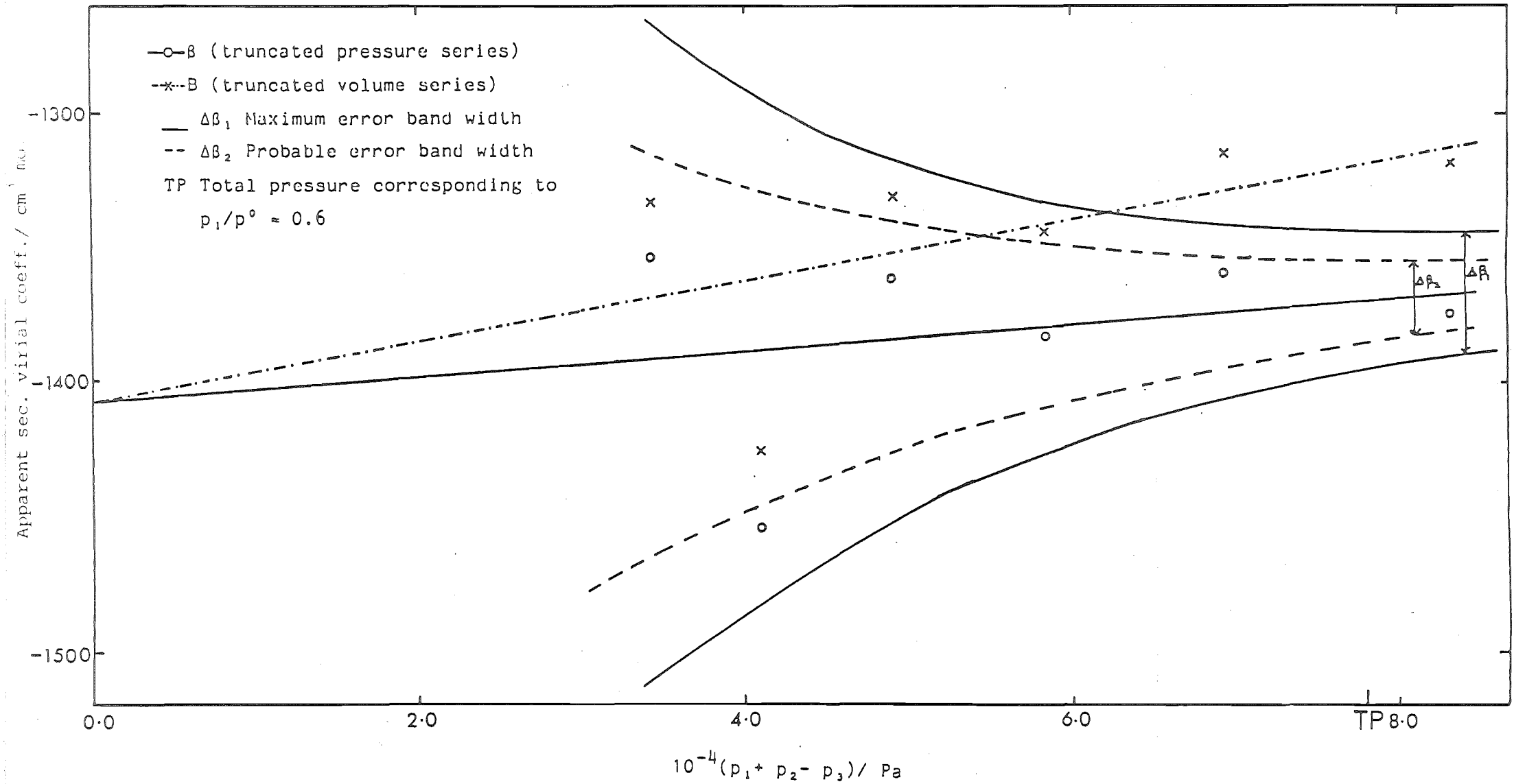

Table 6-4. **Results for Hexane at 348.15 K**

Run No.	$(p_1 + p_2 - p_3)$ / Pa	$\beta_{apparent}$ / $cm^3\ mol^{-1}$	$B_{apparent}$ / $cm^3\ mol^{-1}$
3	78415	-1255	-1213
18	70930	-1258	-1220
9	70120	-1259	-1221
11	66058	-1273	-1237
19	59498	-1266	-1234
12	55383	-1298	-1266
5	55846	-1251	-1221
20	49870	-1225	-1200
13	46432	-1232	-1209
21	41768	-1263	-1241
14	38892	-1354	-1331

Note : All the runs tabulated in Appendix (A7-1.4) having loading pressure greater than 0.55 times saturation vapour pressure at 348.15 K, have been excluded for weighted least square analaysis.

Pressure Series

$a = -1294\ cm^3\ mol^{-1}$ Standard error = $45\ cm^3\ mol^{-1}$

$b = 4.980 \times 10^{-3}\ cm^6\ mol^{-2}$ Standard error = $7.099 \times 10^{-4}\ cm^6\ mol^{-2}$

Volume Series

$a' = -1295\ cm^3\ mol^{-1}$ Standard error = $43\ cm^3\ mol^{-1}$

$b' = 1.039 \times 10^{-4}\ cm^6\ mol^{-2}$ Standard error = $6.823 \times 10^{-4}\ cm^6\ mol^{-2}$

FIGURE 6-5

Extrapolation of observations for n-hexane to zero pressure at 348.15 K

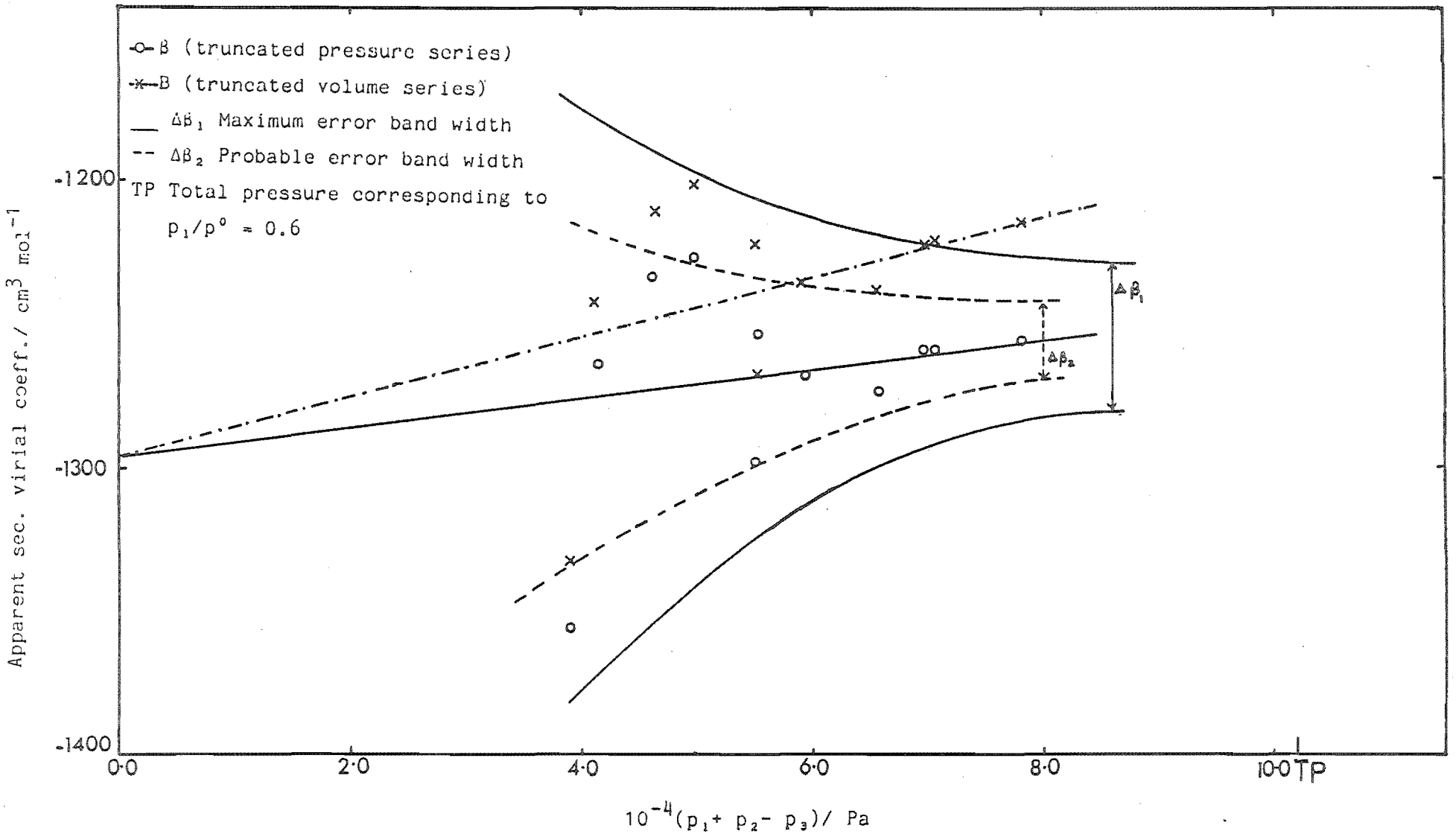

Table 6-5. **Results for Hexane at 358.15 K**

Run No.	$(p_1 + p_2 - p_3)$ / Pa	$\beta_{apparent}$ / $cm^3\ mol^{-1}$	$B_{apparent}$ / $cm^3\ mol^{-1}$
2	105766	-1180	-1131
3	88853	-1177	-1136
4	74575	-1189	-1154
5	62546	-1203	-1173
6	52442	-1159	-1136
7	43918	-1252	-1230
8	36787	-1197	-1181

Pressure Series

$a = -1220\ cm^3\ mol^{-1}$ Standard error = $29\ cm^3\ mol^{-1}$

$b = 4.159 \times 10^{-3}\ cm^6\ mol^{-2}$ Standard error = $3.492 \times 10^{-4}\ cm^6\ mol^{-2}$

Volume Series

$a' = -1220\ cm^3\ mol^{-1}$ Standard error = $28\ cm^3\ mol^{-1}$

$b' = 8.758 \times 10^{-4}\ cm^6\ mol^{-2}$ Standard error = $3.368 \times 10^{-4}\ cm^6\ mol^{-2}$

FIGURE 6-6

Extrapolation of observations for n-hexane to zero pressure at 358.15 K

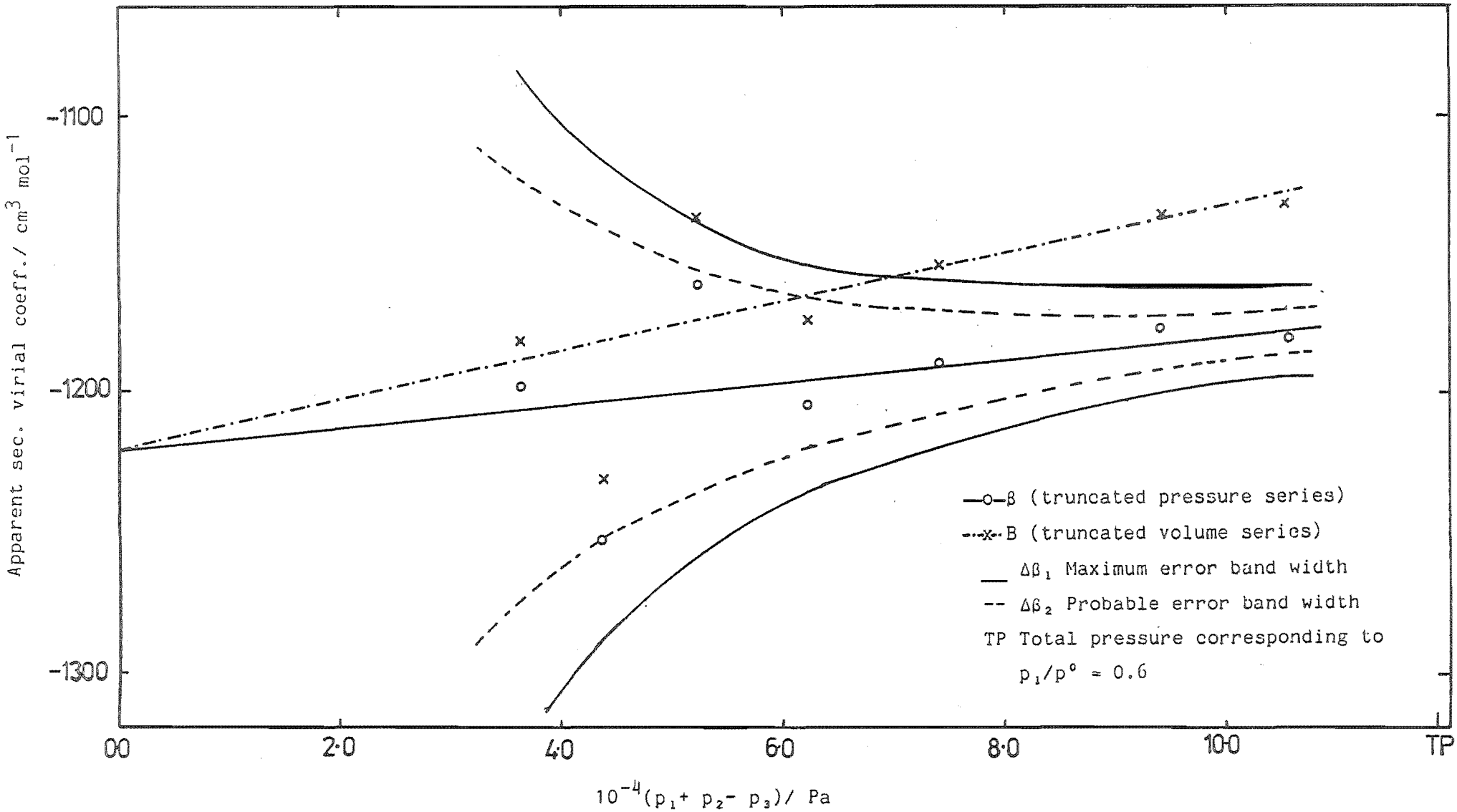

Table 6-6. **Results for Hexane at 373.15 K**

Run No.	$(p_1 + p_2 - p_3)$ / Pa	$\beta_{apparent}$ / $cm^3\ mol^{-1}$	$B_{apparent}$ / $cm^3\ mol^{-1}$
8	133141	-1079	-1038
1	125450	-1107	-1058
9	111975	-1040	-1000
2	104996	-1084	-1044
10	93991	-1034	-1004
3	89552	-1097	-1063
11	78857	-1045	-1021
4	74808	-1139	-1108
12	66107	-1021	-1005
5	63729	-1168	-1140
13	55400	-1124	-1110
6	53191	-1121	-1110
14	46399	-1117	-1111
7	45294	-1056	-1041

Pressure Series

$a = -1101\ cm^3\ mol^{-1}$ Standard error = $41\ cm^3\ mol^{-1}$

$b = 1.943 \times 10^{-3}\ cm^6\ mol^{-2}$ Standard error = $3.938 \times 10^{-4}\ cm^6\ mol^{-2}$

Volume Series

$a' = -1109\ cm^3\ mol^{-1}$ Standard error = $38\ cm^3\ mol^{-1}$

$b' = 6.352 \times 10^{-4}\ cm^6\ mol^{-2}$ Standard error = $3.705 \times 10^{-4}\ cm^6\ mol^{-2}$

FIGURE 6-7

Extrapolation of observations for n-hexane to zero pressure at 373.15 K

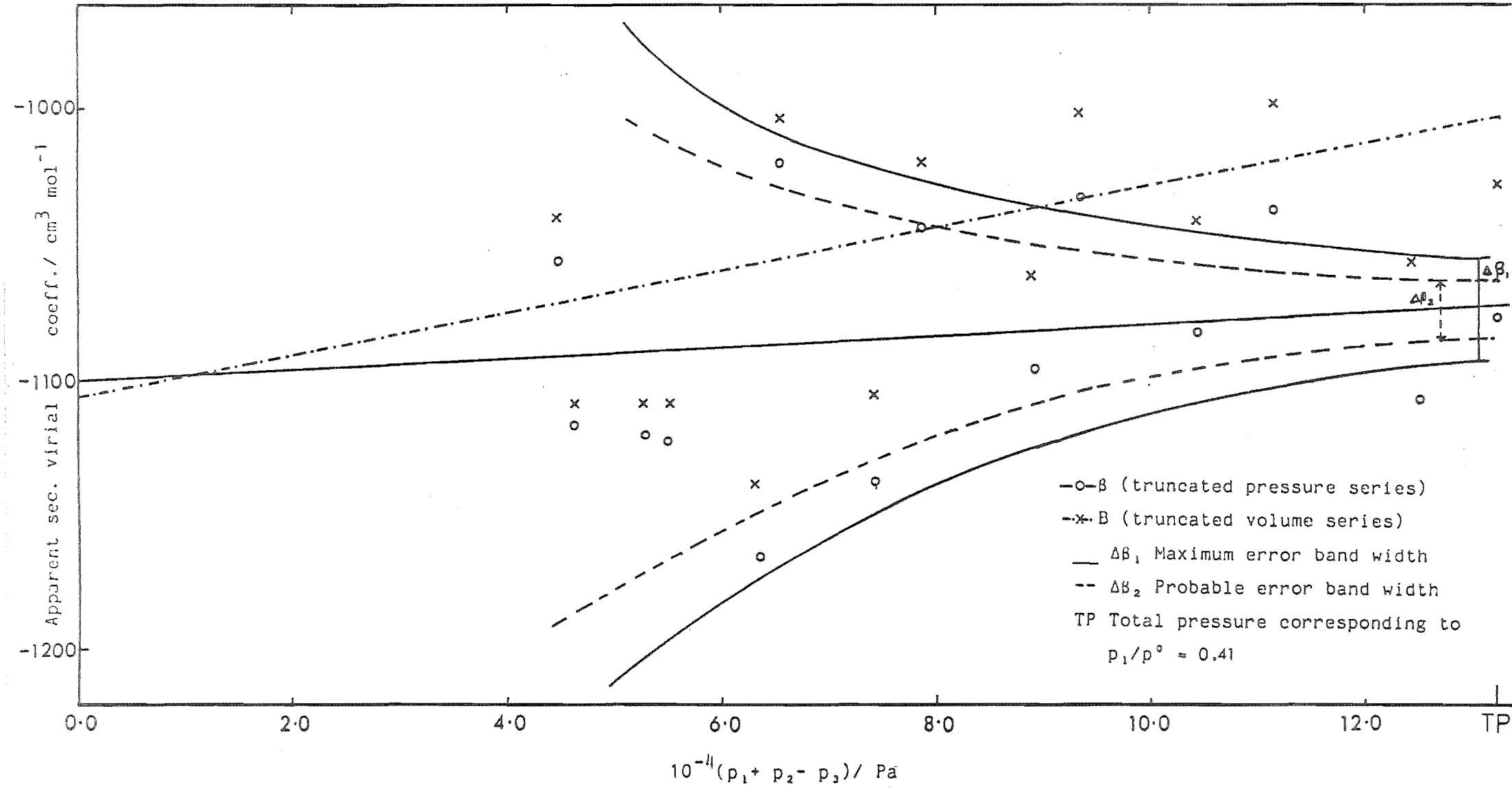

6-3.2 Results for Benzene

Apparent second virial coefficients $B_{apparent}$ and $\beta_{apparent}$ of benzene have been calculated at 323.15 , 348.15, 373.15 K from the raw data in tables A7-2 (Appendix A7). The results are tabulated in Tables 6-7 to 6-9 and are plotted in Figures 6-8 to 6-10. The standard error ranges from ±40 $cm^3\ mol^{-1}$ to ±220 $cm^3\ mol^{-1}$. The maximum difference between β and B for benzene is only 9 $cm^3\ mol^{-1}$ at 323.15 K.

The standard error in the calculation of β at 323.15 K is 200 $cm^3\ mol^{-1}$. The results are suspect however because we are forced to work at very low pressure and do not have a wide working range below p/p^o = 0.6. The error band width, even for the probable error of 3 Pa in pressure measurement, ranges from ±100 $cm^3\ mol^{-1}$ (for corresponding p/p^o equal to 0.72) to ±200 $cm^3\ mol^{-1}$ (for corresponding p/p^o equal to 0.6). The results for benzene at 323.15 K, as plotted in Figure 6-8, show that all the $\beta_{apparent}$, except one, are in the probable error band width. Still $\beta_{apparent}$ at any particular pressure term $(p_1 + p_2 - p_3)$ may vary as much as 70 $cm^3\ mol^{-1}$ to 100 $cm^3\ mol^{-1}$. Thus for this particular case the values of $\beta_{apparent}$ values at different loading pressures, are averaged. Our best estimate is -1125 $cm^3\ mol^{-1}$, between averaged $\beta_{apparent}$ value of -1165 $cm^3\ mol^{-1}$ and extrapolated β having weighted least square straight line regression coefficient of -1079 $cm^3\ mol^{-1}$.

The maximum loading pressure at 323.15 K, corresponds to 0.72 times the saturation vapour pressure of benzene. The errors due to adsorption of the vapours on the surface are also expected as discussed in Section 3-5.

Table 6-7. **Results for Benzene at 323.15 K**

Run No.	$(p_1 + p_2 - p_3)$ / Pa	$\beta_{apparent}$ / $cm^3\ mol^{-1}$	$B_{apparent}$ / $cm^3\ mol^{-1}$
1	35271	-1234	-1216
2	33817	-1179	-1163
3	32409	-1037	-1026
4	31688	-1157	-1143
5	30277	-1179	-1166
6	29535	-1203	-1189
7	28302	-1178	-1166
8	28144	-1221	-1208
9	27119	-1165	-1154
10	26524	-1100	-1091

Pressure Series

$a = -1079\ cm^3\ mol^{-1}$ Standard error = $220\ cm^3\ mol^{-1}$

$b = -2.860 \times 10^{-3}\ cm^6\ mol^{-2}$ Standard error = $7.119 \times 10^{-3}\ cm^6\ mol^{-2}$

Volume Series

$a' = -1088\ cm^3\ mol^{-1}$ Standard error = $215\ cm^3\ mol^{-1}$

$b' = -2.131 \times 10^{-3}\ cm^6\ mol^{-2}$ Standard error = $6.933 \times 10^{-3}\ cm^6\ mol^{-2}$

FIGURE 6-8

Extrapolation of observations for benzene to zero pressure at 323.15 K

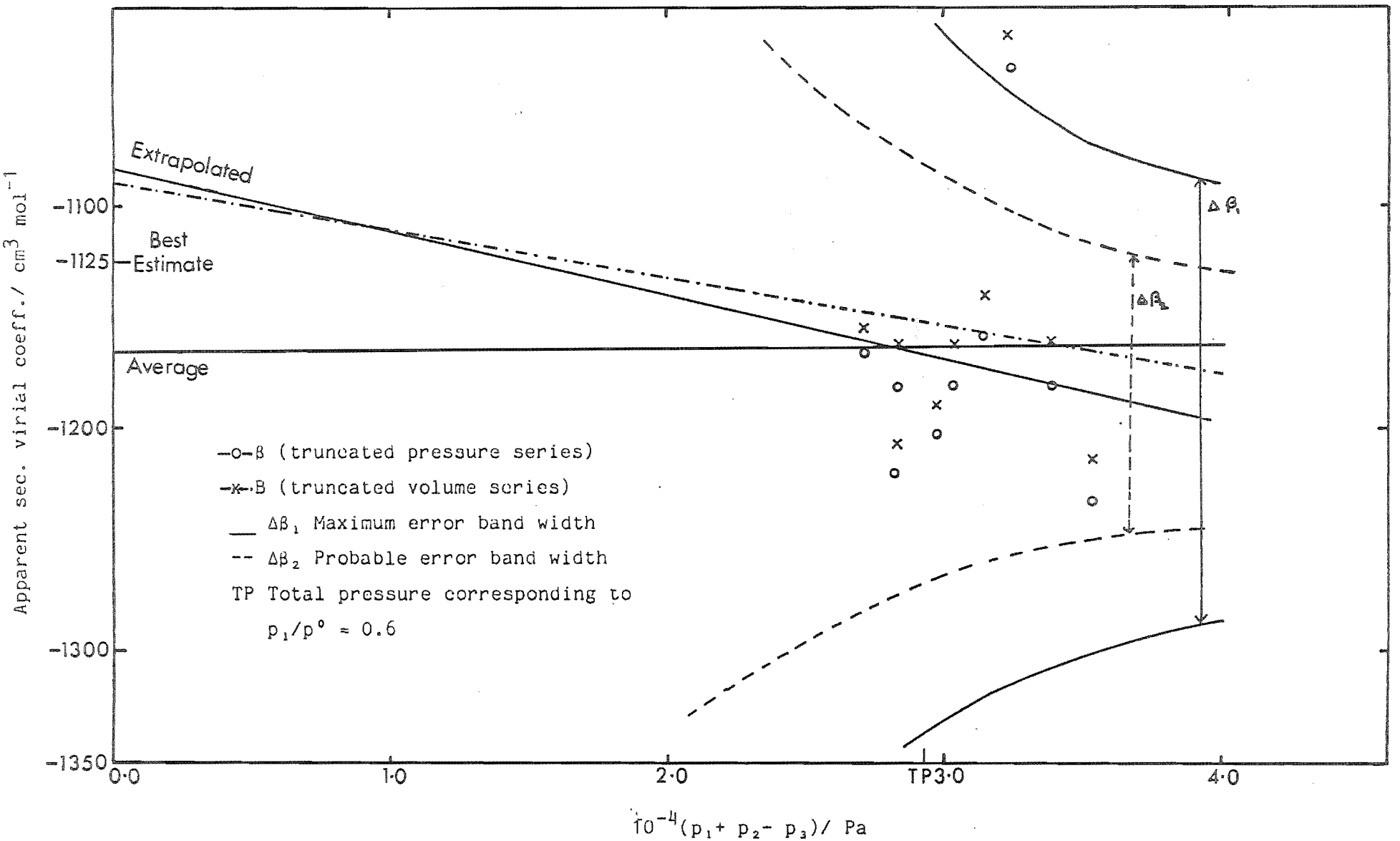

Table 6-8. **Results for Benzene at 348.15 K**

Run No.	$(p_1 + p_2 - p_3)$ / Pa	$\beta_{apparent}$ / $cm^3\ mol^{-1}$	$B_{apparent}$ / $cm^3\ mol^{-1}$
1	73933	-986	-961
2	61973	-1004	-983
3	51909	-1008	-990
4	43490	-928	-916
5	36405	-940	-930
6	30462	-1027	-1018

Pressure Series

$a = -\ 953\ cm^3\ mol^{-1}$ Standard error = $58\ cm^3\ mol^{-1}$

$b = -5.583 \times 10^{-4}\ cm^6\ mol^{-2}$ Standard error = $9.733 \times 10^{-4}\ cm^6\ mol^{-2}$

Volume Series

$a' = -\ 957\ cm^3\ mol^{-1}$ Standard error = $57\ cm^3\ mol^{-1}$

$b' = -1.684 \times 10^{-4}\ cm^6\ mol^{-2}$ Standard error = $9.477 \times 10^{-4}\ cm^6\ mol^{-2}$

FIGURE 6-9

Extrapolation of observations for benzene to zero pressure at 348.15 K

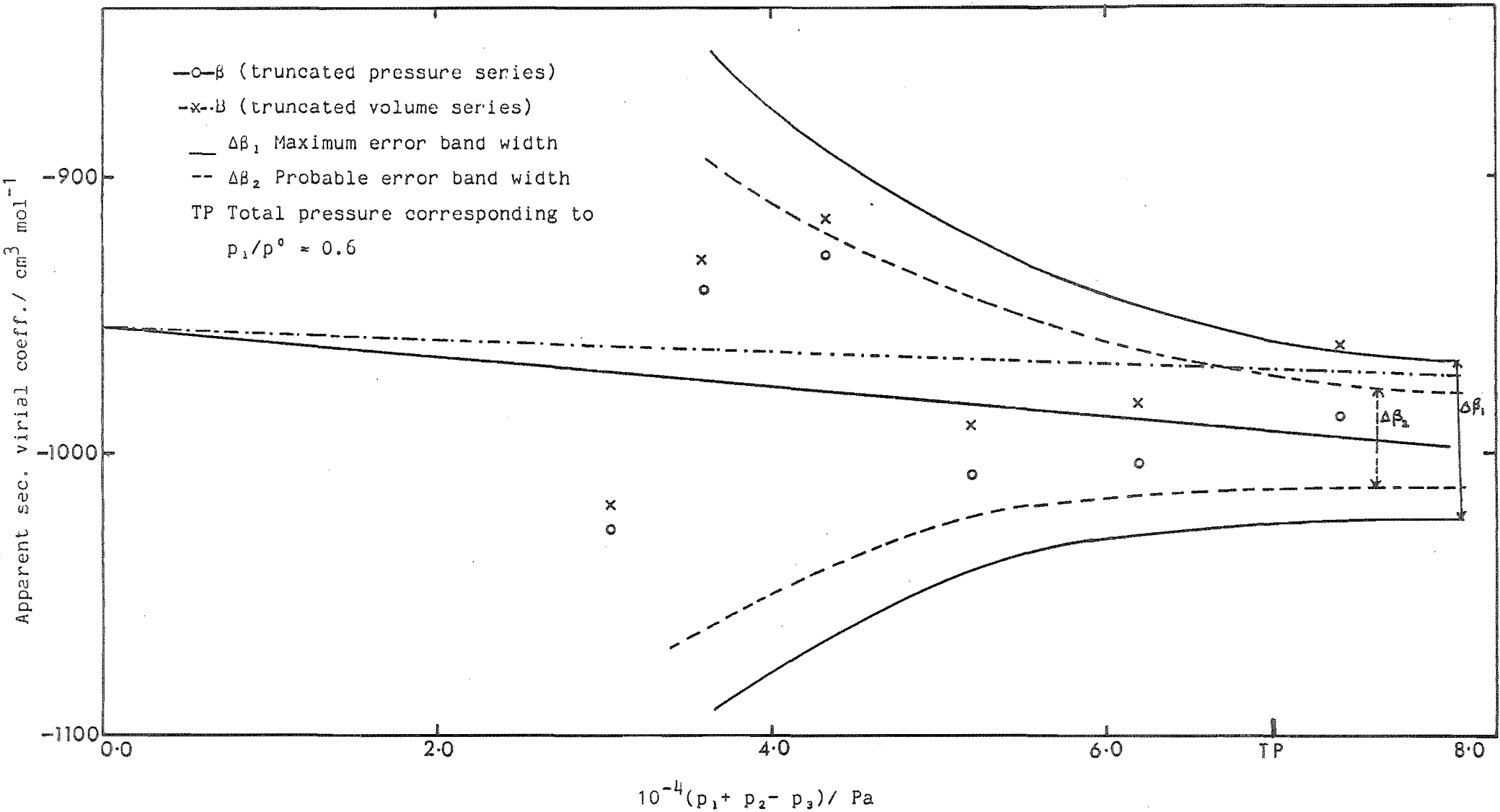

Table 6-9. **Results for Benzene at 373.15 K**

Run No.	$(p_1 + p_2 - p_3)$ / Pa	$\beta_{apparent}$ / $cm^3\ mol^{-1}$	$B_{apparent}$ / $cm^3\ mol^{-1}$
1	132397	-860	-829
2	124907	-856	-827
3	104781	-895	-868
4	91746	-823	-803
5	78167	-824	-807
6	76885	-820	-803
7	64406	-786	-773
8	53887	-828	-817
9	45129	-913	-902

Pressure Series

$a = -799\ cm^3\ mol^{-1}$ Standard error = $41\ cm^3\ mol^{-1}$

$b = -4.905 \times 10^{-4}\ cm^6\ mol^{-2}$ Standard error = $3.890 \times 10^{-4}\ cm^6\ mol^{-2}$

Volume Series

$a' = -801\ cm^3\ mol^{-1}$ Standard error = $39\ cm^3\ mol^{-1}$

$b' = -2.372 \times 10^{-4}\ cm^6\ mol^{-2}$ Standard error = $3.737 \times 10^{-4}\ cm^6\ mol^{-2}$

FIGURE 6-10

Extrapolation of observations for benzene to zero pressure at 373.15 K

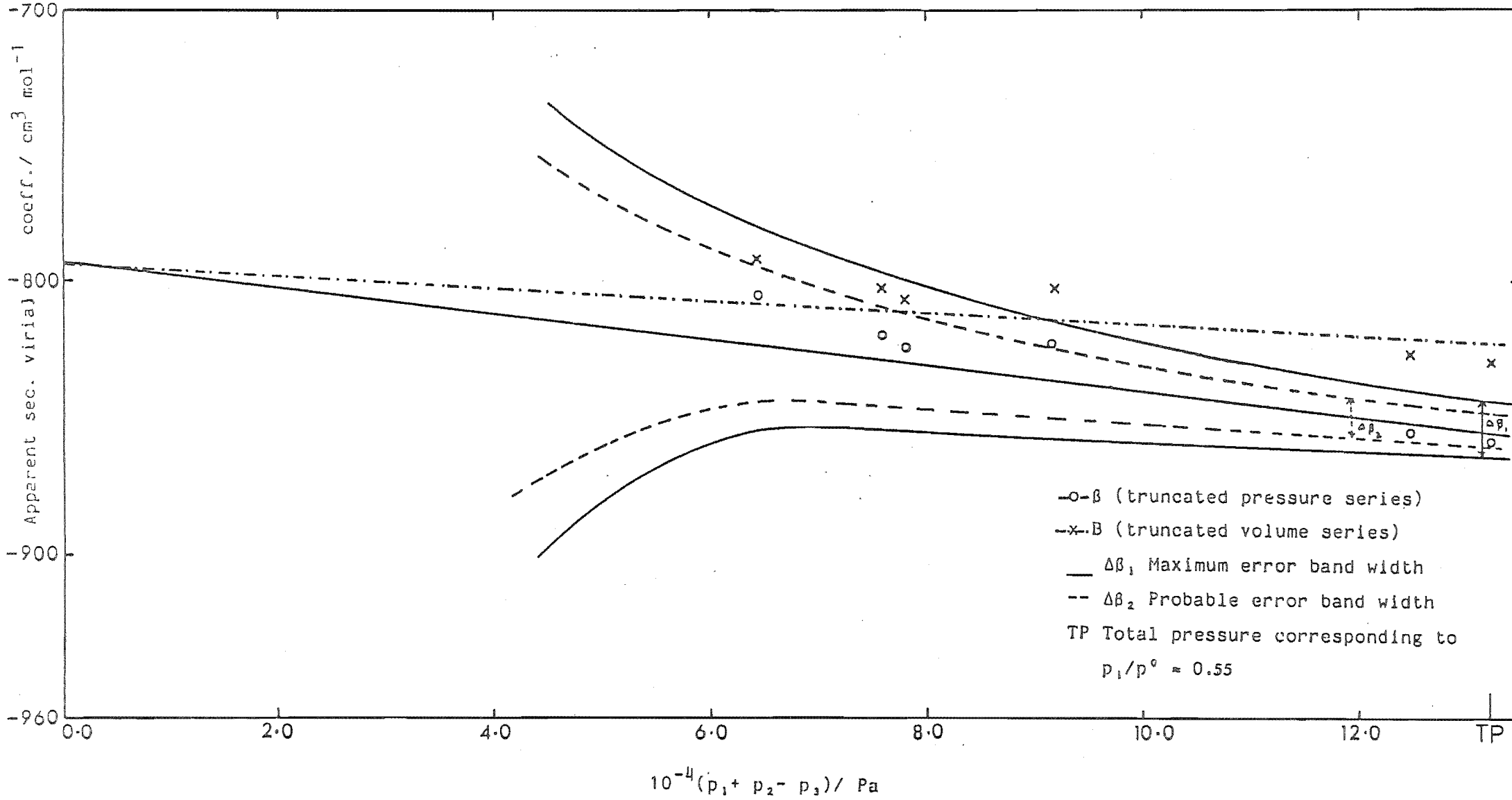

6-3.3 Results for Cyclohexane

Apparent second virial coefficients of cyclohexane have been calculated at 323.15, 348.15, 373.15 K from the raw data in Tables A7-3 (Appendix A7). The results are tabulated in Tables 6-10 to 6-12 and are plotted in Figures 6-11 to 6-13 respectively. The standard error ranges from ±23 $cm^3\ mol^{-1}$ for β at 373.15 K, to maximum of ±143 $cm^3\ mol^{-1}$ for β at 323.15 K. The difference between β and B at any temperature never exceeds 4 $cm^3\ mol^{-1}$.

The results for cyclohexane at 323.15 K are treated in the same way (Section 6-3.2) as those for benzene. Thus the best estimate for β, is -1384 $cm^3\ mol^{-1}$, which lies between the averaged $\beta_{apparent}$ value of -1308 $cm^3\ mol^{-1}$ and extrapolated β having weighted least squares straight line regression coefficient equal to -1460 $cm^3\ mol^{-1}$. At 323.15 K, all loading pressures except the first one, are below the pressure corresponding to 0.6 times the saturation vapour pressure of cyclohexane.

Table 6-10. **Results for Cyclohexane at 323.15 K**

Run No.	$(p_1 + p_2 - p_3)$ / Pa	$\beta_{apparent}$ / $cm^3\ mol^{-1}$	$B_{apparent}$ / $cm^3\ mol^{-1}$
1	33867	-1250	-1232
2	28829	-1296	-1280
3	28337	-1341	-1325
4	24601	-1308	-1296
5	24116	-1397	-1383
6	20578	-1259	-1252

Pressure Series

$a = -1459\ cm^3\ mol^{-1}$ Standard error = $143\ cm^3\ mol^{-1}$

$b = 5.526 \times 10^{-3}\ cm^6\ mol^{-2}$ Standard error = $5.040 \times 10^{-3}\ cm^6\ mol^{-2}$

Volume Series

$a' = -1463\ cm^3\ mol^{-1}$ Standard error = $139\ cm^3\ mol^{-1}$

$b' = 6.218 \times 10^{-4}\ cm^6\ mol^{-2}$ Standard error = $4.896 \times 10^{-4}\ cm^6\ mol^{-2}$

FIGURE 6-11

Extrapolation of observations for cyclohexane to zero pressure at 323.15 K

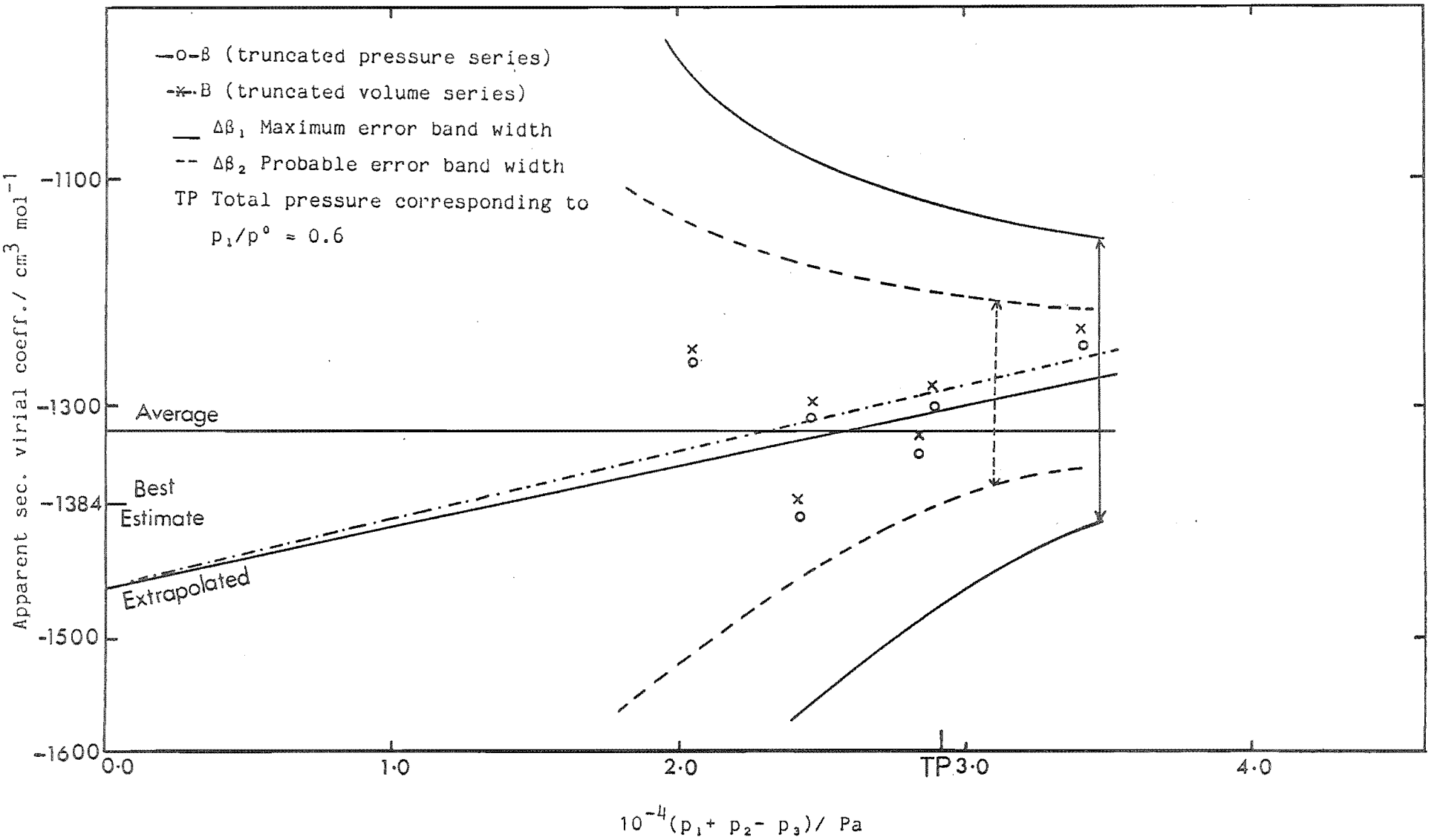

Table 6-11. **Results for Cyclohexane at 348.15 K**

Run No.	$(p_1 + p_2 - p_3)$ / Pa	$\beta_{apparent}$ / $cm^3\ mol^{-1}$	$B_{apparent}$ / $cm^3\ mol^{-1}$
1	68303	-1070	-1043
2	58225	-1024	-1003
3	57259	-1066	-1044
4	48772	-1032	-1015
5	47973	-1067	-1049
6	33615	-1154	-1141
7	28138	-1122	-1113

Pressure Series

$a = -1140\ cm^3\ mol^{-1}$ Standard error = $67\ cm^3\ mol^{-1}$

$b = 1.400 \times 10^{-3}\ cm^6\ mol^{-2}$ Standard error = $1.191 \times 10^{-3}\ cm^6\ mol^{-2}$

Volume Series

$a' = -1143\ cm^3\ mol^{-1}$ Standard error = $65\ cm^3\ mol^{-1}$

$b' = 1.831 \times 10^{-4}\ cm^6\ mol^{-2}$ Standard error = $1.161 \times 10^{-4}\ cm^6\ mol^{-2}$

FIGURE 6-12

Extrapolation of observations for cyclohexane to zero pressure at 348.15 K

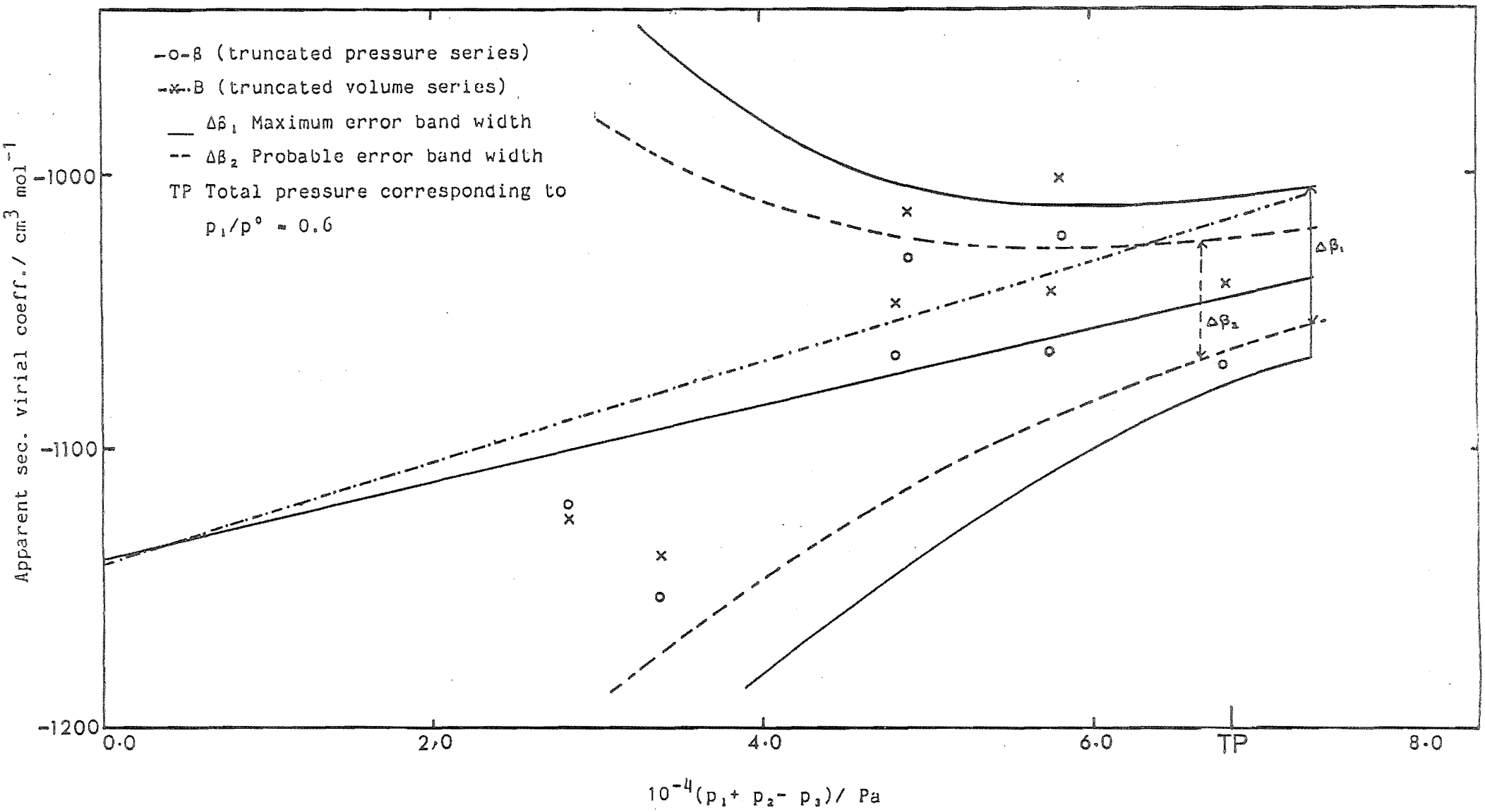

Table 6-12. **Results for Cyclohexane at 373.15 K**

Run No.	$(p_1 + p_2 - p_3)$ / Pa	$\beta_{apparent}$ / $cm^3\ mol^{-1}$	$B_{apparent}$ / $cm^3\ mol^{-1}$
1	125473	-975	-935
2	105379	-956	-925
3	88408	-953	-927
4	74157	-940	-919
5	62126	-977	-958
6	52046	-903	-890
7	43561	-977	-965
8	36458	-948	-939

Pressure Series

$a = -925\ cm^3\ mol^{-1}$ Standard error = $23\ cm^3\ mol^{-1}$

$b = -3.521 \times 10^{-4}\ cm^6\ mol^{-2}$ Standard error = $2.360 \times 10^{-4}\ cm^6\ mol^{-2}$

Volume Series

$a' = -930\ cm^3\ mol^{-1}$ Standard error = $22\ cm^3\ mol^{-1}$

$b' = -5.666 \times 10^{-6}\ cm^6\ mol^{-2}$ Standard error = $2.253 \times 10^{-4}\ cm^6\ mol^{-2}$

FIGURE 6-13

Extrapolation of observations for cyclohexane to zero pressure at 373.15 K

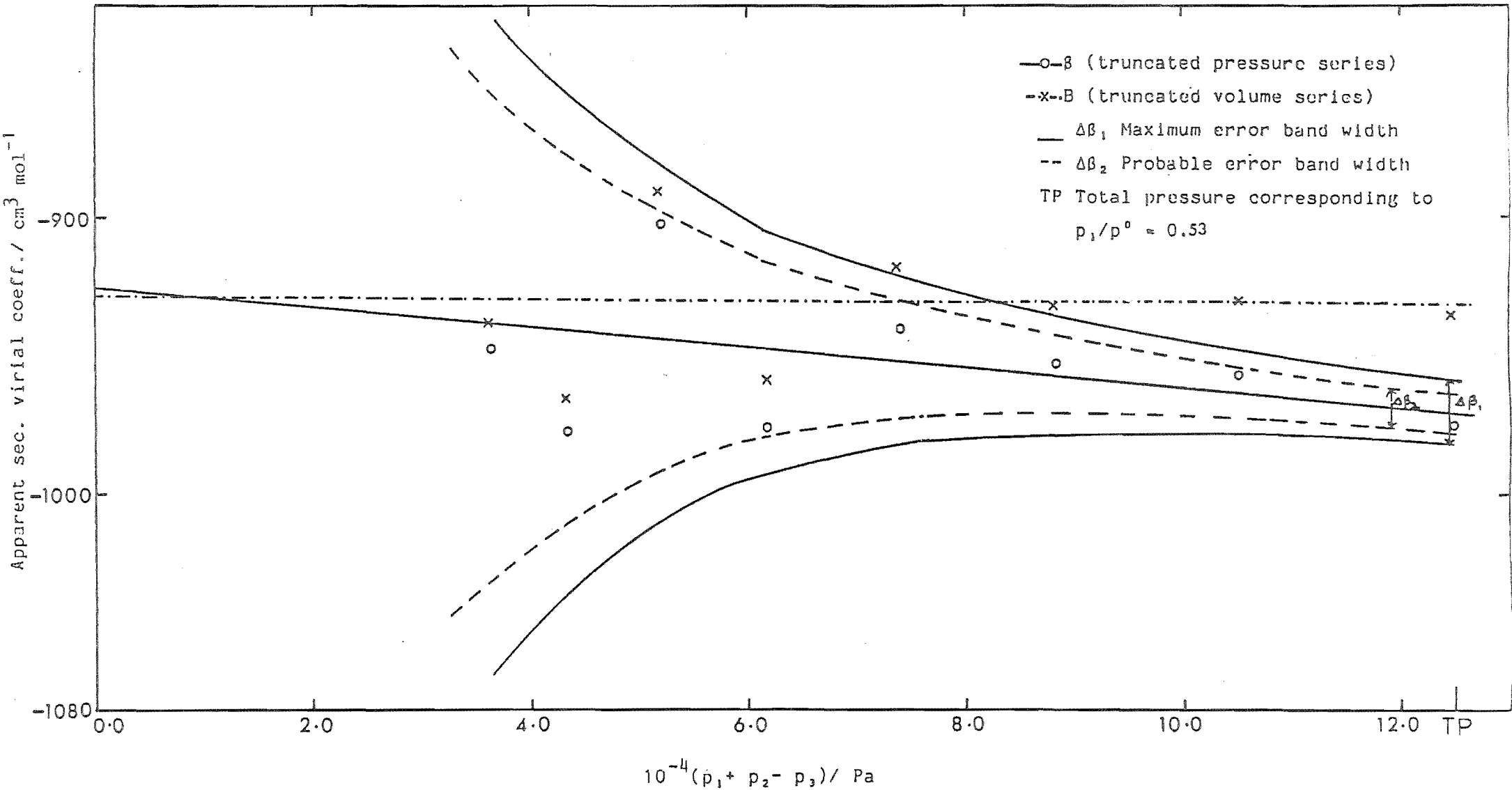

B. MIXTURES

6-4 Calculation Procedure and Organisation of Raw Data

The raw data for each experimental run comprises,

1. bath temperature (T),
2. loading pressure (p) of the reference component and
3. pressure difference (Δp) between the initial identical pressures of the pure components and the pressure of the mixture after mixing, at the equilibrium.

6-4.1 Loading Pressure

The loading pressure of the sample was the same as that of the reference gas nitrogen, measured by the mercury manometer. It was calculated using the equation

$$p = \rho_{Hg}(t^{o}C) \times g_{local} \times \Delta h \qquad (6.13)$$

where $\rho_{Hg}(t^{o}C)$ was obtained from the tabulation by Bigg (1964) of the variation in the densities of mercury with temperature. Δh is the difference in the two heights of the mercury levels in the mercury manometer. The value of g_{local}, provided by the Christchurch Meterological service, is 980.48 cm sec^{-2}.

6-4.2 Pressure Difference

The pressure differences between the initial pressure of the pure components and final pressure of the mixture at equilibrium was recorded on the pressure transducer (Section 5-5) at 5 minute interval for 40 to 50 minutes and the average of the final steady values was corrected for any shift in the gauge zero.

6-4.3 Organisation of Data

Appendix A10 (Part I) gives one complete set of the original instrumental readings and sample calculations to determine the loading pressure and pressure difference measurements. The raw data for each run, comprising of T, p and Δp for each system at the various temperatures are tabulated in Appendix A10.2 (Part II).

6-5 Calculation Procedure For the Results

The results, tabulated in the Tables 6-13 to 6-15 and plotted in Figures 6-14 to 6-16, are calculated using a truncated form of equation (3.38)

$$\varepsilon \simeq \frac{2RT\Delta p}{p^2 (1 + \Delta p/p)} \qquad (6.14)$$

where $2x_1x_2$ term is approximated to 0.5. The value of R = 8.3144 $Pa\ m^3$

mol^{-1} K^{-1} is used throughout, as the universal gas constant. The major source of error is in Δp and may be ten times greater than that in the x_1x_2, p or T terms. The uncertainty, quoted for $\varepsilon_{uncorr.}$ in Tables 6-13 to 6-15, is the result of uncertainties (equation 3.48) in measurement of p, Δp and T.

The results have been adjusted, assuming the correction necessary for adsorption. The correction $\delta\varepsilon_{adsorption}$ has been determined as detailed in Appendix A11. The error $\delta\varepsilon$ assigned to Avg. ε is either the half of the spread of corrected results or the measurement errors (equation 3.48), whichever is the larger.

A multivariant curve fitting program (Mayhew, 1978) described in Appendix (A12), is used to fit the excess second virial coefficient $\varepsilon_{corr.}$ to a function of the form

$$\varepsilon_{corr.} = a + bx10^{-4}\exp(c/T) \qquad (6.15)$$

where a, b and c are the regression coefficients and $\varepsilon_{corr.}$ is the interaction second virial coefficient at temperature T, corrected for adsorption of the vapours on to the surface.

The sum of the deviations of the results from the fitted curve can be expressed as

$$y = \varepsilon_{corr.} - \varepsilon_{calc.} \qquad (6.16)$$

The tables also report Σy^2, where Σy^2 is the sum of the square of deviations of the experimental results from the fitted curve.

Table 6-13 **Results corrected for Adsorption**

Benzene (1) + Cyclohexane (2)

Temp.	Loading Pressure	$\delta\varepsilon$ adsorp.	Excess Virial Coefficient		
			ε uncorr.	ε corr.	Avg. ε
K ±0.005	Pa ±10	$cm^3\ mol^{-1}$	$cm^3\ mol^{-1}$	$cm^3\ mol^{-1}$	$cm^3\ mol^{-1}$
298.15	9678	-28.0	147.0±6	119.0	
298.15	6138	53.0	120.0±14	173.0	146±27
323.15	24080	-0.2	51.9±1	51.7	
323.15	25210	-1.4	48.7±1	47.3	50±2
348.15	44950	1.1	27.6±1	28.7	
348.15	51110	0.5	28.3±1	28.8	29±1
373.15	47090	1.8	24.2±1	26.0	
373.15	46860	1.8	24.2±1	26.0	26±1
398.15	46370	2.0	19.7±0.6	21.7	
398.15	48320	1.9	18.8±1	20.7	
398.15	46820	2.0	19.3±1	21.3	
398.15	47340	1.9	16.5±1	18.4	21±1

The regression coefficients obtained using equation (6.13) are

$a = 21.35\ cm^3\ mol^{-1}$ $\quad b = 0.007\ cm^3\ mol^{-1}$

$c = 5662\ K$ $\quad \Sigma y^2 = 82\ cm^6\ mol^{-2}$

where Σy^2 is the sum of square of deviations of experimental results from the fitted curve.

FIGURE 6-14

The Excess Second Virial Coefficient of

Benzene (1) + Cyclohexane (2)

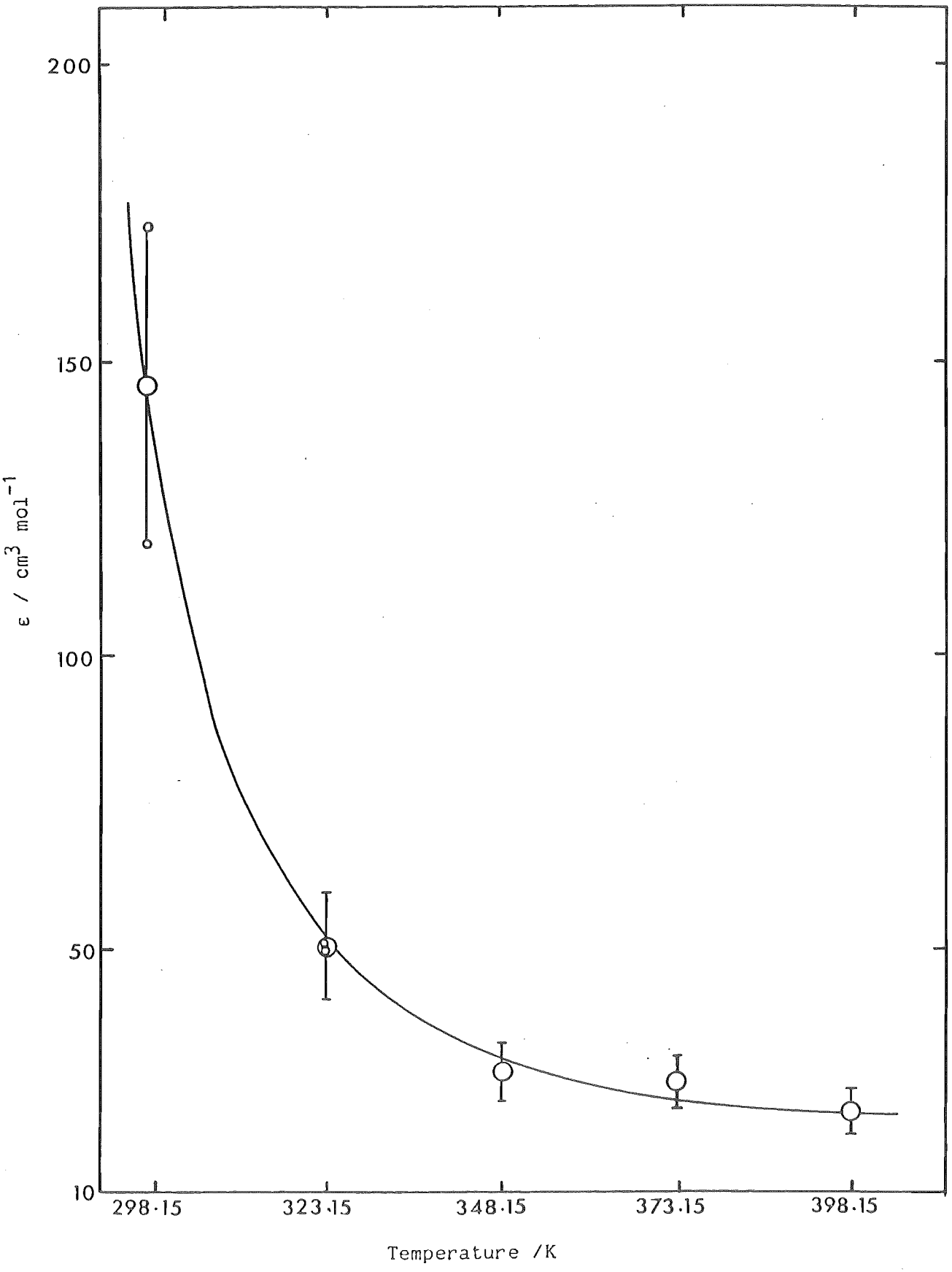

Table 6-14 **Results corrected for Adsorption**

Benzene (1) + n-Hexane (2)

Temp.	Loading Pressure	adsorp.	Excess Virial Coefficient		
			εuncorr.	εcorr.	Avg. ε
K ±0.005	Pa ±10	$cm^3\ mol^{-1}$	$cm^3\ mol^{-1}$	$cm^3\ mol^{-1}$	$cm^3\ mol^{-1}$
298.15	7649	17.0	48.0±8	65.0	
298.15	8428	8.0	59.0±7	67.0	66±8
323.15	20450	3.1	30.5±1.4	33.6	
323.15	22300	2.1	29.1±1.2	31.2	32±1.4
348.15	40770	1.1	22.3±0.4	23.4	
348.15	43440	0.9	25.5±0.3	26.4	
348.15	46590	0.7	19.7±0.3	20.4	
348.15	40680	1.1	19.6±0.5	20.7	23±3
373.15	46560	1.1	18.6±0.4	19.7	
373.15	47300	0.7	22.8±0.2	23.5	
373.15	45190	1.2	20.9±0.3	22.1	21.8±2
398.15	48950	1.1	15.5±0.3	16.6	
398.15	47170	1.2	15.4±0.6	16.6	
398.15	51500	1.0	15.4±0.5	16.4	16.6±0.6

The regression coefficients obtained using equation (6.13) are

$a = 17.09\ cm^3\ mol^{-1}$ $\quad b = 0.3\ cm^3\ mol^{-1}$

$c = 4256\ K$ $\quad \Sigma y^2 = 114\ cm^6\ mol^{-2}$

where Σy^2 is the sum of square of deviations of experimental results from the fitted curve.

FIGURE 6-15

The Excess Second Virial Coefficient of

Benzene (1) + n-Hexane (2)

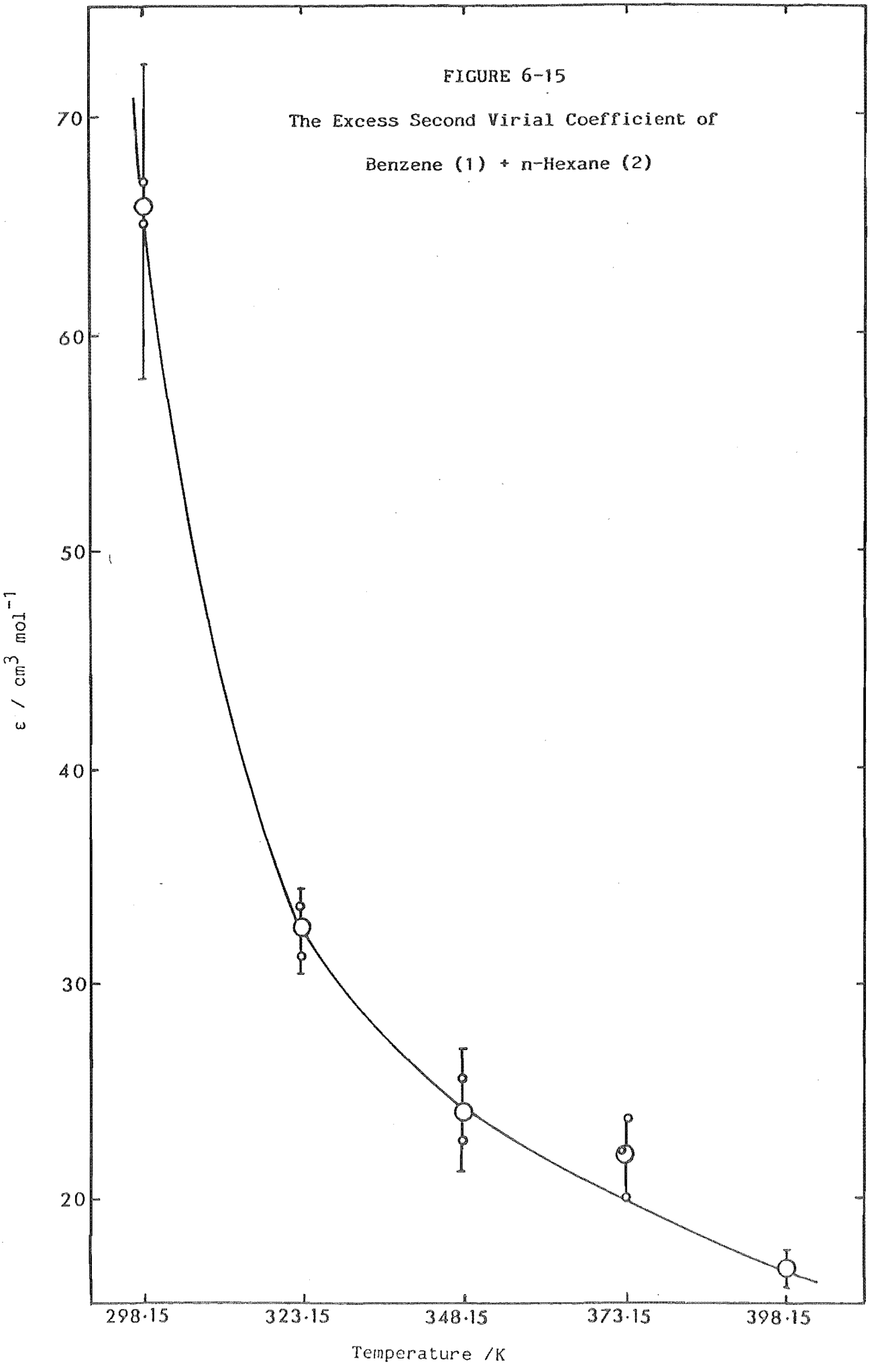

Table 6-15 **Results corrected for Adsorption**

Cyclohexane (1) + n-Hexane (2)

Temp.	Loading Pressure	$\delta\varepsilon_{adsorp.}$	Excess Virial Coefficient		
			$\varepsilon_{uncorr.}$	$\varepsilon_{corr.}$	Avg. ε
K ±0.005	Pa ±10	$cm^3\ mol^{-1}$	$cm^3\ mol^{-1}$	$cm^3\ mol^{-1}$	$cm^3\ mol^{-1}$
* 298.15	9034	1.0	3.1±6	4.1	
298.15	8679	7.7	-12.5±6.7	-4.8	
298.15	9017	1.0	-15.2±6	-14.2	-9.5±7
323.15	23950	1.2	-6.7±1	-5.5	
323.15	21740	3.2	-7.3±1.2	-4.1	-4.8±1.2
348.15	44440	1.3	-4.7±0.3	-3.4	
348.15	47930	0.9	-4.2±0.3	-3.3	-3.3±0.3
373.15	47180	1.7	-4.2±0.8	-2.5	
373.15	45080	1.9	-2.9±0.3	-1.0	
373.15	47840	1.7	-4.0±0.5	-2.3	-1.9±0.8
398.15	44170	2.0	-4.1±0.3	-2.1	
398.15	49400	1.7	-3.1±0.3	-1.4	-1.8±0.3

* See Section 7-6.1

The regression coefficients obtained using equation (6.13) are

$a = -1.125\ cm^3\ mol^{-1}$ $\quad b = -15.313\ cm^3\ mol^{-1}$

$c = 2487.5\ K$ $\quad \Sigma y^2 = 8\ cm^6\ mol^{-2}$

where Σy^2 is the sum of square of deviations of experimental results from the fitted curve.

FIGURE 6-16

The Excess Second Virial Coefficient of

Cyclohexane (1) + n-Hexane

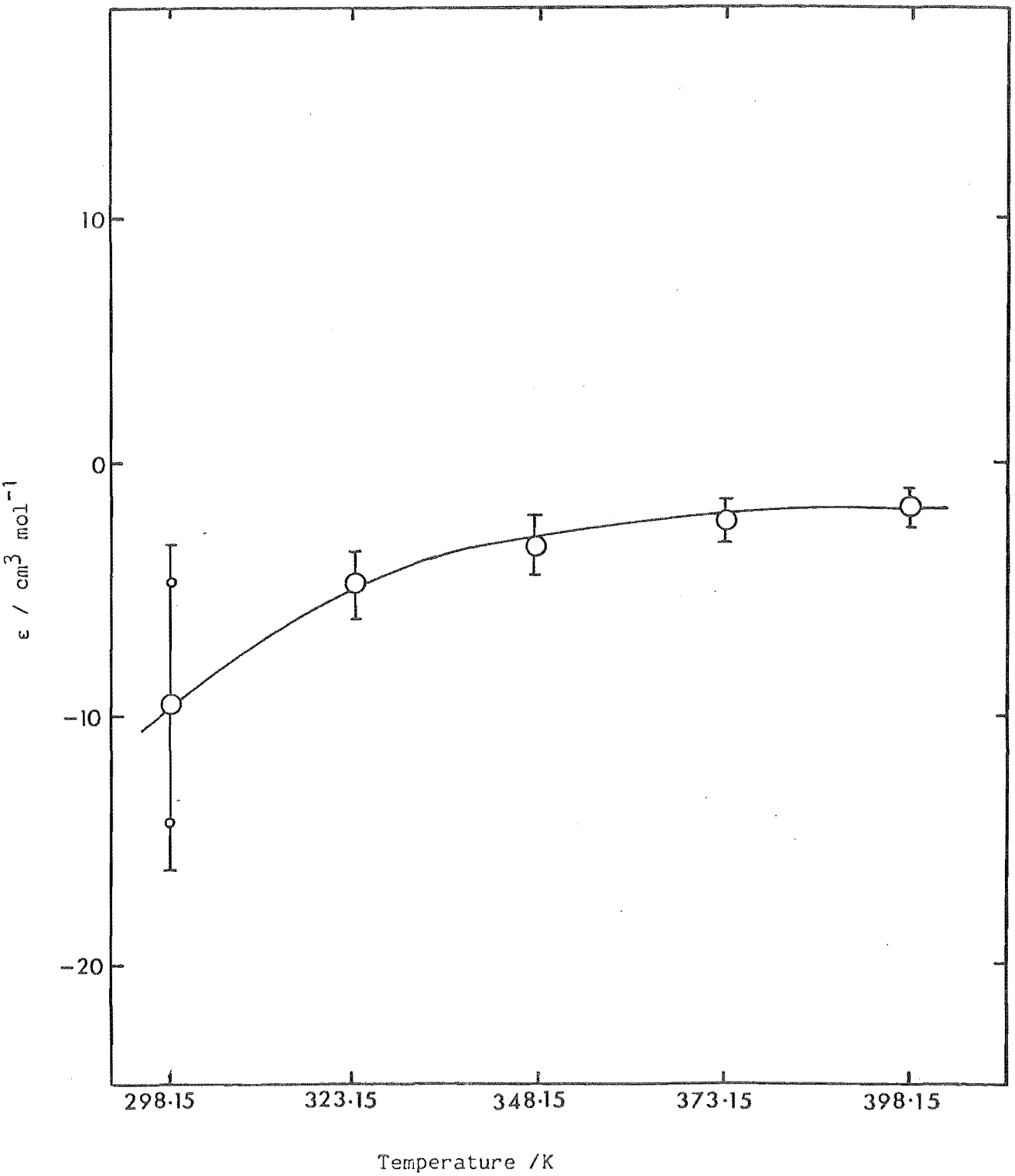

CHAPTER 7

DISCUSSION

A. PURE COMPONENT

7-1 Significance of B

The analysis of the results embodied in this thesis for the second virial coefficients of n-hexane, benzene and cyclohexane assures that meaningful second virial coefficients have been obtained. The agreement between the extrapolated values of β and B at zero pressure indicates the theoretical significance of the quantities obtained (Scott and Dunlap, 1962). These results are at variance with those reported in the literature (Dymond and Smith, 1980) and we believe that the literature results are not "true" second virial coefficients.

Most of the literature values are the results of measurements at comparatively high pressure and are derived using truncated forms of the virial equation of state to include only the linear terms. In the determination of the molecular weights of gas by the limiting density method, Bottomley et al. (1950) questioned the assumption that pV/p isotherms for 1 atmosphere downwards were strictly linear. They

concluded that failure to detect with certainty any curvature with propane shows that any departure from linearity of pV/p isotherms at 295 K is very small.

Hamann and Pearse (1952) attempted to improve upon the accuracy obtained in the low pressure measurements of second virial coefficients. They observed that their differential compressibility method gave two values of second virial coefficients $\beta(T)$ based on the first approximation

$$\beta(T) = (1/n)[(pV)/p] \tag{7.1}$$

where n is the number of moles of the comparison gas (found by extrapolating pV to p=0, Section 2-2.4) and signifies the change in the compression step. They concluded that the complicating effects of adsorption or of the higher terms contribution were causing an apparent increase in $\beta(T)$ with increasing pressure. They also observed the apparent non-linearity of pV with p, for methyl chloride at 295.2 K.

McGlashan and Potter (1958) indicated that the values of B calculated from the experimental results by the relation

$$pV = nRT(1 + nB/V) \tag{7.2}$$

are by no means the same as those obtained by the relation

$$pV = nRT + n\beta p \tag{7.3}$$

They asserted that at least for the molecules which obey reasonably, the principle of corresponding states at temperatures below critical, the omission of higher terms in the equation (7.2) affects the

calculated value of B to a much smaller extent than the omission of higher terms in equation (7.3). Hence the values of β calculated from the latter relation should show a trend in the expected direction with pressure (McGlashan and Potter, 1958).

McGlashan and Potter (1962) analysed their second virial coefficient measurements on n-heptane, using the differential compression method as discussed in Section 2-3.1.6, assuming both $\gamma=0$ and $C=0$, to examine the accuracy of either of the approximations. They looked for systematic differences between β_{12} and β_{13} on one hand, and between B_{12} and B_{13} on the other hand. They justified the conclusion $C=0$ to be a much better assumption than the assumption $\gamma=0$ (or $C=B^2$), as the systematic differences between β_{12} and β_{13} were much greater than the systematic differences, if any, between B_{12} and B_{13}.

Bottomley and Reeves (1958c) justified the use of equation (7.3) on the basis of the pV-p line being linear to high accuracy up to 70% of the saturation pressure. They also found the pV versus 1/V plot drawn from their observations, to be very nearly linear, when drawn on quartograph paper, since their data consisted of the determination of volumes of the system at various pressures in each expansion. However, they reserved comment on the relative merits of pV-p and pV-(1/V) plots unless the experimental results include measurements of pV at several widely spaced pressures for each expansion.

Bottomley and Spurling (1964) used a differential thermal expansion method as detailed in Section 2-3.1.5. Their method involved the measurement of $\Delta\beta$ (difference between pressure series second virial ceofficients at the temperatures T_1 and T_2), or the measurement of ΔB (difference between volume series second virial coefficients at temperature T_1 and T_2) to obtain the absolute values of β and B of any substance at temperature T. Bottomley and

Spurling (1966) reported the analysis to ascertain the possible influence of the third virial coefficient. They observed that their experimentally determined quantities provided only apparent values of $\Delta\beta$ and ΔB, and also that the apparent $\Delta\beta$ is not equal to the apparent ΔB. They suggested the discrepencies between two values can be quantitatively accounted by neglect of the third virial coefficients in equations (3.1 and 3.9). Thus it necessitated knowing the value of the third virial coefficient.

Bottomley and Spurling (1967) analysed the data for methanol using pressure and volume series expansions, first truncating the equations at the second and then at the third virial coefficients. As shown in Table 7-1, in the former case, they reported a difference of 15 $cm^3\ mol^{-1}$ between β and B but only of 1 $cm^3\ mol^{-1}$ in the latter case.

Table 7-1. **Second Virial Coefficients for Methanol at 323.15 K**

(Bottomley and Spurling, 1967)

$\frac{B}{(cm^3\ mol^{-1})}$	$\frac{C}{(cm^3\ mol^{-1})^2}$	$\frac{\beta}{(cm^3\ mol^{-1})}$	$\frac{\gamma}{(cm^3\ mol^{-1})^2}$
-1276 -1144	-1.297×10^7	-1291 -1145	-1.429×10^7

The difference between two values of β by these methods can be as much as 146 $cm^3\ mol^{-1}$.

Eubank and Angus (1973) have also shown concern in the danger of deriving the second virial coefficients from the truncated series

virial expansions as the equation of state. They have analysed the results for methane and ethylene using the virial equation of state including the square terms. Lee S-M et al. (1977) have drawn generalized plots suggesting optimal truncation of virial equation and other generalized plots which indicate probable errors associated with the most common truncation.

Hauthal and Sackmann (1969) also calculated β and B for methyl isobutyl ketone at 393 K and found apparent β and B values to be -1650 and -1580 $cm^3\ mol^{-1}$. Besides being difference in apparent β and "true " β values, the difference in apparent values of β and B can also be as much as 70 $cm^3\ mol^{-1}$.

Since $C-RT\gamma = B^2$, manifestly C and γ can not both be zero. This work is also suggestive of the influence of the values of C and γ. The method of measurement of "true" B values (Section 3-2) for this work, suggests that it is possible to calculate "true" B values using equations (3.5 and 3.6), overcoming the difficulty of knowing the absolute value of C and γ. Hence, the quantities quoted in the literature (Dymond and Smith, 1980) are not "true" (infinite series) second virial coefficients. It is suggested that the second virial coefficients of substances, in the literature, may deviate by as much as 100 $cm^3\ mol^{-1}$ from the "true" second virial coefficients.

The values of $\beta_{apparent}$ and $B_{apparent}$ obtained in the present work are in very good agreement with those of the literature, for the particular truncated linear series used. The observations for n-hexane are interpreted in the same way as in the literature (eg. McGlashan and Potter, 1962) at a given loading pressure and the accuracy of apparent second virial coefficient of n-hexane is comparable with those of the literature, at our range of loading pressure. Similarily the observations for benzene are interpreted in the same way as those in

the literature and comparison is discussed in Section 7-3.2.

The slopes of plots of $\beta_{apparent}$ against $(p_1 + p_2 - p_3)$ at the various temperatures, as shown later in Figure 7-3 and discussed in Section 7-3.1D, also indicate the influence of the third virial coefficients C or γ, at those temperatures. But pressure and volume measurements in the low pressure region are rarely accurate enough to yield meaningful values of the third virial coefficients. Though n-hexane, benzene and cyclohexane are not true Lennard-Jones molecules, one can determine the force constants in the Lennard-Jones (6-12) potential, from the experimental second virial coefficients. One can then estimate the value of the third virial coefficients, and examine the reasonableness or otherwise the trend of the slopes of the plots of $\beta_{apparent}$ versus $(p_1 + p_2 - p_3)$.

7-2 Accuracy of the Experimental Technique and B Measurement

All the pressure measurements are reported within the probable error of 5 Pa. The working range of the pressure is narrowed at both the higher and the lower limits of the degree of saturation, to obtain results with good accuracy. Our experience suggests that the maximum loading pressure is restricted to 60-70% of the saturation vapour pressure of the pure component.

The obvious effect of the greater loading pressure is more adsorption of the vapours on the glass surface. The effect is prominent in cyclohexane. It may be observed as a reading suggesting a differential pressure of the vapours of nearly 4 Pa on "Baratron 1" gauge (reference side under hard vacuum) corresponding to incomplete transfer of nearly 10^{-7} moles of the component from one cell to

another and this is quite significant (Section 3-4.3). This effect decreases at the low working pressure.

A similar situation was encountered for $B_{apparent}$ measurements of n-hexane at 348.15 K. Accidently a few measurements of $\beta_{apparent}$ were obtained at the loading pressure between 70-80% of the saturation vapour pressure, resulting in a change in the slope of the extrapolated line for the plot of $\beta_{apparent}$ versus $(p_1 + p_2 - p_3)$. This resulted in the deviation of the "true" B, from the plot of B against temperature (See Section 7-3.1; Figure 7-1). However, the measurements of $\beta_{apparent}$ above the maximum optimum loading pressure are truncated (Table 6-4) to obtain "true" B at 348.15 K.

At lower loading pressure in the range of 16,000 - 20,000 Pa, the measurements of $\beta_{apparent}$ are still within the limits of the probable errors of ±200-300 $cm^3\ mol^{-1}$ and may be very close to the extrapolated line, but they may contribute to greater uncertainty in the extrapolated (infinite series) second virial coefficients. Especially at 323.15 K, the measurements are confined to a maximum loading pressure below 30,000 Pa. The apparatus is strained to its limitation of accuracy, resulting in greater uncertainty of the extrapolated line. The latter may cause uncertainty in B upto ±300 $cm^3\ mol^{-1}$. Hence, at 323.15 K only, for benzene and cyclohexane, the average of $\beta_{apparent}$ values is taken to give the best estimate of β.

7-3 Comparison of Results with the Literature Values

In this Section, $\beta_{apparent}$, $B_{apparent}$ and "true" (infinite series) B for n-hexane, benzene and cyclohexane are compared with the

literature values (Dymond and Smith, 1980), and with the correlations of Hayden and O'Connell (1975) and Tsonopoulos (1974). The slopes of the extrapolated lines for the plots of $\beta_{apparent}$ versus $(p_1 + p_2 - p_3)$ at the various temperatures are compared with Lennard-Jones (6-12) potential predictions.

7-3.1 n-Hexane

The second virial coefficients of n-hexane determined by different workers, generally agree within an estimated uncertainty ranging from ±20 to ±50 $cm^3\ mol^{-1}$, although some values are less negative (Lambert et al. 1949) and some are more negative (Hajjar et al., 1969) than expected. Al-Bizreh and Wormald (1978) proposed the equation

$$B = 337.4 - 206.8 \exp(703.8K/T) \qquad (7.4)$$

on the basis of the best fit to the second virial coefficient and Joule-Thomson coefficient data.

A. Direct PVT Measurement

Quite a few workers (Lambert et al. (1949), Bottomley and Reeves (1958c), McGlashan and Potter (1962) and Hajjar et al. (1969)) have measured second virial coefficients of n-hexane using direct PVT measurements. Lambert et al. (1949) have estimated the probable error of their result as ±20 to ±100 $cm^3\ mol^{-1}$, showing a considerable scatter of second virial coefficients at various temperatures.

Bottomley and Reeves (1958c) observed their second virial coefficient measurements in agreement with Lambert et al. (1949), but slightly less negative than those of McGlashan and Potter (1962). The difference between the two sets may be speculated on, as $\beta_{apparent}$ is pressure dependent, and McGlashan and Potter (1962) have used a truncated linear volume series equation of state, judging C=0 to be a more accurate approximation than γ=0 (Section 7-1). However, there is no apparent justification for the measurements of McGlashan and Potter's $B_{apparent}$ being unexpectedly lower than the $\beta_{apparent}$, measured by Bottomley and Reeves.

If our observations are interpreted in the same way as McGlashan and Potter (1962) interpret theirs (Appendix A6, Part II), then there is very good agreement between the answers obtained. A comparison, on this basis, of the second virial coefficients of n-hexane (McGlashan and Potter, 1962), with this work and that of Couldwell et al. (1978) tabulated in Table 7-2 and is shown in Figure 7-1.

Table 7-2. **Comparison of Values of $B_{apparent}$ of n-hexane with the Results of Other Workers**

Temp. / K	p_{max} / Pa	B(1) / $cm^3 mol^{-1}$	B(2) / $cm^3 mol^{-1}$	B(3) / $cm^3 mol^{-1}$
323.15	43876	-1520	-1483	
328.15	44530	-1458	-1514	-1504
338.15	71994	-1326	-1298	
348.15	68161	-1233	-1234	
358.15	65000	-1163	-1144	-1170
373.15	81113	-1030	-1030	-1035

1. McGlashan and Potter (1962)
2. This work
3. Couldwell et al. (1978)

FIGURE 7-1

Comparison of Apparent Second Virial Coefficient ($B_{apparent}$)

of n-hexane Versus Temperature

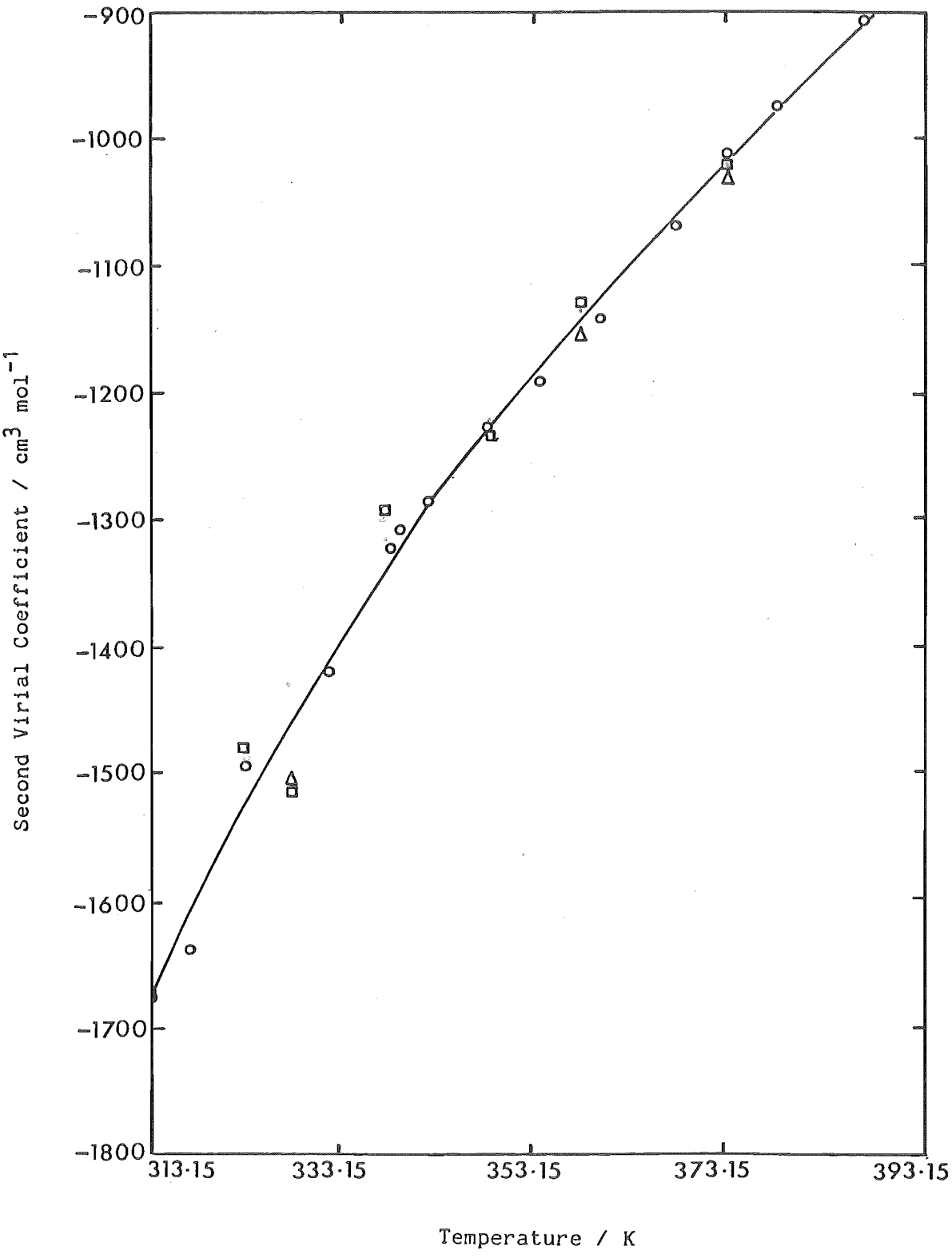

Thus we believe our observations to be of an accuracy comparable with those of McGlashan and Potter, but that the quantities calculated above are not "true" (infinite series) second virial coefficients. We believe that the values quoted for n-hexane, are in error by as much as 100 cm^3 mol^{-1}. Excluding Couldwell's (1975) results for the second virial coefficients of n-hexane at 323.15 and 348.15 K (Section 3-1) and combining the rest with that of Pandya and this work, illustrates the significance of these "true" second virial coefficients (Figure 7-2).

Couldwell et al. (1978) have reported that the two measurements, at 328.15 and 343.15 K in series 2, have been affected by the presence of traces of oil in the apparatus due to incomplete cleaning following an accidental breakage. Couldwell (1975) has presented the quantitative analysis of the effect of oil within one cell of the apparatus. He has concluded that the extra oil terms have a considerable effect, especially at low temperatures.

Hajjar et al. (1969) measured the second virial coefficients of cyclohexane, benzene and n-hexane. They reported plots for the compressibility, z, against 1/V to be linear and concluded that the effect of the third virial coefficient was negligible. Since their isotherms did not extrapolate to unity as p->0, they adjusted the ordinate and compressibility values, downwards accordingly and determined the second virial coefficients. This is difficult to justify and hence we have omitted their results from our comparison. However, their results are less negative by as much as 100 cm^3 mol^{-1} from the apparent second virial coefficients measured by other workers (Dymond and Smith, 1980)

FIGURE 7-2

Second Virial Coefficient of n-hexane Versus Temperature

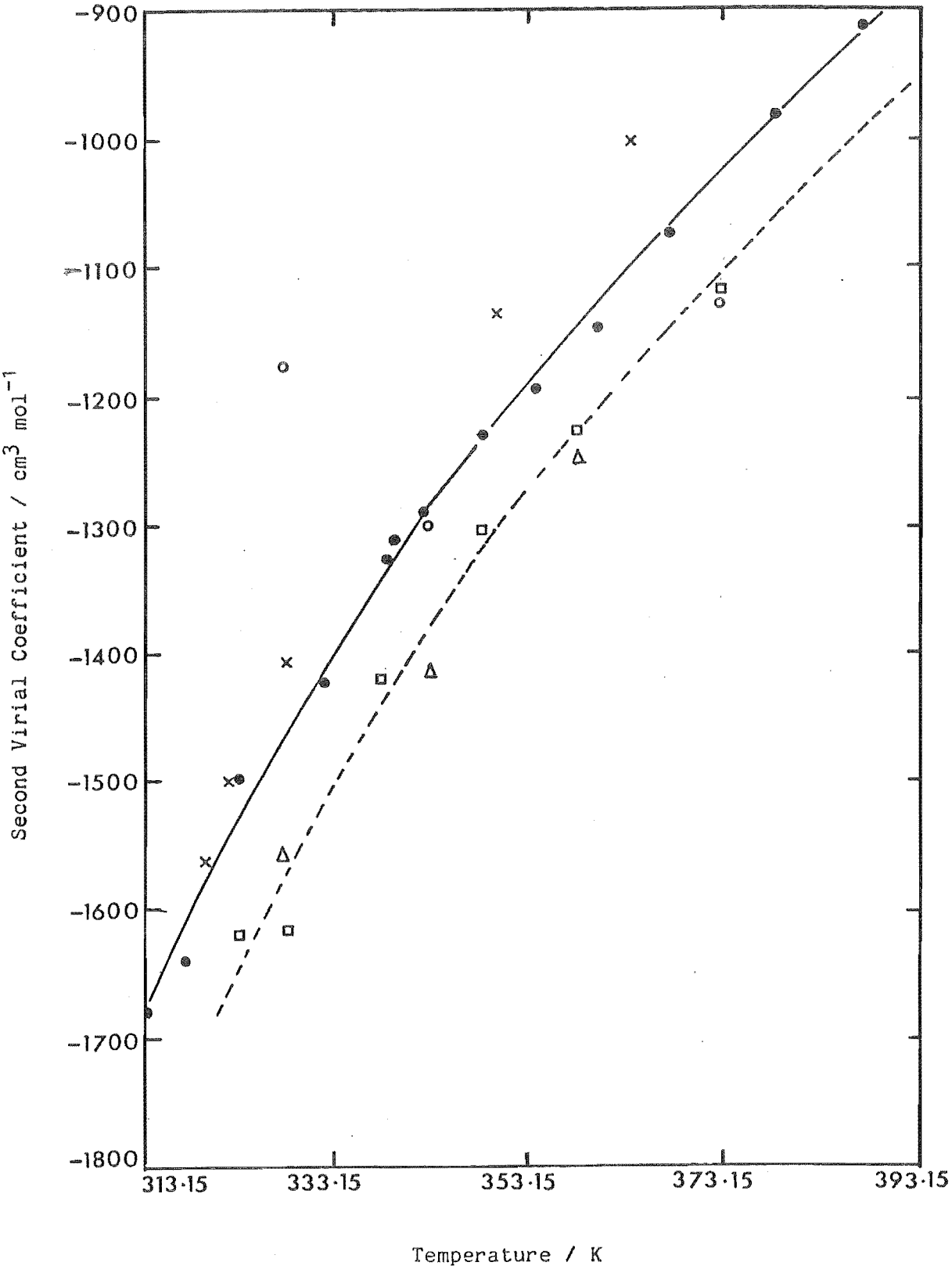

B. Density Balance Method

Di Zio et al. (1966) used a vapour density balance method, as explained in Section 2-3.1.8, for the determination of vapour densities and hence the second virial coefficients of n-hexane over the temperature range 318 to 363 K, without reference to the properties of any other material. Their results correlated well within ±30 cm^3 mol^{-1}, with the smoothing curve proposed by McGlashan and Potter (1962). The pressure range employed was from 250 to 750 mm Hg comparable to the maximum pressure range (Max. pressure ≃ three times the loading pressure) used by McGlashan and Potter. However, density balance measurements are handicapped by the method being more sensitive to the purity of the material than the direct method and not being able to cover a wide temperature range.

C. Indirect Method

Waddington and Douslin (1947) deduced second virial coefficients of n-hexane from the molar volume of the liquid, the calorimetric latent heat of vaporisation and the vapour pressure as a function of temperature. The method has been described in Section 2-3.3.4. They related the second virial coefficient and the absolute temperature by the equation

$$B = -2270 + 6.25 \times 10^5 T^{-1} - 1.306 \times 10^{13} T^{-4} \qquad (7.5)$$

The values of B from this equation at the temperatures of this work with n-hexane, are -1533, -1492, -1420, -1364, -1319, -1269 cm^3 mol^{-1}

and are plotted in Figure 7-2. These values are slightly less negative up to 338.15 K and more negative for temperatures above 348.15 K, in comparison with this work. Hence the agreement is far from impressive.

Al-Bizreh and Wormald (1978) calculated second virial coefficients from the their best fit (equation 7.4) to second virial coefficients and Joule Thomson coefficient data. This correlation is suspect as the best fit is obtained by combining data of apparent β and B, and not "true" B.

D. Analytical Method

The correlations of Hayden and O'Connell (1975) and Tsonopoulos (1974) fit other workers results well (Figure 7-2). However, we believe that new correlations for the "true" second virial coefficients are required.

Considering n-hexane to be represented as a Lennard-Jones molecule, it is possible to fit the Lennard-Jones (6-12) potential (Tee et al., 1966) and to obtain the parameters from the experimental second virial coefficients of n-hexane at the various temperatures. The parameters obtained for this work and that of McGlashan and Potter (1962) are tabulated in Table 7-3.

Table 7-3. **Force Constants for Lennard-Jones (6-12) Potential for n-hexane**

Source	σ / Å	(ε/k) / K	b_0 / $cm^3\ mol^{-1}$
This Work	12.2	170	2300
McGlashan & Potter (1962)	12.2	167	2272

It shows that collision diameters and force constants are comparable. Lennard-Jones reduced temperatures can be calculated using

$$T^* = Tk/\varepsilon \quad \text{(Hirschfelder et al., 1954)} \tag{7.6}$$

where $\varepsilon/k = 0.77T^c$ (Hirschfelder et al., 1954) (7.7)

$$T_B = 0.375T^c \quad \text{(Mason and Spurling, 1969)} \tag{7.8}$$

where T_B is the Boyle temperature, i.e. the temperature at which the second virial coefficient is zero

From equations (7.7 and 7.8)

$$T_B = 0.49/(\varepsilon/k) \tag{7.9}$$

From equations (7.6 and 7.9)

$$T/T_B = 0.49T^* \tag{7.10}$$

Mason and Spurling (1969) have plotted the curves of B/v_B, C/v_B^2, D/v_B^3 and E/v_B^4 versus T/T_B on the basis of theoretical calculations for the Lennard-Jones (6-12) potential. The terms B, C, D, and E are the second, third, fourth and fifth volume series virial coefficients and v_B is the Boyle or van der Waals volume defined as

$$v_B = T(dB/dT)_{T=T_B} \tag{7.11}$$

They expected the general shapes of the curves to be correct for most of the gases, but the curves may be displaced to either side slightly, depending on the substance.

To illustrate the influence of the third virial coefficients in

this work, γ/V_B^2 values are calculated using the values C/v_B^2 on curve for the plot of C/v_B^2 versus T/T_B for Argon (Mason and Spurling, 1969) and equation (1.6)

$$C(T) = \gamma(T)RT + B^2(T) \tag{1.6}$$

These γ/V_B^2 values are plotted versus T/T_B for argon in Figure 7-3.

We compare the trend of γ values as a function of T/T_B for this work, with the plot of theoretically calculated γ/V_B^2 versus T/T_B. This comparison is suitable because our results, being interpreted by equation (3.5)

$$\beta_{apparent} = \beta + \gamma(p_1 + p_2 - p_3) \tag{3.5}$$

using the plots of $\beta_{apparent}$ versus $(p_1 + p_2 - p_3)$, give us "true" values of pressure series third virial coefficient (Section 6-2).

The slopes for plots of $\beta_{apparent}$ versus $(p_1 + p_2 - p_3)$ for n-hexane, at various temperatures, are indicative of the trend of γ (Section 6-2) and are illustrated in Figure 7-4. The slopes show a regular trend of being positive and decreasing steadily with the increasing temperature, with the exception of that at 348.15 K. The latter slope is doubtful as suggested in Section 7-2.

Using (ε/k) value for n-hexane in this work as tabulated in Table 7-3, T^* varies from 1.9 to 2.2 (equation 7.6) for the temperature range from 323.15 to 373.15 K. These T^* values correspond to T/T_B varying from 0.93 to 1.08 (using equtaion 7.10). The γ values for n-hexane in this work are plotted versus corrsponding T/T_B, in Figure 7-5. It is observed that the qualitative trend of γ (Figure 7-5) is comparable with the trend of γ/V_B^2 for Argon, in Figure 7-3, for

FIGURE 7-3

Lennard Jones (12-6) Potential Plot for B/V_B, C/V_B^2

Y/V_B^2 versus T/T_B

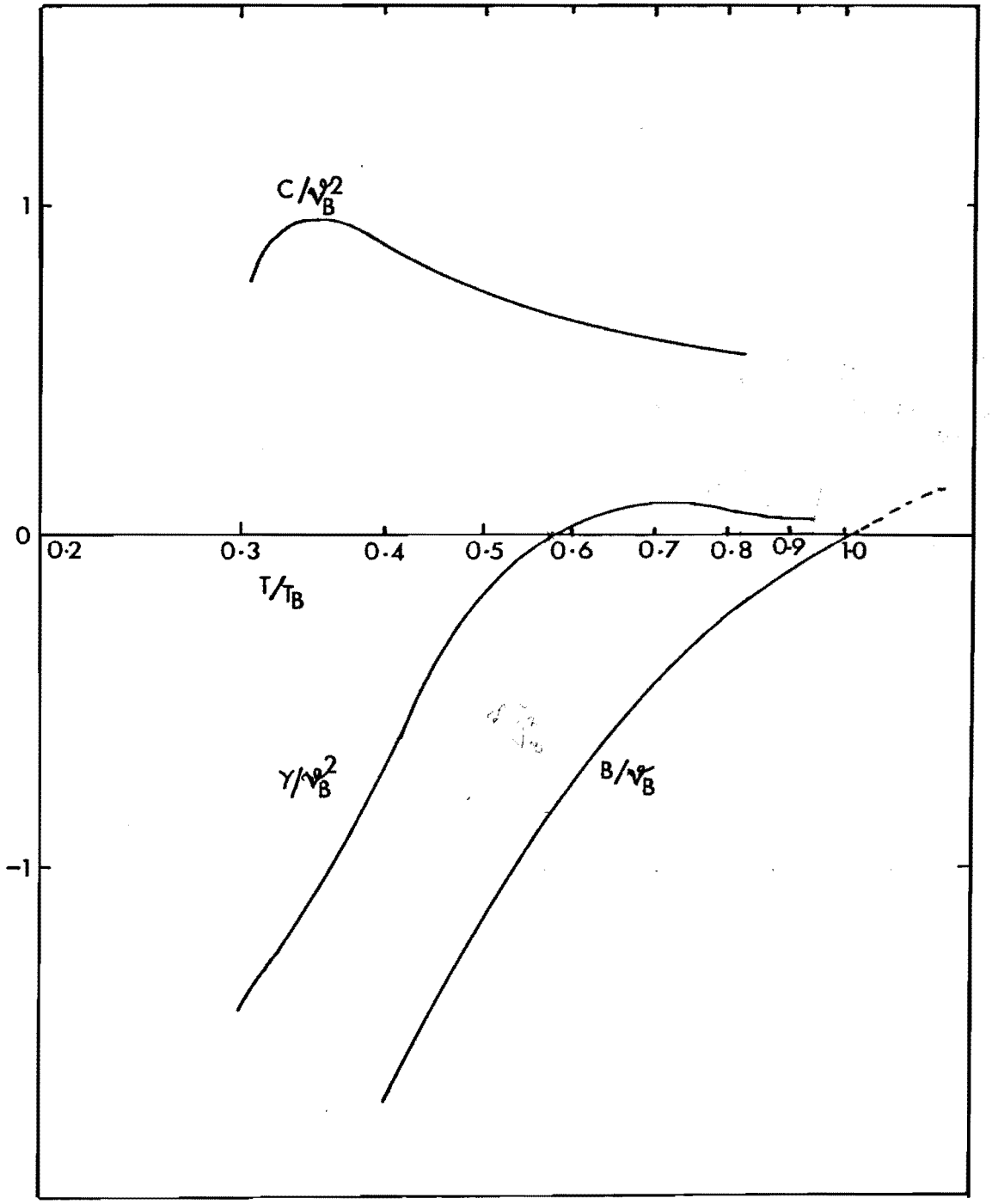

FIGURE 7-4

Comparison of Slopes for Plots of $\beta_{apparent}$ versus $(p_1 + p_2 - p_3)$ for n-hexane

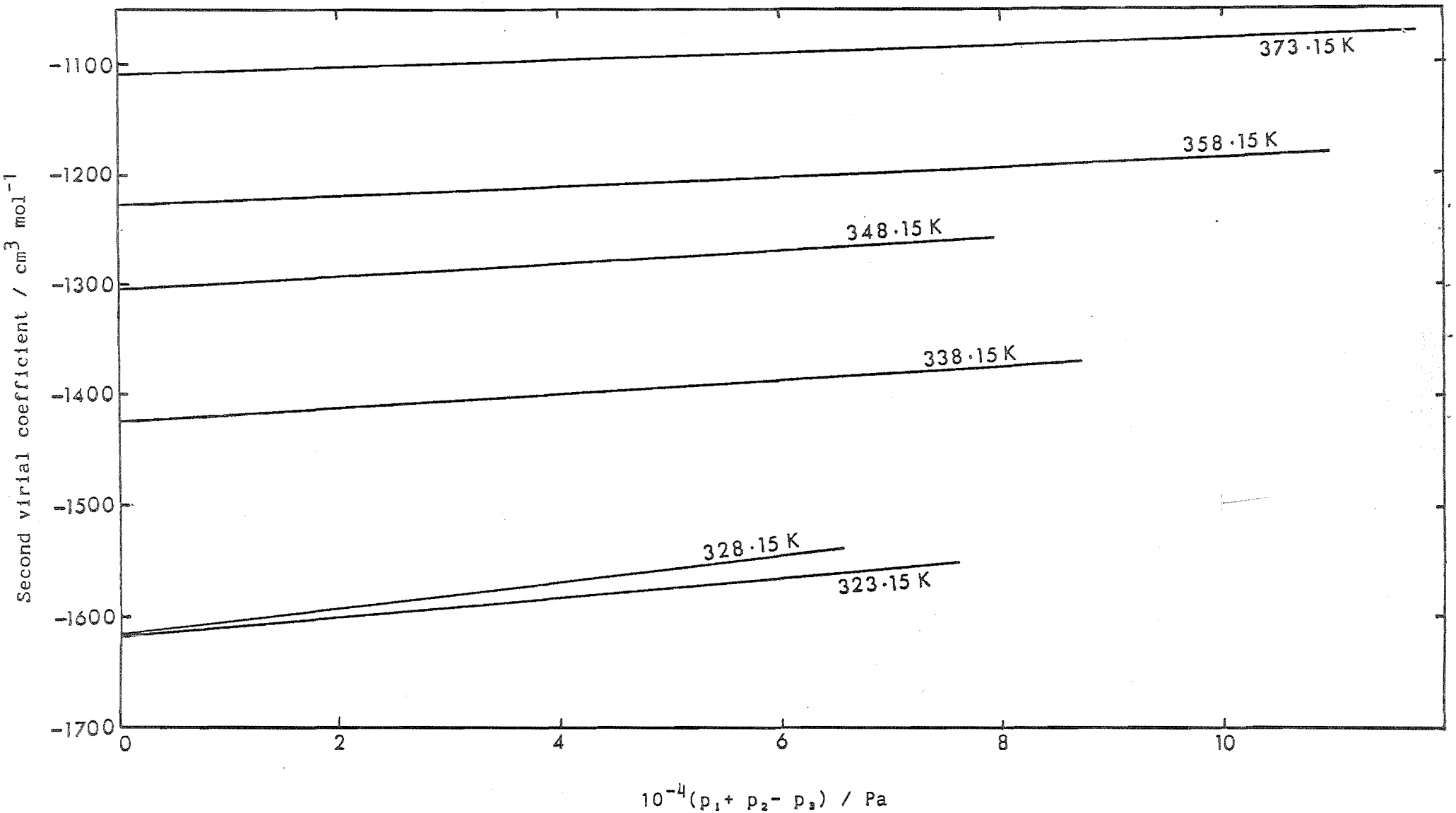

FIGURE 7-5

Plot of Third Virial Coefficient (Y) versus Temperature

for n-hexane

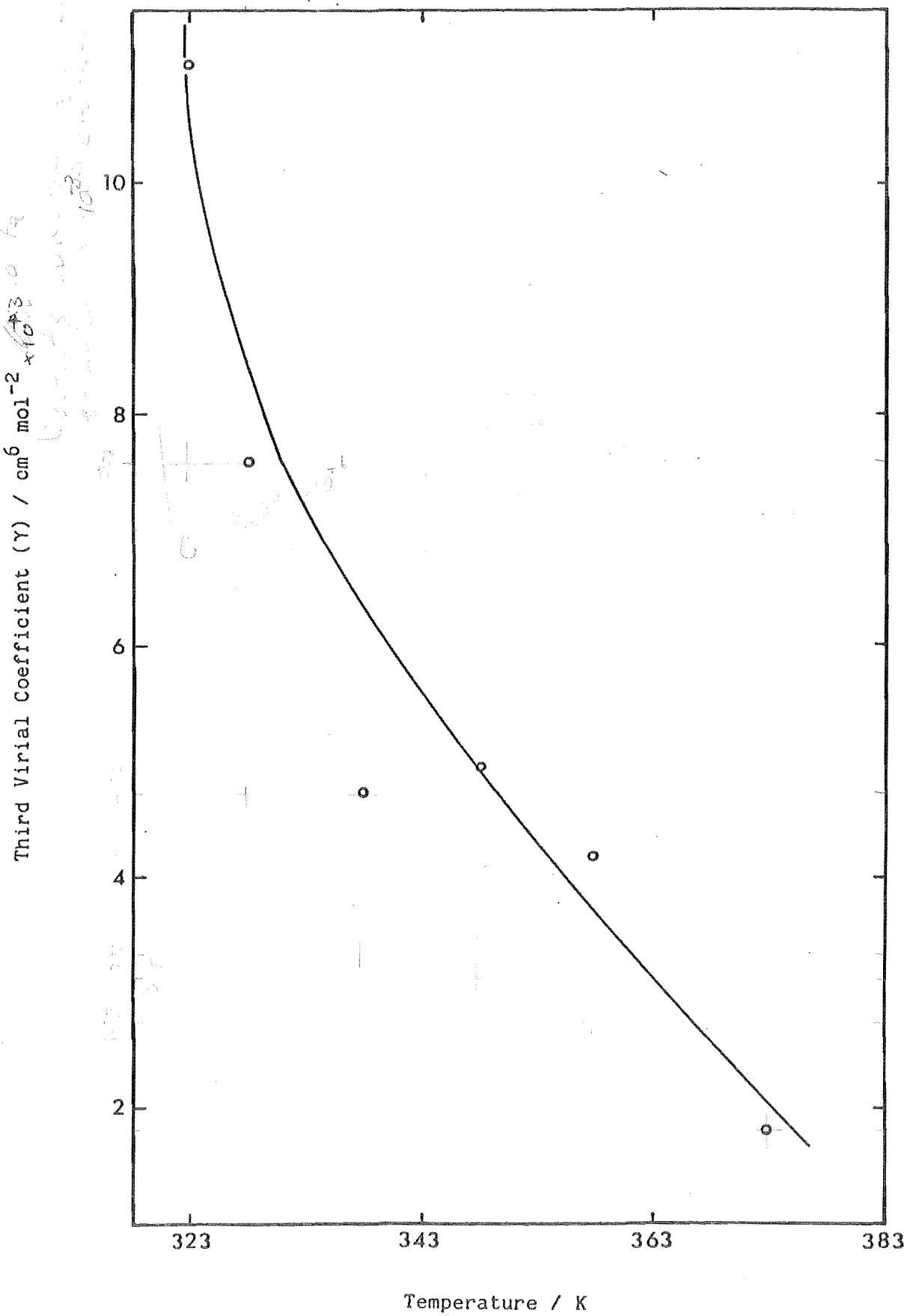

the same range of T/T_B varying from 0.93 to 1.08.

7-3.2 Benzene

The larger error bands at the lower pressures for 323.15 K (Figure 6-8) inhibit the precise extrapolation of the line through the plot of $\beta_{apparent}$ versus $(p_1 + p_2 - p_3)$. Hence for the particular case at 323.15 K, $\beta_{apparent}$ values are averaged and the best β estimated is considered to be $-1125\ cm^3\ mol^{-1}$, i.e., between the averaged $\beta_{apparent}$ values and the extrapolated β (Section 6-3.2).

Allen et al. (1952) drew attention to the disagreement between the results for benzene, of different experimenters (Lambert et al. (1949), Baxendale et al. (1951) and others), especially for the results below 333.15 K. Since then the experimental determinations of the second virial coefficients of benzene vapours have been widely studied. A review of the reults up to 1977 indicates that the controversy surrounding the second virial coefficients of benzene has been resolved by recent measurements which are, with the exception of Hajjar et al. (1969), all consistent with the function of Al-Bizreh and Wormald (1977). They determined the following equation

$$B = 41.5 - 1.118 \times 10^5 T^{-1} - 3.850 \times 10^7 T^{-2} - 1.289 \times 10^9 T^{-3} - 5.158 \times 10^{12} T^{-4} \qquad (7.12)$$

by analysis of available second virial coefficient data, pressure coefficients of heat capacity and and isothermal Joule Thomson coefficient, in the range of 295 to 630 K.

A. Direct PVT Method

The literature results (Dymond and Smith, 1980) of the second virial coefficients versus temperature for benzene are segregated into pressure and volume series, and are illustrated separately in the Figures (7-6 and 7-7). If our observations are interpreted in terms of truncated linear series, in the same way as other workers' results, then there is a good agreement between our observations and the answers obtained for respective series second virial coefficients.

Pressure Series Virial Equation of State

The claim (Allen et al., 1952) of a concealed error in the second virial coefficient values (Baxendale et al. 1951) leading to more negative values than those reported by others, is supported by the work of Andon et al. (1957) using the same Boyle's method as that of Baxendale and Enustun (described in Section 2-3.1.2). Francis et al. (1952) attempted to reslove the discrepancies by two independent series of measurements, but these showed a scatter of values at the same temperature. Bottomley et al. (1958a) measured $\beta_{apparent}$ using a differential expansion method as explained in Section 2-3.1.7. The combined values of the second virial coefficients by several experimenters (Bottomley et al. (1958a), Zaalishvili et al. (1964), Knoebel and Edmister (1968) and Eon et al. (1971)) show a consistent trend in $\beta_{apparent}$ versus T. This work, interpreted at the same pressure range and in the same way as that of others giving $\beta_{apparent}$ values of benzene at temperature T, and literature $\beta_{apparent}$ values are illustrated in Figure 7-6. They show a good agreement.

FIGURE 7-6

Second Virial Coefficient (Pressure Series) of Benzene

Versus Temperature

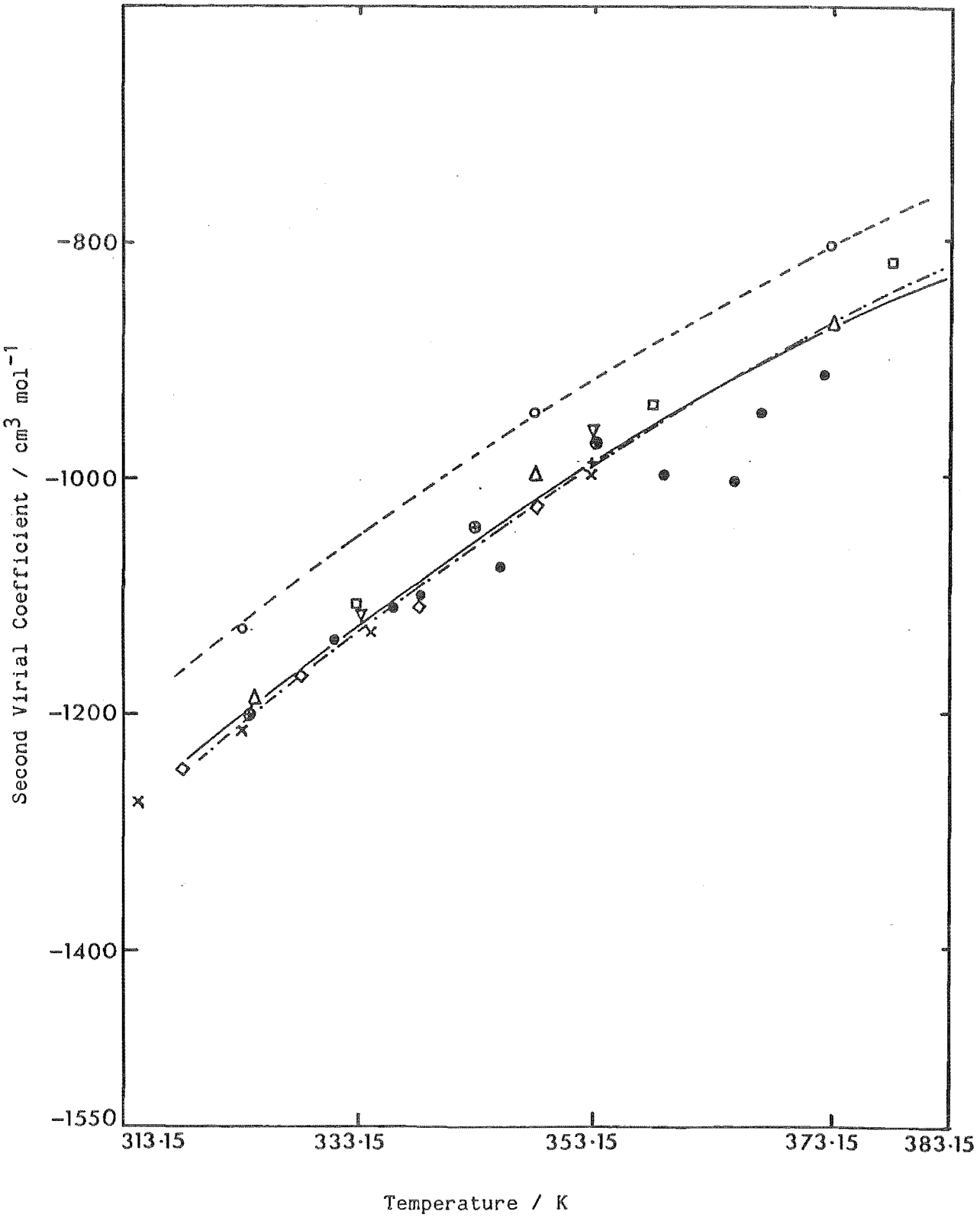

---- This Work
—— Others' apparent β
-·-· Hayden and O'Connell
o This Work (β)
Δ This Work (apparent β)
◇ Allen et al. (1952)
⊛ Bottomley et al. (1958)
▽ Eon et al. (1971)
● Francis et al. (1952)
□ Knoebel and Edmister (1968)
× Scott et al. (1947)
+ Zaalishvili et al. (1965a)

Volume Series Virial Equation of State

Francis et al. (1969) used a differential piezometer (McGlashan and Potter, 1962) as described in Section 2-3.1.6, to make a series of the measurements of the second virial coefficients, B, of benzene, using a truncated linear form of the volume series of virial equation of state to interpret their observations. They also analysed the measured values of B at temperatures from 295 to 628 K, the calorimetric values of (B-TdB/dT) obtained by isothermal throttling from 323 to 403 K, and the calorimetric values of T^2d^2B/dT^2 obtained from measurements of the pressure dependence of the heat capacity from 333 to 527 K both as a test of their mutual consistency and to determine as far as possible the form of B(T). They obtained their best overall fit with an equation of the "Square-Well" form:

$$B/cm^3\ mol^{-1} = -60.1 - 70.4\exp(891.3K/T) \qquad (7.13)$$

Our measurements interpreted (Appendix A6, Part II) in the same way as the careful measurements of Francis et al. (1969) are in extremely good agreement with their results. The comparison is tabulated in Table 7-4.

Since the second virial coefficient for benzene at 323.15 K (Francis et al., 1969) is not measured, B is calculated using equation (7.12). Maximum pressure is assumed to be 0.8 times vapour pressure at that temperature, as their p_{max}/(sat. P) ratio varies from 0.7 to 0.90. The results are plotted in Figure 7-7. This certainly illustrates the capacity of this technique to interpret results in either series in the same way as other workers' results. Volume series second virial coefficients are about 50 $cm^3\ mol^{-1}$ less negative than the pressure

FIGURE 7-7

Second Virial Coefficient (Volume Series) of Benzene

Versus Temperature

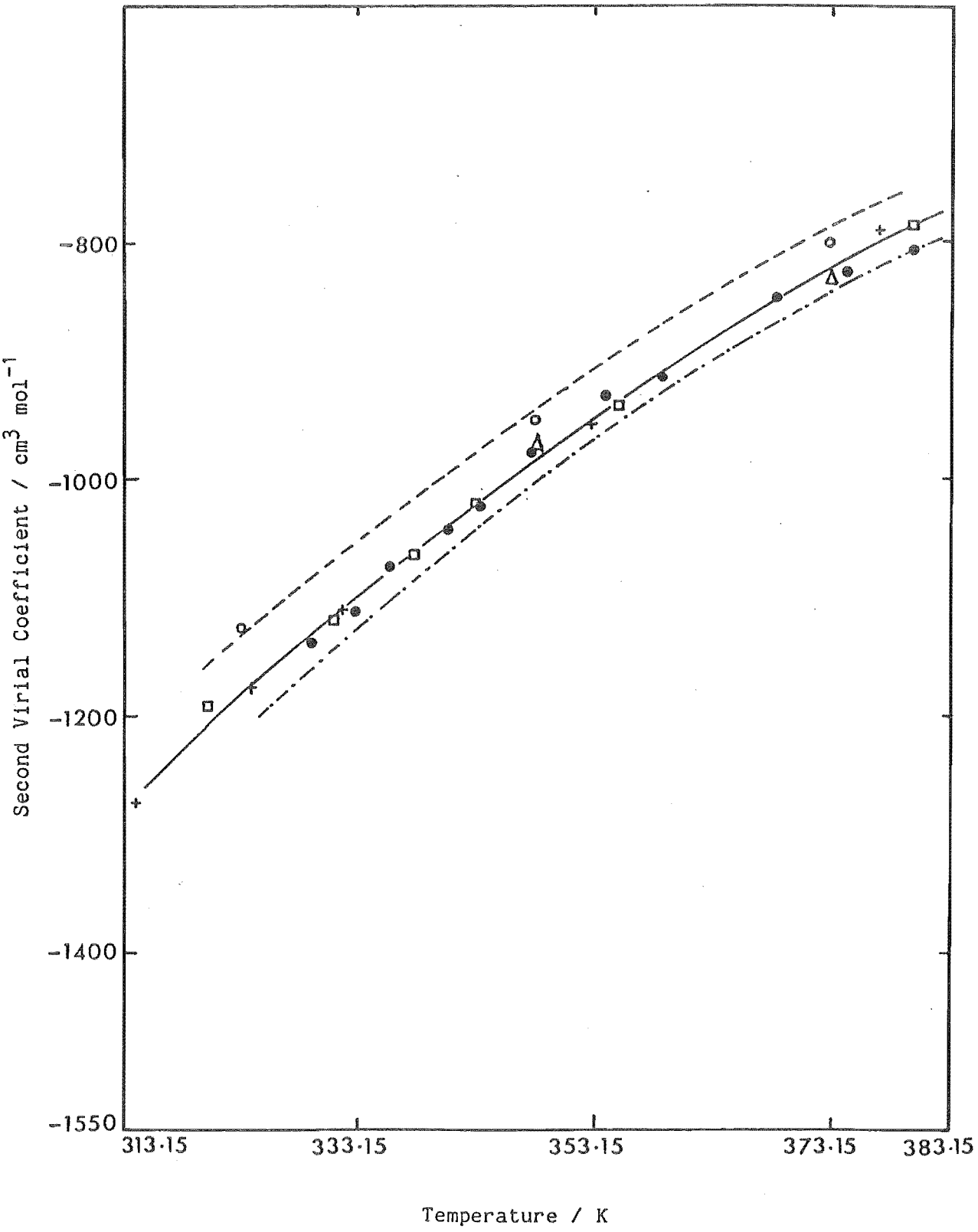

----- This Work
——— Dymond and Smith (1980)
-·-·- Hayden and O'Connell
o This Work (B)
Δ This Work (apparent B)
□ Bottomley and Spurling (1966)
● Francis et al. (1969)
✦ Todd et al. (1978)

Table 7-4. **Comparison of Values of $B_{apparent}$ of benzene with the Results of Other Workers**

Temp. / K	p_{max} / Pa	Francis et al. (1969) / $cm^3 mol^{-1}$	This work / $cm^3 mol^{-1}$
323.15	29740	-1170 *	-1173
348.15	57075	- 972	- 970
373.15	125545	- 830	- 830

* B calculated using equation (7.12)

series second virial coefficients. However, as is apparent, "true" B is 25 cm^3 mol^{-1} less negative than $B_{apparent}$.

Bottomley and Spurling (1966) reported the analysis for benzene ascertaining the influence of third virial coefficients, using the volume series equation of state. They used the differential thermal expansion method as discussed in Sections 2-3.1.5 and 7-1. They reported the difference, k, in ΔB and $\Delta\beta$ as a function C and γ, from 333 K to 430 K. k is expressed as

$$k = \Delta B - \Delta\beta = \frac{n}{V}(C_1 - C_2 - \gamma_1 - \gamma_2) \qquad (7.14)$$

where C_1, C_2, γ_1 and γ_2 are the third virial coefficients of component 1 and 2, at temperatures T_1 and T_2. Substituting for C in

equation (7.14), k is expressed as

$$k = \frac{n}{V} (B_1^2 - B_2^2) \text{ vap.} \qquad (7.15)$$

They observed that k is not greater than the experimental error of the measurement of ΔB results (± 2.0 cm^3 mol^{-1}), at high pressures. They expected the errors in the low pressure values of $\Delta\beta$ to be slightly higher. It is expected when Bottomley and Spurling's (1966) $B_{apparent}$ values corrected for the third virial coefficient effect, should give B values compared to those of "true" B values in this work.

Bich et al. (1979) measured the values of second virial coefficients, by measuring the pressures of fixed amounts of gas in a constant volume at varying temperatures. They analysed their results using the equations

$$V(1-s) = V(1 - \frac{pV}{RT}) = -(B + CV^{-1} + \ldots) \qquad (7.16)$$

and

$$V_{res.} = (\frac{RT}{p} - V) = -(\beta + \gamma p + \ldots) \qquad (7.17)$$

Ignoring C and γ, they would be measuring $B_{apparent}$ and $\beta_{apparent}$. They observed that V(1-s) is mainly temperature dependent and is independent of the density of the gas. The error in V(1-s) is related to the uncertainty in the temperature measurement. They expressed $V_{res.}$ as linear function of the pressure

$$V_{res} = a_0 + a^o p \qquad (7.18)$$

and reported that the error in β can be expressed as an error in the a_0 determination. However, this work shows that both $\beta_{apparent}$ and

$B_{apparent}$ are pressure dependent. This explains why when our results are interpreted at the same loading pressure range, as that of others, the $B_{apparent}$ and $\beta_{apparent}$ agree well with the literature values.

Bich et al.'s (1979) results show that $\beta_{apparent}$ was more negative than $B_{apparent}$ by as much as 17 cm^3 mol^{-1} for temperature at 348.15 K. It seems from the trend of second virial coefficient versus temperature, that the difference decreases with the temperature. The difference between the two is expected to be greater at lower temperatures. This work shows that $B_{apparent}$ is 25 cm^3 mol^{-1} less negative than $\beta_{apparent}$ at any temperature. Considering $\beta_{apparent}$ to be pressure dependent, they derived four orthogonal polynomial relations between $B_{apparent}$ and temperature. Their relations predicted $B_{apparent}$ quite well for temperatures from 303 to 635 K.

B. Density Balance Method

Casado et al. (1951) measured the second virial coefficient of benzene at 295.5 K, using a microbalance method but not claiming a high degree of accuracy. Whytlaw-Gray and Bottomley (1957) suspected that the balance may not have been sufficiently compensated for adsorption and that this imperfect compensation may have affected the value of the virial coefficient significantly. Bottomley et al. (1958b) deduced the second virial coefficient of benzene to be -1528 and -1352 cm^3 mol^{-1} at 295.2 and 308.2 K using a comparative gas density balance method as discussed in Section 2-3.1.5. Unfortunately, this work is not in their range of temperature. However, the B values calculated using equation (7.13) are -1501 and -1329 cm^3 mol^{-1} respectively at 295.2 and 308.2 K.

C. Indirect Methods

Benzene is included as one of the recommended reference material approved in 1974, for heat capacity of the real gas and for the enthalpy of vaporisation by IUPAC Physical Chemistry Division (Herington, 1974). A review of second virial coefficient obtained using indirect determination methods also makes an interesting study. Scott et al. (1947) and Allen et al. (1952) used the truncated pressure series virial equation of state to relate to the variation of the vapour heat capacity with pressure (equation 2.44). It is observed that both workers' results for $\beta_{apparent}$ versus T (Figure 7-6) plot very well.

Scott et al. (1947) also related β to the variation of the vapour heat capacity with pressure by the equation (2.46)

$$\lim_{p \to 0} (\partial Cp/\partial p)_T = - T d^2B/dT^2 \qquad (2.46)$$

They obtained an empirical equation for the second virial coefficient, of the form (Hirschfelder et al., 1942)

$$B = b - c.\exp(a/T) \qquad (7.19)$$

On the basis of this empirical equation, the variation of the heat capacity with pressure is given by

$$(\partial Cp/\partial p)_T = c(a^2/T^3 + 2a/T^2)\exp(a/T) \qquad (7.20)$$

where constants "c" and "a" are selected to fit $(\partial Cp/\partial p)_T$ data. They used the heat of vaporisation data to calculate B using equation

(2.44) and then b using equation (7.19). The resulting equation for the second virial coefficient for benzene, is

$$B = -202 - 53.5\exp(950/T) \qquad (7.21)$$

Todd et al. (1978) calculated the second virial coefficients $B_{apparent}$ from the Clapeyron equation (2.45) at each temperature at which the enthalpy of vaporisation was determined. Their values fitted well with $B_{apparent}$ values of other workers (Figure 7-7) and they were slightly less negative than $\beta_{apparent}$ values calculated by Scott et al. (1947) and Allen et al. (1952). Hence the effect of third virial coefficient is also observed in the indirect measurements.

Todd et al. (1978) also used the variation of heat capacity with pressure data to obtain values of $-T^2d^2B/dT^2$ from the equation (2.46). They correlated the results with the empirical equation for B as a function of temperature T.

$$B = b + d/T + c[\exp(a/T) - 1 - a/T] \qquad (7.22)$$

Equation (7.22) is a modification of equation (7.19). B values obtained by such a method are expected to be free from the possible systematic errors arising from adsorption.

D. Analytical Methods

Both the correlations of Hayden and O'Connell (1975) and Tsonopoulos (1974) fit the pressure series virial coefficients (literature values in Figure 7-6) more closely than the volume series

second virial coefficients (Figure 7-7).

The tabulation of Lennard-Jones (6-12) potential parameters (Table 7-5), for this work differs from Tee et al. (1966) and Sherwood and Prausnitz (1964) estimations of parameters for benzene.

Table 7-5. **Force Constants for Lennard-Jones (6-12) Potential for benzene**

	This work	Tee et al. (1966)	Sherwood et al. (1964)	Bottomley et al. (1966)
ϵ/k	(K) 289.000	247.500	242.700	284.400
σ	(Å) 7.424	8.443	8.569	5.790

However, the ϵ/k value for this work is very close to 284.4 calculated by Bottomley and Spurling (1966). Using ϵ/k equal to 289 and equation (7.6) T^* for benzene varies from 1.12 to 1.30 corresponding to T/T_B varying from 0.55 to 0.64. A plot of γ/v_B^2 versus T/T_B (Figure 7-3) suggests the trend of slopes to be negative and getting less negative for T/T_B varying from 0.55 to 0.64, as obtained experimentally in this work (Figure 7-7).

Zaalishvili et al. (1965a) using their experimental results of benzene (Zaalishvili et al., 1964) found ϵ/k to be equal to 200 K and σ equal to 9.72 Å.

FIGURE 7-8

Comparison of Slopes for Plots of $\beta_{apparent}$ for Benzene

Versus $(p_1 + p_2 - p_3)$

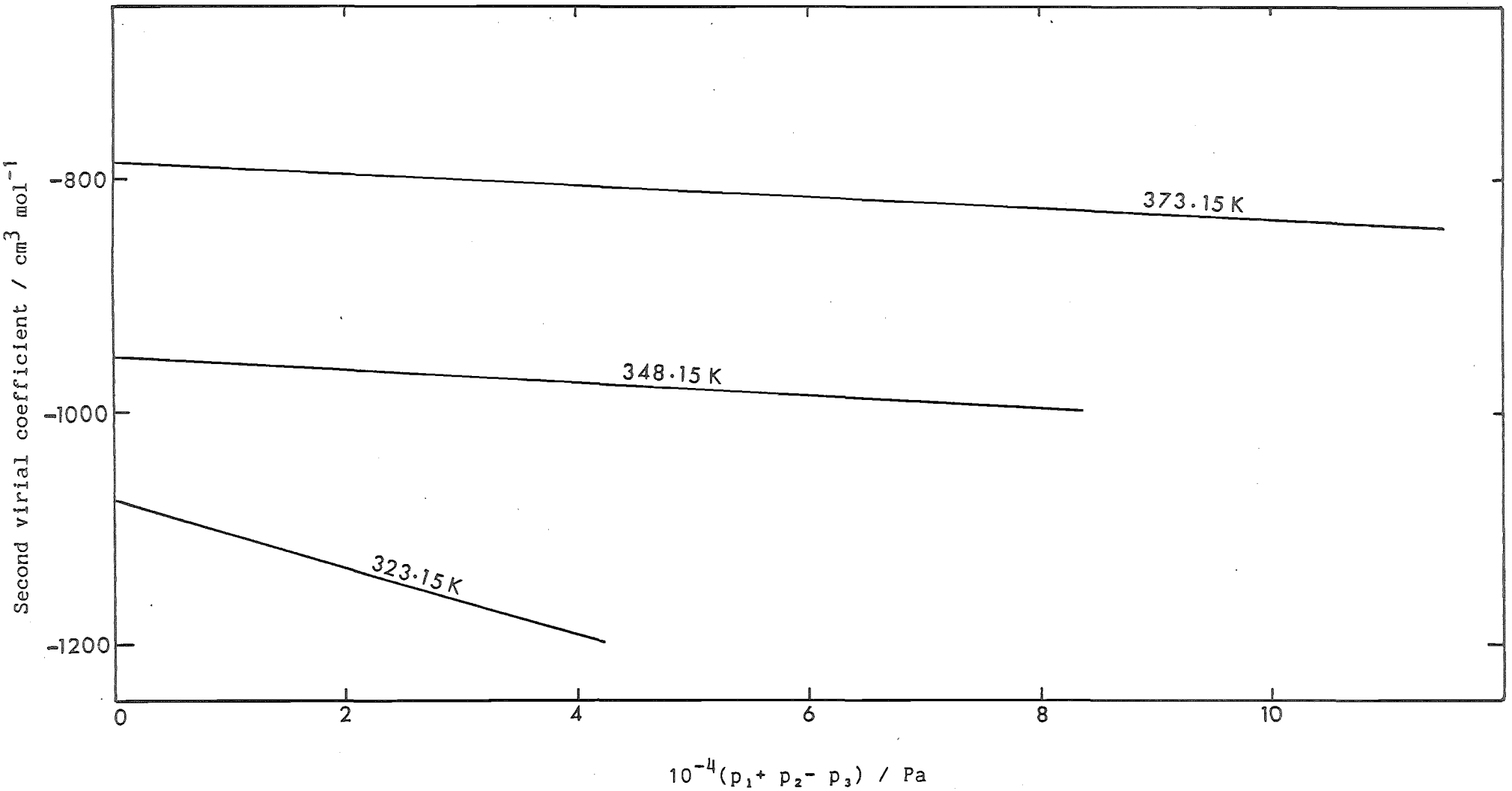

7-3.3 Cyclohexane

The results for cyclohexane have certainly been affected by adsorption, as observed on the "Baratron" gauge, while transferring cyclohexane vapours from one cell to another. The results have not been corrected for adsorption. This effect is more significant for the measurements at 323.15 K, and the larger error bands (Figure 6-10) in the low pressure regions inhibit the precise extrapolation of the line through the plot of $\beta_{apparent}$ versus $(p_1 + p_2 - p_3)$ to the required accuracy. Hence β for cyclohexane is estimated in the same manner as that for benzene (Section 7-3.2). The best estimate of β for cyclohexane at 323.15 K is found to be -1384 $cm^3\ mol^{-1}$.

Dymond and Smith (1980) have recommended values for the second virial coefficients of cyclohexane within the accuracy of ±50 $cm^3\ mol^{-1}$ at temperatures from 300 to 560 K, ignoring the results of Kerns et al. (1974) and Lambert et al. (1949). Most of the previous results are either below 323.15 K or above 373.15 K, with the exception of the work of Lambert et al. (1949), Hajjar et al. (1969) and Waelbroeck (1955), and these available results are not sufficiently accurate enough for a conclusive comparison. It is observed that all the values of $\beta_{apparent}$ averaged at a temperature agree reasonably well with literature values (Figure 7-9).

Bottomley and Remington (1958d) used a microbalance to measure the second virial coefficient of cyclohexane at 295.2 and 308.2 K. They obtained the pressure series second virial coefficient values -1663 $cm^3\ mol^{-1}$ at 298.2 K and -1523 $cm^3\ mol^{-1}$ at 308.2 K. These results are not in our range of temperature. These values are slightly more

FIGURE 7-9

Second Virial Coefficient (Pressure Series) of Cyclohexane Versus Temperature

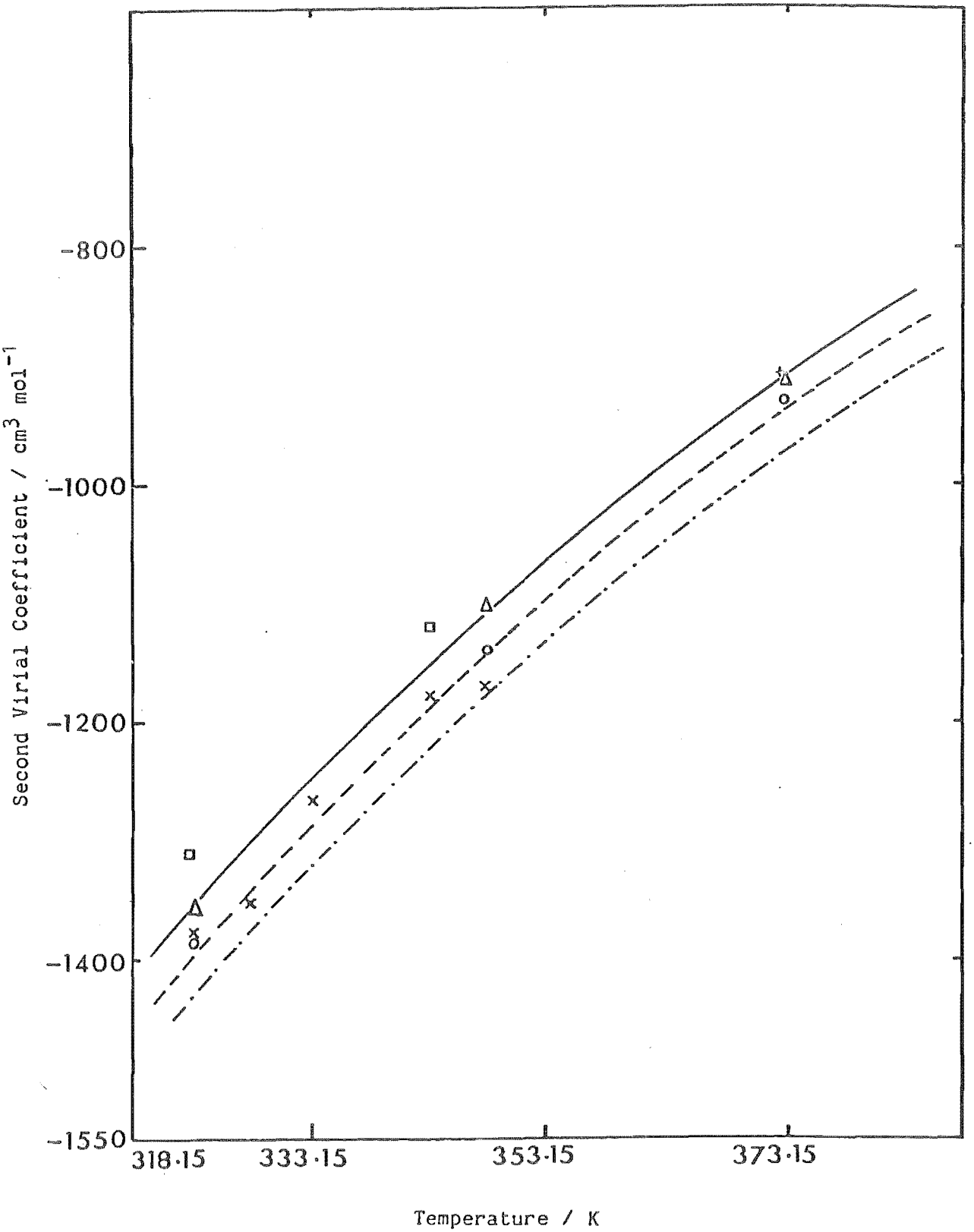

negative than the values on the smooth curve, representing this work, when extended to the temperature 298.2 K.

The Hayden and O'Connell (1975) and Tsonopoulos (1974) correlations seem to fit this work well. However, it is necessary to do more work on cylcohexane at other temperatures to establish any trend different from previous work.

The Lennard-Jones (6-12) potential parameters for cyclohexane in Table 7-6 are comparable with those estimated by Kunz and Kapner (1971).

Table 7-6. **Force Constants for Lennard-Jones (6-12) Potential**

	This work	Kunz and Kapner(1971)
ε/k (K)	175	189
σ (Å)	11.3	10.6

The trend of slopes is expected to be same as that for n-hexane, as T/T_B varies from 0.90 to 1.04. However, in this work, the slope for 373.15 K tends to be negative (Figure 7-10). This work is very close to the Boyle temperature for cyclohexane and it is difficult to establish the expected trend for the slope, as it may be positive or negative, in this region.

FIGURE 7-10

Comparison of Slopes for Plots of $\beta_{apparent}$ for Cycloheane

Versus $(p_1 + p_2 - p_3)$

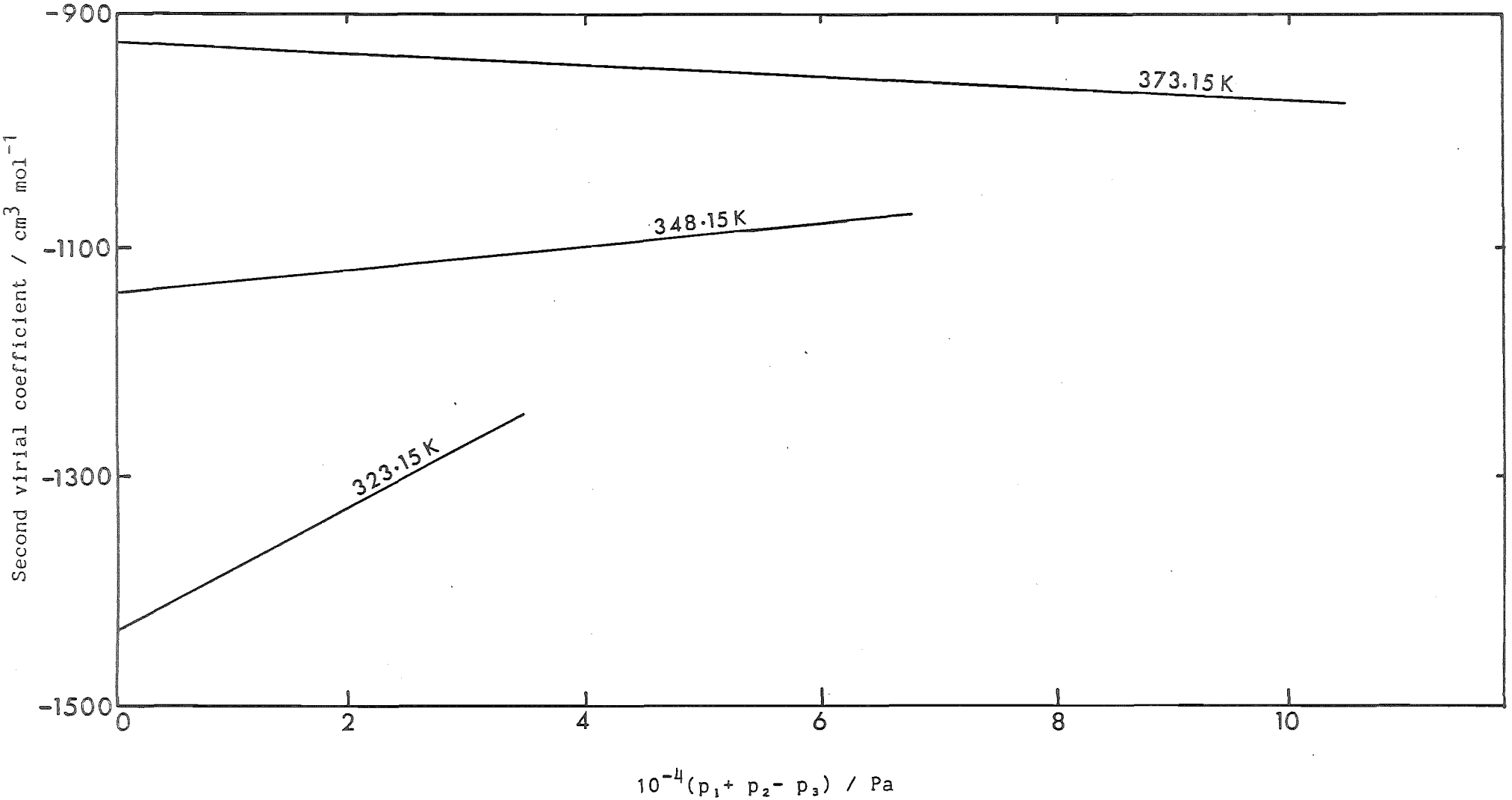

B. MIXTURES

7-4 Significance of ε

The significance of the interaction second virial coefficients of the mixture, has already been discussed in Chapter 1. After obtaining meaningful "true" second virial coefficients for the pure components, it is necessary to study the interaction between the groups of molecules represented by equation (1.7). For a binary mixture, it is convenient to define excess second virial coefficients (equation 1.11), which can be measured with reasonable accuracy, given by equation (3.38).

7-5 Accuracy of the Experimental Techniques and $\mathcal{E}$ Measurement

7-5.1 The "Open Tap" Technique

The "Open Tap" technique (Section 5-5) avoids the effects of the volume changes caused by opening and shutting the valve and reduces the likelihood of zero pressure difference shift. However, this technique involves certain assumptions.

1. Opening valve (H3) before inducing mixing has little effect, during the time (approximately 5 minutes) taken to obtain the zero pressure difference reading.
2. The amount of the vapour left unmixed in the pipe beyond valve (H5) and in the diaphragm chamber is not large enough to affect

the measurement, as the pressure difference on the mixing is dependent on the mole fraction of the product only.

7-5.2 The Temperature Fluctuation

Shannon (1976) reported pressure difference fluctuations of 0.1 Pa caused by the thermostat controller altering the power input to maintain the required temperature. This effect was reduced by controlling the room temperature fluctuations within 0.5 K, using an air conditioning unit, covering the top of the bath with a removable wooden lid, followed by glass wool sheet and blocking the cold fingers with long wooden stoppers. Better bath insulation (especially around the cold finger) has the effect of slowing down these pressure difference fluctuations, but not their magnitude. A better accuracy has been achieved in the results (Section 7-6.1), compared to those obtained by Shannon (1976). The corrected value of excess second virial coefficient for benzene + cyclohexane, at 298.15 K, is reported to be 146 $cm^3\ mol^{-1}$ within ±27 $cm^3\ mol^{-1}$. Shannon (1976) has reported ε for the same mixture, at 300 K, to be 175 $cm^3\ mol^{-1}$, within ±50 $cm^3\ mol^{-1}$ (Section 7-6.1, Table 7-7).

7-5.3 Measurement Errors

The major source of error in the measurement of ε is the uncertainty in the pressure difference (Section 3-7.1). The reproducibility of the measurements of ε at 348.15, 373.15 and 398.15 K are within the pressure difference uncertainty of ±0.1 Pa. The

loading pressure is balanced to better than 0.1 Pa in all cases.

7-5.4 Surface Vapour Adsorption

The model postulated in the Section 3-7.4, is only qualitatively useful. The adsorptive area used for the correction is the geometric area of the cylinder. Several authors (Brunauer et al., 1938; Cusumano and Low, 1970) have claimed monolayer adsorption isotherm up to relative pressure p/p^{o} corresponding to 0.34. Hence at higher loading pressure, there is a possibility of multimolecular layer adsorption, which can result in the effective area being up to ten times or more than the geometric area. Thus the corrections required due to the effect of surface adsorption can be more than ten times greater than reported in this work.

However, using the model postulated, narrows the spread of the results in the "corrected" results at various loading pressures. This indicates that increasing the postulated adsorptive area, may narrow the spread even further.

7-6 Comparison of Results with Literature Values

In this Section, the excess virial coefficients and interaction second virial coefficients are compared and discussed. Pompe and Spurling (1976), Dymond and Smith (1980) and Warowny and Stecki (1979) have compiled the second cross virial coefficients of gaseous mixtures. Attempts to predict and correlate both the excess and interaction second virial coefficients are discussed.

7-6.1 Comparison of Excess Second Virial Coefficients of Mixtures

Benzene(1) + Cyclohexane(2)

The plot of the excess second virial coefficients (ε) of benzene(1) + cyclohexane(2) versus temperature is shown in Figure 6-14. Literature values for the excess second virial coefficients of benzene + cyclohexane are tabulated in Table 7-7 and are illustrated in Figure 7-11 for ε versus T. This work (Table 6-13) has better accuracy than that reported by Shannon (1976) and Pasco et al. (1980) presented in Table 7-7. The results are in good agreement with those of Pasco et al. (1980).

At 298.15 K, the results are scattered. It is possible that the loading pressure (Table A10-1) of 9678 Pa (0.76 fraction of saturated vapour pressure of benzene) may be the cause of error due to adsorption.

Judd et al. (1980) held reservations concerning the literature values of ε at 298.15 K (Pasco et al., 1980) and 300 K (McElroy et al., 1980). They justified their concern by performing the curve fitting using data pairs (ε_i, T_i) and (H^E/p_j, T_j). This was done to examine the effect of using values of H^E/p on the shape of the plot of ε versus T. The predicted ε value at 298 K, is 74.87 $cm^3\ mol^{-1}$ approximately half the experimental measured value. ε equal to 175 $cm^3\ mol^{-1}$ at 300 K (Shannon,1976) seem to be larger than expected. However, this work supports the ε value equal to 135 $cm^3\ mol^{-1}$ (Pasco et al., 1980) at 298.15 K. This view is further strengthened with ε, at 303 K, equal to 140 $cm^3\ mol^{-1}$ (Keller, 1983), which lies very close on the curve (Figure 6-14). Keller (1983) has used a glass apparatus

Table 7-7 **Literature Value of the Excess Second Virial Coefficient of Benzene + Cyclohexane**

T / K	ε / $cm^3\ mol^{-1}$	Source
298	135 ± 80	Pasco et al. (1980)
300	175 ± 50	McElroy et al. (1980)
303	140	Keller (1983)
308	57 ± 10	Pasco et al. (1980)
313	30 ± 45	McElroy (1968)
315	38 ± 16	McElroy et al. (1980)
318	45 ± 20	McElroy (1968)
323	35 ± 10	McElroy (1968)
	44 ± 1	McElroy et al. (1980)
	29 ± 2	Pasco et al. (1980)
	48 ± 2	Keller (1983)
333	14 ± 15	McElroy (1968)
348	19 ± 3	McElroy et al. (1980)
	25 ± 2	Pasco et al. (1980)
	28 ± 1	Keller (1983)
373	21 ± 3	McElroy et al. (1980)
	22 ± 2	Pasco et al. (1980)
	22 ± 1	Pasco et al. (1980)

FIGURE 7-11

The Excess Second Virial Coefficieint (ε) of

Benzene (1) + Cyclohexane (2)

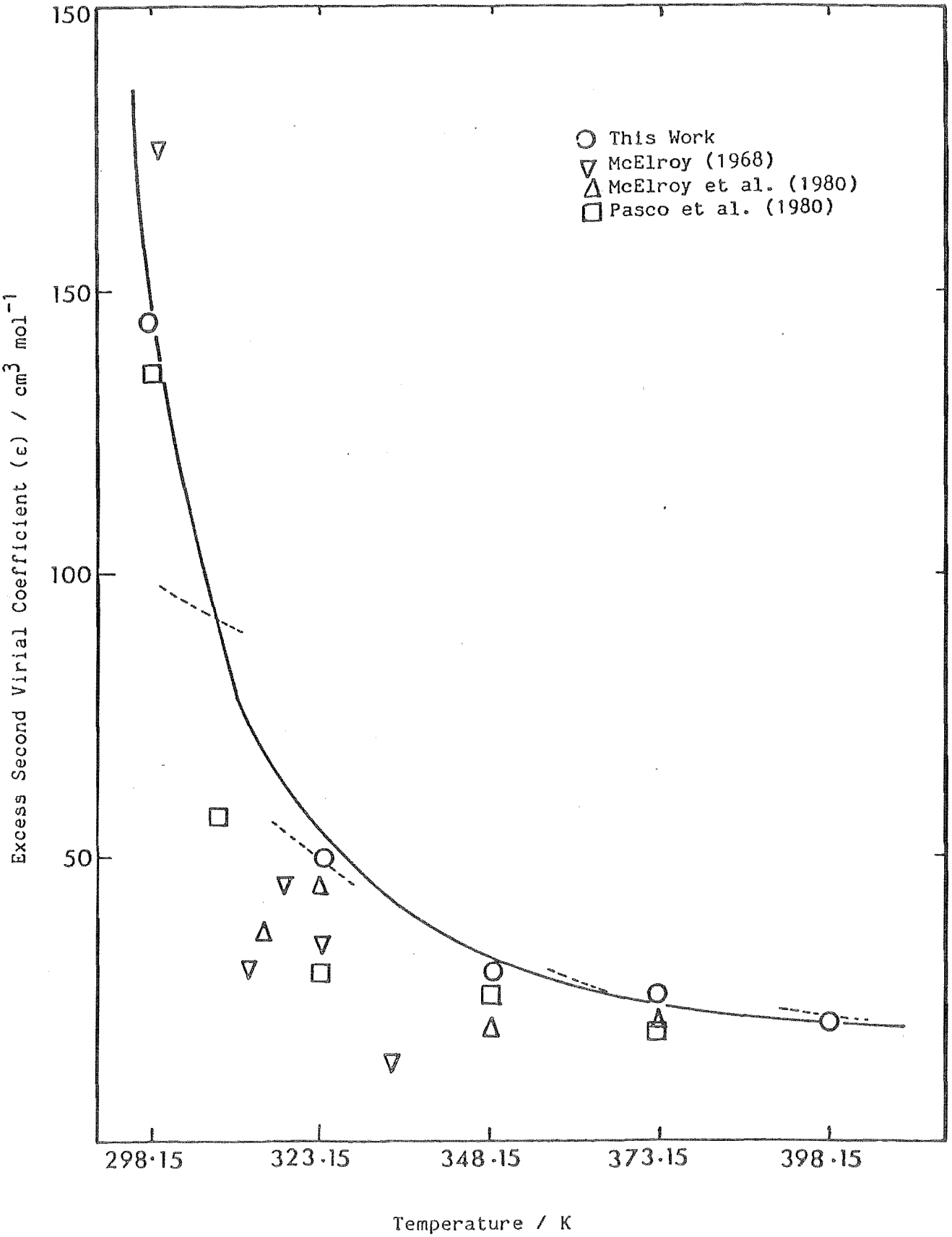

for ε measurements to moderate the effect of surface adsorption. His ε values at 323.15 K and 348.15 K are comparable with those reported in this work. However, he suggests that these values may be in slight error as the pressure transducer, used in the work, needed recalibration

Mayhew (1976) has measured $(H^E/p)_{323}$ = 210 ±30 $cm^3\ mol^{-1}$ and $(H^E/p)_{356}$ = 50 ±4 $cm^3\ mol^{-1}$ in a flow calorimeter, with a mole fraction of benzene at 0.548 in the both cases. Wormald (1969b) measured $(H^E/p)_{373}$ = 40 ±10 $cm^3\ mol^{-1}$. Using equation (1.27) and values of ε, from Figure 6-14, gives

$$(d\varepsilon/dT)_{323} = -1.2\ cm^3\ mol^{-1}\ K^{-1},$$
$$(d\varepsilon/dT)_{356} = -0.72\ cm^3\ mol^{-1}\ K^{-1} \text{ and}$$
$$(d\varepsilon/dT)_{373} = -0.16\ cm^3\ mol^{-1}\ K^{-1}$$

These slopes are shown in Figure 7-11 and they show reasonable agreement with the fit through the results, especially in the higher temperature region. The curve is very steep between 298.15 and 323.15 K. It gradually decreases from 323.15 to 348.15 K, till it is nearly horizontal from 348.15 to 373.15K.

Benzene(1) + n-Hexane(2)

This work results can not be compared with those of others, because of unavailability of literature data, in this temperature range (Dymond and Smith, 1980). No data are available for (H^E/p) for this system, in the vapour state. The excess second virial coefficients, corrected for adsorption, are within the error limit corresponding to that caused by the pressure difference uncertainty.

The results corrected for adsorption are tabulated in Table

6-14, and a smooth curve is drawn through the averaged excess second virial coefficients of the system, versus temperature (Figure 6-15). The trend is slightly different compared to that of benzene(1) + cyclohexane(2) in Figure 6-14. It has uniform dε/dT for the results from 323.15 to 398.15 K. There is a steep slope in the curve from 298.15 to 323.14 K. The excess second virial coefficient for the system is only 66 cm^3 mol^{-1} at 323.15 K, compared to 146 cm^3 mol^{-1} for benzene + cyclohexane, at the same temperature. However, the excess second virial coefficient is only about 6 cm^3 mol^{-1} lower than that of benzene + cyclohexane for temperatures from 348.15 to 398.15 K. This suggests similar interactions between the two systems, for temperatures from 348.15 to 398.15 K.

Cyclohexane(1) + n-Hexane(2)

No literature results are available, for either the excess second virial coefficient or heat of mixing (H^E/p) for this system in the vapour state. The results show negative excess second virial coefficients for all temperatures. The adsorption corrections for this system are less, compared to those for other system, even at nearly the same loading pressure. When corrected for the adsorption at various loading pressures, the spread of the results is narrowed.

The results (Table 6-15) at 323.15 K are suspicious, especially, the one at the loading pressure of 9034 Pa, as the excess second virial coefficient is positive, while for other loadings at 8679 and 9017 Pa, ε is negative. Since it is expected to be negative, ε calculated at the loading pressure of 9034 Pa is discarded. Hence the average ε at 298.15 K is -9.5 cm^3 mol^{-1}.

A smooth curve is plotted through the averaged excess second virial coefficients of cyclohexane + n-hexane, from 298.15 to 398.15 K,

in the steps of 25°C (Figure 6-16). The curve is nearly flat for the temperature from 323.15 to 398.15 K. It shows only a slight slope from 298.15 to 323.15 K.

7-6.2 Comparison of Literature and Experimental Values of the Interaction Second Virial Coefficient

Experimental values of B_{12} are calculated using the equation (1.11)

$$B_{12} = \varepsilon + (B_{11} + B_{22})/2 \qquad (7.23)$$

and substituting the values for ε and the "true" values of B of pure component 1 and 2 obtained in this work. The "true" values of B at the corresponding temperatures are taken from the smooth curves through the experimental values of B versus T. The values of B_{12} calculated in this way for all the three binary mixtures of benzene, cyclohexane and n-hexane are tabulated in Table 7-8.

The uncertainties reported, in Table 7-8, have been calculated by averaging the pure component uncertaintities and adding the excess second virial coefficient uncertainty i.e.

$$\delta B_{12} = \delta\varepsilon + (\delta B_{11} + \delta B_{22})/2 \qquad (7.24)$$

δB_{12} for all the three systems at 323.15 K is large, as B reported for "true" B for benzene and cyclohexane are high.

Table 7-8 **Interaction Second Virial Coefficient B_{12} of the Mixtures**

System T / K	(a)* B_{12} / $cm^3\ mol^{-1}$	(b)* B_{12} / $cm^3\ mol^{-1}$	(c)* B_{12} / $cm^3\ mol^{-1}$
323.15	-1175	-1346	-1458
348.15	- 994 ± 62	-1097 ± 53	-1201 ±55
373.15	- 842 ± 31	- 930 ± 41	-1026 ±31

*(a) Benzene (1) + cyclohexane (2)

(b) Benzene (1) + n-hexane (2)

(c) Cyclohexane (1) + n-hexane (2)

The literature values of B_{12} for benzene + cyclohexane are tabulated in Table 7-9. The comparison of B_{12} values for the system is illustrated in Figure 7-12.

Waelbroeck (1955) calculated interaction virial coefficient B_{12} of the mixture (benzene + cyclohexane) from the equation

$$B_m = x_1^2 B_{11} + 2x_1 x_2 B_{12} + x_2^2 B_{22} \qquad (7.25)$$

where B_{11}, B_{12} and x_1, x_2 are the second virial coefficients and mole fractions of benzene and cyclohexane respectively and B_m is the apparent virial coefficient of the mixture. To obey the corresponding states law, the value of B_{12} should lie between B_{11} and B_{22}. He suggested that in the temperature range for 328 to 348K studied, and

Table 7-9 **Literature Value of the Interaction Second Virial Coefficient of Benzene + Cyclohexane**

T/K	$B_{12}/(cm^3\ mol^{-1})$	Source
298	-1410 ±130	Pasco et al. (1980)
300	-1355 ±100	McElroy et al. (1980)
308	-1346 ±70	Bottomley and Coopes (1962)
	-1364 ±54	Pasco et al. (1980)
313	-1336 ±95	McElroy (1964)
315	-1340 ±60	McElroy et al. (1980)
318	-1272 ±70	McElroy (1968)
323	-1225 ±50	McElroy et al. (1980)
	-1280 ±50	Pasco et al. (1980)
	-1222 ±60	McElroy (1968)
	-1215 ±70	Bottomley and Coopes (1962)
328	-1227 ±70	Waelbroeck (1955)
333	-1144 ±65	McElroy (1968)
	-1203 ±70	Waelbroeck (1955)
343	-1041 ±70	Bottomley and Coopes (1962)
	-1109 ±70	Waelbroeck (1955)
348	-1075 ±70	Waelbroeck (1955)
	-1090 ±46	Pasco et al. (1980)
	-1035 ±47	McElroy et al. (1980)
373	- 910	Cox and Stubley (1960)
	- 844 ±47	McElroy et al. (1980)
	- 840 ±47	Pasco et al. (1980)

within the experimental uncertainties, the pure substances appear to obey the corresponding state law. His B_{12} values are more negative compared to this work values at the same temperature (Figure 7-12).

Cox and Stubley (1960) also measured B_{12} for the mixture benzene(1) + cyclohexane(2) at 373 K, using Boyle method as described in Section 2-3.1.2. They contradicted Waelbroeck's (1955) suggestion of pure substances obeying a corresponding state law. They calculated B_{12} for the mixture at 373.15 K, equal to -918 cm^3 mol^{-1}, while the experimental second virial coefficients for benzene and cyclohexane are -814 cm^3 mol^{-1} and -900 cm^3 mol^{-1} respectively. However, our results show that the pure substances do obey the corresponding state law, as the B_{12} values lie between B_{11} and B_{22}. But it is suggested that still a lot of work has to be put into accurate determination of "true" second virial coefficients of pure components and interaction virial coefficients of the mixtures. Our results are calculated using equation (7.23), expecting to have less uncertainty in B_{12} measurement than Cox and Stubley's (1960) method.

Bottomley and Coopes (1962) used a differential compressibility apparatus (Bottomley et al., 1958a) to measure second virial coefficients of cyclohexane-benzene mixture and the pure component cyclohexane at 308, 323 and 343 K, using benzene as the reference gas with B values from the previous work (Bottomley et al., 1958a). They used the results to calculate the interaction coefficient B_{12} from the equation (7.25), where B_{11}, B_{22} and x_1, x_2 are the second virial coefficients and mole fractions of cyclohexane and benzene respectively.

McElroy (1968), McElroy et al. (1980), and Pasco et al. (1980) used the same method as described in Section 2-4.1 and reported for this work. McElroy et al. (1980) estimated the second virial

FIGURE 7-12

Interaction Second Virial Coefficient (B_{12}) for

Benzene (1) + Cyclohexane (2)

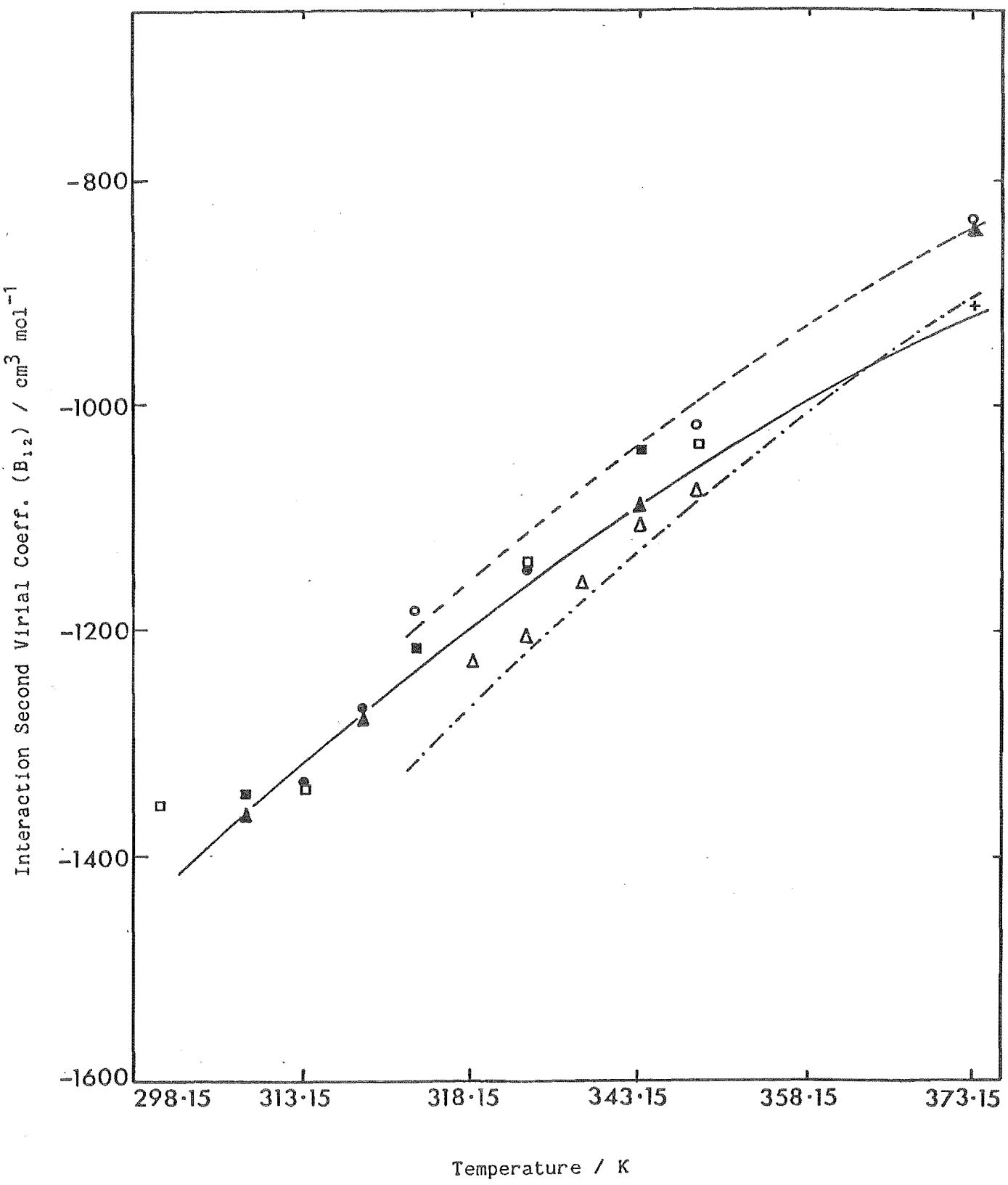

o This Work
+ Cox and Stubley (1960)
□ McElroy et al. (1980)
Δ Waelbroeck (1955)
■ Bottomley and Coopes (1962)
● McElroy (1968)
▲ Pasco et al. (1980)

coefficients using McGlashan and Potter's (1962) correlation, as given in equation (1.17)

$$B/V^c = 0.43 - 0.886T_R^{-1} - 0.694T_R^{-2} - 0.0375(n-1)T_R^{-4.5} \quad (1.17)$$

where n is equal to 3.8 for cyclohexane and 4.1 for benzene. Pasco et al. (1980) used the values of the pure components, as given in the literature (Dymond and Smith, 1980).

The error for the values of ε (Pasco et al., 1980; McElroy, 1968; Shannon, 1976) have been calculated using equation (7.24). The errors assigned to ε (Bottomley and Coopes, 1962; Cox and Stubley, 1960; Waelbroeck, 1955) are as calculated by Shannon (1976). Our results at 373.15 K are comparable with Pasco et al. (1980) and McElroy et al. (1980), but are less negative than those values reported at 323.15 and 348.15 K.

The experimental values of interaction second virial coefficients B_{12} (Table 7-8) for benzene + n-hexane, and cyclohexane + n-hexane are illustrated in Figure 7-13. Zaalishvili et al. (1971) and Belousova and Verkhova (1973) have measured B_{12} for benzene + n-hexane in the range of temperature varying from 433.2 to 493.2 K. It is difficult to directly compare their B_{12} values with this work at lower temperatures. However, a plot of B_{12} versus temperature (Figure 7-14) for benzene + n-hexane shows that their values extrapolated to low temperatures, are more negative than those in this work.

Battino et al. (1983) have reported B_{12} for the systems (benzene + n-hexane, and cyclohexane + n-hexane). The pure component second virial coefficients are calculated using McGlashan and Potter's (1962) equation (1.17).

The equation gave a good fit to existing results considered most accurate, using n=3.8 for cyclohexane, n=4.1 for benzene (Chan,

FIGURE 7-13

Interaction Second Virial Coefficient (B_{12}) for Benzene (1) + n-Hexane (2) and Cyclohexane (1) + n-Hexane (2)

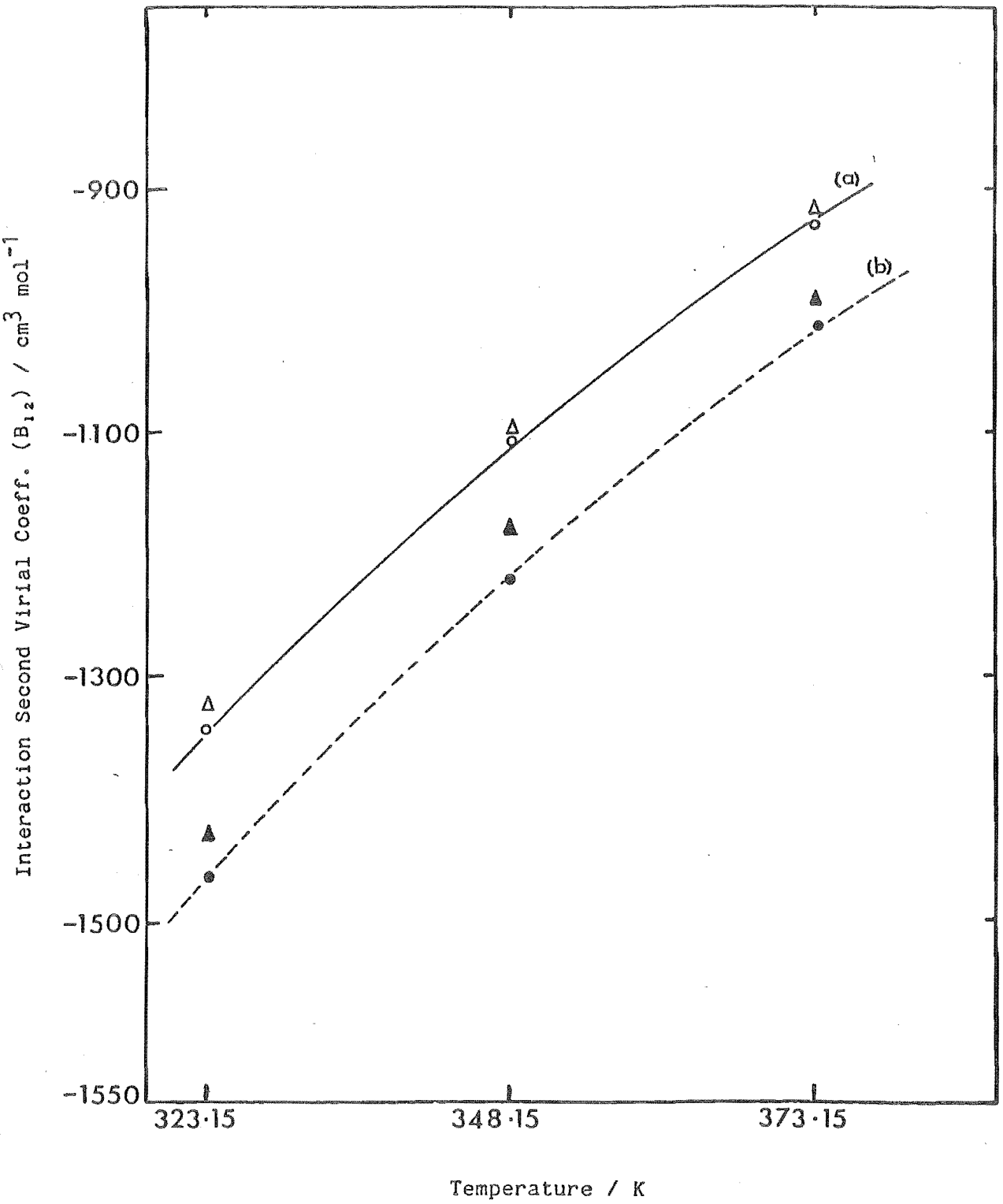

a. Benzene (1) + n-hexane (2)

o This Work
Δ Battino et al. (1983)
—— Hayden and O'Connell (1975)

b. Cyclohexane (1) + n-hexane (2)

● This Work
▲ Battino et al. (1983)
---- Hayden and O'Connell (1975)

FIGURE 7-14

Literature Values for the Interaction Sec. Virial Coeff. (B_{12})

for Benzene (1) + n-Hexane (2)

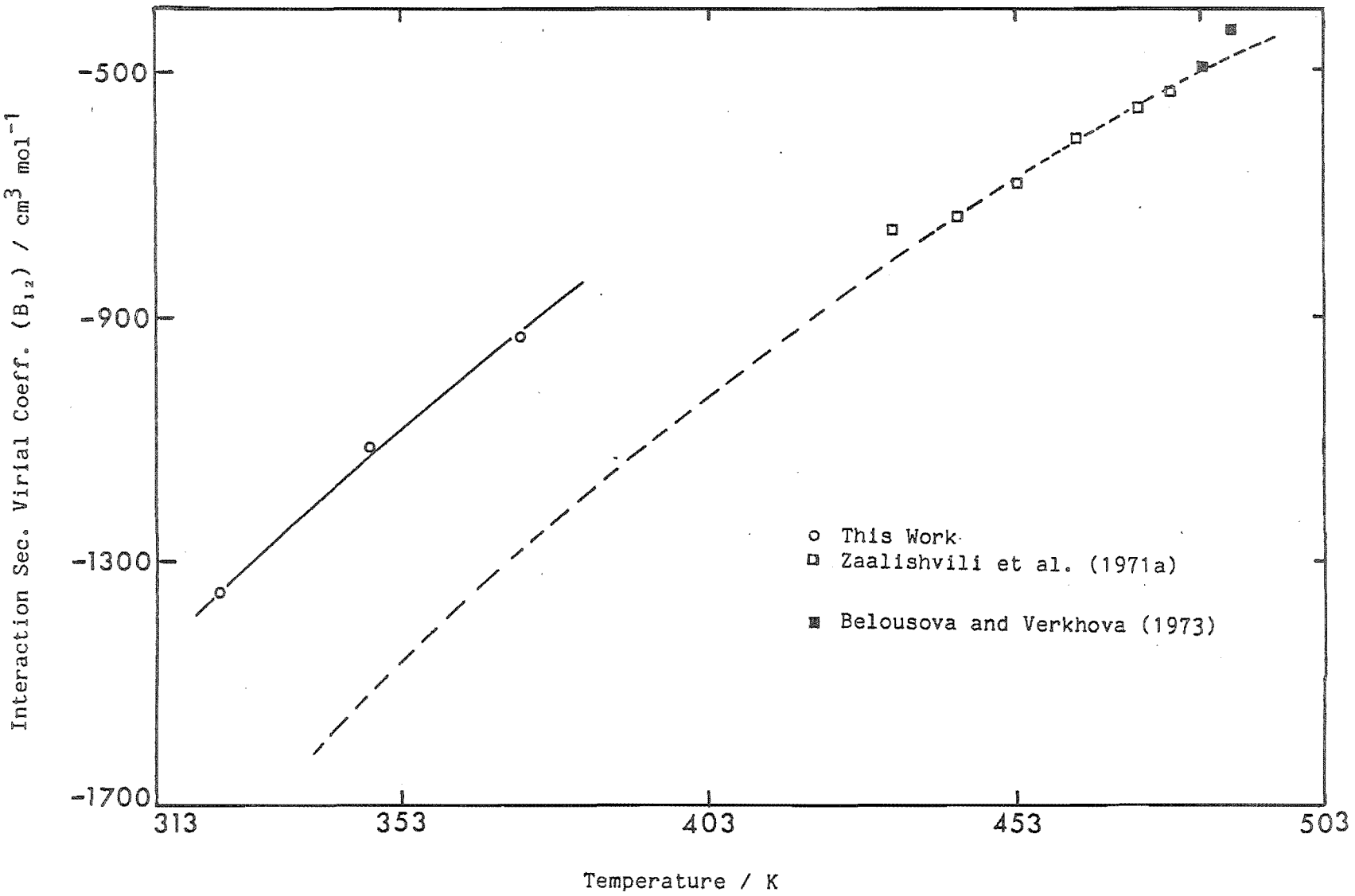

1976). The predicted values agree with the data, but the data consists of apparent values of B and β, and not "true" B values as reported in this work. The Joule - Thomson coefficients for n-hexane (Al-Bizreh and Wormald, 1978) used, assuming a functional form for B, to calculate B values in the limit of zero pressure give values which are in good agreement with McGlashan and Potter's (1962) equation for n-hexane. However, there has been controversy, whether measurements made at sufficiently low pressures, ensure the determination of "true" B, as do the B measurement, determined by extrapolation of apparent values of B and β at zero pressure. This work is not in agreement with the McGlashan-Potter correlation as "true" B for n-hexane are approximately 80 $cm^3\ mol^{-1}$ more negative than those values obtained from equation (1.17) at corresponding temperatures.

Figure 7-13 illustrates the difference in B_{12} values using "true" B (Table 7-8) and those (Table 7-10) calculated using predicted

Table 7-10 **Interaction Second Virial Coefficient B_{12} of the Mixtures (Battino et al., 1983)**

System / T / K	(a)* B_{12} / $cm^3\ mol^{-1}$	(b)* B_{12} / $cm^3\ mol^{-1}$
298.15	-1639	-1781
323.15	-1327	-1428
348.15	-1094	-1177
373.15	- 915	- 989
398.15	- 783	- 846

*(a) Benzene(1) + n-hexane(2)

(b) Cyclohexane(1) + n-hexane(2)

second virial coefficients from the McGlashan-Potter correlation (Battino et al., 1983). However, they are within experimental errors and it certainly needs improved accuracy of pure component "true" B to suggest a different correlation.

7-6.3 Correlation of the Existing Results

Malijevsky and Novak (1980) reported semi-empirical rules for estimating cross second virial coefficients. The simplest estimation rules for B_{12} are as follows

(1) $$B_{12}(T) = [B_{11}(T) + B_{22}(T)]/2 \qquad (7.26)$$

(2) $$B_{12}(T) = [B_{11}(T)B_{22}(T)]^{0.5} \qquad (7.27)$$

where $B_{11}(T)B_{22}(T) > 0$

(3) $$B_{12}(T) = (1/8)[B_{11}^{1/3}(T) + B_{22}^{1/3}(T)]^3 \qquad (7.28)$$

More accurate estimates are obtained by applying the empirical relations for virial coefficients of pure components (Black, 1958; McGlashan and Potter, 1962; Pitzer and Curl, 1957) and using various combination rules for the parameters. Malijevsky and Novak (1980) derived the following new relations estimating B_{12} in terms of the corresponding state theorem.

(4) $$B_{12}(T) = (1/8)[B_{11}^{1/3}(T(\frac{T_1^c}{T_2^c})^{0.5}) + (B_{22}^{1/3}(T(\frac{T_2^c}{T_1^c})^{0.5})]^3 \qquad (7.29)$$

(5) $$B_{12}(T) = (1/16)(V_1^{c\,1/3} + V_2^{c\,1/3})^3[V_1^{c\,-1} B_{11}(T\,(T_2^c/T_1^c)^{0.5}) + V_2^{c\,-1} B_{22}(T\,(T_1^c/T_2^c)^{0.5})] \quad (7.30)$$

(6) $$B_{12}(T) = (1 + \delta^2/12)[B_{11}(T)B_{22}(T)]^{0.5} \quad (7.31)$$

where $\delta = (V_1^c - V_2^c)/V^c$

Other established correlations to predict B_{12} are due to Tsonopoulos (1974), in Appendix A9, Hayden and O'Connell (1975), in Appendix A8, and McGlashan and Potter (1962) correlations. Table 7-11 gives the comparison of experimental B_{12} for benzene + cyclohexane and predicted B_{12} values using semi-empirical rules and established correlations.

McGlashan and Potter (1962) estimations of B_{12} are calculated using the correlation

$$B_{12}/V_{12}^c = 0.430 - 0.886(T_{12}^c/T) - 0.694(T_{12}^c/T)^2 - 0.375(n_{12} - 1)(T_{12}^c/T)^{4.5} \quad (7.32)$$

where the pseudo critical properties V_{12}^c, T_{12}^c and chain length n_{12} are calculated using the combining rules (equations 1.21 to 1.23).

$$T_{12}^c = (T_{11}^c T_{22}^c)^{0.5} \quad (1.21)$$

$$V_{12}^c = 1/8(V_{11}^{c\,1/3} + V_{22}^{c\,1/3})^3 \quad (1.22)$$

$$n_{12} = (n_1 + n_2)/2 \quad (1.23)$$

Table (7.11) shows that semi-empirical rules give better estimation of B_{12}, for benzene + cyclohexane, than the predictive

Table 7-11 **Comparison of Interaction Second Virial Coefficients**

for Benzene (1) + Cyclohexane (2)

Correlation No.	$B_{12}(323.15)$ / $cm^3\ mol^{-1}$	$B_{12}(348.15)$ / $cm^3\ mol^{-1}$	$B_{12}(373.15)$ / $cm^3\ mol^{-1}$
Expt.	-1175	- 994	-842
(1)	-1225	-1023	-868
(2)	-1254	-1042	-859
(3)	-1224	-1021	-866
(4)	-1223	-1020	-865
(5)	-1225	-1021	-866
(6)	-1225	-1022	-866
(7)	-1370	-1105	-919
(8)	-1260	-1050	-895
(9)	-1314	-1078	-905

Expt. This Work

(1) to (6) : Semi-empirical rules (Malijevsky and Novak, 1980)

(1) Equation (7.26)

(2) Equation (7.27)

(3) Equation (7.28)

(4) Equation (7.29)

(5) Equation (7.30)

(6) Equation (7.31)

(7) Tsonopoulos (1974)

(8) McGlashan and Potter (1962)

(9) Hayden and O'Connell (1975)

correlations. The analysis emphasises the need for change in McGlashan and Potter (1962) correlations to justify the combining rules, as the values of n used in equation (1.16) do not represent "true" B values for benzene and cyclohexane. Also the correlation, itself, needs to be modified to predict the "true" values of B, for n having values equal to number of carbon atoms in the hydrocarbon (e.g. n=6 for n-hexane).

Tsonopoulos (1974) and Hayden and O'Connell (1975) predictive correlations are also based on previous apparent values of B measurements. However, it is still essential to know B values of the pure components, accurately, to establish any correlation.

7-7 Correlation of the Excess Second Virial Coefficient Data and Heat of Mixing Data

It was pointed out in Section 2-2.4, that heats of mixing of gases at low pressures can be simply related to the excess second virial coefficient of those gases by equation (2.52)

$$\lim_{p\to 0} H_m^E/p = 2x_1x_2(\varepsilon - d\varepsilon/dT) \qquad (2.52)$$

As shown, in Section 7-6.1, H_m^E/p may be used to find $d\varepsilon/dT$ knowing ε and the corresponding T and comparing slopes of $d\varepsilon/dT$ for the plot of ε versus T (Figure 7-11). Judd et al. (1980) analysed their results assuming a functional form

$$\varepsilon = a + b\exp(c/T) \qquad (7.33)$$

for the relation between ε and T. This function in turn leads to

$$H_m^E/2x_1x_2p = a + b(1 + c/T)\ \exp(c/T) \qquad (7.34)$$

This suggests that the available data for ε fitted along with the measurement of H_m^E/p to a function of the form (equation 7.29) should define the plot of ε versus T. Their best fit of ε and H^E/p to the function (7.34) for benzene (1) + cyclohexane (2) predicted the following correlation

$$\varepsilon(T) = 13.52 + 6.57 \times 10^{-4}\ \exp(3412/T) \qquad (7.35)$$

The value of $\varepsilon(T)$ obtained from the equation (7.35), at 298.15 K is 74.87 $cm^3\ mol^{-1}$, half the experimental value in this work. Their prediction agreed well only at temperatures 348.15 and 373.15 K. This indicates that the use of $(H_m^E/p_j,\ T_j)$ data pairs included in correlating ε_i and T_i values does not improve the quality of the fit to any extent. However, the heats of mixing data in the low temperature region are useful, in indicating the trend of ε at low temperatures, as the experimental values of ε are generally doubtful because of adsorption in this temperature region.

CHAPTER 8

CONCLUSION

A. PURE COMPONENTS

8-1 Review of This Work

The results, incorporated in this thesis for the second virial coefficients of the pure components n-hexane, benzene and cyclohexane, suggest that they are at variance with those reported in the literature (Dymond and Smith, 1980), as discussed in Section 7-3.

It is suggested that the second virial coefficients obtained from the truncated series are pressure dependent, as observed in the plots for $\beta_{apparent}$ of the component versus the pressure term $(p_1 + p_2 - p_3)$. Bich et al. (1979) observed $\beta_{apparent}$ to be linearly dependent on pressure. Our results show that $B_{apparent}$ also is affected by the pressure, at which the property is measured.

A proportional temperature controller used for this work (Section 4-2) holds the bath temperature to better than $\pm 0.005^{o}C$ over a period of the single measurement of the pressure. But it is not unlikely for the temperature of the bath to drift by a few hundredth of

degree, during a subsequent measurement of the pressure in the single run. This affects $\beta_{apparent}$ measurement. The drift may be very close to a tenth of the degree, over a week, i.e. the time taken to complete one set to measure "true" B value of the component at any one temperature. This work has included the correction for the drift in the temperature of the bath, using equation (3.7).

It is suggested that for all the three pressure measurements, there should be no obvious effect of the adsorption (Section 3-5), provided the experiment is performed in the region of monomolecular adsorption. This model suggests that the number of moles adsorbed on the surface remain same, on expansion of the gas into double its original volume, as the expansion doubles the surface area but halves the adsorption of the number of moles per unit area.

It is obvious from Table 3-3, unless the loading pressure is less than or equal to 0.4 times the saturated vapour pressure of the gas, there is an effect due to adsorption. This effect is quite significant at higher pressures. The adsorption effect has been observed at 323.15 K for benzene (Section 7-3.2) and for cyclohexane (Section 7-3.3), where the loading pressure has exceeded 0.6 times the saturation vapour pressure.

8-2 Suggestions for Further Work

8-2.1 Experimental Aspects

The suggestions for experimental problems are incorporated with a few suggestions to improve the present apparatus.

a. Redesign of the Present Apparatus

A proportional integrated controller is suggested to control the bath temperature for further work.

It is desirable to make the measurements at higher temperatures. An earlier attempt, to raise the temperature of the bath above 373.15 K, had caused the metallic joints inside the bath to introduce some leaks into the apparatus. Higher temperature study is advantageous to strengthen the view that this method is not affected by adsorption. One can then work at a series of loading pressures corresponding to less than 0.4 times the saturated vapour pressure of the gas. This pressure range also would be high enough to not to incorporate high errors in $\beta_{apparent}$, associated with the measurements in the low pressure region.

It is also possible to modify the present apparatus, to measure the interaction second virial coefficient of the mixture. The suggested modification to the existing layout of the present apparatus, is shown in Figure 8-1.

To measure the excess second virial coefficient of a mixture, component 1 is loaded into cell 1, with valves H2 and H5 closed. The loading pressure is measured using the differential pressure transducer Baratron 1 and nitrogen as outlined in Section 5-2.2. Valves H1 and H4 are then closed and H3 is opened to evacuate the system. When the evacuation is complete, component 2 is loaded into cell 2 and H2 is closed. Valve H6 is closed and nitrogen is pumped away. H5 is opened to balance the pressure of component 2 using Baratron 1. With valves H3 and H4 closed, the contents of cell 1 and 2 are mixed and the resulting Δp is measured with the transducer.

The possible problem in this modification, is overloading of

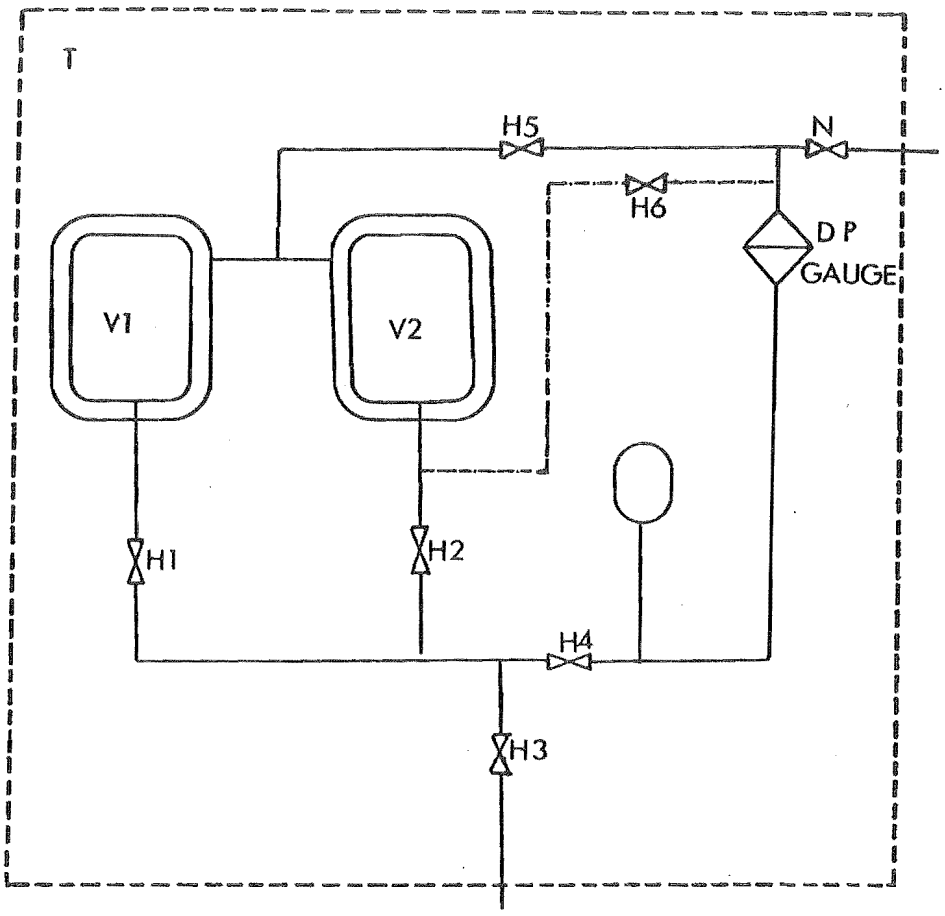

FIGURE 8-1

Modification of the Existing Apparatus to Enable It to be Used for Δp (mixing) Measurements

——— Existing layout of the apparatus

—·—·— Suggested modification

that volume series $B_{apparent}$ are also pressure dependent. At higher pressure, the difference between $\beta_{apparent}$ and $B_{apparent}$ is more than the differences at lower pressure. It is also very likely that any relationship (linear or other) between $B_{apparent}$ and the pressure term should intersect y axis (for p tending to zero,), at a point close to "true" B.

It is concluded that the "true" second virial coefficient values are different from the values cited in the literature (Dymond and Smith, 1980). It is suggested that this method be used to measure second virial coefficients of a series of alkanes over a bigger temperature range, at narrowly separated temperatures. This may lead to a new correlation, similar to that of McGlashan and Potter's (1962), to predict B values.

A theoretical adsorption model may be necessary to apply adsorption corrections to the measurement of B at higher pressure.

B. MIXTURES

8-3 Conclusions

The results embodied in this thesis, suggest that Δp^E method of measuring the excess second virial coefficient is a good one. The minor alterations done to the existing apparatus (Shannon, 1976), for this work, have improved the previous results.

The ΔH^E on mixing measurement permits the measurement of ε to be made in the regions, where adsorption would be troublesome to Δp^E measurement. These two measurements together promise to enable ε measurements to be made accurately over a wide temperature range.

Adsorption problems are still associated with the accuracy of ε measurements. The loading pressure is close to 0.6 times the saturation vapour pressure in a few cases, indicating possible multimolecular adsorption. It seems that the apparatus has an adsorption area about twice the geometric area of the apparatus. It is expected that a smoother surface, such as that obtained with glass, would give a small variation because of adsorption in the useful temperature range.

To enable quantitative corrections to be made, more information is required on the adsorption isotherms of both the pure components and their mixtures. Also it should be possible to estimate the loading pressure as a fraction of saturation vapour pressure that gives a zero adsorption correction.

The apparatus has recently been rebuilt (McElroy, 1982) with glass vessels. The minor modifications, suggested by Shannon (1976),

introduced to the layout of the previous apparatus, has facilitated the measurement of the pure component second virial coefficients as well. The new method of measurement may have an advantage over the existing method (Section 3-2) of measuring the second virial coefficient of pure components, as seven pressure measurements over a five fold density range may be made with one loading. The other possible problem in the 3-bulb system in the new apparatus, is that there will be variation of surface/volume ratio, which may exacerbate the adsorption problem (Marsh and Williamson, 1981), if the adsorption isotherm is non-linear in the pressure range used. The adsorption problem seems to be very obvious in the 2-bulb system, in the existing apparatus.

REFERENCES

Abraham, W. H.; Bennet, C. D. (1960) A.I.Ch.E. Journal, 6(2), 257.

Al-Bizreh, N.; Wormald, C. J. (1977) J. Chem. Thermodynamics, 9, 49.

Al-Bizreh, N.; Wormald, C. J. (1978) J. Chem. Thermodynamics, 10, 31.

Alexander, E. A.; Lambert, J. D. (1941) Trans. Faraday Soc., 37, 421.

Allen, P. W.; Everett, D. H.; Penney, M. F. (1952), Proc. Roy. Soc., A212, 149.

Anderson, L. N.; Kudchadker, A. P.; Eubank, P. T. (1968) J. Chem. Eng. Data, 13(3), 321.

Andon, R. J. L.; Cox, J. D.; Herington, E. F. G.; Martin, J. F. (1957) Trans. Faraday Soc., 53, 1074.

Arora, P. S.; Robjohns, H. L.; Bell, T. N.; Dunlop, P. J. (1980) Aust. J. Chem., 33, 1993.

Ashton, H. M.; Guggenheim, E. A. (1956) Proc. Phys. Soc. London, B69, 693.

Aston, J. G.; Fink, H. L.; Bestul, A. B.; Pace, E. L.; Szasz, G. J. (1946) J. Am. Chem. Soc., 68, 52.

Barker, J. A.; Linton, M. (1963) J. Chem. Phys., 38(8), 1853.

Barton, J. R.; Hsu, C. C. (1969) J. chem. Eng. Data, 14(2), 184.

Battino, R.; Banzhof, M.; Bogan, M.; Wilhelm, E. (1971) Analytical Chemistry, 43, 806.

Battino, R. (1980) Personal communication

Battino, R.; Malhotra, R.; McElroy, P.J.; Williamson, A. G. (1983) J. Chem. Thermodynamics, 15, 83.

Baxendale, J. H.; Enustun, B. V.; Stern, J. (1951) Phil. Trans. A, 243 169.

Bean, H. S. (1930) Bur. Std. J. Res., 4, 645.

Bell, T. N.; Cussler, E. L.; Harris, K. R.; Pepela, C. N.; Dunlop, P. J. (1968) J. Phys. Chem., 72(13), 4693.

Bell, T. N.; Dunlop, P. J. (1981) Chem. Phys. Letters, 84(1), 99.

Bell, T. N.; Dunlop, p. J. (1982) Rev. Sci. Instrum., 53, 83.

Belousova, Z. S.; Verkhova, V. P. (1973) Russian J. Phys. Chem., 47(2), 236.

Benedict, M. (1937) J. Am. Chem. Soc., 59, 2224.

Bich, V. E.; Opel, G. (1979) Wissenschaftiche Zeitschrift : Mathematisch Naturwissenschaftliche Reihe, 28(9), 1979.

Bigg, P. H. (1964) Brit. J. Appl. Phys., 15, 1111.

Black, C. (1958) Ind. Eng. Chem., 50(3), 391.

Bottomley, G. A.; Massie, D.; Whytlaw-Gray, R. (1950) Proc. Roy. Soc. A, 200, 201.

Bottomley, G. A.; Reeves, C. G. (1957) Trans. Faraday Soc., 53, 1455.

Bottomley, G. A.; Reeves, C. G.; Whytlaw-Gray, R. (1958a) Proc. Roy. Soc., A246, 504.

Bottomley, G. A.; Remmington, T. A.; Whytlaw-Gray, R. (1958b) Proc. Roy. Soc., A246, 514.

Bottomley, G. A.; Reeves, C. G. (1958c) J. Chem. Soc., 161, 3794.

Bottomley, G. A.; Remmington, T. A. (1958d) J. Chem. Soc., 3800.

Bottomley, G. A. (1960) Aust. J. Chem., 13, 311.

Bottomley, G. A.; Coopes, I. H. (1962) Nature, 193, 268.

Bottomley, G. A.; Spurling, T. H. (1964) Aust. J. Chem., 17, 501.

Bottomley, G. A.; Coopes, I. H.; Nyberg, G. L.; Spurling, T. H. (1965) Aust. J. Chem., 18, 1105.

Bottomley, G. A.; Spurling, T. H. (1966) Aust. J. Chem., 19, 1331.

Bottomley, G. A.; Spurling, T. H. (1967) Aust. J. Chem., 20, 1789.

Bottomley, G. A.; Nairn, D. B. (1977) Aust. J. Chem., 30(8), 1645.

Boulton, L. H.; Clark, B. R.; Coleman, M. F.; Thorp, J. M. (1966) Trans. Faraday Society, 62, 2928.

Brunauer, S.; Emmett. P. H.; Teller, E. (1938) J. Am. Chem. Soc., 60, 309.

Brownlee, K. A. (1960) 'Statistical theory and methodology in Science and Engineering', Canada, John Wiley & Sons Inc..

Burnett, E. S.(1923) Phys. Rev., 22, 590.

Burnett, E. S. (1936) J. Appl. Mechanics, 3, A-136.

Casado, F. L.; Massie D. S.; Whytlaw-Gray, R. (1951) Proc. Roy. Soc., A207, 483.

Chan, S. H. (1976) Project Report : B.E. :Chemical Engineering, University of Canterbury, Christchurch.

Cawood, W.; Patterson, H. S. (1932) J. Chem. Soc., 135, 2180.

Charnley, A.; Isles, G. L.; Townley, J. R. (1953) Proc. Roy. Soc., 1953, A218, 133.

Cherney, B. J.; Marchman, H.; York, R. (1949) Ind. Eng. Chem., 41(11), 2653.

Chueh, P. L.; Prausnitz, J. M. (1967) A.I.Ch.E. Journal, 13(5), 896.

Clarke, P. H.; Francis, P. G.; George, M.; Phuthela, R. C.; Roberts, G. K. St. C. (1979) J. Chem. Thermodynamics, 11, 125.

Connolly, J. F.; Kandalic, G. A. (1960) Phys. Fluid, 3(3), 463.

Cottrell, T. L.; Hamilton, R. A. (1956) Trans. Faraday Soc., 52, 156.

Couch, E. J.; Kobe, K. A.; Hirth, L. J. (1961) J. Chem. Eng. Data, 1961, 6(2), 229.

Couldwell, C. M. (1975), Thesis : Ph.D : Chemical Engineering, University of Canterbury, Christchurch.

Couldwell, C. M.; O'Neill, S. P.; Pandya, M. V.; Williamson, A. G. (1978) Aust. J. Chem., 31, 231.

Cox, H. E.; Crawford, F. W.; Smith, E. B.; Tindell, A. R. (1980) Mol. Phys., 40(3), 7050.

Cox, J. D.; Andon, R. J. L. (1958) Trans. Faraday Soc., 54, 1622.

Cox, J. D.; Stubley, D., Appendix to Partington et. al. (1960) Trans. Faraday Soc., 56, 484.

Cox, J. D.; Lawrenson,I. J. (1973) 'Chemical Thermodynamics', ed. McGlashan, M. L. (Specialist Periodical Reports) vol. 1, 162.

Cruickshank, A. J. B.; Windsor, M. L.; Young, C. L. (1966) Proc. Roy. Soc., A295, 259.

Cusumano, J. A.; Low, M. J. D. (1970) J. Phys. Chem., 74(41), 792.

Dantzler, E. H.; Knobler, C. M.; Windsor, M. L. (1968) J. Phys. Chem., 72, 676.

Dantzler, E. M.; Knobler, C. M. (1969) J. Phys. Chem., 73, 1335.

David, H. G.; Hamann, S. D. (1953) Trans. Faraday Soc., 49, 711.

D'Avila, S. G.; Kaul, B. K.; Prausnitz, J. M. (1976) J. Chem. Eng. Data, 21(4), 488.

Day, H. O.; Felsing, W. A. (1952) J. Am. Chem. Soc., 74, 1951.

Di Zio, S. F.; Abbott, M. M.; Zibello, D.; Van Ness, H. C. (1966) Ind. & Eng. Chem. Fundamentals, 5(4), 569.

Dixon, L. C. W. (1972) 'Nonlinear Optimisation', The English Universities Press Ltd., London.

Douslin, D. R.; Harrison, R. H.; Moore, R. T. (1969) J. Chem. Thermodynamics, 1, 305.

Doyle, J. A.; Hutchings, D. J.; Mayr, J. C.; Wormald, C. J. (1981) J. Chem. Thermodynamics, 13, 261.

Dymond, J. H.; Smith, E. B. (1980) "The Virial Coefficients of Pure Gases and Mixtures", Oxford, Clarendon Press.

Edwards, A. E.; Roseveare, W. E. (1942) J. Chem. Soc., 64, 2816.

Edwards, J. D. (1917) Ind. Eng. Chem., 9(8), 790.

Elabd, A. A. (1976) The Libyan J. of Science, 6A, 55.

Ellington, R. T.; Eakin, B. E. (1963), Chem. Eng. Prog., 59(11), 80.

Eon, C.; Pommier, C.; Guiochon, G. (1971) J. Chem. Eng. Data, 16(4),408.

Epstein, L. F. (1952) J. Chem. Phys., 20, 1981.

Epstein, L. F. (1953) J. Chem. Phys., 21, 762.

Eubank, P. T.; Angus, S. (1973) J. Chem. Eng. Data, 18(4), 428.

Eubank, P. T.; Kerns, W. J. (1973) A.I.Ch.E. Journal, 19(4), 711.

Ewing, M. B.; Marsh, K. N. (1979) J. Chem. Thermodynamics, 11, 793.

Feng, P. Y.; Melzer, M. (1972) J. Chem. Education, 49(5), 375.

Francis, P. G.; McGlashan, M. L.; Hamann, S. D.; McNanmey, W. J. (1952) J. Chem. Phys., 20, 1341.

Francis, P. G.; McGlashan, M. L.; Wormald, C. J. (1969) J. Chem. Thermodynamics, 1, 441.

Frisch, H. L.; Helfand, E. (1960) J. Chem. Phys., 32(1), 269.

Gawdzik, J.; Suprynowicz, Z.; Jaroniee, M. (1976) J. Chromotography, 121, 185.

Gehrig, M.; Lentz, H. (1977) J. Chem. Thermodynamics, 9, 445.

Giauque, W. F.; Buffington, R. M., Schulze, W. A. (1927) J. Am. Chem. Soc., 49(10), 2343.

Gornowski, E. J.; Amick, E. M. Jr.; Hixson, A. N. (1947) Ind. Eng. ., Chem., 39(10), 1348.

Gorski, R. A.; Miller, J. G. (1953) J. Am. Chem. Soc., 75, 550.

Grimsrud, D. T.; Werntz, J. H. (1967) Phys. Rev., 157(1), 181.

Guggenheim, E. A.; Wormald, C. J. (1965) J. Chem. Phys., 42(11), 3775.

Guggenheim, E. A. (1967) "Thermodynamics; An Advanced Treatment for Chemists and Physicsts", fifth edition, North-Holland Publishing Co. - Amsterdam.

Hajjar, R. F.; MacWood, G. E. (1968) J. Chem. Phys., 49(10), 4567.

Hajjar, R. F.; Kay, W. B.; Leverett, G. F. (1969) J. Chem. Eng. Data, 14(3), 377.

Hajjar, R. F.; MacWood, G. E. (1970) J. Chem. Eng. Data, 15(1), 3.

Hala, E.; Pick, J.; Fried, V.; Vilim, O. (1967) "Vapour-Liquid Equilibrium", Second Edition, Pergamon Press Ltd.

Hall, K. R.; Canfield, F. B. (1970) Physica, 47, 99.

Hall, K. R.; Eubank, P. T. (1973) J. Chem. Phys., 59(2), 709.

Hall, K. R.; Eubank, P. T. (1974) A.I.Ch.E. Journal, 20(4), 815.

Hamann, S. D.; Pearse, J. F. (1952) Trans. Faraday Soc., 48, 101.

Hauthal, W. H.; Sackmann, H. (1969) Proc. 1st. Intern. Conf. Calorimetry and Thermodynamics, 627.

Hayden. J. G.; O'Connell, J. P. (1975) Ind. Eng. Chem., Process Des. Dev., 14, 209.

Haywood, A. T. J. (1977) 'Repeatability and Accuracy', Mechanical Engineering Publications Ltd., London.

Heichelheim, H. R.; Kobe, K. A.; Silberberg, I. H.; McKetta, J. J. (1962) J. Chem. Eng. Data, 7(4), 507.

Herrington, E. F. G. (1974) Pure and Applied Chemistry, 40, 393.

Hill, T. L. (1962), 'Introduction to Statistical Thermodynamics', Reading, Addison - Wesley.

Hirschfelder, J. O.; McClure, F. T.; Weeks, I. F. (1942) J. Chem. Phys., 10, 201.

Hirschfelder, J. O.; Curtiss, c. F.; Bird, R. B. (1954) 'Molecular Theory of Gases and Liquids', New York, Wiley.

Holste, J. C.; Watson, M. Q.; Bellomy, M. T.; Eubank, P. T.; Hall, K. R. (1980) A.I.Ch.E. Journal, 26(6), 954.

Hou, Y. C.; Martin, J. J. (1959) A.I.Ch.E. Journal, 5(1), 125.

Johnston, H. L.; Weimer, H. R. (1934) J. Am. Chem. Soc., 56, 625.

Johnston, H. L. (1946) J. Am. Chem. soc., 68, 2362.

Judd, N. F.; Mayhew, C. J.; McElroy, P. J.; Williamson, A. G. (1980) J. Chem. Themodynamics, 12, 465.

Kamenetskii, V. R.; Russian (1973) J. Phys. Chem., 47(4), 471.

Kappallo, W.; Lund, N., Schafer, K. (1963) Z. Phys. Chem., 37(8), 196.

Katayama, T.; Ohgaki, K.; Ohmori, H. (1980) J. Chem. Eng. of Japan, 13(4), 257.

Kell, G. S.; Whalley, E. (1965) Phil. Trans. Roy. Soc. London, A258, 565.

Kell, G. S.; McLaurin, G. E.; Whalley, E. (1968) J. Chem. Phys., 48(8), 3805.

Kell, G. S.; McLaurin, G. E.; Whalley, E. (1978) J. Chem. Phys., 68(5), 2199.

Kell, G. S. (1982) Ind. Eng. Chem. Fundam., 21(1), 56.

Keller, J. B.; Zumino, B. (1959) J. Chem. Phys., 30(5), 1351.

Keller, P. (1983) Project Report : B.E. : Chemical Engineering, University of Canterbury, Christchurch.

Keller, W. E. (1955) Phys. Rev., 97(1),1

Kemball, C.; Rideal, E. K. (1946) Proc. Roy. Soc., A187, 53.

Kerl, K. (1982) Z. Phys. Chemie Neue Folge, 129, 129.

Kerns, W. J.; Anthony, R. G.; Eubank, P. T. (1974) A.I.Ch.E. Symposium Series, 70(140), 14.

Kessler, W. D.; Osborne, D. V. (1980a) J. Phys. C., 13, 1571.

Kessler, W. D.; Osborne, D. V. (1980b) J. Phys. C., 13, 2097.

Khodeeva, S. M.; Labedeva, E. S.; Belousova, Z. S. (1966) Russian J. Phys.Chem., 40(12), 1669.

King, R. C.; Potter, J. H. (1962) Trans. ASME, Series B, 84, 180.

Kistemaker, J.; Keesom, W. H. (1946) Physica, 12(4), 227.

Knobler, C. M.; Beenakker, J. J. M.; Knaap, H. F. P. (1959) Physica, 25, 909.

Knobler, C. M. (1967) Rev. Sci. Inst., 38(2), 184.

Knobler, C. M. (1978) 'Chemical Thermodynamics' ed. McGlashan, M. L. (Specialist Periodical Reports), vol. 2, 199.

Knobler, C. M. (1983) Pure & Applied Chemistry, 55(3), 455.

Knoebel, D. H.; Edmister, W. C. (1968) J. Chem. Eng. Data, 13, 312.

Koh, S. P.; Williamson, A. G. (1980) J. Chem. Eng., 19, 85.

Kolysko, L. E.; Mozhginskaya, L. V.; Gorodinskaya, E. Ya. (1972) Russian J. Phys. Chem., 46(4), 614.

Kretschmer, C. B.; Wiebe, R. J. (1951) J. Am. Chem. Soc., 73, 3778.

Kunz, R. G.; Kapner, R. S. (1971) A.I.Ch.E. Journal, 17(3), 562.

Lambert, J. D.; Roberts, A. H.; Rowlinson, J. S.; Wilkinson, V. J. (1949) Proc. Roy. Soc., A196, 113.

Laub, R. J.; Pecsok, R. L. (1974) J. Chromatography, 98, 511.

Leaver, R. H.; Thomas, T. R. (1974) 'Analysis and presentation of experimental results', London, The MacMillan Press Ltd.

Lee, R. C.; Edmister, W. C. (1970) A.I.Ch.E. Journal, 16, 1047.

Lee,S-M.; Eubank, P. T.; Hall, K. R. (1977) Fluid Phase Equilibria, 1, 219.

Lentz, H. (1969) Rev. Sci. Instrum., 40, 371.

Lipsicas, M.; Bloom, M.; Muller, B. H. (1961) J. Chem. Phys., 34, 1813.

Long, E. A.; Gulbransen, E. A. (1936) J. Am. Chem. Soc., 58, 203.

Maher, P. J.; Smith, B. D. (1979) J. Chem. Eng. Data, 24, 16.

Malesinska, B. (1980) Polish J. of Chem., 54(7-8), 1527.

Malijevsky, A.; Novak, J. P. (1980) Collect. Czech. Chem. Commun., 45, 1155.

Mansoorian, H.; Hall, K. R.; Eubank, P. T. (1977) Proc. of the Symposium on Thermoplhysical properties, 456.

Marsh, K. N.; Williamson, A. G. (1981) Proc. Second Aust. Thermodynamics Cong., 429.

Marsh, K. N.; Rogers, H. P. D. (1983) Ind. Eng. Chem. Fundam., 22, 1.

Mason. E. A.; spurling, T. H. (1969) 'The Virial Equation of State', Pergaman, New York.

Martin, M. L., Trengove, R. D.; Harris, K. R.; Dunlop, P. J. (1982) Aust. J. Chem., 35, 1525.

Mavridis, A. (1976) Chimica Chronika, 5, 333.

Mayhew, C. J. (1976) Ph.D. Thesis, University of Canterbury, Christchurch, NZ.

McCullough, J. P.; Waddington, G.. (1968) 'Experimental Thermodynamics, Calorimetry of Non-reacting System', Ed. McCullough, J. P.; Scott, D. W.; Vol. I, 369.

McElroy, P. J. (1968) Ph.D Thesis, University of Otago, Dunedin. NZ.

McElroy, P. J.; Shannon, T. W.; Williamson, A. G. (1980) J. Chem. Thermodynamics, 12, 371.

McElroy, P. J. (1982) Personal Communication.

McGlashan, M. L.; Potter, D. J. B. (1958) Proceedings of the Joint Conference on Thermodynamics and Transport Properties of Fluids, London: Inst. of Mech. Engineers, 60.

McGlashan, M. L.; Potter, D. J. B. (1962) Proc. Roy. Soc., A267, 478.

Meyer, E. F.; Awe, M. J.; Wagner, R. E. (1980) J. Chem. Eng. Data, 25, 371.

Michels, A.; Michels, C.; Wouters, H. (1935) Proc. Roy. Soc., A153, 214.

Michels, A.; Wassenaar, T.; Zwietering, Th. N. (1952) Physica, 18, 6.

Miller, I.; Freund, J. E. (1965) 'Probability and Statistics for Engineers,' New Jersey, Prentice-Hall Inc., Englewood, Cliffs.

Miller, R. C.; Kidnay, A. J.; Hiza, M. J. (1972) J. Chem. Thermodyn., 4, 807.

MKS Baratron Precision Pressure Measurement (1975), 'Design Note', MKS Instruments Inc., Massachusetts.

MKS Baratron Precision Meter Type 170 (1977), 'Instruction Manual', MKS Instruments Inc., Massachusetts.

Najour, G. C.; King, A. D. (1966) J. Chem. Phys., 45(6), 1915.

Nicholas, J. V.; White, D. R. (1981) 'Temperature Measurement and Calibration Workshop Notes', Physics and Engineering Laboratory Report No. 707, DSIR NZ.

Ohgaki, K.; Mizuhaya, T.; Katayama, T. (1982) J. Chem. Eng. of Japan, 15(2), 85.

Orentlicher, M.; Prausnitz, J. M. (1967) Canad. J. Chem., 45, 373.

Pandya, M. V.; Williamson, A. G. (1971) Aust. J. Chem., 1971, 24, 465.

Pasco, N. F.; Handa, Y. P.; Scott, R. L.; Knobler, C. M. (1980), J. Chem. Thermodynamics, 12, 11.

Pathak, G. (1979) Indian J. of Technology, 17(3), 119.

Pavlyuchenko, N. M. (1970) Russian J. Phys. Chem., 44, 152.

Pecsok, R. L.; Windsor, M. L. (1968) Analytical Chemistry, 40 (8), 1238.

Pitzer, K. S.; Lippmann, D. Z.; Curl, R. F. Jr.; Huggins, C. M.; Peterson, D. E. (1955) J. Am. Chem. Soc., 77, 3433.

Pitzer, K. S.; Curl, R. F. (1957) J. Am. Chem. Soc., 79, 2369.

Pocock, G.; Wormald, C. J. (1975) J. Chem. Soc. Faraday Trans. 1, 71(4), 705.

Polak, J.; Lu, B. C-Y (1972) Can. J. Chem. Eng., 50, 553.

Pompe, A.; Spurling, T. H. (1976) CSIRO Aust. Div. Appl. Organic Chem. Tech. Pep. NO. 3.

Prasad, D. H. L.; Viswanath, D. S. (1980) J. Chem. Eng. Data, 25, 374.

Prasad, M.; Kudchadker, A. P. (1978) J. Chem. Eng. Data, 23(3), 190.

Prausnitz, J. M. (1969) 'Molecualr Thermodynamics of Fluid Phase Equilibria', Prantice-Hall, Englewood Cliffs, N. J.

Prausnitz, J. M.; Anderson, T.; Grens, E.; Eckert, C.; Hsieh, R.; O'Connell, J. (1980) 'Computer Calculations for multicomponent vapour - liquid and liquid - liquid equilibria', Prentice Hall Inc., Englewood Cliff, N. J.

Putnam, W. E.; Kilpatrick, J. E. (1953) Nature, 951.

Ratzsch, M.; Freydank, H. (1971) J. Chem. Thermodynamics, 3, 861.

Reid, C. R.; Prausnitz, J. M.; Sherwood, T. K. (1977) 'The Properties of Gases and Liquids', mcGraw-Hill Book Co.

Roper, E. E. (1940) J. Phys. Chem., 44, 835.

Rossini, F. D. (1970) J. Chem. Thermodynamics, 2, 447.

RUSKA Dead Weight Gauge (1976)'Operating Manual, for Model No. 2465-751-00, Serial No.: 23165 (gauge); 22910 (weights)', Ruska Instrument Corporation, Houston, Texas.

Rybolt, T. R. (1981) J. Chem. Education, 58(8), 620.

Sage, B. H.; Kennedy, E. R.; Lacey, W. N. (1936) Ind. Eng. Chem., 28, 601.

Schamp, H. W.; Mason, E. A.; Richardson, A. C. B.; Altman, A. (1958) Phys. Fluid, 1(4), 1958.

Scott, D. W.; Waddington, G.; Smith, J. C.; Huffman, H. M. (1947) J. Chem. Phys., 15(8), 565.

Scott, R. L.; Dunlap, R. D. (1962) J. Phys. Chem., 66, 639.

Scott, R. L. (1976), 'Statistical Thermodynamics', University of California, Los Angeles.

Shannon, T. W. (1976)Ph. D. Thesis, University of Canterbury, Christchurch, NZ.

Sherwood, A. E.; Prausnitz, J. M. (1964) J. Chem. Phys., 41(2), 429.

Silberberg, I. H.; Kobe, K. A.; McKetta, J. J. (1959) J. Chem. Eng. Data, 4(4), 314.

Silberberg, I. H.; Lin, D. C. K.; McKetta, J. J. (1967) J. Chem. Eng. Data, 12, 226.

Singh, R. P. (1979) Personal Communication.

Singh, R. P.; Kudchadker, A. P. (1979) J. Chem. Thermodynamics, 11, 205.

Slawsky, Z. I.; Seigel, A. E.; Ho, L. T.; Kopp, H. J.; Vanderslice, J. T. (1959) Rev. Sci. Instr., 30, 679.

Smith, E. B.; Tindell, A. R.; Wells, B. H.; Tildesley, D. J. (1980) Molecualr Phys., 40(4), 997.

Smith, E. B.; Tindell, A. R.; Wells, B. H.; Crawford, F. W. (1981) Molecular Phys., 42(4), 937.

Solbrig, C. W.; Ellington, R. T. (1963) Chem. Eng. Prog. Sym. Series, 59(44), 127.

Spertell, R. B.; Chang, G. T. (1972) J. Chromatog. Sci., 10, 60.

Stockett, A. L.; Wenzel, L. A. (1964) A.I.Ch.E. Journal, 10, 557.

Straty, G. C.; Prydz, R. (1970) Rev. Sci. Instr., 41, 1223.

Tee, L. S.; Gotoh, S.; Stewart, W. E. (1966) Ind. Eng. Chem. Fundamentals, 5(3), 356.

Thomaes, G.; Van Steenwinkel, R. (1960) Rev. Sci. Instr., 31, 825.

Todd, S. S.; Hossenlop, I. A.; Scott, D. W. (1978) J. Chem. Thermodynamics, 10, 641.

Topping, J. (1955) 'Errors of Observation and their Measurements', London, Institute of Physics.

Tsonopoulos, C. (1974) A.I.Ch.E. Journal, 20, 263.

Varekamp, F. H.; Beenakker, J. J. M. (1959) Physica, 25, 809.

Vilcu, R.; Birhala, Al. (1975) Revue Roumaine de Chimie, 20(7), 889.

Waddington, G.; Todd, S. S.; Huffman, H. M. (1947) J. Am. Chem. Soc., 69, 22.

Waddington, G.; Douslin, D. R. (1947) J. Am. Chem. Soc., 69, 2275.

Waelbroeck, F. G. (1955) J. Chem. Phys., 23, 749.

Wallace, C. B.; Silberberg, I. H.; McKetta, J. J. (1964) Hydrocarbon Processing, 43(10), 177.

Walters, C. J.; Smith, J. M. (1952) Chem. Eng. Prog., 48, 337.

Warowny, W.; Stecki, J. (1978a) J. Chem. Eng. Data, 23, 212.

Warowny, W.; Wielopolski, P.; Stecki, J. (1978b) Physica, 19A, 73.

Warowny, W.; Stecki, J. (1979) ' The Second Cross Virial Coefficients of Gaseous Mixtures', Polish Scientific Publishers, Warszawa.

Waxman, M.; Hastings, J. R. (1971) J. Res. C, US Nat. Bureau of Stds. - Eng. and Instrumentations, 75C, 165.

Weir, R. D.; Jones, I. W.; Rowlinson, J. S.; Saville, G. (1967) Trans. Faraday Soc., 63, 1320.

White, D.; Hu, J-H.; Johnston, H. (1953) J. Chem. Phys., 21, 1149.

White, D.; Rubin, T.; Camky, P.; Johnston, H. L. (1960) J. Phys. Chem., 64, 1607.

Whytlaw-Gray, R.; Patterson, H. S.; Cawood, W. (1931) Proc. Roy. Soc., A134, 7.

Whytlaw-Gray, R.; Bottomley, G. A. (1957) Nature, 180, 1252.

Wielopolski, P.; Warowny, W. (1978) Physica 91A, 66.

Wormald, C. J.; Francis, P. G.; McGlashan, M. L. (1969a) J. Chem. Thermodynamics, 1, 441.

Wormald, C. J. (1969 b) Proc. 1st. Internat. Conf. of Calorimetry of Thermodynamics, Warsaw, 601.

Wormald, C. J. (1975) J. Chem. Soc. Faraday Trans. 1, 71, 726.

Wormald, C. J. (1977) J. Chem. Thermodynamics, 9, 901.

Zaalishvili, Sh. D.; Belousova, Z. S. (1964) Russian J. Phys. Chem., 38(2), 269.

Zaalishvili, Sh. D.; Belousova, Z. S.; Kolysko, L. E. (1965a) Russian J. Phys. chem., 39(2), 232.

Zaalishvili, Sh. D.; Kolysko, L. E. (1965b) Russian J. Phys. Chem., 39(4) 539.

Zaalishvili, Sh. D.; Belousova, Z. S.; Verkhova, V. P. (1971a) Russian J. Phys. Chem., 45, 149.

APPENDIX A1

Platinum Resistance Temperature

The programme "RMPRT/BAS" calculates the working temperature of the bath, given the ratio (R) of the resistance of the standard resistor [Type 'Tinsley'; Grade 'S'] to that of the probe at the working temperature. The method is iterative. It first corrects the resistance of the standard resistor for the room temperature using the relation

$$R_2 = R_3[1 + c(T-20)] \qquad (A1.1)$$

where R_2 is the resistance of the standard resistor at its working temperature, T.

R_3 is the resistance of the standard resistor at $20^{o}C$.

T is the temperature of the standard resistor.

c is the temperature coefficient of resistance of the standard resistor and is 4 ppm/^{o}C.

The initial temperature (S) is estimated using the relation

$$S = (R_1 - R_4)/(R_4 A) \qquad (A1.2)$$

where R_1 is the resistance of the probe at the bath temperature.

R_4 is the resistance of the probe at $0^{o}C$ and is 25.5035 ohms for the Pt. Resistance Probe No. 409, used in this work.

A is a constant equal to 3.920×10^{-3}.

The estimated final temperature is given by the expression

$$T_{(i+1)} = S + [D(S_i/100 - 1)(S_i/100)] \qquad (A1.3)$$

where D is a constant equal to 1.4856. If the absolute value of the difference of $T_{(i+1)}$ and S_i is greater than $1x10^{-4}$ degree C, then S_i inside the bracket is estimated equal to $T_{(i+1)}$ from equation (A1.3) and the iterative process is continued.

```
10 REM ** PROGRAMME "RMPRT/BAS" CALCULATES THE WORKING **
15 REM ** TEMPERATURE OF THE SYSTEM USING A PLATINUM **
20 REM ** RESISTANCE THERMOMETER **
30 REM ** R3= RESISTANCE OF STANDARD RESISTOR**
40 REM ** R4= RESISTANCE OF PROBE AT ZERO DEGREE**
50 REM ** R= RATIO OF RESISTANCE OF STANDARD RESISTOR**
60 REM ** TO PROBE AT WORKING TEMPERATURE **
70 REM ** R1= RESISTANCE OF PROBE AT WORKING TEMPERATURE**
80 REM ** C=THERMAL COEFFICIENT FOR STANDARD RESISTOR**
90 REM ** T1= TEMPERATURE OF STANDARD RESISTOR**
100 REM ** R2= CORRECTED RESISTANCE OF STANDARD RESISTOR**
110 PRINT "INPUT TITLE"
120 INPUT A$
130 PRINT "HAVE YOU CHANGED STATEMENT NO. 150, YES/NO?"
133 INPUT A$
135 IF A$ = "YES" THEN 140
137 PRINT "READ STATEMENTS 151-153"
138 GOTO 430
140 R3=25.4999
150 R4 = 25.5035
151 REM ** R4=25.5035 IS THE VALUE FOR PT. RES. PROBE 409**
152 REM ** FOR PROBE 240, (R4= 25.5213)**
153 REM ** CHANGE STATEMENT NO. 150**
160 A=3.924E-3
170 D=1.4856
180 REM ** A= CONSTANT ALPH**
190 REM ** D= CONSTANT DELTA**
200 C=4 E-6
210 PRINT "INPUT T1,R"
220 INPUT T1,R
230 R2=R3*(1+C*(T1-20))
240 N=1
260 R1=R2/R
270 REM **STEP 260 IS BECAUSE R IS THE RATIO OF STANDARD**
280 REM **RESISTOR TO PROBE AT WORKING TEMPERATURE **
282 REM ** FOR R BEING THE RATIO OF RESISTANCES OF PROBE TO**
283 REM **STANDARD RESISTANCE; STATEMENT 260 IS CHANGED**
284 REM ** HENCE; 260 R1=R2*R **
290 S= (R1-R4)/(R4*A)
300 REM ** S=STARTING INITIAL TEMPERATURE **
310 T4=(R1-R4)/(R4*A)
320 T2=T4+D*((S/100)-1)*(S/100)
330 B=ABS(T2-S)
335 IF B<=1.0E-4 THEN 380
350 S=T2
360 N=N+1
370 GOTO 320
380 T3=T2+273.15
410 PRINT "TEMP./K= ";T3,"TEMP./C= ";T2
413 PRINT "ANY MORE CONVERSIONS? YES/NO"
415 INPUT K$
420 IF K$ = "YES" THEN 210
430 END
```

APPENDIX A2

Dead Weight Gauge Pressure

The programme "RMRUSK/BAS" gives tables for the pressures in Pa for the weights on piston. The area of the piston is calibrated for the piston temperature at the time of the measurement using the relation

$$D = A_0[1 + c(T-23)] \qquad (A2.1)$$

where D is the calibrated area of the piston at temperature T.

A_0 is the area of the piston (equal to 3.35678×10^{-11} m^2 at $23^{\circ}C$) according to Ruska DWG (1976).

c is the thermal coefficient of piston material (equal to 1.5×10^{-4} m^2 deg^{-1}).

Total pressure exerted by the different combination of weights is summed by the relation

$$\text{DWG Pressure} = \Sigma p_i \qquad (A2.2)$$

where p_i is the pressure exerted by the individual weight having mass, m_i, given by

$$p_i = m_i g_{local}/D \qquad (A2.3)$$

where g_{local} is the acceleration due to gravity (equal to 9.8048 m sec^{-2} (Christchurch Metrological Service)).

```
10 REM ** RMRUSK IS TO CALCULATE PRESSURES IN **
20 REM ** NEWTONS/MM FOR RUSKA AIR PISTON DEAD WEIGHT**
21 REM ** GAUGE **
22 REM ** G = LOCAL ACCELERATION DUE TO GRAVITY **
24 REM ** C = THERMAL COEFFICIENT OF PISTON MATERIAL **
26 REM ** AO = AREA OF PISTON AT 23 DEG C **
28 REM ** D = CALIBRATED AREA OF PISTON AT TEMP., T **
30 REM ** P(I) = PRESSURE EXERTED BY EACH WEIGHT **
40 DIM M(15),P(15)
50 LPRINT
51 LPRINT
52 LPRINT
70 M(1)=.855775
80 M(2)=.855767
90 M(3)=.855793
100 M(4)=0
110 M(5)=.342327
120 M(6)=.342324
130 M(7)=.17115
140 M(8)=.0855824
150 M(9)=.0342329
160 M(10)=.0342329
170 M(11)=.0171173
180 M(12)=8.56170E-3
190 M(13)=4.278E-3
195 M(14)=.047921
200 G=980.48
210 T1=23
220 C=1.5E-5
225 A0=3.35678E-4
228 T=20
230 T=T+.2
233 LPRINT "Temp.= ";T;"Deg. C"
234 LPRINT
235 LPRINT "Wt. No.","Press./Pa"
236 LPRINT "--------","---------"
237 LPRINT
240 FOR I=1 TO 14
260 T2=T-T1
270 D=A0*(1+C*T2)
280 P(I)=(M(I)*G)/(D*100)
290 LPRINT I,:LPRINT USING "######.#";P(I)
300 NEXT I
320 LPRINT
330 LPRINT
340 LPRINT
350 LPRINT
355 GOTO 230
360 END
```

APPENDIX A3

Pressure and Volume Series Virial Coefficient

The programme "RMDSVC/BAS" determines pressure series apparent second virial coefficients ($\beta_{apparent}$), using the raw data p_1, p_2 p_3, T_1, T_2, T_3 and then uses $\beta_{apparent}$ as the first approximation to calculate the volume series apparent second virial coefficient ($B_{apparent}$).

A. Pressure Series Virial Coefficient, $\beta_{apparent}$

$\beta_{apparent}$ is calculated at temperature T_1 correcting for temperature variation in T_2 and T_3, using relation

$$\beta_{apparent} = R\left(\frac{T_3}{p_3} - \frac{T_1}{p_1} - \frac{T_2}{p_2}\right) \qquad (A3.1)$$

where p_1, p_2 and p_3 are the pressures of n moles of the sample in the volumes $v_1(T_1)$, $v_2(T_2)$ and $v_3(T_3)$ respectively. The volume v_3 is the sum of volumes v_1 and v_2.

B. Volume Series Virial Coefficient $B_{apparent}$

The volume explicit virial equation of state can be expressed as

$$pv = RT(1 + B/v) \qquad (A3.2)$$

where v is the molar volume of the gas given by V/n and n is the number of moles of gas. In the volume series, the difference in temperatures T_1, T_2 and T_3 for the three pressure measurements can not be accounted for, as in pressure series using direct relation (A3.1) for β. Assuming the system as a perfect gas thermometer, initially pressure $p_2(T_2)$ and $p_3(T_3)$ are also approximated at temperature T_1, using the equations

$$p_2' = (p_2/T_2).T_1 \qquad (A3.3)$$

$$p_3' = (p_3/T_3).T_1 \qquad (A3.4)$$

The imperfection in the equation of state is negligible for a few hundredths of degree. Equation (A3.2) can be written in quadratic form

$$p/v^2 - RTv - RTB = 0 \qquad (A3.5)$$

Hence using this form, and approximating first $B_{apparent}$ as $\beta_{apparent}$, the two volumes can be approximated using relations

$$v_1' = \frac{RT + \sqrt{(RT)^2 + 4p_1(RTB)}}{2p_1} \qquad (A3.6)$$

$$v_2' = \frac{RT + \sqrt{(RT)^2 + 4p_2(RTB)}}{2p_2'} \qquad (A3.7)$$

Using approximated B, p_3'' and the values of v_1' and v_2' from equations (A3.6 and A3.7) can be calculated using the relation

$$p_3'' = (RT/v_3)(1 + B/v_3) \qquad (A3.8)$$

where $v_3 = v_1' + v_2'$ (A3.9)

The calculated p_3'' is compared with the experimental p_3'. B is changed in consecutive steps and v_1', v_2' are approximated again. The process is iterative, till p_3'' (calculated) is within 0.1 Pa of the experimental p_3' value. The final approximated B value is the volume series apparent second virial coefficient ($B_{apparent}$).

Programme "RMSVCD/BAS"

The programme "RMSVCD/BAS" creates a data file of the raw data as given in Tables in Appendix A7. These data files are recalled in the programme "RMDSVC/BAS" to calculate $\beta_{apparent}$ and $B_{apparent}$ values.

```
10 REM ** PROGRAMME "RMDSVC/BAS" DETERMINES SEC. VIRIAL **
20 REM ** COEFFICIENT ON THE BASIS OF PRESSURE SERIES **
21 REN ** VIRIAL EQUATION OF STATE AND THEN USES THIS **
30 REM ** VALUE TO DETERMINE DENSITY SEC. VIRIAL COEFF. **
40 REM ** USING DENSITY SERIES VIRIAL EQUATION OF STATE **
50 REM ** BY ITERATIVE METHOD. **
55 REM ** P1= PRESURE OF THE SAMPLE IN BULB 1          **
60 REM ** P2= PRESSURE OF THE SMAPLE IN BULB 2         **
70 REM ** P3= PRESSURE OF THE SAMPLE IN BULB (1&2)     **
75 REM ** T1,T2,T3= TEMPERATURE OF THE BATH FOR P1,P2,P3**
80 REM ** R= GAS CONSTANT IN UNITS "PA.M3.MOL-1.K-1"   **
100 R=8.3144
110 GOSUB 700
115 GOSUB 1000
120 FOR I=1 TO N
130 P1=P1(I) : P2=P2(I) : P3=P3(I) : T1=T1(I)
135 T2=T2(I) : T3=T3(I)
150 LPRINT : LPRINT : LPRINT : LPRINT : LPRINT
160 LPRINT "Sec. virial coeff. for run";I
165 LPRINT "-------------------------------"
168 LPRINT
170 LPRINT "Pressure 1= ";P1;"Pa","Temp. 1= ";T1;"K"
180 LPRINT "Pressure 2= ";P2;"Pa","Temp. 2= ";T2;"K"
185 LPRINT "Pressure 3= ";P3;"Pa","Temp. 3= ";T3;"K"
190 LPRINT : LPRINT " Temperature of the bath= ";T1;"K" : LPRINT
200 B=R*((T3/P3)-(T1/P1)-(T2/P2))
205 B2=B*10[6
210 LPRINT "Sec. virial coeff. (Press. ser.)= ";B;"m3 mol-1"
215 LPRINT "                                 = ";B2;"cm3 mol-1"
225 T4=T2-T1 : T5=T3-T1
230 LPRINT "Drift in temp.2 for P2 measurement= ";T4;"K"
240 LPRINT "Drift in temp.3 for P3 measurement= ";T5;"K"
260 LPRINT : LPRINT : LPRINT
270 LPRINT " Second Part "
275 LPRINT " ------------ " : LPRINT
276 LPRINT "Sec. virial coeff. of Hexane (density series)"
280 LPRINT "-------------------------------------------"
285 LPRINT
300 REM ** SECOND PART **
310 REM ** V1 = V1/n m3. mol-1, WHERE V1 IS THE VOLUME **
315 REM ** OF THE BULB 1                               **
320 REM ** n IS THE NUMBER OF MOLES OF THE SAMPLE IN   **
325 REM ** THE BULB 1                                  **
330 REM ** V2 = V2/n, WHERE V2 IS THE VOLUME OF BULB 2 **
340 REM ** V3 = V3/n, WHERE V3 IS THE VOLUME FOR THE   **
345 REM ** WHEN IT IS EXPANDED TO BOTH BULBS 1 AND 2   **
350 REM ** V3 IS ALSO EQUAL TO V1 + V2 **
360 REM ** B = SECOND VIRIAL COEFFICIENT OF SAMPLE FROM **
365 REM ** PRESSURE SERIES, FIRST APPROXIMATION FOR     **
367 REM ** VOLUME SERIES EQUATION OF STATE.            **
370 REM ** DENSITY SERIES EQUATION IS ; PV = RT(1 + B/V) **
380 REM ** WRITTEN IN QUADRATIC FORM; V CAN BE SOLVED **
381 P2= (P2*T1)/T2 : P3= (P3*T1)/T3
382 LPRINT "Corr. P2 and P3 for the temp. of bath for P1 are"
383 LPRINT "corr. P2= ";P2;"Pa","corr. P3= ";P3;"Pa"
385 LPRINT
386 B3= R*T1*((1/P3)-(1/P1)-(1/P2))
```

```
387 LPRINT "Press. series using P1,P2,P3 at T1= "B3;"m3 mol-1"
388 B4= B3*10[6
389 LPRINT                                          =";B4;"CM3. MOL-1"
390 LPRINT : LPRINT
391 LPRINT "estimated","calculated","observed"
392 LPRINT "vir. coeff.","pressure 3","pressure 3"
393 LPRINT "------------","------------","----------"
400 V1=(R*T1+((R*T1)[2+(4*P1*B*R*T1))[0.5)/(2*P1)
410 V2=(R*T1+((R*T1)[2+(4*P2*B*R*T1))[0.5)/(2*P2)
420 V3=V1+V2
430 P4= ((R*T1)/V3)*(1+(B/V3))
440 REM ** P4 = PRESSURE OF THE SAMPLE, WHEN EXPANDED **
442 REM ** INTO BOTH BULBS 1 AND 2, AND              **
450 REM ** CALCULATED ON THE BASIS OF DENSITY SERIES **
460 LPRINT B,P4,P3
470 IF P4-P3<8 THEN GOTO 500
480 B=B+.00002
490 GOTO 400
500 IF P4-P3<1 THEN GOTO 512
510 B=B+.000002
511 GOTO 400
512 IF P4-P3<.1 THEN 540
514 B=B+.000001
520 GOTO 400
540 LPRINT : LPRINT : LPRINT
541 B=B*10[6
542 LPRINT "Sec. Virial Coeff. (dens. Series)= ";B;"cm3 mol-1"
545 LPRINT : LPRINT "Pressure 3.,calc.= ";P4;"Pa"
555 A=V2/V1
556 LPRINT "Ratio of vols. of cell 2 and cell 1; V2/V1= ";A
565 P4=P1+P2-P3 : LPRINT
567 LPRINT "( P1 + P2 - P3 ) = ";P4;"Pa"
568 LPRINT
569 LPRINT "-------------------------------------------------------"
570 PRINT #3,P1,P4,B2,B
580 NEXT I
590 CLOSE #3
610 GOTO 1300
700 REM ** THIS IS A SUBROUTINE TO OPEN AND READ THE   **
710 REM ** DATA FILE OF P1,P2,P3,T1,T2,T3.             **
720 PRINT "INPUT THE FILE NAME"
730 INPUT B$
740 LPRINT "DATA FILE= ";B$
750 OPEN "I", 2, B$
760 INPUT #2, C$
765 INPUT #2, N,T
766 LPRINT : LPRINT CHR$(27)"E"
767 LPRINT CHR$(27)"G"
770 LPRINT "-------------------------------------------------------"
773 LPRINT : LPRINT
774 LPRINT CHR$(14) "at "; T; " K"
780 LPRINT "------------------------------"
782 LPRINT CHR$(27)"F"
783 LPRINT CHR$(27)"H"
785 LPRINT CHR$(146)
800 LPRINT : LPRINT "Number of the data points = ";N
802 LPRINT : LPRINT CHR$(15)
805 LPRINT "Run No.","P1(I)","P2(I)","P3(I)","T1(I)","T2(I)","T3(I)"
807 LPRINT : LPRINT
```

```
810 FOR I=1 TO N
820 INPUT #2, P1(I),P2(I),P3(I),T1(I),T2(I),T3(I)
860 LPRINT I,P1(I),P2(I),P3(I),T1(I),T2(I),T3(I)
870 LPRINT
880 NEXT I
890 INPUT #2, D$
895 CLOSE #2
900 LPRINT CHR$(140)
910 LPRINT CHR$(146)
920 RETURN
1000 REM ** THIS SUBROUTINE IS TO CREATE A FILE TO STORE **
1010 REM ** THE DATA FOR WEIGHTED LEAST SQUARE ANALYSIS  **
1020 REM ** OF APPARENT PRESSURE/DENSITY SERIES SECOND   **
1030 REM ** VIRIAL COEFFICIENT AND (P1+P2-P3)            **
1035 A$=D$
1040 OPEN "O", 3,D$
1050 PRINT #3,C$
1060 PRINT #3,N;",";T
1110 REM ** C$ = COMPONENT7S NAME                        **
1120 REM ** N,T = NUMBER OF DATA POINTS AND TEMPERATURE **
1140 RETURN
1280 REM **
1290 REM **
1300 REM ** THIS SUBROUTINE OPENS THE CREATED DATA FILE **
1310 REM ** AND DISPLAYS ON THE PRINTER                 **
1320 REM **
1330 REM **
1340 LPRINT CHR$(140)
1345 PRINT C$
1350 LPRINT CHR$(27)"E"
1355 PRINT N,T
1360 LPRINT CHR$(27)"G"
1370 A$=D$
1380 OPEN "I", 1,A$
1390 LPRINT "Data File--";A$
1400 LPRINT "-------------------------"
1410 LPRINT : LPRINT : LPRINT
1420 INPUT #1,C$
1430 INPUT #1,N,T
1470 LPRINT CHR$(14) "Apparent B of ";C$ ;" at" ;T ;" K"
1480 LPRINT "-------------------------------------------------"
1490 LPRINT : LPRINT
1492 LPRINT CHR$(27)"F"
1494 LPRINT CHR$(27)"H"
1496 LPRINT CHR$(146)
1500 LPRINT "Press 1","(P1+P2-P3)","B (press)","B (dens)"
1505 LPRINT "Pascal","Pascal","cm3.mol-1","cm3.mol-1"
1510 LPRINT "-------","----------","---------","---------"
1515 LPRINT : LPRINT
1520 FOR I=1 TO N
1530 INPUT #1,P1,P4,B2,B
1540 LPRINT P1,P4,B2,B
1550 LPRINT
1555 NEXT I
1560 CLOSE #1
1600 LPRINT CHR$(140)
2000 END
```

```
10 REM ** PROGRAMME "RMSVCD/BAS" CREATES THE FILE FOR **
20 REM ** THE PROGREAMME "RMDSVC/BAS"                  **
30 PRINT "INPUT THE FILE NAME"
40 INPUT A$
50 OPEN "O", 1, A$
60 PRINT "INPUT THE COMPONENT NAME"
70 INPUT B$
80 PRINT #1,B$
90 PRINT "INPUT THE NUMBER OF THE DATA POINTS AND TEMPERATURE"
100 INPUT N,T
105 PRINT #1,N;",";T
110 FOR I=1 TO N
120 READ P1(I),P2(I),P3(I),T1(I),T2(I),T3(I)
130 PRINT P1(I),P2(I),P3(I),T1(I),T2(I),T3(I)
140 PRINT #1,P1(I);",";P2(I);",";P3(I);",";T1(I);",";T2(I);",";T3(I)
150 NEXT I
160 PRINT "INPUT THE NAME FOR THE FILE TO BE CREATED"
170 INPUT C$
180 PRINT #1, C$
250 DATA 25196,19745,11124,323.165,323.161,323.163
260 DATA 25054,19629,11066,323.175,323.188,323.181
270 DATA 23609,18497,10418,323.158,323.155,323.160
280 DATA 21080,16522,9300,323.166,323.169,323.163
290 DATA 20968,16425,9249,323.175,323.19,323.184
300 DATA 20204,15823,8908,323.182,323.177,323.185
310 DATA 19763,15468,8708,323.177,323.165,323.178
350 END
```

APPENDIX A4

Weighted Least Squares Straight Line Analysis

The programme "RMWLS/BAS" fits the weighted least squares straight line to the data pairs of $\beta_{apparent}$ and $(p_1 + p_2 - P_3)$ or $B_{apparent}$ and $(p_1 + p_2 - p_3)$, and calculates β and B respectively. $\beta_{apparent}$ and $B_{apparent}$ are functions of the pressure term $(p_1 + p_2 - p_3)$ at a given temperature. A least-squares straight line, through a plot of $\beta_{apparent}$ and $B_{apparent}$ versus the pressure term, should give "true" β and B respectively for the pressure term tending to zero as explained in Section 3-2.

For n paired observations (x_i, y_i), the error E_i in predicting the value of y_i corresponding to given x_i, is

$$y_i - y_i' = E_i \qquad (A4.1)$$

where $$y_i' = a + bx_i \qquad (A4.2)$$

and a,b are constants. Miller and Freund (1965) showed that a and b should be chosen such that the sum of squares of E_i, represented as

$$Q = \sum_{i=1}^{n} [y_i - (a + bx_i)]^2 \qquad (A4.3)$$

is minimised. Hence

$$\frac{\partial Q}{\partial a} = \sum_{i=1}^{n} [y_i - (a + bx_i)](-2) = 0 \qquad (A4.4)$$

$$\frac{\partial Q}{\partial b} = \sum_{i=1}^{n} [y_i - (a + bx_i)](-2x_i) = 0 \qquad (A4.5)$$

From equations (A4.4 and A4.5) the convenient form for $n(x_i, y_i)$ data pairs is

$$\Sigma y = Na + b\Sigma x \qquad (A4.6)$$

$$\Sigma xy = a\Sigma x + b\Sigma x^2 \qquad (A4.7)$$

Solving for a and b

$$a = \frac{\Sigma y.\Sigma x^2 - \Sigma x.\Sigma xy}{N\Sigma x^2 - (\Sigma x)^2} \qquad (A4.8)$$

$$b = \frac{N\Sigma xy - \Sigma x.\Sigma y}{N\Sigma x^2 - (\Sigma x)^2} \qquad (A4.9)$$

Leaver and Thomas (1974) have given other convenient forms for calculating a and b.

The accuracy of the values of the apparent second virial coefficient, $\beta_{apparent}$, is a function of pressure term $(p_1 + p_2 - p_3)$ at a given temperature. The estimated probable error, $E1_i$, in a particular run as given in Section 3-3, can be determined by the following equation

$$E1_i = \left[\left(\frac{6RT\delta p}{p_i}\right)^2 + \left(\frac{4\delta T p_i}{p_i}\right)^2\right]^{0.5} \qquad (A4.10)$$

where δp is the probable error in the pressure measurement and is equal to 5 Pa,

δT is the probable error in the temperature measurement, equal to 0.2 K and

p_i is the maximum pressure, p_1, at each loading in a run. A weighting factor w_i given by

$$w_i = 1/E1_i \qquad (A4.11)$$

is applied to the deviation $(y_i - (a + bx_i))$ where w_i bears a relation to $(p_1 + p_2 - p_3)$.

Brownlee (1960) showed that for the weighted sums of the squares of the deviations to be a minimum, the regression coefficients are given by

$$a = \frac{\Sigma yw.\Sigma x^2w - \Sigma xw.\Sigma xyw}{\Sigma w.\Sigma x^2w - (\Sigma xw)^2} \qquad (A4.12)$$

$$b = \frac{\Sigma w.\Sigma xyw - \Sigma xw.\Sigma yw}{\Sigma w.\Sigma x^2w - (\Sigma xw)^2} \qquad (A4.13)$$

The accuracy of the regression coefficients is given by the standard error of a and b (Topping, 1955).

$$\text{standard error of b} = \sqrt{\frac{\Sigma w.\Sigma E_i^2}{(n-2)[\Sigma w.\Sigma x^2.(\Sigma x)^2]}} \qquad (A4.14)$$

$$\text{standard error of a} = \sqrt{\frac{\Sigma x^2.\Sigma E_i^2}{(n-2)[\Sigma w.\Sigma x^2.(\Sigma x)^2]}} \qquad (A4.15)$$

where E_i is given by equation (A4.1) and in the programme is expressed as R[I].

```
10 REM ** PROGRAMME "RMWLS/BAS" FITS THE WEIGHTED LEAST **
15 REM ** SQUARES METHOD ANALYSIS OF STRAIGHT LINE       **
20 REM ** FOR A PLOT OF (P1+P2-P3) ON X AXIS AND         **
30 REM ** RESPECTIVE VIRIAL COEFFICIENT ON Y AXIS       **
40 REM ** E1= ERROR IN THE MEASUREMENT OF VIRIAL COEFF.  **
50 REM ** E2= POSSIBLE ERROR IN MEASURING PRESS. IN PA   **
60 REM ** E3= POSSIBLE ERROR IN MEASURING TEMPERATURE    **
70 REM ** T = TEMPERATURE IN KELVIN                      **
80 REM ** P = P1 IN EACH MEASUREMENT OF VIRIAL COEFF.    **
90 REM ** X = (P1+P2-P3)/PASCALS                         **
100 REM ** Y = SECOND VIRIAL COEFFICIENT/ CM3 MOL-1      **
110 REM ** W = WEIGHTAGE GIVEN TO A PARTICULAR POINT     **
120 R=8.3144
130 REM ** R= GAS CONSTANT IN PA. M3. K-1. MOL-1**
150 E2=5 :E3=.005
160 DIM P(50),X(50),Y(50),B(50)
170 DIM E1(50),E2(50),E3(50),E4(50),E5(50),E6(50),E7(50),R(50)
180 DIM W1(50),X1(50),Y1(50),P1(50),X2(50)
185 GOSUB 1300
190 E2=5 : E3=0.005
200 LPRINT CHR$(27)"E"
210 LPRINT CHR$(27)"G"
220 LPRINT CHR$(14) "B of ";C$;" (press series) "
221 LPRINT "-------------------------------------------------"
222 LPRINT CHR$(14) "at "; T ; " K"
224 LPRINT "----------------------------"
225 LPRINT CHR$(27)"F" : LPRINT CHR$(27)"H"
228 FOR I=1 TO N : Y(I)=B2(I)
230 NEXT I
235 GOSUB 280
236 FOR I=1 TO N : Y(I)=B(I) : NEXT I
240 LPRINT CHR$(27)"E"
245 LPRINT CHR$(27)"G"
250 LPRINT CHR$(14) "B of ";C$;" (dens. series) "
252 LPRINT "-------------------------------------------------"
255 LPRINT CHR$(14) "at "; T ;" K"
257 LPRINT "------------------------"
260 LPRINT CHR$(27)"F" : LPRINT CHR$(27)"H"
265 GOSUB 280
270 GOTO 1800
280 REM ** THIS IS SUBROUTINE TO FIT WEIGHTED LEAST SQ. **
282 REM ** EQUATION TO THE DATA                          **
285 LPRINT "Possible errors: in press.=";E2; "Pa"
287 LPRINT "                 in temperature = ";E3; "K"
290 FOR I=1 TO N
300 E4(I)= (6*R*T*E2*10[6)/(P(I)*P(I))
310 E5(I)= (4*E3*R*10[6)/P(I)
320 E6(I)= - 4*E2*Y(I)/P(I)
330 E7(I)=E4(I)[2 + E5(I)[2
340 E1(I)=E7(I)[0.5+E6(I)
350 W1(I)= 1/E1(I)
360 NEXT I
365 LPRINT : LPRINT
370 LPRINT " P1/","(P1+P2-P3)/","VIRIAL COEFF/","PROB. ERROR/"
380 LPRINT "Pascals","Pascals","Cm3. Mol-1","Cm3. Mol-1"
390 LPRINT "--------","--------","-----------","-----------"
395 LPRINT
400 FOR I= 1 TO N
```

```
410 LPRINT P(I),X(I),Y(I),E1(I)
415 NEXT I
421 FOR I=1 TO N : X1(I)=X(I)*W1(I) : Y1(I)= Y(I)*W1(I)
422 P1(I)= X(I)*Y(I)*W1(I) :X2(I)= X(I)[2*W1(I)
425 NEXT I
426 LPRINT : LPRINT
430 W1=0 : X1=0 : Y1=0 : P1=0 : X2=0
440 FOR I = 1 TO N
450 W1= W1+W1(I)
460 X1= X1+X(I)*W1(I)
470 Y1= Y1+Y(I)*W1(I)
480 P1= P1+X(I)*Y(I)*W1(I)
490 X2= X2+X(I)[2*W1(I)
500 NEXT I
510 D=X2*W1-X1*X1
530 B= (P1*W1-X1*Y1)/D
540 A= (Y1-B*X1)/W1
550 LPRINT : LPRINT
560 LPRINT "SLOPE= "B,"INTERCEPT= ";A
570 LPRINT : LPRINT
580 LPRINT " X  "," Y  "," Y. calc. "," R(I) "
590 LPRINT "(P1+P2-P3)","Vir. coeff","V C calc.","Y - Y.calc"
600 LPRINT "----------","----------","----------","----------"
610 S1=0 : S2=0
620 FOR I=1 TO N
630 Y=A+B*X(I)
640 R(I)= Y(I)-Y
650 LPRINT X(I),Y(I),Y,R(I)
660 S1=S1+R(I)*R(I)*W1(I)
670 S2= S2+ R(I)*R(I)
680 NEXT I
685 S3=S1/((N-1)*W1)
690 S3= S3[0.5
695 LPRINT : LPRINT
700 LPRINT "According to Topping (1955, page 88)"
701 LPRINT "---------------------------------------"
702 LPRINT "Standard error of weighted mean is "
710 LPRINT "Standard deviation= ";S3
720 REM ** A1=STANDARD ERROR OF SLOPE,B **
730 REM ** B1= STANDARD ERROR OF INTERCEPT,A**
740 B1=(W1*S1)/((N-2)*D)
750 B1=B1[0.5
760 A1=(X2*S1)/((N-2)*D)
770 A1=A1[0.5
780 LPRINT "Standard error in Slope, B= ";B1
790 LPRINT : LPRINT "Standard error in Intercept, A= ";A1
800 LPRINT : LPRINT
810 LPRINT "Virial Coefficient for this run is ";A;"cm3 mol-1"
815 LPRINT "with a standard error of ";A1;"cm3 mol-1"
820 LPRINT CHR$(140)
830 RETURN
1300 REM ** THIS SUBROUTINE OPENS THE CREATED DATA FILE **
1310 REM ** AND DISPLAYS ON THE PRINTER                 **
1320 REM **
1330 REM **
1350 LPRINT CHR$(27)"E"
```

```
1360 LPRINT CHR$(27)"G"
1365 PRINT "INPUT THE DATA FILE NAME"
1370 INPUT A$
1380 OPEN "I", 1,A$
1390 LPRINT "Data File--";A$
1400 LPRINT "------------------------"
1410 LPRINT : LPRINT : LPRINT
1420 INPUT #1,C$
1430 INPUT #1,N,T
1470 LPRINT CHR$(14) "Apparent B of ";C$ ;" at" ;T ;" K"
1480 LPRINT "-----------------------------------------------------------"
1490 LPRINT : LPRINT
1492 LPRINT CHR$(27)"F"
1494 LPRINT CHR$(27)"H"
1496 LPRINT CHR$(146)
1500 LPRINT "Press 1","(P1+P2-P3)","B (press)","B (dens)"
1505 LPRINT "Pascal","Pascal","cm3.mol-1","cm3.mol-1"
1510 LPRINT "-------","----------","---------","--------"
1515 LPRINT : LPRINT
1520 FOR I=1 TO N
1530 INPUT #1,P(I),X(I),B2(I),B(I)
1540 LPRINT P(I),X(I),B2(I),B(I)
1550 LPRINT
1555 NEXT I
1560 CLOSE #1
1600 LPRINT CHR$(140)
1610 RETURN
1800 END
```

APPENDIX A5

Calibration Charts for Bar_1 Measurement

Appendix A5 gives the plots of the calibration charts for conversion of measurements of pressure in Bar_1 units into the values in Bar_2 units, as explained in Section 5-3.2. The curves are plotted for the sum of the two Baratron readings ($\Delta s = Bar_1 + Bar_2$) corresponding to same pressure on two gauges, versus Bar_1 readings.

FIGURE A5-1

Calibration of Baratron 1 Against Baratron 2 at 323.15 K

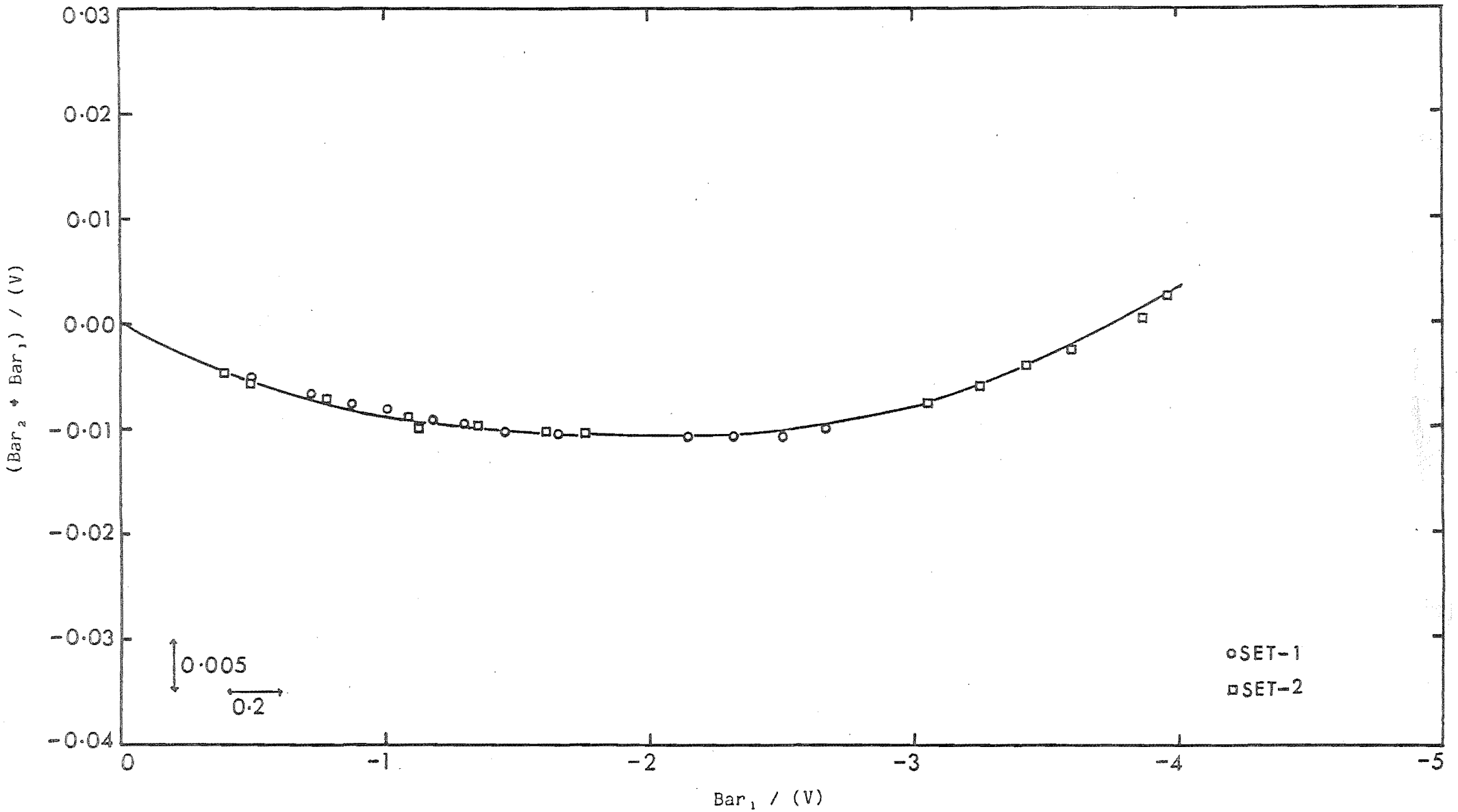

FIGURE A5-2

Calibration of Baratron 1 Against Baratron 2 at 338.15 K

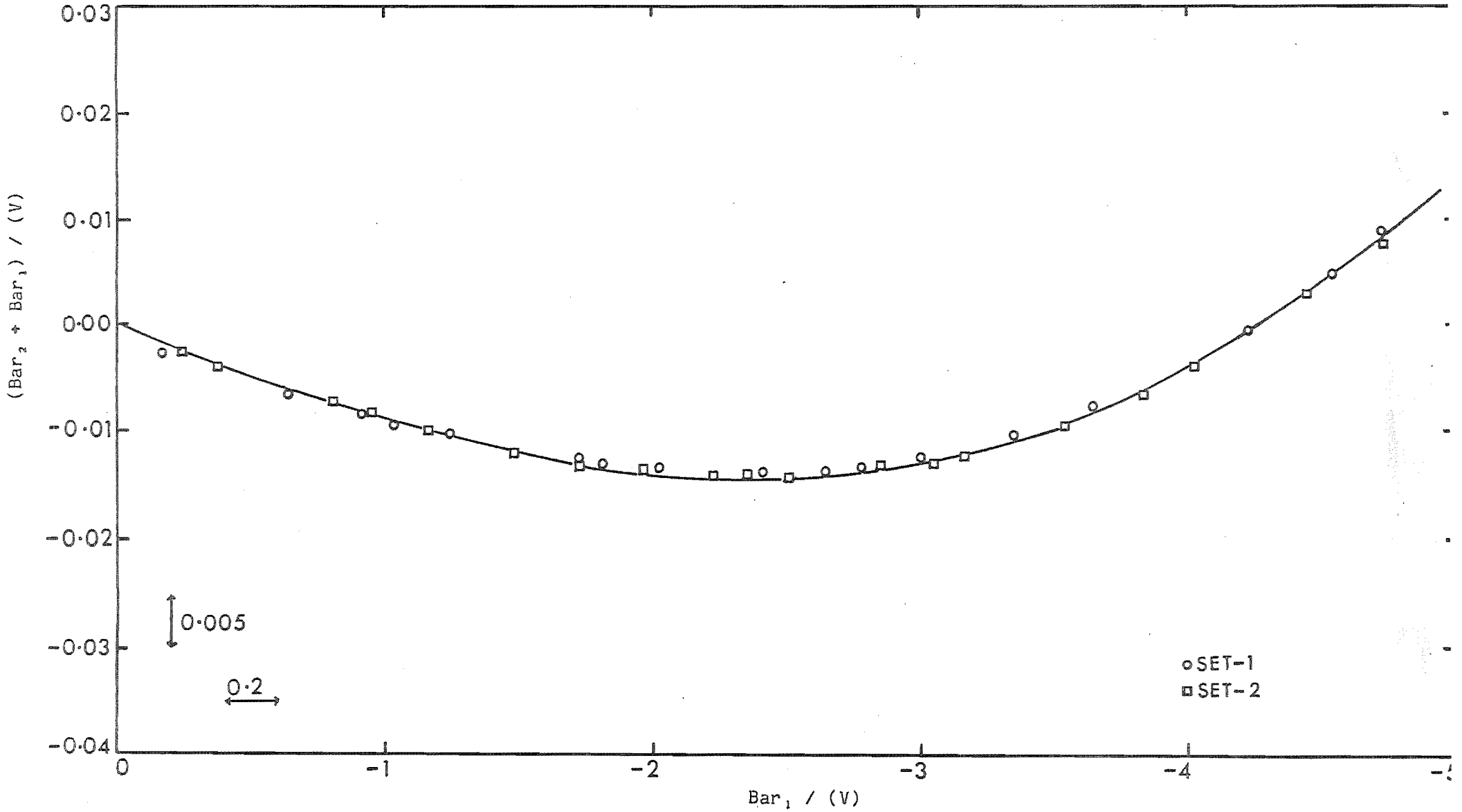

FIGURE A5-3

Calibration of Baratron 1 Against Baratron 2 at 348.15 K

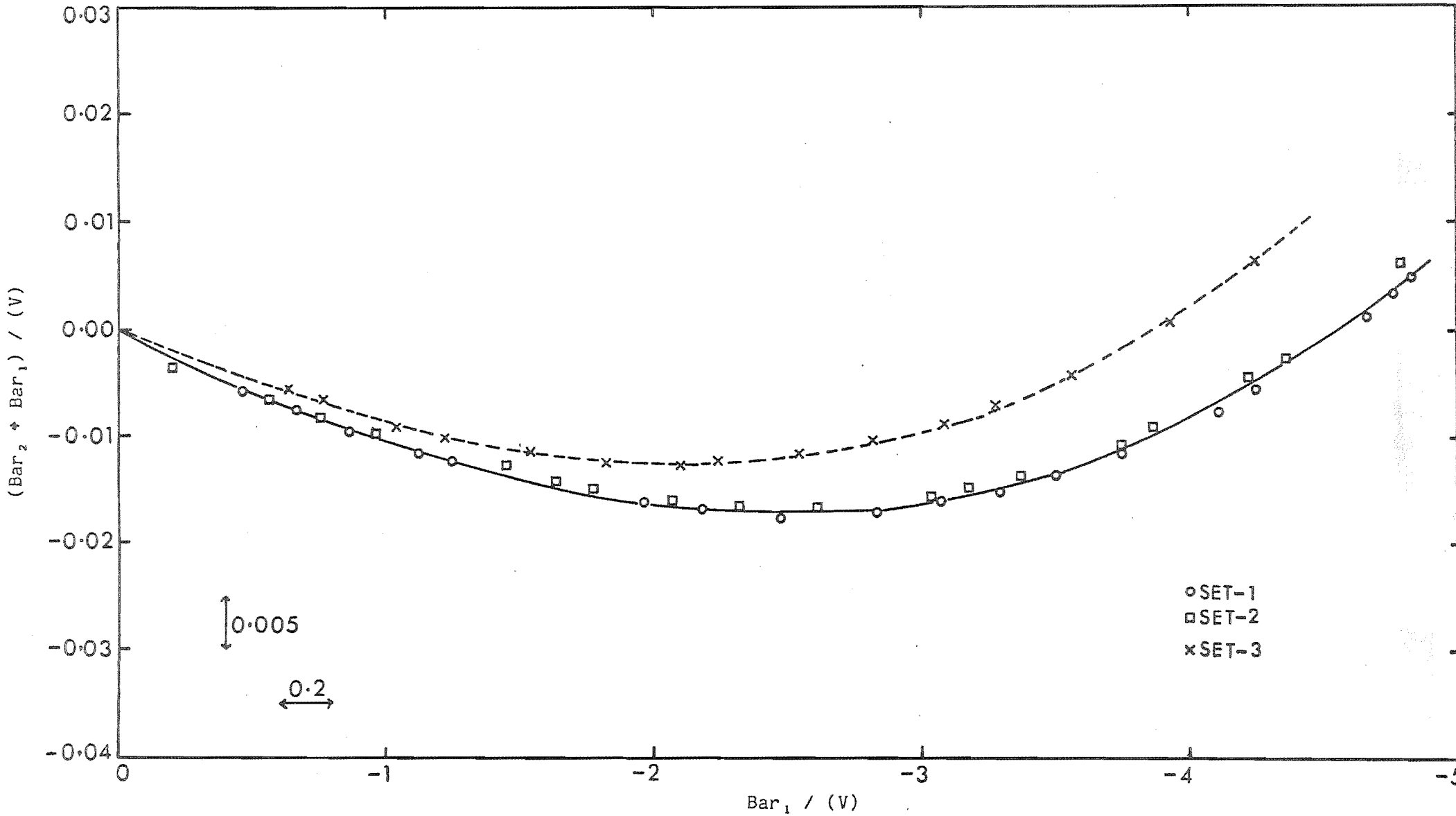

FIGURE A5-4

Calibration of Baratron 1 Against Baratron 2 at 358.15 K

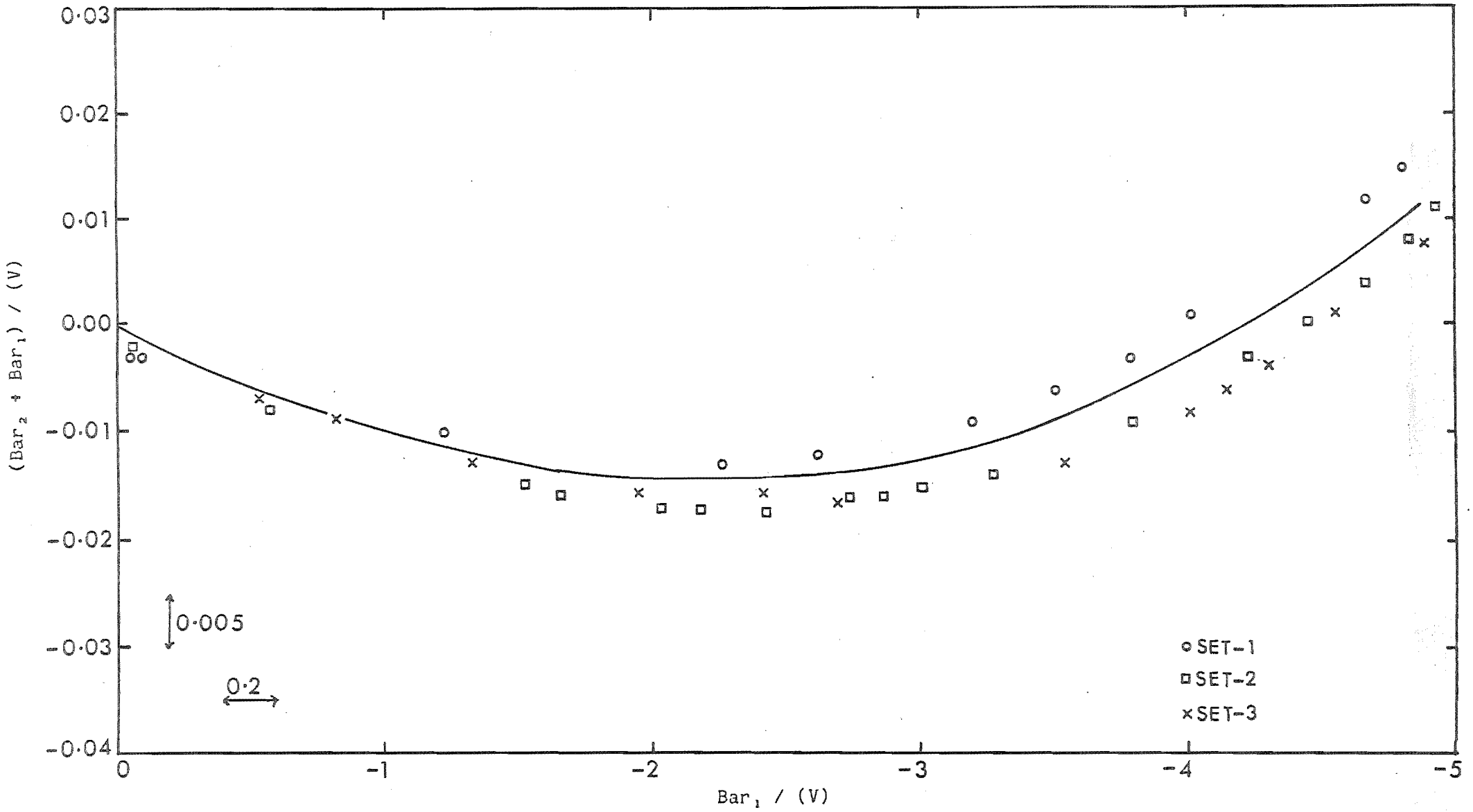

FIGURE A5-5

Calibration of Baratron 1 Against Baratron 2 at 373.15 K

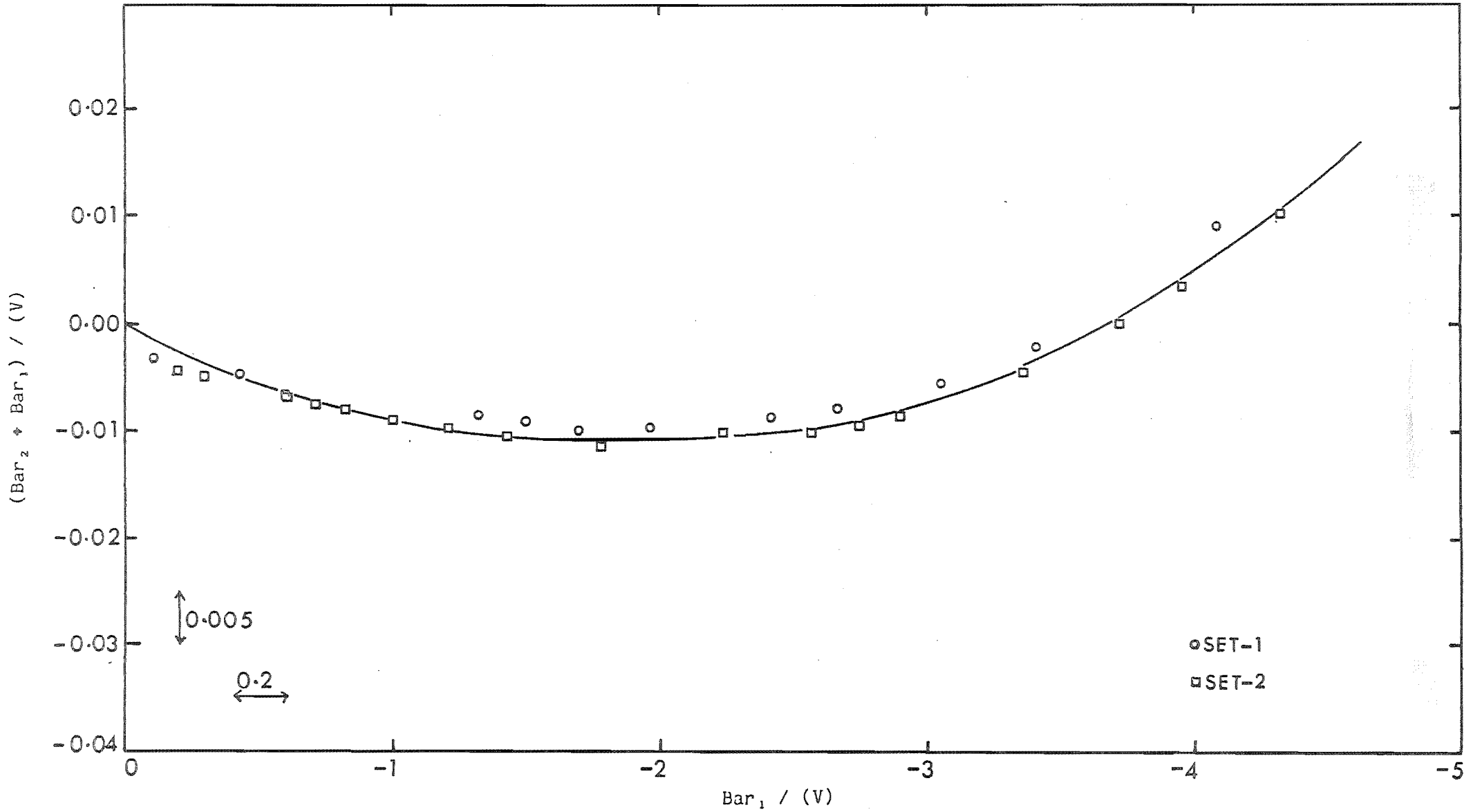

APPENDIX A6

Appendix A6 consists of two parts. Part I describes the calculations of raw data (tabulated in Appendix A7), using original instrumental readings. Part II describes the calculations of $B_{apparent}$ and $\beta_{apparent}$ and comparison of others' work with this one, at the same maximum loading pressure.

Part I

The raw data, for each pressure measurement of the gas in a run, comprises of measurements of the bath temperature (Section 4-3) and piston temperature (Section 4-4D). The data also need designation of the weights on the piston of the dead weight gauge (DWG) to balance the reference gas (nitrogen) pressure (Section 5-2.2) and the measurements of outputs of both "Baratron" pressure gauges for balanced DWG piston position (Section 5-2.2).

This section explains the sample calculations taking a particular example of raw data for meaurement of p_1 of n-hexane at 373.15 K for Run 1.

Measurement of p_1, Run 1 of Hexane at 373.15 K

Instrumental Readings

Bath Temperature (Quartz Thermometer) = 99.942°C

Piston Temperature =20.0°C

Weights on Piston = 1, 2, 3, 5, 6, 8, 12

(Note : The numbers designate the weight)

Table A6-1 **Original Instrumental Readings for Balanced DWG Piston Position**

Bar 2 (Volts)	Bar 1 (Volts)
1.990	-0.6686
1.986	-0.6659
1.975	-0.6503
1.970	-0.6454
1.966	-0.6426
1.985	-0.6668
1.982	-0.6637
1.980	-0.6616

Room temperature was stable within ±1°C as indicated by hygrothermograph.

Sample Calculation

1. The bath temperature is corrected for the zero shift in quartz thermometer (Section 6-1.1)

Corrected bath temperature = 99.942 + 0.045^{o}C

= 99.987^{o}C

2. DWG pressure for piston temperature 20^{o}C are calculated for corresponding weight as described in Appendix A2 and are tabulated in Table A6-2.

Table A6-2 **Piston Weights Denomination in Pa at 20^{o}C**

Wt. No.	DWG Pressure Pascal
1	24997.4
2	24997.2
3	24997.9
5	9999.5
6	9999.4
8	2499.9
12	250.1
TC	1399.8
Total Pressure =	99141.2

where TC is the tare component, i.e. pressure exerted by piston itself.

Bar_1 reading is corrected to read in inetrumental units

(Volts) of Bar_2, as explained in Section 5-3.2 and using the calibration plot for Bar_1 versus Bar_2 at 373.15 K (Appendix A5). For each pair of both "Baratron" pressure gauge' readings, the total pressure is obtained as the sum of Bar_1, Bar_2 and DWG observations, given by equation (6.5) and is tabulated in Table A6-3.

Table A6-3 **Total Pressure**

Bar_2 (Volts)	Bar_1 (Volts)'**	Bar_1corr. (Volts)	Bar_1corr. + Bar_2 (Volts)	P_s* (Pascal)
1.990	-0.6686	-0.6611	1.3289	99318.4
1.986	-0.6659	-0.6590	1.3270	99318.1
1.975	-0.6503	-0.643	1.3320	99318.8
1.970	-0.6454	-0.638	1.3320	99318.8
1.966	-0.6426	-0.635	1.3310	99318.7
1.985	-0.6668	-0.659	1.3260	99318.0
1.982	-0.6637	-0.656	1.3260	99318.0
1.980	-0.6616	-0.654	1.3260	99318.0

(Note: * P_s = (Bar_1corr. + Bar_2)133.3224/0.999602 + DWG)

** (Volts)' = the differential pressure as read on Baratron 1 gauge in its units.

Average total pressure = 99318.4±0.4 Pa

Hence, p_1 = 99318 Pa; and T_1 = 373.137 K

Raw data for the calculation of the second virial coefficients B and β, are tabulated in Table A7-1.6 (Appendix A7).

Part II

The raw data tabulated in Table A7-1.6 (Appendix A7) are used to calculate $\beta_{apparent}$ and $B_{apparent}$, using computor programme "RMDSVC/BAS" as detailed in Appendix A3. The apprent second virial coefficients corresponding to the pressure term $(p_1 + p_2 - p_3)$ for n-hexane at 373.15 K are tabulated in Table 6-6, and are plotted in Figure 6-7. The plot shows that the difference in two apparent second virial coefficients decreases as $(p_1 + p_2 - p_3)$ decreases. β andB are nearly the same for $(p_1 + p_2 - p_3)$ approaching zero.

Comparison

The results are compared with those of McGlashan and Potter (1962) for n-hexane at 373.15 K. Table 6-4 gives their $B_{apparent}$ values for n-hexane at temperatures close to 373.15 K.

Table A6-4 $B_{apparent}$ for n-hexane

(McGlashan and Potter, 1962)

T_1 / K	p_1 / mm	$B_{apparent}$ / $cm^3\ mol^{-1}$
	Series 1	
368.0	200	-1075
378.4	200	-981
	Series 2	
370.5	230	-1050
377.7	230	-992

From Table A6-4, B for n-hexane at 373.15 K for both series is approximately -1030 $cm^3\ mol^{-1}$.

McGlashan and Potter (1962) have reported the initial pressure p_1, choosing as high a value of p_1 as was consistent with the condition that condensation should not occur when the gas was compressed to a pressure of about $3p_1$. Thus on the final compression their maximum pressure is approximately $3p_1$.

p_1 = 200.0 mm

Max. pressure $\simeq 3p_1$ = 600.0 mm

80000 Pa

This Work

$$\text{Max. pressure (this work)} = 0.745(p_1 + p_2 - p_3) \qquad \text{(A6.1)}$$

The factor 0.745 was approximated by dividing the actual pressure term $(p_1 + p_2 - p_3)$ by p_1, using raw data from Table A7-1.6.

To compare the second virial coefficients of this work with those of the literature (eg. McGlashan and Potter, 1962), the total pressure term $(p_1 + p_2 - p_3)$ is approximated using equation (A6.1) corresponding to their maximum pressure $(3p_1)$. Hence

$$(p_1 + p_2 - p_3) = 80{,}000/0.745$$

$$= 10.74 \times 10^4 \text{ Pa}$$

From the plot for $\beta_{apparent}$ and $B_{apparent}$ versus the pressure term $(p_1 + p_2 - p_3)$ for this work, for n-hexane at 373.15 K in Figure 6-7, the value of $\beta_{apparent}$ and $B_{apparent}$ can be determined corresponding to McGlashan and Potter's (1962) approximated $(p_1 + p_2 - p_3)$ term. Hence at p_{max} corresponding to 80,000 Pa, the apparent second virial coefficients are

$$\beta_{apparent} = -(1075 \pm 20) \text{ cm}^3 \text{ mol}^{-1}$$

$$B_{apparent} = -(1030 \pm 20) \text{ cm}^3 \text{ mol}^{-1}$$

Hence $B_{apparent}$ for this measurement at 373.15 K, at initial loading pressure equal to 80,000 Pa, is equal to -1030 $\text{cm}^3 \text{ mol}^{-1}$ (McGlashan and Potter, 1962) within the experimental probable error of

$B_{apparent}$ calculated for truncated linear series. It is also observed that at the higher pressure, $B_{apparent}$ is less negative than $\beta_{apparent}$ by 5%.

The extrapolated values of the second virial coefficients on ordinate for $(p_1 + p_2 - p_3)$ tending to zero are

"True" $\beta = -1100 \pm 41$ cm^3 mol^{-1}

"True" $B = -1109 \pm 38$ cm^3 mol^{-1}

As is obvious in this work, β and B are close enough to satisfy the condition of them being equal as conditioned in equation (1.5).

APPENDIX A7

A7-1 Second Virial Coefficient of Hexane

Table : A7-1.1 Raw Data at 323.15 K

	Run No.	p_1 / Pa	p_2 / Pa	p_3 / Pa	T_1 / K	T_2 / K	T_3 / K
a.	1	42870	33687	19066	323.234	323.224	323.229
	2	33687	30512	16165	323.224	323.224	323.224
	3	30512	23939	13517	323.224	323.222	323.222
	4	23939	21675	11449	323.222	323.221	323.224
	5	21675	16978	9577	323.221	323.220	323.227
b.	6	46474	36557	20704	323.263	323.220	323.263
	7	39012	30646	17336	323.182	323.182	323.174
	8	32708	25674	14504	323.169	323.169	323.169
	9	27412	21500	12131	323.176	323.169	323.169
	10	22948	17993	10147	323.169	323.192	323.180
c.	11	45123	35488	20096	323.140	323.139	323.139
	12	37868	29741	16820	323.142	323.142	323.142
	13	31758	24908	14074	323.143	323.144	323.146
	14	26609	20858	11772	323.142	323.142	323.142
	15	22276	17460	9844	323.142	323.134	323.136

Table : A7-1.2 **Raw Data at 328.15 K**

	Run No.	p_1 / Pa	p_2 / Pa	p_3 / Pa	T_1 / K	T_2 / K	T_3 / K
a.	1	53582	44507	24649	328.143	328.140	328.134
	2	44507	37800	20683	328.140	328.140	328.138
	3	37800	31343	17307	328.140	328.138	328.145
	4	31343	26585	14505	328.138	328.136	328.149
	5	26585	22031	12140	328.136	328.131	328.136
b.	6	56797	47178	26139	328.157	328.157	328.157
	7	47178	40088	21946	328.157	328.159	328.162
	8	40088	33258	18371	328.159	328.148	328.157
	9	33258	28216	15397	328.148	328.148	328.152

Table : A7-1.3 **Raw Data at 338.15 K**

Run No.	p_1 / Pa	p_2 / Pa	p_3 / Pa	T_1 / K	T_2 / K	T_3 / K
1	61741	48583	27555	338.174	338.172	338.174
2	51849	40756	23074	338.172	338.167	338.178
3	43500	34154	19314	338.177	338.172	338.177
4	36473	28616	16161	338.168	338.164	338.167
5	30543	23973	13526	338.177	338.166	338.184
6	25604	20064	11310	338.171	338.165	338.174

Table : A7-1.4 Raw Data at 348.15 K

	Run No.	p_1 / Pa	p_2 / Pa	p_3 / Pa	T_1 / K	T_2 / K	T_3 / K
a.	1	77086	69905	37272	348.157	348.157	348.159
	2	69905	54998	31206	348.157	348.187	348.157
	3	54998	49869	26454	348.187	348.171	348.179
	4	49869	39154	22132	348.171	348.171	348.174
	5	39154	35447	18755	348.171	348.171	348.171
b.	6	87481	68959	39259	348.151	348.151	348.179
	7	68959	62542	33280	348.151	348.149	348.157
	8	62542	49172	27871	348.149	348.140	348.149
	9	49172	44569	23618	348.140	348.167	348.140
c.	10	58730	46124	26119	348.187	348.187	348.180
	11	49252	38680	21873	348.198	348.199	348.195
	12	41285	32402	18303	348.191	348.198	348.204
	13	34603	27137	15309	348.197	348.196	348.197
	14	28985	22720	12813	348.200	348.198	348.200
d.	15	89215	70336	40054	348.151	348.143	348.149
	16	75008	59062	33542	348.141	348.143	348.148
	17	63024	49559	28083	348.127	348.133	348.131
	18	52888	41549	23507	348.134	348.138	348.142
	19	44366	34808	19671	348.136	348.138	348.132
	20	37169	29153	16452	348.137	348.135	348.134
	21	31124	24405	13761	348.135	348.130	348.128

Table : A7-1.5 Raw Data at 358.15 K

Run No.	p_1 / Pa	p_2 / Pa	p_3 / Pa	T_1 / K	T_2 / K	T_3 / K
1	93795	73955	42056	358.224	358.217	358.216
2	78909	62089	35233	358.222	358.215	358.217
3	66263	52094	29505	358.224	358.202	358.213
4	55611	43663	24700	358.209	358.194	358.203
5	46626	36615	20674	358.189	358.399	358.198
6	39086	30650	17295	358.263	358.262	358.273
7	32741	25648	14470	358.257	358.279	358.282
8	27416	21470	12099	358.263	358.271	358.259

Table : A7-1.6 **Raw Data at 373.15 K**

	Run No.	p_1 / Pa	p_2 / Pa	p_3 / Pa	T_1 / K	T_2 / K	T_3 / K
a.	1	93613	73680	41845	373.147	373.138	373.143
	2	73680	66783	35467	373.138	373.151	373.164
	3	66783	52454	29688	373.151	373.135	373.154
	4	52454	47516	25162	373.135	373.133	373.137
	5	47516	37262	21050	373.133	373.122	373.128
	6	37262	33762	17825	373.122	373.211	373.128
	7	33762	26926	14901	373.211	373.122	373.221
b.	8	99318	78275	44452	373.137	373.149	373.149
	9	83532	65647	37212	373.171	373.065	373.060
	10	70089	55059	31156	373.130	373.137	373.140
	11	58783	46157	26083	373.139	373.150	373.152
	12	49260	38665	21818	373.156	373.162	373.158
	13	41299	32364	18277	373.161	373.124	373.379
	14	34582	27092	15275	373.121	373.133	373.145

A7-2 **Second Virial Coefficient of Benzene**

Table : A7-2.1 **Raw Data at 323.15 K**

Run No.	p_1 / Pa	p_2 / Pa	p_3 / Pa	T_1 / K	T_2 / K	T_3 / K
1	26284	20596	11609	323.166	323.167	323.165
2	25196	19745	11124	323.165	323.161	323.163
3	24142	18919	10650	323.175	323.186	323.173
4	23609	18497	10418	323.158	323.155	323.160
5	22557	17671	9952	323.170	323.151	323.162
6	22003	17239	9708	323.178	323.165	323.173
7	21080	16522	9300	323.166	323.169	323.163
8	20968	16425	9249	323.175	323.190	323.184
9	20204	15823	8908	323.182	323.177	323.185
10	19763	15468	8708	323.177	323.165	323.178

Table : A7-2.2 **Raw Data at 348.15 K**

Run No.	p_1 / Pa	p_2 / Pa	p_3 / Pa	T_1 / K	T_2 / K	T_3 / K
1	55098	43276	24440	348.155	348.160	348.155
2	46180	36244	20451	348.155	348.160	348.165
3	38687	30326	17100	348.160	348.210	348.162
4	32401	25389	14300	348.228	348.226	348.226
5	27120	21244	11959	348.192	348.201	348.204
6	22695	17768	10001	348.197	348.199	348.194

Table : A7-2.3 **Raw Data at 373.15 K**

Run No.	p_1 / Pa	p_2 / Pa	p_3 / Pa	T_1 / K	T_2 / K	T_3 / K
1	98731	77666	44002	373.144	373.136	373.149
2	93139	73232	41465	373.089	373.072	373.069
3	78139	61357	34713	373.060	373.075	373.062
4	68397	53658	30311	373.064	373.053	373.063
5	58233	45722	25787	373.101	373.108	373.095
6	57325	44909	25351	373.053	373.037	373.054
7	47987	37621	21201	373.031	373.045	373.029
8	40119	31493	17727	373.054	373.024	373.042
9	33628	26337	14834	372.997	373.030	373.013

A7-3 **Second Virial Coefficient of Cyclohexane**

Table : A7-3.1 **Raw Data at 323.15 K**

Run No.	p_1 / Pa	p_2 / Pa	p_3 / Pa	T_1 / K	T_2 / K	T_3 / K
1	25234	19778	11145	323.204	323.207	323.202
2	21481	16827	9479	323.198	323.200	323.206
3	21108	16547	9319	323.214	323.202	323.215
4	18326	14357	8082	323.180	323.175	323.180
5	17968	14072	7924	323.181	323.181	323.178
6	15318	12014	6754	323.175	323.155	323.142

Table : A7-3.2 **Raw Data at 348.15 K**

Run No.	p_1 / Pa	p_2 / Pa	p_3 / Pa	T_1 / K	T_2 / K	T_3 / K
1	50921	39958	22576	348.196	348.201	348.200
2	43407	34020	19202	348.167	348.168	348.171
3	42674	33475	18890	348.196	348.200	348.199
4	36331	28505	16064	348.169	348.165	348.159
5	35749	28023	15800	348.199	348.173	348.173
6	25051	19613	11049	348.170	348.167	348.171
7	20961	16416	9239	348.168	348.165	348.165

Table : A7-3.2 Raw Data at 348.15 K

Run No.	p_1 / Pa	p_2 / Pa	p_3 / Pa	T_1 / K	T_2 / K	T_3 / K
1	93609	73610	41747	373.163	373.152	373.154
2	78579	61752	34950	373.143	373.156	373.143
3	65884	51775	29252	373.155	373.148	373.149
4	55267	43370	24481	373.149	373.143	373.150
5	46305	36299	20479	373.160	373.148	373.150
6	38781	30387	17122	373.148	373.154	373.147
7	32453	25428	14321	373.179	373.158	373.157
8	27148	21284	11974	373.164	373.171	373.163

APPENDIX A8

Hayden and O'Connell's Method

Estimation of the second virial coefficient of a pure substance using the method of Hayden and O'Connell (1975), requires only a knowledge of its critical temperature, pressure and mean radius of gyration. Cross parameters, for calculations of cross second virial coefficients, are obtained using mixing rules and pure component parameters. The pure component and cross second virial coefficients B_{ij} are given by the sum of the several contributions.

$$B_{ij} = (B^F_{nonpolar})_{ij} + (B^F_{polar})_{ij} + (B^D_{metastable})_{ij} + (B^D_{bound})_{ij} + (B^D_{chemical})_{ij} \qquad (A8.1)$$

Prausnitz et al. (1980) list the individual contributions, calculated from temperature correlations

$(B^F_{nonpolar})_{ij}$

$$(B^F_{nonpolar})_{ij} = (b_0)_{ij} \left[0.94 - \frac{1.47}{T^{*'}_{ij}} - \frac{0.85}{T^{*'2}_{ij}} + \frac{1.015}{T^{*'3}_{ij}}\right] \qquad (A8.2)$$

where $(b_0)_{ij}$ = equivalent hard sphere volume of molecules, in units

$cm^3\ g\text{-}mole^{-1}$

$T^{*'}_{ij}$ = the reduced temperature

$$\frac{1}{T^{*'}_{ij}} = \frac{1}{T^{*}_{ij}} - 1.6\omega_{ij} \qquad (A8.3)$$

$$T^{*}_{ij} = \frac{T}{(\varepsilon_{ij}/k)} \qquad (A8.4)$$

where ω_{ij} = nonpolar acentric factor

(ε_{ij}/k) = characteristic energy for the i-j interaction, K.

$$(b_0)_{ij} = 1.26184\ \sigma^3_{ij} \qquad (A8.5)$$

where σ_{ij} = molecular size, A

For i=j parameters, ω_{ii}, (ε_{ii}/k) and σ_{ii} in equations (A8.3 to A8.5) are predicted from pure component properties.

$$\omega_{ii} = 0.006026R_{D_i} + 0.02096R_{D_i}^2 - 0.001366R_{D_i}^3 \qquad (A8.6)$$

where R_{D_i} = mean radius of gyration of component i.

$$(\varepsilon_{ii}/k) = (\varepsilon_{ii}/k)'[1 - \xi C_1(1 - \frac{\xi(1 + C_1)}{2})] \qquad (A8.7)$$

where (ε_{ii}/k) = characteristic energy parameter for pure non-polar pairs, K

k = Boltzmann constant = 1.3805×10^{-16} ergs molecule-1 K

$\xi = 0$ for $\mu_i < 1.45$ or

$$\xi = \frac{1.7941 \times 10^7 \mu_i^4}{\left[\left(2.882 - \frac{1.882\omega_{ii}}{0.03\omega_{ii}}\right) T_i^c \sigma'^6_{ii} (\varepsilon_{ii}/k)'\right]} \qquad \text{(A8.8)}$$

for $\mu_i \geq 1.45$

where μ_i = molecular dipole moment, D (10^{-18} esu)

σ'_{ii} = molecular size parameter for pure polar and associating pairs

$(\varepsilon_{ii}/k)'$ = characteristic energy parameter for pure polar and associating pairs

$$(\varepsilon_{ii}/k)' = T_i^c[0.748 + 0.91\omega_{ii} - \frac{0.4\eta_{ii}}{2 + 20\omega_{ii}}] \qquad \text{(A8.9)}$$

where T_i^c = critical temperature of component i

η_{ii} = association parameter for pure interaction

$$C_1 = \frac{16 + 400\omega_{ii}}{10 + 400\omega_{ii}} \qquad \text{(A8.10)}$$

$$\sigma'_{ii} = (2.44 - \omega_{ii})(1.0133T_i^c/P_i^c)^{1/3} \qquad \text{(A8.11)}$$

where P_i^c = critical pressure of component i

$$\sigma_{ii} = \sigma'_{ii}(1 + \xi C_2)^{1/3} \qquad \text{(A8.12)}$$

$$C_2 = \frac{3}{10 + 400\omega_{ii}} \qquad \text{(A8.13)}$$

$(B^F_{polar})_{ij}$

$$(B^F_{polar})_{ij} = -(b_0)_{ij} \mu^{*'}_{ij}\left(0.74 - \frac{3.0}{T^{*'}_{ij}} + \frac{2.1}{T^{*',2}_{ij}} + \frac{2.1}{T^{*',3}_{ij}}\right) \qquad (A8.14)$$

$$\mu^{*'}_{ij} = \mu^{*}_{ij} \qquad \mu^{*}_{ij} < 0.4$$

$$= 0 \qquad 0.04 \leq \mu^{*}_{ij} < 0.25$$

$$= \mu^{*}_{ij} - 0.25 \qquad \mu^{*}_{ij} \geq 0.25 \qquad (A8.15)$$

where μ^{*}_{ij} = molecular dipole moment, $D(10^{-18}$ esu)

$$\mu^{*}_{ij} = \frac{7243.8\mu_i\mu_j}{(\varepsilon_{ij}/k)\sigma_{ij}} \qquad (A8.16)$$

$(B^D_{metastable})_{ij} + (B^D_{bound})_{ij}$

$$(B_{metastable})_{ij} + (B_{bound})_{ij} = (b_0)_{ij} A_{ij} \exp\left(\frac{\Delta h_{ij}}{T^{*}_{ij}}\right) \qquad (A8.17)$$

where A_{ij} = parameter in correlation

Δh_{ij} = effective enthalpy of formation of physically bound pairs, ergs molecule^{-1}.

$$A_{ij} = -0.3 - 0.05\mu^{*}_{ij} \qquad (A8.18)$$

$$h_{ij} = 1.99 + 0.2\mu^{*2}_{ij} \qquad (A8.19)$$

$\underline{(B^{D}_{chemical})_{ij}}$

$$(B^{D}_{chemical})_{ij} = (b_0)_{ij} E_{ij}[1 - \exp(\frac{1500\mu_{ij}}{T})] \qquad (A8.20)$$

where

$$E_{ij} = \exp[\eta_{ij}(\frac{650}{(\varepsilon_{ij}/k) + 300} - 4.27)] \qquad \text{for } \eta_{ij}<4.5$$

$$\varepsilon_{ij} = \exp[\eta_{ij}(\frac{42800}{(\varepsilon_{ij}/k) + 22400} - 4.27)] \qquad (A8.21)$$

To calculate the interaction second virial coefficient of the mixture, the cross parameters(ε_{ij}/k), σ_{ij}, and ω_{ij} ($i \neq j$) are calculated using suitable mixing rules and pure-component parameters given by equations (A8.6) through (A8.13).

$$\omega_{ij} = (\omega_{ii} + \omega_{jj})/2 \qquad (A8.22)$$

$$(\varepsilon_{ij}/k) = (\varepsilon_{ij}/k)'(1 + \xi' C_1') \qquad (A8.23)$$

where $(\varepsilon_{ij}/k)'$

$$= 0.7[(\varepsilon_{ii}/k)(\varepsilon_{jj}/k)]^{1/2} + \frac{0.6}{[1/(\varepsilon_{ii}/k)+(1/(\varepsilon_{jj}/k)]} \qquad (A8.24)$$

$$\xi' = \frac{\mu_i^2(\varepsilon_{jj}/k)^{2/3}\sigma_{jj}^4}{(\varepsilon_{ij}/k)'\sigma_{ij}'^6} \qquad \text{for } \mu_i \geq 2 \text{ and } \mu_j = 0 \qquad (A8.25)$$

or

$$\xi' = \frac{\mu_j^2(\varepsilon_{ii}/k)^{2/3}\sigma_{ii}^4}{(\varepsilon_{ij}/k)'\sigma_{ij}'^6} \qquad \text{for } \mu_j \geq 2 \text{ and } \mu_i = 0 \qquad (A8.26)$$

or $\xi' = 0.0$ for all other values of μ_i and μ_j (A8.27)

$$C_1' = \frac{16 + 400\omega_{ij}}{10 + 400\omega_{ij}} \qquad (A8.28)$$

σ_{ij} for $i \neq j$, is expressed as

$$\sigma_{ij} = \sigma'_{ij}(1 - \xi' C'_2) \qquad (A8.29)$$

where

$$\sigma'_{ij} = (\sigma_{ii}\sigma_{jj})^{1/2} \qquad (A8.30)$$

and

$$C'_2 = \frac{3}{10 + 400\omega_{ij}} \qquad (A8.31)$$

The programme "RMHSVC/BAS" is used to estimate second virial coefficient of pure components and their mixtures, at the various temperatures using Hayden and O'Connell correlation. The programme needs input of only, critical temperature (T^c), critical pressure (P^c), mean radius of gyration (R_D) and dipole moment (μ) of pure components (Prausnitz et al., 1980). The list of computer symbols, used instead of the conventional nomenclature above, is given below.

Conventional Nomenclature	Equation No.	Computer Symbol
$(B^F_{nonpolar})_{ij}$	(A8.1)	B1
$(B^F_{ploar})_{ij}$	(A8.1)	B2
$(B^D_{metastable})_{ij}$	(A8.1)	B3
$(B_{bound})_{ij}$	(A8.1)	B4
$(B_{chemical})_{ij}$	(A8.1)	B5
$(b_0)_{ij}$	(A8.2)	V

Conventional Nomenclature	Equation No.	Computer Symbol
$T^{*'}_{ij}$	(A8.2)	T3
T^{*}_{ij}	(A8.4)	T4
σ_{ii}	(A8.5)	S
σ'_{ii}	(A8.8)	S1
ξ	(A8.7)	D
T^{c}_{i}	(A8.8)	T1
P^{c}_{i}	(A8.11)	P1
ω_{ii}	(A8.3)	W(I)
$(\varepsilon_{ii}/k)'$	(A8.7)	E3
η_{ii}	(A8.9)	N
(ε_{ii}/k)	(A8.7)	E1
μ_{i}	(A8.8)	D1
μ^{*}_{ii}	(A8.15)	D3
$\mu^{*'}_{ii}$	(A8.14)	D4
Δh_{ij}	(A8.19)	H
A_{ij}	(A8.18)	A
E_{ij}	(A8.20)	E5
ω_{ij}	(A8.22)	W(J)

```
10 REM ************************************************************
20 REM ** RMHSVC.BAS ESTIMATES SECOND VIRIAL COEFF. OF PURE      **
30 REM ** COMPONENTS AND THEIR MIXTURE, AT THE VARIOUS TEMP.     **
50 REM ** USING HAYDEN AND O'CONNELL 'S METHOD.                  **
60 REM ************************************************************
70 PRINT "DO YOU NEED INFORMATION ? Y/N."
80 INPUT X$ \ IF X$="N" THEN 230
90 PRINT "ESTIMATION OF SECOND VIRIAL COEFF. OF PURE COMPONENT"
100 PRINT "AND MIXTURE, USING HAYDEN AND O'CONNELL METHOD (1975)"
110 PRINT "REQUIRES TO KNOW PURE COMPONENT'S CRITICA TEMP."
120 PRINT "CRITICAL PRESS., MEAN RADIUS OF GYRATION AND DIPOLE"
130 PRINT "MOMENT. THESE VALUES ARE USED FROM REFERENCE :"
140 PRINT "PRAUSNITZ ET AL., 'COMPUTER CALCULATIONS FOR MULTI-"
150 PRINT "COMPONENT VAPOUR-LIQUID AND LIQUID-LIQUID "
151 PRINT "EQUILIBRIAL.', (1980)"
160 PRINT
170 PRINT "B FOR PURE COMPONENT AND MIXTURES IS SUM OF SEVERAL"
180 PRINT "CONTRIBUTIONS, CALCULATED FROM TEMPERATURE DEPENDENT"
190 PRINT " CORRELATIONS GIVEN IN THE REFERENCE" \ PRINT  \ PRINT
200 PRINT " DATA FILE IS PUT AT THE END  IN LINES 3000-3020"
210 PRINT "3010 DATA T1,P1,R1,D1"
215 REM ** ALL SYMBOLS USED IN THE PROGRAMME ARE DEFINED IN **
216 REM ** APPENDIX A8 OF PH.D THESIS (MALHOTRA, 1983)      **
217 REM ** CHEM. ENG., SUBMITTED TO UNIV. OF CANTERBURY     **
218 REM ** CHRISTCHURCH, NEW ZEALAND.                       **
220 PRINT
230 OPEN "LP:" FOR OUTPUT AS FILE #1
240 PRINT #1,DAT$
245 PRINT #1 \ PRINT #1
250 PRINT "INPUT TITLE"
260 INPUT A$
270 PRINT #1,A$
275 PRINT #1,"_____________________________________________________"
280 PRINT #1 \ PRINT #1 \ PRINT #1
300 READ T,T5,T6
310 FOR I=1 TO 2
320 READ T(I),P(I),R(I),D(I),N(I)
330 NEXT I
340 READ N(3)
350 PRINT #1,"PARAMETERS FOR COMPONENT (1)"
351 PRINT #1,"------------------------------"
352 PRINT #1 \ PRINT #1
355 PRINT #1,"CRITICAL TEMPERATURE = ";T(1)
357 PRINT #1,"CRITICAL PRESSURE = ";P(1)
360 PRINT #1,"RADIUS OF GYRATION = ";R(1)
363 PRINT #1,"DIPOLE MOMENT  = D(1)
365 PRINT #1,"ASSOCIATION NUMBER =";N(1) \ PRINT #1
370 PRINT #1,"PARAMETERS FOR COMPONENT (2)"
375 PRINT #1,"------------------------------" \ PRINT #1
380 PRINT #1,"CRITICAL TEMPERATURE = ";T(2)
382 PRINT #1,"CRITICAL PRESSURE = ";P(2)
385 PRINT #1,"RADIUS OF GYRATION =";R(2)
387 PRINT #1,"DIPOLE MOMENT = ";D(2)
390 PRINT #1,"ASSOCIATION NUMBER = ";N(2)
395 PRINT #1 \ PRINT #1
400 PRINT #1,"SOLVATION NUMNER FOR THE MIXTURE= ";N(3)
405 PRINT #1,"COMPONENT 1","COMPONENT 2","MIXTURE (1+2)","TEMP."
410 PRINT #1,"-----------","-----------","--------------","-------"
415 PRINT #1
```

```
500 REM ** THIS PART CALCULATES THE PARAMETERS FOR THE PURE      **
510 REM ** COMPONENTS.                                           **
550 FOR I=1 TO 2
560 W(I)=6.02600E-03*R(I)+.02096*R(I)^2-1.36600E-03*R(I)^3
570 C1=(16+400*W(I))/(10+400*W(I))
580 C2=3/(10+400*W(I))
590 S1=(2.44-W(I))*((1.0133*T(I))/P(I))^(1/3)
600 E3=T(I)*(.748+.91*W(I)-(.4*N(I)/(2+20*W(I))))
610 IF D(I)>=1.45 THEN  GO TO 630
620 D=0 \ GO TO 650
630 C=2.882-((1.882*W(I))/(.03+W(I)))
640 D=(1.7941*10^7*D(I)^4)/(C*T(I)*S1^6*E3)
650 E(I)=E3*(1-(D*C1*(1-(D*(1+C1)/2))))
660 S(I)=S1*((1+D*C2)^(1/3))
670 D3(I)=(7243.8*D(I)^2)/(E(I)*S(I)^3)
680 NEXT I
800 REM ** THIS PART CALCULATES THE PARAMETER FOR THE MIXTURE   **
820 J=3
830 W(J)=(1/2)*(W(1)+W(2))
840 C1=(16+400*W(J))/(10+400*W(J))
850 C2=3/(10+400*W(J))
860 S1=(S(1)*S(2))^(1/2)
870 E3=.7*(E(1)*E(2))^(1/2)+.6/((1/E(1))+(1/E(2)))
880 IF D(1)>=2 THEN IF D(2)=0 THEN  GO TO 900
890 IF D(2)>=2 THEN IF D(1)=0 THEN  GO TO 940
895 D=0 \ GO TO 950
900 D=(D(1)^2*(E(2)^(2/3)*S(2)^4)/(E3*S1^6) \ GO TO 950
940 D=D(2)^2*(E(1)^(2/3)*S(1)^4)/(E3*S1^6)
950 E(J)=E3*(1+D*C1)
960 S(J)=S1*(1-D*C2)
970 D3(J)=(7243.8*D(1)*D(2))/(E(J)*S(J)^3)
980 FOR I=1 TO 3
1000 NEXT I
1300 REM ** THIS PART CALCULATES THE SECOND VIRIAL COEFF.       **
1310 REM ** OF PURE COMPONENT AND THEIR MIXTURE.                **
1320 FOR I=1 TO 3
1330 V=1.26184*S(I)^3
1340 IF D3(I)<.04 THEN  GO TO 1380
1350 IF D3(I)>=.04 THEN IF D3(I)<.25 THEN  GO TO 1390
1360 IF D3(I)>=.25 THEN  GO TO 1400
1370 GO TO 1410
1380 D4=D3(I) \ GO TO 1410
1390 D4=0 \ GO TO 1410
1400 D4=D3(I)-.25
1410 A=-.3-.05*D3(I)
1420 H=1.99+.2*D3(I)^2
1425 IF N(I)<4.5 THEN  GO TO 1435
1430 IF N(I)>=4.5 THEN  GO TO 1440
1435 E=EXP(N(I)*(650/(E(I)+300)-4.27)) \ GO TO 1450
1437 GO TO 1450
1440 E=EXP(N(I)*(42800/(E(I)+22400)-4.27))
1450 T4(I)=T/E(I)
1460 T3=(1/T4(I))-(1.6*W(I))
1470 B1=V*(.94-(1.47*T3)-(.85*T3^2)+(1.015*T3^3))
1480 B2=-V*D4*(.74-(3*T3)+(2.1*T3^2)+(2.1*T3^3))
1490 B3=V*A*EXP(H/T4(I))
1500 B4=V*E*(1-EXP((1500*N(I))/T))
1600 B(I)=B1+B2+B3+B4
1610 NEXT I
1620 PRINT B(1),B(2),B(3),T
```

```
1770 PRINT #1,B(1),B(2),B(3),T
1780 T=T+5
1790 IF T5>=T THEN  GO TO 500
1800 PRINT #1,CHR$(12)
1900 CLOSE #1
2000 DATA 323.15,373.15,5
2010 DATA 562.1,48.6,3.004,0,0
2020 DATA 509.1,47,2.74,2.88,0.9
2030 DATA 0.5
2050 END
```

APPENDIX A9

Tsonopoulos Estimation of Second Virial Coefficient

The programme "RMSVCT.BAS" estimates the second virial coefficients of the pure components using Tsonopoulos (1974) correlation, as discussed in Section 1-4. The method only needs to know the critical pressure (P^c), critical temperature (T^c) and acentric factor (ω) of the pure component, and can be obtained from the reference Reid et al. (1977).

The programme calculates B using the relations

$$B = \frac{RT^c}{P^c}(f^{(0)} + \omega f^{(1)}) \qquad \text{(A9.1)}$$

where

$$f^{(0)} = 0.1445 - 0.33/T_R - 0.1385/T_R^2 - 0.0121/T_R^3 - 0.000607/T_R^8 \qquad \text{(A9.2)}$$

$$f^{(1)} = 0.637 + 0.331/T_R^2 - 0.423/T_R^3 - 0.008T_R^8 \qquad \text{(A9.3)}$$

and $T_R = T/T^c$

The second virial cross coefficient B_{12} has the same temperature dependence that B_{11} and B_{22} have, but the parameters T^c_{12}, ω_{12} required in equations (A9.1 to A9.3) are calculated using mixing rules

$$T_{12}^{c} = (T_{11}^{c} \cdot T_{22}^{c})^{0.5} \qquad \text{(A9.4)}$$

$$\omega_{12} = (\omega_{11} + \omega_{22})/2 \qquad \text{(A9.5)}$$

```
10 REM ************************************************************
20 REM ** RMSVCT.BAS ESTIMATES SECOND VIRIAL COEFFICEINTS OF **
30 REM ** PURE NON-POLAR COMPONENTS USING CONSTANTINE          **
40 REM ** TSONOPOULOS'  METHOD OF EMPIRICAL CORRELATION.      **
50 REM ************************************************************
55 REM
60 PRINT "ESTIMATION OF SECOND VIRIAL COEFFICIENT OF PURE AND"
70 PRINT "NON-POLAR" COMPONENT USING CONSTANTINE TSONOPOULOS'S"
75 PRINT "METHOD OF EMPIRICALCORRELATIONS REQUIRES TO"
80 PRINT "KNOW CRITICAL TEMPERATURE, CRITICAL PRESSURE AND "
90 PRINT "VAPOUR PRESSURE AT REDUCED TEMPERATURE EQUAL TO 0.7"
100 PRINT
110 OPEN "LP:" FOR OUTPUT AS FILE #1
120 PRINT "INPUT TITLE" \ PRINT
130 INPUT A$
140 PRINT #1,A$ \ PRINT #1 \ PRINT #1
150 PRINT "REM: P1=CRITICAL PRESS. OF THE PURE COMPONENT, (ATM.)"
160 PRINT "REM: T1=CRITICAL TEMP. OF THE PURE COMPONENT, (K)"
170 PRINT "REM: W =OMEGA, ACENTRIC FACTOR "
180 PRINT  \ PRINT
190 PRINT "VALUES P1,T1,W FOR MOST OF THE PURE COMPONETS CAN BE"
200 PRINT "USED FROM THE REFERENCE: REID,C.R.; PRAUSNITZ, J.M,; "
210 PRINT "SHERWOOD,T.S, 'THE PROPERTIES OF GASES AND LIQUIDS' "
220 PRINT "THIRD EDITION, 1977, APPENDIX A: PAGE 629."
230 PRINT  \ PRINT "INPUT T1,P1,W"
240 INPUT T1,P1,W
250 PRINT #1,"CRITICAL TEMPERATURE = ";T1;"K"
260 PRINT #1,"CRITICAL PRESSURE = ";P1;"ATM."
270 PRINT #1,"PITZER'S ACENTRIC FACTOR = ";W
280 PRINT #1
290 PRINT "REM: T = THE MINIMUM TEMPERATURE FOR WHICH SECOND "
300 PRINT "           VIRIAL COEFFICIENT HAS TO BE ESTIMATED."
310 PRINT "REM: T5= THE FINAL TEMPERATURE FOR THE SEC. VIRIAL"
320 PRINT "            COEFF. "ESTIMATION."
330 PRINT "REM: T6= STEP BETWEEN EACH CONSTICUTIVE TEMPERATURE, "
340 PRINT "           FOR SEC. VIRIAL COEFFICIENT ESTIMATION."
350 PRINT  \ PRINT "INPUT T,T5,T6"
360 INPUT T,T5,T6
370 PRINT #1,"INITIAL TEMPERATURE = ";T;"K"
380 PRINT #1,"FINAL TEMPERATURE = ";T5;"K"
390 PRINT #1,"DIFFERENCE IN CONSICUTIVE TEMPERATURE = ";T6;"K"
400 PRINT #1 \ PRINT #1
410 REM ** B = ESTIMATED SECOND VIRIAL  COEFFICIENT.     **
420 REM ** F0,F1= TSONOPOULOUS'S MODIFIED CONSTANT       **
430 REM ** R = GAS CONSTANT (CM3OATM.GMOLE-1.K-1)        **
440 REM ** T2= REDUCED TEMPERATURE.                      **
450 PRINT #1,"SEC. VIRIAL COEFF. ESTIMATION (TSONOPOULOUS'S )"
460 PRINT #1,"-------------------------------------------------"
470 R=82.057
480 T2=T/T1
490 F0=.1445-.33/T2-.1385/(T2^2)-.0121/(T2^3)
500 F0=F0-6.07000E-04/(T2^8)
510 F1=.0637+.331/(T2^2)-.423/(T2^3)-8.00000E-03/(T2^8)
520 B=((R*T1)/P1)*(F0+W*F1)
530 PRINT #1
540 PRINT #1,"B (";T;"K ) = ";B;"CM3. MOLE-1"
550 PRINT #1 \ PRINT #1
560 T=T+T6
570 IF T5>=T GO TO 480
580 CLOSE #1
590 END
```

APPENDIX A10

Calculation and Tabulation of Raw Data for Mixtures

Appendix A10 consists of two parts. Part I contains calculations of raw data as obtained, using the original instrumental readings. The original instrumental readings comprise temperature of the bath (T), temperature of the manometer bath (T_1), the difference in the heights (Δh) of the mercury levels in the manometer, zero pressure adjustment reading on the Baratron (B_{zero}) and pressure difference measurement (Δp) using the Baratron gauge.

Bath temperature (T) = 323.15 K

Mercury manometer thermostat temperature (T_1) = 296.65 K

* Difference in mercury heights (Δh) = 18.14 cms.

* Zero pressure adjustment, i.e.,Reference pressure higher than mixture = 0.8 μm Hg

* Pressure difference (Δp) = 41.2±0.6 μm Hg

Acceleration due to gravity (g_{local}) = 980.48 cm sec^{-1}

ρ_{Hg}(296.65 K) = 13.53731 gm. cm^{-3} (Bigg, 1964)

* These are the averages of a few readings observed.

Using equation (6.12)

$$p = 13.53731 \times 980.48 \times 18.14/10$$

$$= 2.408 \times 10^4 \text{ Pa} \simeq 180.6 \text{ mm Hg}$$

Zero pressure adjustment i.e.

Reference pressure is higher than system pressure by 0.8 μm Hg before mixing. Therefore

Average Δp (mixture higher than reference) = 41.2±0.6 μm Hg

Corrected Δp = 41.2 + 0.8 = 42.0 μm Hg

or $\Delta p = 0.042 \times 133.3224 = 5.6$ Pa

Part II

Part II tabulates the raw data consisting of loading pressure (p) and pressure change (Δp) after mixing of the components at temperature (T).

Table A10-1 **Raw Data for Benzene (1) + Cyclohexane (2)**

Temperature K	Loading Pressure Pa	Fraction of Saturated Vapour Pressure of benzene	Pressure Change Pa	
298.15	9678	0.76	2.77±0.1	
298.15	6138	0.48	0.91±0.1	
323.15	24080	0.66	5.60±0.1	
323.15	25210	0.77	5.76±0.1	
348.15	44950	0.52	9.64±0.1	B
348.15	51110	0.59	12.75±0.1	B
373.15	47090	0.26	9.09±0.1	B
373.15	46860	0.26	8.55±0.2	B
* 398.15	46370	0.14	6.39±0.1	B
398.15	48320	0.14	6.64±0.1	
398.15	46820	0.14	6.40±0.4	
398.15	47340	0.14	5.60±0.2	

* First component is cyclohexane

B Data measured by Prof. Rubin Battino (1979-80), Wright State University, Dayton, Ohio, USA. during his stay in this department.

Table A10-2 **Raw Data for Benzene (1) + n-Hexane (2)**

Temperature K	Loading Pressure Pa	Fraction of Saturated Vapour Pressure of benzene	Pressure Change Pa	
298.15	7649	0.60	0.57±0.1	
298.15	8428	0.67	0.85±0.1	
323.15	20450	0.56	2.37±0.1	B
323.15	22300	0.62	2.69±0.1	
348.15	40770	0.47	6.40±0.1	
348.15	43440	0.50	8.30±0.1	
348.15	46590	0.54	7.40±0.1	B
348.15	40680	0.47	5.60±0.1	B
373.15	46560	0.26	6.49±0.1	B
373.15	57300	0.32	12.07±0.1	B
373.15	45190	0.25	6.88±0.1	
398.15	48950	0.14	5.60±0.1	B
398.15	47170	0.14	5.16±0.2	B
398.15	51500	0.15	6.15±0.2	

B Data measured by Prof. Rubin Battino.

Table A10-3 **Raw Data for Cyclohexane (1) + n-Hexane (2)**

Temperature K	Loading Pressure Pa	Fraction of Saturated Vapour Pressure of cyclohexane	Pressure Change Pa	
298.15	9034	0.69	0.51±0.1	
298.15	8679	0.66	-0.19±0.1	
298.15	9017	0.69	-0.25±0.1	
323.15	23950	0.66	-0.72±0.1	
323.15	21740	0.60	0.77±0.1	
348.15	44400	0.52	-1.59±0.1	B
348.15	47930	0.56	-1.67±0.1	B
373.15	47180	0.27	-1.51±0.1	B
373.15	45080	0.26	-0.96±0.1	
373.15	47840	0.27	-1.49±0.2	B
398.15	44170	0.14	-1.20±0.1	
398.15	49400	0.15	-1.12±0.1	B

B Data measured by Prof. Rubin Battino

APPENDIX A11

Adsorption Correction to Apparent Excess Second Virial Coefficient

The analysis for the effect of adsorption of the component on the vessel surface has already been discussed (section 3-7.4). A short program "RBEPS/BAS" (Battino, 1980) is used to calculate $\delta\varepsilon_{adsorption}$. It requires the input values of adsorption area (A), volume of the vessel (V), isotherm parameter (C), number of moles per unit area, N_i^0 of each component (1) and (2) to form monolayer and saturated vapour pressures of the components (1) and (2) at the working temperature. The values of the apparatus constants used in this work are

$A = 0.24\ m^2$

$V = 6.0$ litres

$C = 100$

Moles per unit area (N^0) for monolayer

$N^0(\text{benzene}) = 4.0 \times 10^{-6}\ \text{mol}\ m^{-2}$

$N^0(\text{cyclohexane}) = 8.3 \times 10^{-6}\ \text{mol}\ m^{-2}$

$N^0(\text{n-hexane}) = 3.5 \times 10^{-6}\ \text{mol}\ m^{-2}$

Saturated vapour pressure

Saturated vapour pressure at the various temperatures were observed from the tabulation of selected values of properties of hydrocarbon and related compounds (American Partroleum Institute Research Project 44, 1975). In addition it requires the loading pressure (p) of each component at temperature (T). The number of moles (n_{a_i}) of each component adsorbed before mixing are calculated using equation (3.65). On rearranging, we obtain

$$n_{a_i} = \frac{N_i^0 ACp/p_i^0}{(1 - p/p_i^0)[1 + (C - 1)p/p_i^0]} \qquad (A11.1)$$

No. of moles (Na_i) of each component adsorbed after mixing are calculated using equation (3.66). On rearranging we obtain

$$n'_{a_i} = \frac{N_i^0 ACp/p_i^0}{(1 - p/2p_i^0)[1 + (C - 1)p/2p_i^0]} \qquad (A11.2)$$

$\delta\varepsilon_{adsorption}$ is calcualted using equation (3.64)

$$\delta\varepsilon_{adsorption} = V(n_{a_1} - n'_{a_1} + n_{a_2} - n'_{a_2})/n_1^2 \qquad (3.64)$$

Where $n_1 \simeq n_2 \simeq n$, and subscripts 1 and 2 represent components (1) and (2).

```
5  REM ************************************************************
10 REM ** PROGRAM RBEPS.BAS TO CALCULATE DELPSILON CORRECTION **
20 REM ** FOR ADSORPTION OF HYDROCARBONS ON METALS USING THE  **
30 REM ** BET ISOTHERM.  SEE SHANNON'S THESIS PAGES 37-38     **
40 REM ** BATTINO MAY 1980                                    **
45 REM ************************************************************
50 REM A = ADSORPTIVE AREA = 0.24 M^2
60 REM C = CONSTANT = 100
70 REM N1 = NO. MOLES/AREA TO FORM MONOLAYER. COMPONENT 1.
80 REM N2 =                                   COMPONENT 2.
90 REM N = NO. MOLES OF EACH COMPONENT START WITH.
100 REM V = VOLUME OF VESSEL = 6.0 LITERS
110 REM P = PRESSURE OF MEASUREMENT IN MM HG
120 REM P1 = SATURATION VAPOR PRESSURE OF COMPONENT 1
130 REM P2 =                             COMPONENT 2
140 REM T = KELVIN TEMP
150 REM R = GAS CONSTANT
160 REM D1 = COMPONENT 1 PRIME; D2 = COMPONENT 1 DOUBLE PRIME
170 REM E1 =           2      ; E2 =           2
180 REM
190 OPEN "LP:" FOR OUTPUT AS FILE #1
200 PRINT #1
210 PRINT #1,"INPUT TITLE"
220 INPUT A$
230 PRINT #1,A$
240 PRINT A$
250 PRINT #1
260 PRINT
270 R=.08205
280 A=.24
290 C=100
300 V=6
310 PRINT #1
320 PRINT
330 PRINT #1,"INPUT T/K, N1, N2 ...NO. MOLES/AREA"
340 PRINT "IMPUT T/K, N1, N2"
350 INPUT T,N1,N2
360 PRINT #1
370 PRINT
380 PRINT #1,"T/K = ";T,"N1 = ";N1,"N2 = ";N2
390 PRINT "T/K = ";T,"N1 = ";N1,"N2 = ";N2
400 PRINT #1
410 PRINT
420 PRINT #1,"INPUT P/MM HG, P1, P2 ...SATN V.PS."
430 PRINT "INPUT P/MM HG, P1, P2"
440 INPUT P,P1,P2
450 PRINT #1
460 PRINT
470 PRINT #1,"P/MM HG = ";P,"P1 = ";P1,"P2 = ";P2
480 PRINT "P/MM HG = ";P,"P1 = ";P1,"P2 = ";P2
490 N=(P*V)/(760*R*T)
500 D3=N1*A*C*P/P1
510 D1=(1-(P/P1))*(1+(C-1)*(P/P1))
520 D1=D3/D1
530 D2=(1-(P/(2*P1)))*(1+(C-1)*(P/(2*P1)))
540 D2=D3/D2
550 E3=N2*A*C*P/P2
560 E1=(1-(P/P2))*(1+(C-1)*(P/P2))
570 E1=E3/E1
580 E2=(1-(P/(2*P2)))*(1+(C-1)*(P/(2*P2)))
```

```
590 E2=E3/E2
600 E=V*(D2-D1+E2-E1)/(N*N)
610 E=E*1000
620 PRINT #1
630 PRINT
640 PRINT #1
650 PRINT
660 PRINT "DELTA EPSILON/(CM^3/MOL) = ";E
670 PRINT #1,"DELTA E[SILON/(CM^3/MOL) = ";E
680 PRINT #1
690 PRINT
700 PRINT #1,"D1 = ";D1,"D2 = ";D2,"N = ";N
710 PRINT "D1 = ";D1,"D2 = ";D2,"N = ";N
720 PRINT #1,"E1 = ";E1,"E2 = ";E2
730 PRINT "E1 = ";E1,"E2 = ";E2
740 PRINT #1
750 PRINT
760 CLOSE
770 GO TO 190
780 END
```

APPENDIX A12

Curve Fitting

The curve fitting to data pairs comprising ε_i and T_i is accomplished by using a multivariant - variable optimisation routine. The programme "RMCFP.BAS" fits a specific function to a set of data pairs by minimising the sum of squares of deviation of the data from the fitted function and is designed for the use with an interactive terminal. It uses a 'Hooke and Jeeves' pattern search method (Dixon, 1972) to change the value of the constants in the function, in a search for the optimum sum of squares of deviations. A modified multivariant - variable optimisation routine programme "RMCFP2.BAS" may be used to fit curve to combined data pairs comprising of ε_i, T_i and H_m^E/p_j, T_j. The appendix lists both curve fitting programmes used.

A12-1 Program for Fitting (ε_i, T_i) Data Only

The function to be fitted to data pair (ε_i, T_i) is, namely

$$\varepsilon/10^{-6}\ m^3\ mol^{-1} = a + (b \times 10^{-4})\exp(100c/T) \qquad (A12.1)$$

where the constants in

$$\varepsilon = A + B\exp(C/T) \qquad (A12.2)$$

have been scaled so that they are of the same order of magnitude. The inputs required are

(1) No. of (ε_i, T_i) data pairs to be fitted.

(2) No. of variables (constants) in the function.

(3) Initial step size in the variables for the search method.

(4) Final step size in the variables for the search method.

(5) Step size reduction factor.

(6) Initial values of a, b and c

Generally the initial step size used is 2, going through a reduction factor of 0.5 to a final step size equal to 0.001. Initial values of a, b and c used are by random hit and trial method and getting more selective at the end of search. The (ε_i, T_i) and weighting w_i, data is already included in the program, by means of DATA statement lines 6000 to 6002. The weight w_i, given to the ith data pair (ε_i, T_i) is given by

$$w_i = E/\delta\varepsilon_i \qquad \text{(A12.3)}$$

where E is the maximum error in the measurement of ε in the set of data pairs.

A dummy input in statement 4010, stops program execution after the search has been terminated and optimum values found. This enables the interim output to be suppressed thus saving time. Upon entering the dummy input by any integer, the final output is printed, having the following form.

(1) The optimum values of the sum of squares of deviations.

(2) A listing of the final values of the constants a, b and c.

(3) A listing of the numbers of explorations, pattern moves and function evaluation required to find the optimum.

```
5  REM ************************************************************
10 REM ** PROGRAMME "RMCFP.BAS" USES THE MULTI                    **
20 REM ** VARIABLE OPTIMISATION BY HOOKE AND JEEVES PATTERN       **
30 REM ** SEARCH METHOD.                                          **
40 REM ** SEE DIXON "NONLINEAR OPTIMISATION" P 69.               **
50 REM ** THE FUNCTION TO BE OPTIMISED IS DEFINED IN A           **
60 REM ** SUBROUTINE AT LINE 5000                                **
65 REM ************************************************************
70 DEF FNA(A,B,C,T)=A+1.00000E-04*B*EXP(100*C/T)
80 DIM P(20),T(20),W(20)
90 PRINT "NUMBER OF DATA POINTS/" \ INPUT N9
100 FOR M=1 TO N9
110 READ P(M),T(M),W(M)
120 NEXT M
130 DIM X(10),X1(10),X2(10),X3(10)
200 PRINT "INPUT NUMBER OF VARIABLES N"
220 INPUT N
300 PRINT "INPUT INITIAL STEP SIZE K" \ INPUT K
340 PRINT "INPUT FINAL STEP SIZE K1" \ INPUT K1
360 PRINT "INPUT STEP SIZE REDUCTION FACTOR" \ INPUT K2
430 LET K9=K
480 REM INPUT STARTING POINT X
500 FOR I=1 TO N
520 PRINT "X("I")= ", \ INPUT X(I)
540 NEXT I
550 PRINT  \ PRINT
560 K=K9
600 REM INITIALISE COUNTERS
620 LET J=0 \ LET J1=0 \ LET J2=0
2000 REM START SEARCH
2020 REM EVALUATE FUNCTION AT STARTING POINT
2040 FOR I=1 TO N
2060 LET X1(I)=X(I) \ LET X2(I)=X(I)
2080 NEXT I
2100 GOSUB 5000
2120 LET Y=Y1 \ LET Y2=Y1
2140 PRINT "AT INITIAL BASE POINT Y= ";Y
2160 FOR I=1 TO N
2170 PRINT "X("I")= ";X(I)
2220 NEXT I
2240 PRINT
2300 REM START EXPLORATION
2320 LET J=J+1
2340 PRINT "EXPLORATION NUMBER =";J
2360 FOR I=1 TO N
2380 LET X1(I)=X2(I)+K
2400 GOSUB 5000
2420 LET Z=Y1
2460 IF Z>Y2 THEN 2700
2480 REM FAILURE. CHANGE SIGN OF STEP.
2520 LET X1(I)=X2(I)-K \ LET K=-K
2540 GOSUB 5000
2560 LET Z=Y1
2600 IF Z>Y2 THEN 2700
2620 REM FAILURE AGAIN. GO ON TO NEXT DIRECTION
2660 LET X3(I)=X2(I)
2670 LET X1(I)=X2(I)
2680 GO TO 2780
```

```
2700 ** REM SUCCESS                                                **
2740 LET X3(I)=X1(I)
2760 LET Y2=Z
2780 NEXT I
2800 REM END OF EXPLORATION
2820 PRINT "AFTER EXPLORATION Y2=";Y2
2840 PRINT "X3=";
2860 FOR I=1 TO N
2880 PRINT X3(I);
2900 NEXT I
2920 PRINT
2940 REM TEST WHETHER EXPLORATION HAS IMPROVED OVER BASE POINT
2960 PRINT "EXPLORATION HAS";
2980 IF Y2>Y THEN 3000
2990 PRINT "NOT";
3000 PRINT "IMPROVED ON BASE POINT"
3020 IF Y2<=Y THEN 3500
3040 PRINT "MAKE PATTERN MOVE"
3060 FOR I=1 TO N
3080 LET X2(I)=X3(I)*2-X(I)
3100 LET X(I)=X3(I)
3110 LET X1(I)=X2(I)
3120 NEXT I
3140 LET Y=Y2
3160 GOSUB 5000
3180 LET Y2=Y1
3200 LET J2=J2+1
3220 PRINT "PATTERN MOVE "J2" IS TO X2=";
3260 FOR I=1 TO N
3280 PRINT X2(I);
3300 NEXT I
3320 PRINT  \ PRINT "WHERE Y2=";Y2
3340 PRINT "BASE POINT NUMBER "J2+1" BECOMES"
3350 PRINT "X= ";
3360 FOR I=1 TO N
3380 PRINT X(I);
3400 NEXT I
3420 PRINT  \ PRINT "WHERE Y= "Y
3440 GO TO 2320
3500 REM NO IMPROVEMENT FROM EXPLORATION . HAVE WE EXPLORED
3510 REM   FROM THE BASE POINT?
3520 FOR I=1 TO N
3540 IF X2(I)=X(I) THEN 3580
3560 GO TO 3700
3580 NEXT I
3590 GO TO 3900
3700 PRINT "START NEXT EXPLORATION FROM THE BASE POINT."
3720 FOR I=1 TO N
3740 LET X2(I)=X(I)
3760 NEXT I
3780 LET Y2=Y
3800 GO TO 2320
3900 PRINT "HAVE ALREADY EXPLORED FROM THE BASE POINT."
3910 PRINT "DECREASE STEP SIZE"
3920 LET K=K*K2 \ PRINT "K= ";K
3940 REM TEST FOR TERMINATION
3960 IF ABS(K)>=K1 THEN 2320
4000 REM TEST FOR TERMINATION
4010 INPUT A9
4020 PRINT  \ PRINT "OPTIMUM VALUE IS";Y
```

```
4040 FOR I=1 TO N
4060 PRINT "X("I")= ";X(I)
4080 NEXT I
4100 PRINT J"EXPLORATIONS"
4120 PRINT J2"PATTERN MOVES"
4140 PRINT J1"FUNCTION EVALUATIONS"
4300 STOP
5000 REM SUM OF SQUARES SUBROUTINE
5020 LET Y1=0
5040 LET J1=J1+1
5060 FOR M=1 TO N9
5080 Y9=P(M)-FNA(X1(1),X1(2),X1(3),T(M))
5100 LET Y9=Y9*Y9
5110 Y9=Y9*W(M)
5120 LET Y1=Y1-Y9
5140 NEXT M
5160 RETURN
6000 DATA 57,308,8,22,373,80,35,323,8,25,348,40,22,373,40
6001 DATA 38,315,5,21,373,26.7,45,318,4,29,323,40,44,323,80
6002 DATA 19,348,26.7,30,313,1.78,14,333,5.33,135,298,1,175,300,1.6
8190 END
```

A12-2 Program for Fitting Both (ε_i, T_i) and (H_m^E/p_j, T_j) Data

A previous program (Appendix A12.1) is modified to include the contribution attributable to the deviation of the (H_m^E/p_j, T_j) data to the sum of squares of deviations. Additional inputs required are

(1) Overall weighting of the (H_m^E/p_j, T_j) data points.

(2) Overall weighting of the (ε_i, T_i) data points.

The (H_m^E/p_j, T_j) data is read by the means of the DATA statements 5998 amd 5999. The final output is the same as for the other program with the addition of the contribution of each set of data to the final sum of squares of deviations.

```
5  REM ************************************************************
10 REM ** PROGRAMME RMCFP2.BAS USES THE MULTI VARIABLE           **
20 REM ** OPTIMISATION BY HOOKE AND JEEVES PATTERN SEARCH       **
30 REM ** METHOD TO FIT A SUITABLE RELATION TO THE DATA         **
35 REM ** OF EXCESS SECOND VIRIAL COEFF. AT VARIOUS TEMP.       **
36 REM ** AND HEAT OF MIXING OF VAPOURS AT VARIOUS TEMP.        **
40 REM ** SEE DIXON "NONLINEAR OPTIMISATION" P 69.              **
50 REM ** THE FUNCTION TO BE OPTIMISED IS DEFINED IN A          **
60 REM ** SUBROUTINE AT LINE 5000                               **
65 REM ************************************************************
62 DIM R(10),T1(10),W1(10)
63 DEF FNB(A,B,C,T)=A+1.00000E-04*B*EXP(100*C/T)*(1+100*C/T)
64 PRINT "OVERALL WEIGHTING OF HE/P DATA POINTS?"; \ INPUT Q
65 REM N8 IS THE NUMBER OF HE/P DTA POINTS
66 N8=10
67 FOR M1=1 TO N8
68 READ R(M1),T1(M1),W1(M1)
69 NEXT M1
70 DEF FNA(A,B,C,T)=A+1.00000E-04*B*EXP(100*C/T)
80 DIM P(20),T(20),W(20)
81 PRINT "OVERALL WEIGHTING OF DATA POINTS?"; \ INPUT P
90 PRINT "NUMBER OF DATA POINTS/" \ INPUT N9
100 FOR M=1 TO N9
110 READ P(M),T(M),W(M)
120 NEXT M
130 DIM X(10),X1(10),X2(10),X3(10)
200 PRINT "INPUT NUMBER OF VARIABLES N"
220 INPUT N
300 PRINT "INPUT INITIAL STEP SIZE K" \ INPUT K
340 PRINT "INPUT FINAL STEP SIZE K1" \ INPUT K1
360 PRINT "INPUT STEP SIZE REDUCTION FACTOR" \ INPUT K2
430 LET K9=K
480 REM INPUT STARTING POINT X
500 FOR I=1 TO N
520 PRINT "X("I")= ", \ INPUT X(I)
540 NEXT I
550 PRINT  \ PRINT
560 K=K9
600 REM INITIALISE COUNTERS
620 LET J=0 \ LET J1=0 \ LET J2=0
2000 REM START SEARCH
2020 REM EVALUATE FUNCTION AT STARTING POINT
2040 FOR I=1 TO N
2060 LET X1(I)=X(I) \ LET X2(I)=X(I)
2080 NEXT I
2100 GOSUB 5000
2120 LET Y=Y1 \ LET Y2=Y1
2140 PRINT "AT INITIAL BASE POINT Y= ";Y
2160 FOR I=1 TO N
2170 PRINT "X("I")= ";X(I)
2220 NEXT I
2240 PRINT
2300 REM START EXPLORATION
2320 LET J=J+1
2340 PRINT "EXPLORATION NUMBER =";J
2360 FOR I=1 TO N
2380 LET X1(I)=X2(I)+K
2400 GOSUB 5000
2420 LET Z=Y1
2460 IF Z>Y2 THEN 2700
```

```
2480 REM FAILURE. CHANGE SIGN OF STEP.
2520 LET X1(I)=X2(I)-K \ LET K=-K
2540 GOSUB 5000
2560 LET Z=Y1
2600 IF Z>Y2 THEN 2700
2620 REM FAILURE AGAIN. GO ON TO NEXT DIRECTION
2660 LET X3(I)=X2(I)
2670 LET X1(I)=X2(I)
2680 GO TO 2780
2700 REM SUCCESS
2740 LET X3(I)=X1(I)
2760 LET Y2=Z
2780 NEXT I
2800 REM END OF EXPLORATION
2820 PRINT "AFTER EXPLORATION Y2=";Y2
2840 PRINT "X3=";
2860 FOR I=1 TO N
2880 PRINT X3(I);
2900 NEXT I
2920 PRINT
2940 REM TEST WHETHER EXPLORATION HAS IMPROVED OVER BASE POINT
2960 PRINT "EXPLORATION HAS";
2980 IF Y2>Y THEN 3000
2990 PRINT "NOT";
3000 PRINT "IMPROVED ON BASE POINT"
3020 IF Y2<=Y THEN 3500
3040 PRINT "MAKE PATTERN MOVE"
3060 FOR I=1 TO N
3080 LET X2(I)=X3(I)*2-X(I)
3100 LET X(I)=X3(I)
3110 LET X1(I)=X2(I)
3120 NEXT I
3140 LET Y=Y2
3160 GOSUB 5000
3180 LET Y2=Y1
3200 LET J2=J2+1
3220 PRINT "PATTERN MOVE "J2" IS TO X2=";
3260 FOR I=1 TO N
3280 PRINT X2(I);
3300 NEXT I
3320 PRINT  \ PRINT "WHERE Y2=";Y2
3340 PRINT "BASE POINT NUMBER "J2+1" BECOMES"
3350 PRINT "X= ";
3360 FOR I=1 TO N
3380 PRINT X(I);
3400 NEXT I
3420 PRINT  \ PRINT "WHERE Y= "Y
3440 GO TO 2320
3500 REM NO IMPROVEMENT FROM EXPLORATION . HAVE WE EXPLORED
3510 REM   FROM THE BASE POINT?
3520 FOR I=1 TO N
3540 IF X2(I)=X(I) THEN 3580
3560 GO TO 3700
3580 NEXT I
3590 GO TO 3900
3700 PRINT "START NEXT EXPLORATION FROM THE BASE POINT."
3720 FOR I=1 TO N
3740 LET X2(I)=X(I)
3760 NEXT I
3780 LET Y2=Y
```

```
3800 GO TO 2320
3900 PRINT "HAVE ALREADY EXPLORED FROM THE BASE POINT."
3910 PRINT "DECREASE STEP SIZE"
3920 LET K=K*K2 \ PRINT "K= ";K
3940 REM TEST FOR TERMINATION
3960 IF ABS(K)>=K1 THEN 2320
4000 REM TEST FOR TERMINATION
4010 INPUT A9
4020 PRINT  \ PRINT "OPTIMUM VALUE IS";Y
4040 FOR I=1 TO N
4060 PRINT "X("I")= ";X(I)
4080 NEXT I
4100 PRINT J"EXPLORATIONS"
4120 PRINT J2"PATTERN MOVES"
4140 PRINT J1"FUNCTION EVALUATIONS"
4300 STOP
5000 REM SUM OF SQUARES SUBROUTINE
5020 LET Y1=0
5030 S1=0 \ S2=0
5040 LET J1=J1+1
5060 FOR M=1 TO N9
5080 Y9=P(M)-FNA(X1(1),X1(2),X1(3),T(M))
5100 LET Y9=Y9*Y9
5110 Y9=Y9*W(M)
5120 S1=W(M)*Y9+S1
5140 NEXT M
5160 FOR M1=1 TO N8
5180 Y8=P(M1)-FNB(X1(1),X1(2),X1(3),T1(M1))
5200 Y8=Y8*Y8
5220 S2=W1(M1)*Y8+S2
5240 NEXT M1
5260 S=P*S1+Q*S2
5280 Y1=Y1-S
5300 RETURN
5998 DATA 110,359,16.7,105,358,20,100,358,20,105,358,20,100,358,20
5999 DATA 100,358,20,100,358,6.3,400,323,1.3,440,315,1.33,480,305,1
6000 DATA 57,308,8,22,373,80,35,323,8,25,348,40,22,373,40
6001 DATA 38,315,5,21,373,26.7,45,318,4,29,323,40,44,323,80
6002 DATA 19,348,26.7,30,313,1.78,14,333,5.33,135,298,1,175,300,1.6
8190 END
```